UNIVERSITÀ DEL SALENTO
Dipartimento di Ingegneria dell'Innovazione
Dipartimento di Scienza dei Materiali

Società Chimica Italiana
Divisione di Chimica Fisica

XXXVI Congresso Nazionale di Chimica Fisica

Gallipoli, 17-22 Giugno 2007

Con il patrocinio di

Camera di Commercio, Industria, Artigianato e Agricoltura di Lecce

Provincia di Lecce

Comune di Gallipoli

Si ringraziano gli Sponsor:

Costruzioni Solari S.r.l., Zona P.I.P.-73020 Cavallino (Lecce), Italy

Comitato Scientifico

Vincenzo Barone
Angela Agostiano
Piero Baglioni
Stefania Milioto
Nicolae Viorel Pavel
Vincenzo Schettino
Mariano Venanzi
Ludovico Valli

Comitato Organizzatore

Ugo Lamanna
Angela Agostiano
Serena Casilli
Lucia Catucci
Fulvio Ciriaco
Pinalysa Cosma
Lucia Curri
Luigi Dimo
Ameriga Fanigliulo
Paola Fini
Alessandra Genga
Gabriele Giancane
Livia Giotta
Disma Mastrogiacomo
Francesco Milano
Massimo Trotta
Ludovico Valli

Segreteria Organizzativa

Luigi Dimo
Gabriele Giancane
Serena Casilli
Natalia Guerra Carbajo

Dipartimento di Ingegneria dell'Innovazione
Università del Salento
Via Monteroni
73100 Lecce
Tel. 0832 297374/ 325

PROGRAMMA DEL CONGRESSO

Domenica 17 Giugno	
16.00 – 20.00	*Registrazione Delegati*
20.30 – on	*Welcome Reception*

Lunedì 18 Giugno	
8.45 – 9.15	*Inaugurazione lavori*
9.15 – 10.00	*Relazione Plenaria* ***Prof. P. Rich*** *(University College, London):* **New methods to study protein chemistry with ATR infrared spectroscopy**
10.00 - 10.20	***Bocchinfuso Gianfranco*** *(Università di Roma "Tor Vergata"):* **A polysaccharide forming nanochannels in the hydrogel phase: study of static and dynamic effects induced by a soft-confinement**
10.20 – 10.40	***Cannistraro Salvatore*** *(Università della Tuscia):* **Yeast Cytochrome c molecules immobilized on carbon nanotubes: A Conductive Atomic Force Microscopy characterization at the single molecule level**
10.40 – 11.00	***Carlotti Benedetta*** *(Università di Perugia):* **AFM force curve investigation of DNA elasticity**
11.00 – 11.30	*Coffee Break*
11.30 – 11.50	***Mavelli Fabio*** *(Università di Bari):* **Stochastic simulations of proto-cell dynamics**
11.50 – 12.10	***Moncelli Maria Rosa*** *(Università di Firenze):* **ATPasi di tipo P in modelli di membrane biologiche: studio delle proprietà funzionali**
12.10 - 12.30	***Satriano Cristina*** *(Università di Catania):* **Physico-chemical aspects of peptide adsorption onto hydrophilic and hydrophobic substrates**
12.30 – 12.50	***Scipioni Anita*** *(Università di Roma "La Sapienza"):* **Structural analysis of 30 nm chromatin fiber architecture**
12.50 – 13.10	***Narducci Dario*** *(Università di Milano Bicocca):* **Bioinspired Chemical Sensing: Molecular Recognition of Gaseous Species at Nanostructured Surfaces**
15.00 – 17.00	***Sessione Poster***
17.00 – 17.30	*Coffee Break*
17.30 – 18.45	***Rassegna critica di Poster sezione "Chimica Fisica dei Materiali" Breve presentazione di poster selezionati***

Martedì 19 Giugno	
9.00 – 9.45	*Relazione Plenaria* ***Prof. M. Becucci*** *(Università di Firenze):* **Struttura e reattività di molecole isolate e clusters**
9.45 - 10.05	***Cimino Paola*** *(Università di Salerno):* **Calculation of EPR parameters in solution by a recent integrated computational approach**
10.05 – 10.25	***De Filpo Giovanni*** *(Università della Calabria):* **Flexible nano-photo-electrochromic film**
10.25 – 10.45	***Ferrante Camilla*** *(Università di Padova):* **Role of excitonic interactions on the nonlinear absorption spectra of porphyrin J-aggregates**
10.45 – 11.15	*Coffee Break*
11.15 – 11.35	***Melandri Sonia*** *(Università di Bologna):* **Importance of the hydrogen bond in tautomeric equilibria and in molecular complex formation. Rotational spectroscopy in supersonic expansions**
11.35 – 11.55	***Morresi Assunta*** *(Università di Perugia):* **Trehalose and glucose dynamics by low-frequency scattering techniques**
11.55 - 12.15	***Selli Elena*** *(Università di Milano):* **Photocatalytic activity of surface fluorinated and/or Au-modified titanium dioxide**
12.15 – 12.35	***Scaranto Jessica*** *(Università di Venezia):* **Study on the adsorbate-substrate interaction between halogenated ethenes and TiO_2: IR spectroscopy and quantum-mechanical calculations**
15.00 – 16.00	***Sessione Poster***
16.00 – 17.15	***Rassegna critica di Poster per la sezione "Colloidi ed Interfasi"*** ***Breve presentazione di poster selezionati***
17.15 – 17.45	*Coffee Break*
17.45 – 19.00	***Rassegna critica di Poster per la sezione "Spettroscopia e Fotochimica"*** ***Breve presentazione di poster selezionati***

Mercoledì 20 Giugno	
9.00 – 9.45	*Relazione Plenaria* ***Prof. G. Ruocco*** *(Università di Roma "La Sapienza"):* **Aging and flow in a colloidal suspension**
9.45 - 10.05	***Caminati Gabriella*** *(Università di Firenze):* **Addressable DNA architectures anchored to Supported Lipid Bilayers**
10.05 – 10.25	***Caracciolo Giulio*** *(Università di Roma "La Sapienza"):* **Structural Stability Against Disintegration by Anionic Lipids Rationalizes the Efficiency of Cationic Liposome/DNA Complexes**
10.25 – 10.45	***Lazzara Giuseppe*** *(Università di Palermo):* **Aggregation of triblock copolymers in water induced by chlorinated oils**
10.45 – 11.15	*Coffee Break*
11.15 – 11.35	***Marini Alberto*** *(Scuola Normale Superiore di Pisa):* **Orientational order properties of nematic and smectic B phases of fluorinated liquid crystals by means of ^{13}C NMR, optical and dielectric studies**
11.35 – 11.55	***Peddis Davide*** *(Università di Cagliari):* **Magnetic properties of ultra-small nanoparticles: beyond the influence of particles size**
11.55 - 12.15	***Ricchiardi Gabriele*** *(Università di Torino):* **Computational and spectroscopic screening of microporous materials for molecular hydrogen storage**
12.15 – 12.35	***Striccoli Marinella*** *(CNR-IPCF, Bari):* **Luminescent Nanocrystals in PMMA Based Co-polymers: Novel Nanocomposite Materials for Nano Imprint Lithography**
15.00 – 16.15	***Rassegna critica di Poster per la sezione "Chimica Fisica Biologica ed Ambientale"*** ***Breve presentazione di poster selezionati***
17.00	***Gita e Cena Sociale***

Giovedì 21 Giugno	
9.00 – 9.45	*Relazione Plenaria* ***Prof. D. M. Guldi*** *(Università di Erlangen):* **Carbon Based Electron Donor Acceptor Hybrids for Solar Energy Conversion**
9.45 – 10.05	***Bee Antonio*** *(Costruzioni Solari):* **Stato dell'Arte e Potenzialità del Solare Termico**
10.05 – 10.25	***Binetti Simona*** *(Università di Milano "Bicocca"* **Role of defects and defect interactions on the photovoltaic properties of solar grade silicon*)***
10.25 – 10.45	***Torsi Luisa*** *(Università di Bari):* **Chiral recognition with enhanced sensing organic thin-film transistors**
10.45 – 11.15	*Coffee Break*
11.15 – 11.35	***Bisio Chiara*** *(Università del Piemonte Orientale):* **Structural and physico-chemical studies of innovative layered Al-modified magadiite materials**
11.35 – 11.55	***Latterini Loredana*** *(Università di Perugia):* **Preparation and optical properties of metal nanostructures**
11.55 - 12.15	***Manzoli Maela*** *(Università di Torino):* **Characterisation of highly dispersed gold on ZrO_2 catalysts active in the WGS reaction**
12.15 – 12.35	***Massarotti Vincenzo*** *(Università di Pavia):* **Sostituzione cationica e proprietà in "bronzi di tungsteno"**
12.35 – 12.55	***Bystrenova Eva*** *(ISMN-CNR Bologna):* **Growth of neural cells on ultra thin organic semiconductors**
15.00 – 16.15	***Rassegna critica di Poster per la sezione "Chimica Fisica Teorica e Computazionale"*** ***Breve presentazione di poster selezionati***
16.15 – 16.45	*Coffee Break*
16.45 – 18.15	*Tavola Rotonda*
18.15 – 19.45	***Assemblea Divisione***

Venerdì 22 Giugno	
9.00 – 9.45	*Relazione Plenaria* ***Prof.ssa N. Rega*** *(Università di Napoli):* **Ab-initio molecular dynamics of solute-solvent systems based on non periodic boundary conditions: applications to spectroscopic properties**
9.45 - 10.05	***Tabacchi Gloria*** *(Universita' degli Studi dell'Insubria):* **On the active role of substrate reactivity in the context of enzymatic dehydrogenations: a theoretical investigation**
10.05 – 10.25	***Puzzarini Cristina*** *(Università di Bologna):* **Vibrational Corrections to Dipolar Coupling Constants: an Alternative for Determining Equilibrium Distances from Rotational Spectroscopy**
10.25 – 10.45	***Di Pietro Elisa*** *(Università di Firenze):* **Reazione di idrolisi della molecola di diborano in soluzione tramite simulazioni di dinamica molecolare ab initio**
10.45 – 11.15	*Coffee Break*
11.15 – 11.35	***Monaco Guglielmo*** *(Università di Salerno):* **From paratropic ring currents to closed-shell molecular magnets**
11.35 – 11.55	***Pavone Michele*** *(Università di Napoli "Federico II"):* **DFT-D study of the benzene dimer: structural minima, energies and molecular dynamics**
11.55 - 12.15	***Santoro Fabrizio*** *(IPCF – CNR, Pisa):* **Dynamics of the Photodeactivation processes in DNA nucleobases**
12.15 – 12.35	***Manca Gabriele*** *(Università di Pisa):* **A combined approach of theory and experiment for the study of platinum clusters derivatives**
12.35 – 12.55	***Pedone Alfonso*** *(Università di Modena e Reggio Emilia)* **Insight into Elastic Properties of binary alkali silicate glasses: prediction and Interpretation through atomistic simulation techniques**
12.55 – 13.15	***Cerimonia di chiusura***

ELENCO POSTER DELLA SEZIONE
CHIMICA FISICA BIOLOGICA ED AMBIENTALE

P1.1 Nuclear Magnetic Resonance of ^{129}Xe and ^{1}H: structural characterization of hydrophobic cavities of Myoglobins.
Roberto Anedda, Benedetta Era, Antonella Fais, Matteo Ceccarelli, Marcella Corda, Mariano Casu and Paolo Ruggerone

P1.2 Application of ISORROPIA and SOAP modules within CAMx model for PM simulation.
Elena Chianese, Guido Barone, Angelo Riccio

P1.3 An Application of OSAT Probing Tool in Southern Italy.
Elena Chianese, Alessia Riccio, Guido Barone, Angelo Riccio

P1.4 PM Indoor Pollution Reduction by TiO_2 Films.
Elena Chianese, Giuseppina Pironti, Guido Barone, Angelo Riccio

P1.5 Il metano ed il futuro del clima.
Elena Chianese, Guido Barone, Angelo Riccio

P1.6 Conformational stability of a thermostable phosphotriesterase from the archaeon *Sulfolobus solfataricus* (SsoPox)
P. Del Vecchio, P. Carullo, G. Barone, L. Merone, M. Rossi, G. Manco

P1.7 Mn^{2+} in marmi bianchi antichi. Determinazione della cava con spettroscopia EPR tramite parametri magnetici
Alfonso Zoleo and Marina Brustolon

P1.8 Osservazione diretta dell'effetto dell'associazione con la base complementare sul potenziale di ossidazione di guanosina e adenosina
Amedeo Capobianco, Tonino Caruso, Andrea Peluso

P1.9 Spectroscopic study of ochratoxin A and its interaction with cyclodextrins
R. Verrone, L. Catucci, P. Fini, P. Cosma, A. Agostiano, V. Lippolis, M. Pascale

P1.10 Activity of photosynthetic membrane proteins of *Rhodobacter sphaeroides*: a possible role of cardiolipin
Vincenzo De Leo, Lucia Catucci, Francesco Milano, Angela Corcelli, Angela Agostiano

P1.11 Photosystem II thermal stability and pigment photobleaching: Effect of membrane lipids
Andrea Ventrella, Lucia Catucci, Giuseppe Mascolo, Angela Corcelli, Angela Agostano

P1.12 Studio sul metabolismo dell'arsenico attraverso spettroscopia NMR *in vivo*.
Marianna Aggravi, Claudia Bonechi, Claudio Rossi, Nadia Marchettini, Enzo Tiezzi, Alessandro Donati

P1.13 Investigation of Self-Assembling Ionic Peptides
M. Alderighi, C. Duce, S. Monti, R. Solaro, M.R. Tiné

P1.14 Use of Cyclodextrins to Improve the Photostability of RB in Aqueous Solutions
P. Fini, A.E. Di Mauro, S. Rochira, P. Cosma, L. Catucci, M. Castagnolo, A. Agostiano

P1.15 Studio del meccanismo di degrado di vetri antichi rinvenuti nel parco archeologico di Siponto (Foggia)
A. Genga, M. Siciliano, L. Famà, D. Manno, T. Siciliano, A. Mangone, A. Traini, C. Laganara

P1.16 Uno studio combinato spettroscopico-teorico della struttura dell'ottasilicato di sodio RUB18
M. F. Iozzi, M. Cossi, C. Bisio, T. R. Macedo, L. Marchese

P1.17 Influence Of Crowded/Confined Environments On Dynamics Of Amyloidogenic Protein Self-Assenbling
A. N. Lazar, E Bystrenova, C. Dionigi, P. Greco, S. Dutta, P. Stoliar, M.G. Cacace and F. Biscarini

P1.18 Studio strutturale del processo di "unfolding" dell'albumina umana
Claudia Leggio, Luciano Galantini, Nicolae Viorel Pavel

P1.19 Stabilità termodinamica del multimero del telomero umano ed energetica dell'interazione con la porfirina cationica

Luigi Petraccone, Luigi Martino, Bruno Pagano, Guido Barone, Concetta Giancola

P1.20 ATPasi di tipo P in modelli di membrane biologiche: studio delle proprietà funzionali
M.R. Moncelli, G. Bartolommei, F. Tadini-Buoninsegni

P1.21 Direct micelles as microreactors for the tuning of cobalt ferrite nanoparticle sizes
A. Ardu, C. Cannas, A. Musinu, D. Peddis, G.Piccaluga, D. Gatteschi, C. Sangregorio

P1.22 Analisi termodinamica dell'interazione tra ligandi e quadruple eliche del DNA telomerico umano
Bruno Pagano, Antonio Randazzo, Gary N. Parkinson, Carlo A. Mattia, Concetta Giancola

P1.23 Sintesi stereoselettiva di 1,2,3-triaril aziridine e risoluzione strutturale via H^1-NMR di derivati con Pt(II)
E. Pindinelli, M. Fabio, L. Troisi

P1.24 Evidence for different routes of oxidation in the laccase-mediator system: a multifrequency EPR and DFT study.
R. Pogni, B. Brogioni, A. Sinicropi, M. C. Baratto, P. Giardina, G. Sannia, R. Basosi

P1.25 Membrane insertion and bilayer perturbation by antimicrobial peptide
Sara Pistolesi, Jimmy B. Feix, Rebecca Pogni

P1.26 The Fluorescence of Tryptophan in Monellin and Parvalbumin Resolved at the ab initio Multiconfigurational Perturbation Theory Level
Adalgisa Sinicropi, Sara Pistolesi, Rebecca Pogni, Riccardo Basosi, Massimo Olivucci

P1.27 Monitoring of the aggregation behaviour of a catalytic protein targeted by anticancer drugs through analysis of its intrinsic fluorescence
Stefania Ferrari, Maria Paola Costi, Monica Caselli, Glauco Ponterini

P1.28 Multicomponent cationic liposome/DNA complexes: efficient vectors for gene delivery
G. Caracciolo, D. Pozzi, R. Caminiti, C. Marchini, M. Montani, A. Amici, H. Amenitsch

P1.29 Aspetti dinamici su scala macroscpopica derivanti da organizzazione mesoscopica
Grazia Biosa, Marcus Hauser, Sandra Ristori, Eugenio Simoncini, Enzo Tiezzi e Mauro Rustici

P1.30 Superstructural Organization of a G-Quadruplex Forming Homopuryne-Homopyrimidine Tract belonging to the Human Telomerase Reverse Transcriptase (H-Tert) Gene Promoter.
Maria Savino, Sabrina Pisano, Michela Varra, Emanuela Micheli, Teresa Coppola, Luciano Mayol, Pasquale De Santis

P1.31 Analisi Emergetica dell'impatto ambientale delle faggete cedue lombarde
Alberto Schiraldi, Thomas Epis

P1.32 Scuola Nazionale Di Metodologie Chimico Fisiche Per Lo Studio Dei Sistemi Biologici
Alberto Schiraldi

P1.33 Peptides with regular enantiomeric sequences as self-assembling nanotubes for nanotechnology.
A. Scipioni, S. Morosetti, P. De Santis

P1.34 Isotopic effect on the kinetics of the Belousov-Zhabotinsky reaction: Cerium-Malonic subsystem.
Simoncini E., Rossi F., Rustici M., Marchettini N.

P1.35 Theoretical Studies on the Structure of Polycyclic Aromatic Hydrocarbons (PAHs) and Soot Platelets and Their Oxidative Functionalization
Anna Giordana, Andrea Maranzana, Giovanni Ghigo, Mauro Causà, G. Tonachini

P1.36 Vapor pressures, sublimation and vaporization enthalpies using isothermal and non-isothermal thermogravimetry
S. Vecchio

P1.37 Vaporization study of acetaminophen and three of its derivatives using isothermal and non-isothermal thermogravimetry
V. Rossi, M. Tomassetti, S. Vecchio

P1.38 Monitoring peptide folding by Time-Resolved Spectroscopies: the effect of a single Gly to Aib susbtitution
Mariano Venanzi, Emanuela Gatto, Gianfranco Bocchinfuso, Antonio Palleschi, Lorenzo Stella, Chiara Baldini, Fernando Formaggio, Claudio Toniolo, Basilio Pispisa

P1.39 Antimicrobial peptides chelating lanthanide ions: the case of Trichogin GAIV analogs and Terbium(III)
Mariano Venanzi, Emanuela Gatto, Lorenzo Stella, Gianfranco Bocchinfuso, Antonio Palleschi, Fernando Formaggio, Claudio Toniolo

P1.40 Effect of aggregation and membrane-water partition on peptide antimicrobial activity: a lesson learned from spectroscopic studies.
L. Stella, C. Mazzuca, G. Bocchinfuso, F. Formaggio, E. Gatto, K. S. Hahm, A. Palleschi, B. Pispisa, C. Toniolo, M. Venanzi

P1.41 A novel method for detection of Se-Met inclusion into protein crystals *via* Raman microscopy
Alessandro Vergara, Antonello Merlino, Elio Pizzo, Giuseppe D'Alessio, Lelio Mozzarella

P1.42 Nanovoid-structured TiO_2 encapsulating $(I_2)n$ molecules: a way to tune the photoactivity in the visible region
A. Zecchina, G. Ricchiardi, S. Usseglio, A. Damin, D. Scarano, C. Lamberti, S. Bordiga

P1.43 MeCAL-2: New catalysts for methane combustion
G. A. V. Martins, G. Berlier, M. Strauss, S. Coluccia, L. Marchese, Heloise O. Pastore, A. Scarpa, R. Pirone

P1.44 Pt-Ba/Al_2O_3 LNT catalysts: TRM and FT-IR analysis of the reduction of stored NO_x in different model atmospheres
F. Frola, F. Prinetto, G. Ghiotti, I. Nova, L. Lietti, P. Forzatti

ELENCO POSTER DELLA SEZIONE
SPETTROSCOPIA E FOTOCHIMICA

P2.1 Small, Infrared, Luminescent Type II Semiconductor Nanocrystals for Animal Imaging
Matteo Amelia, Loredana Latterini, Gian Gaetano Aloisi, Fausto Elisei

P2.2 Doped Nanocrystals: Coupling Optical and Magnetic Properties
Matteo Amelia, Loredana Latterini, Gian Gaetano Aloisi, Fausto Elisei

P2.3 Magnetic Resonance investigations on Cultural Heritage materials.
Alfonso Zoleo, Marco Ruzzi, Lorenzo Franco, Daria Confortin, Marina Brustolon

P2.4 The triplet of DCM observed for the first time: a TR-EPR study of the dye inclusion in a KH Phthalate single crystal.
Marina Brustolon, Roberto Zanré, Antonio Barbon, Kristin L. Wustholz, Bart Kahr

P2.5 Laser Ablation-Inductively Coupled Plasma Mass Spectrometry For The Determination Of Heavy Metals In Airborne Pariculate Matter (PM10)
Ameriga Fanigliulo, Giuseppe E. De Benedetto

P2.6 Spectral studies of Nicotinamide and Zinc phthalocyanine complexes
R. Del Sole, M. R. Lazzoi, A. De Luca, G. Vasapollo

P2.7 Studio degli ioni Mg^{2+} e Ca^{2+} in metanolo liquido attraverso dinamica molecolare *ab initio* Car-Parrinello
Cristian Faralli, Marco Pagliai, Gianni Cardini e Vincenzo Schettino

P2.8 Low-frequency Raman scattering from aqueous solutions of carbohydrates
S. Perticaroli, P. Sassi, A. Morresi, M. Paolantoni

P2.9 Competitive photoisomerization pathways of 1,2-diarylethenes and related compounds
G. Bartocci, S. Ciorba, G.Ginocchietti, U. Mazzucato, A. Spalletti

P2.10 FTIR spectroscopy and thermodynamics of hydrogen adsorbed in a cross-linked polymer
Olena Zavorotynska, Giuseppe Spoto, Jenny Vitillo, Alessandro Damin, Francesca Bonino, Adriano Zecchina

P2.11 Quinol re-oxidation in the Reaction Center photocycle in vitro
Nicola De Nicolò, Péter Maróti, László Nagy, Massimo Trotta, Francesco Milano, Angela Agostiano.

P2.12 Studio di processi di binding a carico di cellule batteriche mediante spettroscopia ATR-FTIR differenziale
Livia Giotta, Disma Mastrogiacomo, Francesca Italiano, Angela Agostiano, Francesco Milano, Massimo Trotta

P2.13 Does the lipid environment influence the spectral and kinetic properties of semiquinones in bacterial photosynthetic reaction centres?
F. Milano, E. Altamura, A. Agostiano, L. Giotta, L. Nagy, P. Maroti, M. Trotta

P2.14 The hydrophobic chain length of phospholipids influences the functioning of photosynthetic Reaction Centres reconstituted in proteoliposomes.
M. Trotta, F. Milano, N. De Nicolò, L. Giotta, L. Nagy, P. Maroti, A. Agostiano

P2.15 New Sol-Gel Hybrid Materials for High Energy Applications in Nonlinear Optics
I.Fortunati; R.Signorini; R.Bozio; G.Brusatin; M.Guglielmi; S.Dirè

ELENCO POSTER DELLA SEZIONE
COLLOIDI ED INTERFASI

P3.1 Thermal Analysis Characterization of Some Cationic Liposomes
Bonicelli M. G., Giansanti L., Mancini G., Pascale F.

P3.2 Effect of dopant (Nd, Er, Eu and Ce) amount on yttrium aluminum garnet nanoparticles structure
Eugenio Caponetti, Delia Chillura Martino, Maria Luisa Saladino, Stefano Enzo, Giulio Ibba

P3.3 Studio strutturale di polimeri supramolecolari host-guest
Luciano Galantini, Claudia Leggio, Nicolae Viorel Pavel, Massimiliano Anselmi, Alfredo Di Nola, Aida Jover, Francisco Meijide, Victor Hugo Soto Tellini, José Vázquez Tato

P3.4 Physico-Chemical and Structural Properties of hydrogels formed by Chitosan, in the Presence and Absence of Poly(vinylpyrrolidone) and Sodium decylsulfate
Gaetano Mangiapia , Luigi Paduano, Henrich Frielinghaus, Gerardino D'Errico, Ornella Ortona, Roberto Sartorio

P3.5 Self-assembly of starch stabilized Ag nanocrystals into ribbon-like and globular agglomerate structures for biosensors application.
A. Serra, D. Manno, E. Filippo, T. Siciliano, A. Tepore

P3.6 Kinetics of Gelation of Aqueous Laponite Dispersions in the Presence of Tri-block Copolymers and their Homopolymers. Rheological and Dynamic Light Scattering Studies
R. De Lisi, M. Gradzielski, G. Lazzara, S. Milioto and N. Muratore

P3.7 The aggregative behavior of hydrophobically modified chitosans of 10% level substitution
Ornella Ortona, G. D'Errico, G. Mangiapia, L. Paduano

P3.8 Modeling of H_2 adsorption and spectroscopic observation of the ortho-para conversion on the ETS-10 titanosilicate
G. Ricchiardi, J. G. Vitillo, D. Cocina, G. Spoto, A. Zecchina

P3.9 Structure and nuclearity of active sites in Fe-zeolites: comparison with iron sites in enzymes and homogeneous catalysts
Gabriele Ricchiardi, Mickaël Rivallan, Gloria Berlier, Carlo Lamberti, Adriano Zecchina

P3.10 FT-IR Study of the State of Iron(III) Chloride Clusters Confined in AOT Reverse Micelles
V. Turco Liveri, R. Biancheri, L. Ceraulo, S. Fanara, C. Giordano, A. Ruggirello

P3.11 Investigation of the adsorption of PEG1500-12-acyloxystearate surfactants into phospholipids bilayers: An Ellipsometry and Cryo-TEM study.
Mauro Vaccaro, Christian von Corswant, Olle Söderman

P3.12 Characterisation of new gold catalysts supported on mixed ceria-titania oxides for the water-gas shift and preferential CO oxidation reactions
Floriana Vindigni, Maela Manzoli, Anna Chiorino, Tatyana Tabakova, Vasko Idakiev, Flora Boccuzzi

P3.13 Gas-phase photocatalytic reduction of NO_x onto immobilized colloidal TiO_2 nanocrystals: a preliminary study
P. Ielpo, G. Lasorella, R. Comparelli, A. Panniello, M. Striccoli, M. Caselli, A. Agostiano, M. L. Curri

ELENCO POSTER PER LA SEZIONE
CHIMICA FISICA DEI MATERIALI

P4.1 Nuclear Magnetic Resonance of ^{129}Xe used as a probe for the characterization of void space in crystalline microporous dipeptides: thermodynamics and molecular details of sorption.
Roberto Anedda, Dmitriy V. Soldatov, Igor L. Moudrakovski, Mariano Casu, John A. Ripmeester

P4.2 SiO_x and SiN_x layers with improved barrier effect and tribological properties
E. Angelini, R. d'Agostino, S. Grassini, F. Palumbo, F. Rosalbino

P4.3 Synthesis and characterization of hybrid organic/inorganic mesoporous photoactive nanoparticles
Bertolino, C.A., Caputo, G., Gianotti, E.

P4.4 Thermal Analysis Characterization of Some Processes Related to Disproportionation of Stannous Oxide
Bonicelli M. G., Ceccaroni G., Gauzzi F, Mariano G.

P4.5 Surface Chemistry Effects on the Early Growth Stages of Pentacene Films from a Soluble Precursor on Silicon-Based Materials
C. Musumeci, C. Cascio, A. Scandurra, G.F. Indelli, C. Bongiorno, S. Ravesi, B. Pignataro

P4.6 New advances in the high temperature decomposition of H_2SO_4
S. Brutti, L. Bencivenni, V. Barbarossa, G. De Maria

P4.7 Lithium Order-Disorder in Superionic LLTO: Theory and Experiment
M. Catti

P4.8 Tuning of chemical and physical properties of Poly(methyl metacrylate)- TiO_2 nanocrystals based nanocomposites for sensing applications
A. Convertino, G. Leo, M. Striccoli, M. Tamborra, C. Sciancalepore, M. L. Curri

P4.9 A computational multiscale approach to the modelling of 45S5 Bioglass®
M. Corno, A. Pedone, B. Civalleri, M.C. Menziani, P. Ugliengo

P4.10 Structural and chemical properties of the hydroxyapatite surface. A computational *ab initio* and a microcalorimetric/IR spectroscopic characterization
M. Corno, L. Bertinetti, V. Bolis, C. Busco, G. Martra, P. Ugliengo

P4.11 Tailored functionalization of luminescent colloidal nanocrystals for selective 2/3D assembly
M.Corricelli, R. Comparelli, N. Depalo, M. Striccoli, V. Saadhu, J. Huskens, M.L. Curri

P4.12 Physical properties of the magnetic superconductor Ru – 1222 obtained from Ru–1212 and $Ce_{0.6}Gd_{0.4}O_{1.8}$ powders
G. A. Costa, C. Artini, M. M. Carnasciali, R. Masini, A. Ubaldini

P4.13 Fluorination of TiO_2: effects on surface hydroxyl groups and photoreactivity
M.G. Faga, M. Minella, V. Maurino, G. Martra, C. Minero, E. Pelizzetti, S. Coluccia

P4.14 Transient Absorption properties of the monomer and dimer of TTF radical cation
Eleonora Garbin, Elisabetta Collini, Camilla Ferrante, Renato Bozio

P4.15 Squaraine dyes as powerful nonlinear absorbers in the NIR region
Elisabetta Collini, Ilaria Fortunati, Luca Ciaffoni, Camilla Ferrante, Renato Bozio, Luca Beverina, Alessandro Abbotto, Giorgio A. Pagani

P4.16 TPA Absorption properties of octupolar metal complexes
Simone Mazzucato, Ilaria Fortunati, Sara Scolaro, Michele Zerbetto, Camilla Ferrante, Raffaella Signorini, Danilo Pedron, Renato Bozio, Danika Locatelli, Stefania Righetto, Dominique Roberto, Renato Ugo, Alessandro Abbotto, Graziano Archetti, Luca Beverina, Sergio Ghezzi

P4.17 Effect of Grain Size on The Magnetic Properties of $La_{1-X}Ca_xMnO_3$ Manganites Nanoparticles
C. Castellano, M.R. Cimberle, M. Ferretti, A. Martinelli, R. Masini

P4.18 A multi-frequency EPR study on TiO_2 colloidal nanocrystals: a closer insight on the catalytic activity
M. Fittipaldi, C. Sangregorio, D. Gatteschi, N. Grassi, M. L. Curri, R. Comparelli, M. Striccoli, A. Agostiano

P4.19 Correlation between transport properties and lattice effects in the $NdCoO_3$ based catalysts and sensor materials
G. Flor, C. Tealdi, L. Malavasi, F. Gozzo, G. Chiodelli

P4.20 Challenges In Biocatalysis: Immobilization Of Porcine Pepsin In Mesoporous Silicas
Haresh G. Manyar, Simonetta Tumbiolo, Enrica Gianotti, Salvatore Coluccia, Osamu Terasaki

P4.21 Luminescent nanocrystal modified epoxy photoresist for the fabrication of 3-D high aspect-ratio microstructures
C. Ingrosso, V. Fakhfouri, M. Striccoli, A. Voigt, G. Gruetzner, M. L. Curri, J. Brugger

P4.22 Characterization of nanocrystalline semiconductor/metal phthalocyanine hybrid junctions and applications as photoconverter and sensor devices
C. Ingrosso, P. Cosma, P. Fini, M. L. Curri, G. Giancane, L. Valli, A. Agostiano

P4.23 Modification of UHMWPE processed by laser ion implantation
A. Lorusso, F. Paladini, L. Velardi, D. Margarone, N. Campo, L. Torrisi, V. Nassisi

P4.24 Structure, orientational order and dynamics of HAB by ^{2}H and ^{13}C NMR spectroscopy and DFT calculations
Alberto Marini, Lucia Calucci, Marco Geppi, Carlo Alberto Veracini

P4.25 Surface structure of nanohydroxyapatite: effects on water and protein adsorption
Luca Bertinetti, Raffaella Ceschino, Gabriele Alberto, Daniele Bollati, Gianmario Martra

P4.26 Structural and spectroscopic characterisation of $Mo_{1-x}W_xO_{3-\delta}$ oxides.
S. Morandi, G. Ghiotti, M. C. Paganini, E. Giamello, M. Bini, D. Capsoni, V. Massarotti

P4.27 Redox behaviour of Co species in microporous CoAPO-5: a spectroscopic study
M. Vishnuvarthan, G. Berlier, E. Gianotti, D. Davit, V. Murugesan, S. Coluccia

P4.28 Effect of the substrate type/composition and deposition techniques on the photocatalytic activity of semiconducting nanocrystalline films for environmental applications
A. Panniello, R. Comparelli, D. Diso, A. Licciulli, G. Mascolo, A. S. Franza, M. Striccoli, A. Agostiano, M.L. Curri

P4.29 Silver ions mediated photochemical synthesis of water soluble gold nanoparticles with control over size and morphology
T. Placido, R. Comparelli, P.D. Cozzoli, M. Striccoli, G. Capitani, F. Giannici, M.L. Curri

P4.30 Protein Adsorption on Chemically and Topographically Nanopatterned Polymer Surfaces
C. Satriano, G.M.L. Messina, G. Marletta

P4.31 A quantum-mechanical study on the adsorption of CO on TiO_2: comparison between the Lewis acidity of the rutile (110) and the anatase (101) surfaces.
Jessica Scaranto, Santi Giorgianni

P4.32 Photocatalytic H_2 production from water splitting on one step flame synthesised TiO_2 and Au/TiO_2
Elena Selli, Gian Luca Chiarello, Ilenia Rossetti, Lucio Forni

P4.33 Si nanocrystals obtained in SiO_2 matrix by low energy ion implantation
L. Velardi, A. Lorusso, M. Traversa, P. Prete, V. Nassisi, N. Lovergine

P4.34 New methodology for Brønsted quantification in microporous materials: FTIR and themogravimetry
G. A. V. Martins, G. Berlier, G. Gatti, S. Coluccia, L. Marchese

ELENCO POSTER PER LA SEZIONE
CHIMICA FISICA TEORICA E COMPUTAZIONALE

P5.1 DPD Simulations to investigate polymer nanocomposites morphology
E.Bianchino, S.Piotto, C. Sciancalepore, M. L. Curri, A. Agostiano, M. Striccoli, F.Ciriaco, F.Mavelli

P5.2 Polarizzabilità ed iperpolarizzabilità statiche di semplici molecole: studio degli effetti vibrazionali.
S. Bruzzone, U.T. Lamanna, C. Guidotti, G.P. Arrighini

P5.3 Characterization of a New Candidate as Contrast Agent for Magentic Resonance Molecular Imaging
U. Cosentino, D. Pitea, G. Moro, G.A.A Saracino, L. Cipolla, M. Gregori, F. Nicotra, A. Villa

P5.4 Theoretical and experimental studies of layered alkylamine-aluminophosphates.
M. D'Amore, C.Bisio, G. Talarico, M. Cossi, L. Marchese

P5.5 Sviluppo e applicazione di metodi basati su Orbitali Molecolari Estremamente Localizzati
Michela Ghitti, Alessandro Genoni, Stefano Pieraccini, Maurizio Sironi

P5.6 Potenziali chimici in eccesso in liquidi ionici tramite 1D-RISM
M. Malvaldi, S.Bruzzone, C. Chiappe

P5.7 Synthetic, electrochemical and theoretical investigation of encumbered triangular cluster units
Gabriele Manca, Alberto Albinati, Samantha Bruzzone, Fabrizia Fabrizi de Biani, Carla Guidotti, Piero Leoni, Lorella Marchetti, Swagat K. Mohapatra, Eliseo Ruiz, Piero Zanello

P5.8 Combined X-ray absorption spectroscopy and Molecular Dynamics study of the $Hg2^{+}$ aqua ion.
Giordano Mancini, Nico Sanna, Vincenzo Barone, Paola D'Angelo, Giovanni Chillemi

P5.9 *Ab Initio* calculation and experimental determination of ^{13}C And ^{19}F Chemical Shielding Tensors of some fluorinated toluenes dissolved in a nematic LC mixture
Alberto Marini, Donata Catalano, Benedetta Mennucci, Carlo Alberto Veracini

P5.10 A non conventional molecular dynamics approach for determining interactions in MAPKs protein complexes.
M. C. Menziani, F.Filomia, F. De Rienzo

P5.11 Interpretation of CW-ESR spectroscopy of tempo-palmitate in the 5CB liquid crystal
Antonino Polimeno, Mirco Zerbetto, Paola Cimino

P5.12 Multivariate analysis of glass structures obtainted by molecular dynamics simulations
M. Pota, A. Pedone, G. Malavasi, M. Cocchi, U. Segre, M. C. Menziani

P5.13 Molecular dynamics simulation of carboxy and deoxy murine Neuroglobin
Massimiliano Anselmi, Beatrice Vallone, Maurizio Brunori and Alfredo Di Nola

P5.14 Studio DFT della riduzione catalitica di acetofenone ad 1feniletanolo mediante $[Ru(HPN)(pcym)Cl]^{+}$.
V.Verdolino, R.Cammi, P.Pelagatti, M.Balordi, C.Pelizzi

CONTRIBUTI ORALI

SEZIONE

CHIMICA FISICA BIOLOGICA ED AMBIENTALE

I1

New methods to study protein chemistry with ATR infrared spectroscopy

Prof. Peter Rich
University College London, Glynn Laboratory of Bioenergetics

New techniques that can be used in conjunction with modern attenuated total reflection (ATR) infrared microprisms will be described. These methods allow proteins to be manipulated cyclically between different states whilst simultaneously monitoring both mid-IR and UV/visible/near IR changes, providing increased flexibility in comparison to transmission methods of the types of changes that can be induced in proteins and allowing quantitative measurements of vibrational changes associated with conversion between stable catalytic reaction intermediates, ligand binding and oxidation/reduction. Both hydrophobic and soluble proteins can be analysed and the ability to induce transitions repetitively allows IR difference spectra to be acquired at a signal/noise sufficient to resolve changes due to specific cofactors or amino acids that can often be interpreted at the atomic level by standard IR methods of comparisons with model compounds, by isotope and mutation effects and, increasingly, by *ab initio* simulations. Combination of such analyses with atomic 3D structural models derived from X-ray and NMR studies can lead to a deeper understanding of molecular mechanisms of enzymatic reactions.

O 1.1

A polysaccharide forming nanochannels in the hydrogel phase: study of static and dynamic effects induced by a *soft*-confinement.

Bocchinfuso Gianfranco[a], Mazzuca Claudia[a], Marletta Giovanni[b], Coviello Tommasina[c], Alhaique Franco[c], Palleschi Antonio[a]
[a]*Department of Chemical Sciences and Technologies, University of Rome "Tor Vergata", Via della Ricerca Scientifica, 00133 Rome, Italy, gianfranco.bocchinfuso@uniroma2.it*
[b]*Laboratory for Molecular Surfaces and Nanotechnology, Dipartimento di Scienze Chimiche and CSGI, University of Catania, V.le A. Doria 6, 95125 Catania, Italy.*
[c]*Department of Chemistry and Technology of Biologically Active Compounds, Faculty of Pharmacy, University of Rome "La Sapienza", P.le Aldo Moro 5, 00185 Rome, Italy*

The polysaccharide Scleroglucan (Sclg) has been successfully used for various applications (secondary oil recovery, ceramic glazes, food, paints, cosmetics, etc); from a structural point of view it exhibits a triple helix conformation (triplex) both in aqueous solution and in the solid state. It is known that the Sclg hydrogels are influenced by the presence of borax, in terms of reological and drug release properties[1]. In previous works, we have shown that the presence of borax stabilizes the inter-triplex interactions and that the variation of the induced properties can be fully explained considering that the Sclg triplexes can form nanochannel-like structures[2,3]. Now, the stability of these aggregates has been investigated by means of Molecular Dynamics (MD) simulations and acquiring nanoscopic images by means of AFM techniques. Our simulations indicate that borax stabilizes nanochannel-like structures when at least seven triplexes of polysaccharide are considered (see figure). The simultaneous presence of different Sclg triplexes in a narrow space strongly influences the properties of confined water molecules in a manner similar, under many aspects, to that of water molecules inside 'canonical' nanochannels (e.g. carbon nanotubes). As a consequence, also the conformational properties of flanking regions of Sclg triplexes are influenced.

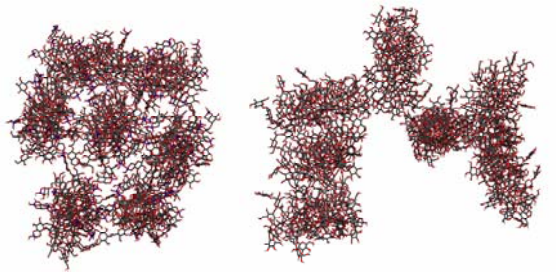

Figure 1: Top view of final structure (5 ns) in the MD simulations of scleroglucan with borax (left) and without borax (right).

Furthermore, Differential Scanning Calorimetry (DSC) data show that the well known conformational transition occurring at 280 K for Sclg does not take place in the presence of borax. The MD simulations show that such lack of transition is a direct consequence of the presence of borax, while the confinement effects of water molecules appear to play a less important role. The role of Na^+ counterions in the hydrogel structure is also investigated.

1. Coviello, T.; Grassi, M.; Palleschi, A.; Bocchinfuso, G.; Coluzzi, G.; Banishoeib, F.; Alhaique, F. *Int. J. Pharm.,* 2005, 289, 97-107. 2. Palleschi, A.; Bocchinfuso, G.; Coviello, T.; Alhaique, F. *Carbohydr. Res.,* **2005**, 340, 2154-2162. 3. Palleschi, A.; Coviello, T.;Bocchinfuso, G.; Alhaique, F. *Int. J. Pharm.,* **2006** , 322, 13-21.

O 1.2

Yeast Cytochrome c molecules immobilized on carbon nanotubes: A Conductive Atomic Force Microscopy characterization at the single molecule level

Chiara Baldacchini, Laura Andolfi, Salvatore Cannistraro
BIOPHYSICS & NANOSCIENCE CENTRE, CNISM, Università della Tuscia, P.le dell'Università, 01100 VITERBO, Italy.E-mail: cannistr@unitus.it.

The integration between metalloproteins and single-walled carbon nanotubes (SWNTs) is an active field of research, with the goal of optimizing electronic signal transduction in advanced and highly sensitive nano-biosensors. A crucial role is played by the immobilization strategy of proteins on SWNTs, because it determines the molecular orientation, which may influence the conduction properties. It is known that metalloproteins adsorbed on SWNTs *via* amide bonds preserve their redox functionality [1], but any characterization of the single molecule conduction is still missing. To this aim, Conductive Atomic Force Microscopy (C-AFM) is the appropriate tool, since it can couple imaging at the single molecule level of redox proteins with the investigation of their conduction properties [2].

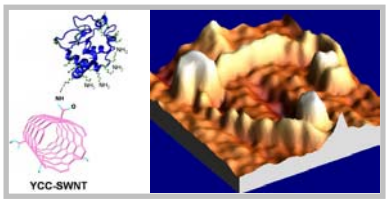

Fig. 1

We functionalized SWNTs with Yeast Cytochrome c (YCC) molecules *via* amide bonds, as shown on the left of Fig. 1. A representative 3D Tapping-Mode AFM image of a functionalized SWNT on a gold surface is shown on the right of Fig. 1. By means of C-AFM, simultaneous topography and current images are obtained (the current image of a functionalized SWNT is shown in Fig. 2, left panel). By positioning the C-AFM tip on top of a functionalized SWNT, we can record, as a function of the applied bias (I/V), the current flowing between tip and metal substrate, *i.e.* through both the SWNT and the adsorbed protein. Series of I/V curves have been recorded as a function of the applied force load (a representative set is shown in the central panel of Fig. 2). The current present a typical increasing-decreasing behaviour as a function of the applied force, indicative of the presence of SWNTs (the current recorded through YCC molecules adsorbed on bare gold surfaces always increases with the applied force, until the protein break [3]). Moreover, by using SWNTs as spacers between redox proteins and metal surfaces, at low applied bias, lower applied forces are needed to record higher currents, with respect to proteins directly assembled on gold surfaces (see Fig. 2, right panel).

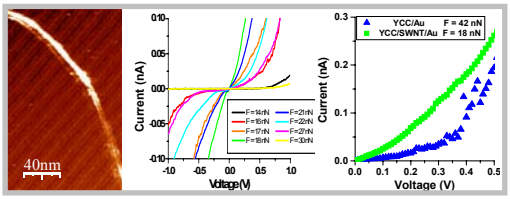

Fig. 2

As a future perspective, we will investigate the role played by the protein-SWNT interaction in the transport mechanism, by comparing the conductive behaviour of YCC molecules as a function of the immobilization strategy on the SWNT sidewalls.

1. Gooding, J. J.; Wibowo, R.; Liu, J.; Yang, W.; Losic, D.; Orbons, S.; Mearns, F. J.; Shapter, J. C.; Hibbert, D. B.; *Journal of the American Chemical Society*, **2003**, 125, 9006 - 9007. 2. Andolfi, L.; Cannistraro, S.; *Surface Science*, **2005**, 598, 68 – 77. 3. Delfino, I.; Bonanni, B.; Andolfi, L.; Baldacchini, C.; Bizzarri, A. R.; Cannistraro, S.; *Journal of Physics:Condensed Matter,* **2007**, 19, 225009 – 225027.

O 1.3

AFM force curve investigation of DNA elasticity

Benedetta Carlotti[a], Fausto Elisei[a], Loredana Latterini[a], Lawrence A. Bottomley[b], Nicholas V. Hud[b], Catherine T. Santai[b].

[a]*Dipartimento di Chimica and Centro di Eccellenza per i Materiali Innovativi Nanostrutturati-Universita' degli Studi di Perugia, Via Elce di Sotto n.8, 06123 Perugia, carlotti@unipg.it*

[b]*School of Chemistry and Biochemistry-Georgia Institute of Technology, 311 Ferst Drive, N.W., 30332-0100 Atlanta, GA, USA*

Atomic force microscopy is a useful tool for determining the mechanical properties of single biomolecules. Our efforts are devoted to correlating the mechanical properties with nucleotide sequence and orientation. Biotinylated oligos are covalently immobilized onto a tip array; streptavidin is covalently attached to a tipless cantilever. When the cantilever makes contact with the tip, biotin-streptavidin conjugation establishes contact at a known position on the oligomer. Retraction of the scanner results in controlled stretching of the nucleic acid and mechanical unfolding of streptavidin. The latter occurs at loads less than that required to pull the nucleic acid off the tip.

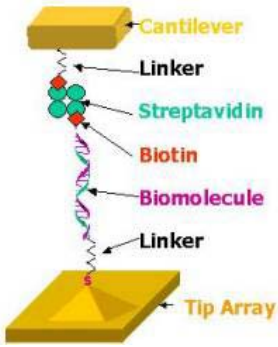

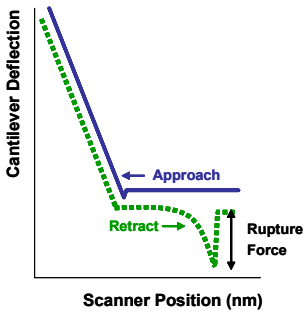

Rapid refolding of streptavidin enables replicate measurements on the same oligo. This strategy provides a rapid and reliable method for analysis of the mechanical properties of these biomolecules that is free of the artifacts and assumptions implicit in data acquisition and interpretation found with conventional methods. The DNA stretching event is studied throughout the acquisition of force-distance curves. Cantilever deflection is monitored as the tip and the beam are brought into contact (biotin-streptavidin conjunction occurs) and subsequently separated. Upon retraction the biomolecule is stretched and the force is recorded by the deflection on the cantilever. The use of a tip array-tipless beam set up instead of the common tip-substrate enables us to explore several tips during the same experiment and to look for the single molecule tips (there may be tips that have no molecules or multiple molecules as well, but we are only interested in the single molecule pulling events).

Lebrun and Lavery[1] have predicted that the stretching of DNA will differ markedly with its orientation. To test this prediction, we have constructed three oligos of exactly the same sequence, biotinylated at either the 5' or 3' terminus and possessing an amino anchoring moiety at the other terminus, (i.e. 5'-5', 3'-3' modified oligos). Each was subjected to AFM-based stretching. The resultant force curves were statistically analyzed and compared with theory . In this presentation, we critically examine our experimental approach and findings in light of the prediction.

1. Lebrun, A.; Lavery, R.; *Nucleic Acids Research*, **1996**, *24(12)*, 2260 – 2267.

O 1.4

Stochastic simulations of proto-cell dynamics.

F.Mavelli[a], K.Ruiz-Mirazo[b], F.Ciriaco[a], U.T.Lamanna[a]

[a] *Chemistry Department, University of Bari, Via Orabona 4 – 70125 Bari*
[b] *Biophysics Research Unit (CSIC-UPV/EHU) University of the Basque Country, Spain*

A computational platform developed to simulate the stochastic time evolution of homogeneous, fixed-volume, chemically reacting systems[i] has been recently extended to apply it to volume-changing, globally heterogeneous, systems[ii]. This improvement made the software 'ENVIRONMENT' suitable for developing and testing realistic proto-cell models and possible explanations for their spontaneous emergence in pre-biotic conditions. In fact, we defend a view[iii] that puts proto-metabolic cellular organization at the core of the problem of the transition to life, in contrast with the mainstream research in the field, which considers the synthesis and properties of biomolecules ('self-replicating' RNA or DNA) as the key point. A much more plausible prebiotic scenario involves the early appearance of compartments[iv] and their 'co-evolution' with reaction networks, so that both get increasingly complex, until the living threshold is eventually achieved. In this framework, lipid membranes can not be considered as mere containers of a set of reactants in relevant concentration levels, but as a supramolecular structure that plays a crucial role in the control of the matter-energy flow through the system, by means of very diverse transport and transduction mechanisms. In order to test and further elaborate our ideas and working hypotheses, as well as their theoretical/experimental implications, we will use the computational approach and the ENVIRONMENT program to simulate the stochastic time behaviour of realistic proto-cellular models, i.e. models that can be tested *in vitro* or that can suggest real lines of experimental research, trying to bridge the traditional gap between theorists and experimentalists.

There are two main lines of research we would like to illustrate in this contribution:
1) First, we will explore how far it is possible to go with cell models that keep a low degree of molecular complexity, i.e. made of relatively simple and, therefore, prebiotically plausible components, like fatty acids, aminoacids and short peptide chains. More concretely, we will tackle the problem of minimal 'lipid-peptide' cells (see Figure 1), already introduced in our recent works[v]. In particular, we will investigate the possibility that molecular transport across the cell membrane mediated by polypeptides channels can be activated/deactivated by the elastic energy of the lipid bilayer and, as a result, function as a primitive mechanism for protocells to regulate their growth and reproduction.
2) Second, we aim to develop a model that addresses more directly the problem of bridging the gap between experimental (*in vitro*) and theoretical (*in silico*) results[ii]. Specifically, we would model the experimental structural and kinetic properties of vesicular aggregates[vi] and address the differences between standard lipid and fatty acid vesicles[vii], including the possible transition from one to the other, since the former are closer to present biomembranes but the latter have higher prebiotic relevance.

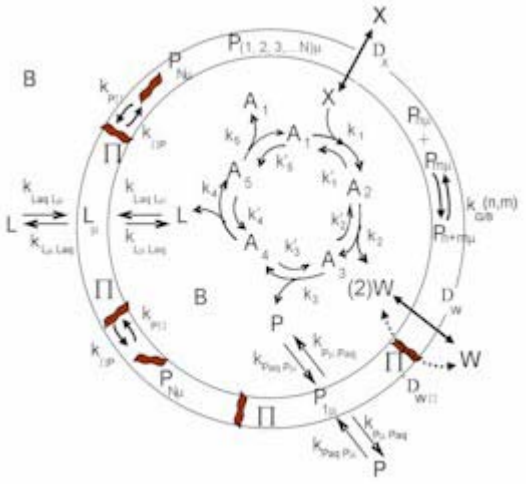

Fig. 1: Schematic draw of the minimal lipid-peptide cell.

[i] Mavelli F.,Piotto S.*J. Mol.Struct*. **2006**, 771 55

[ii] Mavelli F.,Ruiz-Mirazo K., *Phil.Trans.R.Soc.B.* **2007** (in press); *Orig.Life Evol.Biosphere,* **2007** (in press).

[iii] Ruiz-Mirazo K.,Moreno A., *Artificial Life* **2004**, 10(3), 235

[iv] Luisi, P. L., *The Emergence of Life*, **2006** Cambridge University Press, Cambridge

[v] Ruiz-Mirazo K., Mavelli F. *Orig. Life Evol. Biosphere* **2007** (in press); *BioSystems,* **2007,** (accepted).

[vi] Chen, I., Roberts R.W., Szostak J.W., *Science* **2004,** 305, 1474; Chen, I., Szostak J.W., *Biophysical Journal,* **2004,**87**,** 988**.**

[vii] Cheng, Z., Luisi P.L, *J.Phys.Chem.B,* **2003**, 107, 10940; S. Rasi, F. Mavelli, P.L. Luisi,, *J. Phys. Chem. B,* **2003**, 107, 14068; Rasi, S., Mavelli F., Luisi P.L., *Orig.Life Evol.Biosphere,* **2004,** 34, 215

O 1.5

ATPasi di tipo P in modelli di membrane biologiche: studio delle proprietà funzionali

M.R. Moncelli, G. Bartolommei, F. Tadini-Buoninsegni
Dipartimento di Chimica, Università di Firenze, BioElectroLab, via della Lastruccia 3, 50019 Sesto Fiorentino (FI); moncelli@unifi.it

Nel nostro laboratorio si studiano da diversi anni proteine di membrana in modelli sperimentali di membrane biologiche. In modo particolare si studiano ATPasi di tipo P con metodi chimico fisici. Recentemente abbiamo focalizzato la nostra attenzione sullo studio delle interazioni della Ca-ATPasi e della Na,K-ATPasi con alcuni farmaci. Si illustreranno:
- le caratteristiche generali delle ATPasi;
- i metodi di indagine utilizzati: **a)** spettrofluorimetria con sonde stiriliche elettrocromiche e **b)** tecnica per salti di concentrazione su SSM (Solid Supported Membrane)[1,2].

Si presenteranno alcuni risultati:
- interazione della Ca-ATPasi con inibitori a differente affinità (clotrimazolo [3], tapsigargina, acido ciclopiazonico, curcumina);
- interazione della Na,K-ATPasi con clotrimazolo.

1. Tadini-Buoninsegni, F.; Bartolommei, G.; Moncelli, M.R.; Inesi, G.; Guidelli, R.; *Biophys. J.*, **2004**, *86*, 3671-3686. 2. Tadini-Buoninsegni, F.; Bartolommei, G.; Moncelli, M.R.; Guidelli, R.; Inesi, G.; *J. Biol. Chem*., **2006**, *281*, 37720-37727. 3. Bartolommei, G.; Tadini-Buoninsegni, F.; Hua, S.; Moncelli, M.R.; Inesi, G.; Guidelli, R.; *J. Biol. Chem.*, **2006**, *281*, 9547-9551.

O 1.6

Physico-chemical aspects of peptide adsorption onto hydrophilic and hydrophobic substrates

Cristina Satriano, G.M.L. Messina and Giovanni Marletta
Laboratory for Molecular Surfaces and Nanotechnologies (LAMSUN) - Dept. of Chemical Sciences - University of Catania and CSGI, viale A. Doria 6- 95125 Catania, Italy. csatriano@unict.it

The cell-adhesive peptide sequences PHSRN and RGD were adsorbed onto hydrophobic polysiloxane surfaces (HYB) and the corresponding hydrophilic ones (HYL) obtained by UV-O_3 treatments of the HYB surfaces.
Peptides adsorption kinetics as well as coverage and orientation were investigated by Quartz Crystal Microbalance with Dissipation monitoring (QCM-D) and Atomic Force Microscopy (AFM) measurements.
Two different adsorption mechanisms were observed, consisting in a "Langmuir-like" process, with adsorption/desorption equilibrium of basically random coiled molecules, and a "Lundstrom-like" process, involving the irreversible adsorption probably due to the change in the peptide conformation.
The first process was shown to occur for PHSRN onto HYB substrates and RGD on both HYB and HYL substrates, while the second one occurred only for PHSRN onto HYL surfaces. The biological response of bare and peptide-immobilized surfaces was tested by studying their short term interaction with McCoy fibroblast cells by means of QCM-D and optical microscopy for 2 hours incubation in medium-free solutions.
It turned out that both peptide immobilized-HYL as well as control HYL surfaces exhibited a larger number of adhered and viable cells compared to the HYB ones. Moreover, it was found that only PHSRN-HYL substrates prompt the cell spreading process.
The observed effects have been interpreted in terms of the different adsorption state of immobilized peptides on the various surfaces, depending on the tuning of peptide and surface charges, or the occurrence of preferential PHSRN unfolding processes on the highly polar HYL surfaces.

O 1.7

Structural analysis of 30 nm chromatin fiber architecture.

A. Scipioni[a], S. Morosetti[b], G. Turchetti[b], P. De Santis[b]
[a]*Dipartimento di Chimica, La Sapienza Università di Roma, Piazzale A. Moro, 5, 00185 Roma; anita.scipioni@uniroma1.it*
[b]*Dipartimento di Chimica, La Sapienza Università di Roma, P. le A. Moro5, 00185 Roma, Italy*

Chromatin architecture plays an important role in the regulation of nuclear processes of the eukaryotic genomes. It is the result of complex hierarchic assembly of a nucleosome array in a compact structure.
Although the nucleosome structure is known in its molecular details at near-atomic resolution (1), the most fundamental information about the pattern of the organization of nucleosomes in the chromatin fiber is still debated and not fully clarified.

Compaction of nucleosomes in chromatin *in vivo* depends on their positioning along DNA and therefore on the DNA linkers that bridge and mutually rotate the adjacent nucleosomes in the space. Experimental data reveal the presence of some regularity in which the nucleosome repeat length in chromatin fibers differs of multiple of about 10 bp. This suggests the existence of orientational constraints between the nucleosomes and between nucleosomes and the fiber axis as well. Moreover, experimental evidence indicates that the nucleosome super-helical axis is nearly perpendicular to the fiber axis. Recently, the elucidation of the X-ray crystal structure of a reconstituted nucleosome tetramer array (2) and the more recent proposal of the 30 nm fiber interdigitated structure based on the interpretation of EM and cryo-EM images of multimeric nucleosome arrays (3), suggest two apparently different architectures of chromatin fibers. The two models of chromatin are reported in the figure: A) the single helix model with inter-digitized nucleosomes as proposed by Rhodes and cows (3), B) the two-start helix with straight linkers as suggested by Richmond and cows (2).
The crystal structure of the tetranucleosome shows that linker DNA zigzags back and forth between two stacks of nucleosome cores, which appears to form a truncated two-start helix. This nucleosome organization however appears to be not consistent with the EM experiments that are characterized by a more compact packing of nucleosomes and interpreted with an inter-digitized model (3). Furthermore, the modular increasing of linker lengths by 10 bp results in an apparent transition of nucleosome density along the fiber and radial dimension occurring at multimeric DNA periodicity between 207 and 217 bp.
Therefore, the sequential organization of nucleosomes remains a still controversial question.
A theoretical study of the possible nucleosome packing in the chromatin fiber is proposed. Some general features of the fiber structure emerge. The nucleosome density along the fiber and the orientation of nucleosome helical axis with respect to the local fiber axis strongly discriminate the possible architecture of nucleosome assembly and the path of DNA linkers, under the hypothesis of the minimum distortion of the nucleosome and linker DNA intrinsic structure.
In fact, the packing resulting from the EM visualizations of a nucleosome array in the chromatin 30 nm fibers is mainly dependent on the orientational parameters. Their study however implicitly produces useful suggestions about the structure and mutual arrangement of the linkers. Assuming the X-ray crystal structure for the nucleosome and the dinucleosome as a repeating unit of the chain, the helical parameters of the fiber and the orientation of the nucleosome axis with respect to the fiber axis are obtained in terms of the internal twist of the two linkers connecting adjacent nucleosomes. The results indicate that fixing the orientational parameters strongly restricts the linker length to values that differ by integral turns of double helix. However, the linker lengthening by DNA steps of 10 bp increases twist deviation from integral turns of the canonical B-DNA, which is characterized by a periodicity of 10.4 bp. As a consequence, the conservation of a basic structure stable at lowest linker length results in the increasing of the torsional energy, which can be the driving force of a transition to a different class of structures. This is also due to the progressive relaxing of inter-nucleosome contacts consequent to the increase of the radial dimension of the fiber.
Considering the nucleosome packing as a function of

couples of linkers, which determine the mutual arrangement of three adjacent nucleosomes, permits to analyze all the possible assemblies where the interactions between alternating nucleosomes are determinant in the fiber best packing. In particular, we analyzed the architectures characterized by high nucleosome density as those indicated by EM visualizations ranging between 10 and 15 nucleosome per 11 nm for DNA multimeric repeats from 177 to 237 bp, with a fixed increment of 10 bp.

The conformational map of the angles between the nucleosome helical axis and the chromatin fiber axis shows that the possible structures should lie in those regions where one or both the twist angles correspond to the adjacent nucleosomes in trans with respect to the linker.

In the same angular positions high nucleosome packing density, given as the number of nucleosomes in a helical slice of 11 nm, lies nearby the inversion of fiber chirality through formal planar spires where the helical repeat vanishes.

In a previous paper we tried to analyze the nucleosome packing adopting a rough model, where the nucleosomes were modeled as oblate symmetrical tops with dimensions resembling those of the crystal structure. The best packing was driven using an appropriate Gay-Berne potential for oblate ellipsoids (4). At present, we are refining our model by evaluating the energy map taking into account the interactions between all the DNA phosphate groups adopting a Lennard-Jones potential with the minimum localized at 7 Å so that the nearest-neighbor DNA axes lie at a distance of about 26 Å, as found in DNA fibers. The histone octamer is not considered; as a consequence the energy map represents a necessary but not sufficient condition for localizing the nucleosome best packing. Nevertheless, the obtained results permits to identify a class of architectures that account for the experimental data and suggest interesting and dynamical features of chromatin fibers.

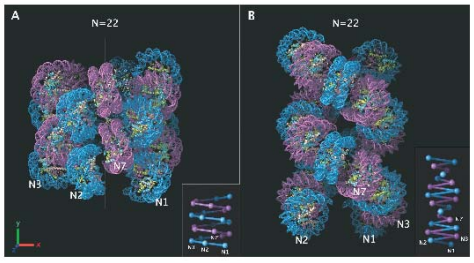

1. Luger, K.; Mäder A. W.; Richmond R. K.; Sargent D. F.; Richmond T. J.; *Nature,* **1997**, *389*, 251-260.
2. Schalch T.; Duda S.; Sargent D. F.; Richmond T. J.; *Nature*, **2005**, *436***,** 138-141.
3. Robinson, P. J. J.; Fairall, L.; Huyhn, V. A. T.; Rhodes, D.**;** *Proc. Natl. Acad. Sci. USA*, **2006**, *103*, 6506-6511.
4. Besker N; Anselmi C; Paparcone R.; Scipioni A.; Savino M.; De Santis P.; *FEBS Lett*., **2003**, *554*, 369-372.

O 1.8

Bioinspired Chemical Sensing: Molecular Recognition of Gaseous Species at Nanostructured Surfaces

Dario Narducci[a], Edoardo Di Vita[a], and Jenni Portman[a]

[a]*CNISM e Dipartimento di Scienza dei Materiali, Università di Milano Bicocca, via R. Cozzi 53, 20125 Milano, dario.narducci@unimib.it*

Chemical sensing has a self-evident relevance to modern robotics. Improvements in the capabilities of detecting chemicals in solution and gas phase has an immediate impact on a variety of fields, such as environmental monitoring, food quality assurance, chemical plant control, and biomedical analyses. However, further to its applications, chemical sensing is also a promising arena where nanotechnology and bioinspired strategies can meet. In this contribution recent advances in the development of a novel class of bioinspired gas sensors will be presented.

An approach based on the use of covalent organic moieties grafted onto single-crystal Si surfaces has been developed in recent years at the University of Milano Bicocca. An organic moiety gets covalently grafted by wet chemistry methods onto a Si surface, and a Metal-Insulator-Semiconductor (MIS) junction is obtained thereof, where the grafted monolayer plays the role of the insulator, and a metal layer is intentionally deposited on top of it as a discontinuous ultrathin film so as to allow gas to diffuse toward the grafted Si surface. Upon molecular recognition of the target gas molecule, the additional dipolar momentum associated to the gas molecule oriented by the interaction with the grafted layers is expected to lead to a modulation of the barrier height at the MIS junction.

To quantitatively verify the detection mechanism, a H-terminated Si(100) surface was hydrosilylated [1-4] with substituted phenylacetylenes using $[HRu(CO)(PPh_3)_3Cl]$ as catalyst. Two types of grafted surfaces were studied, functionalized with either the benzyl ester of 1-vinyl-4-carboxy-benzene or its relevant acid. A lift-off technique was adopted [5] to prevent the damage of the organic monolayer upon metal deposition. Current-voltage characteristics were measured by exposing the MIS device to NH_3 in synthetic air at different temperatures to verify their sensing capabilities and to investigate the pertinent detection mechanism.

An extension of Campbell's model [6] for a grafted Si-based MIS junctions was proposed [7] and systematically compared with the experimental dynamic barrier height modulation in the presence of ammonia. The model was found to be in excellent agreement with the experimental data in the whole range of gas partial pressure considered. The results have a general relevance for sensing devices where the modulation of the barrier heights by molecular units assembled or grafted onto semiconductors. Further patented applications to gas sensing [8] will be briefly outlined.

1. Sudo, T.; Asao, N.; Yamamoto, Y.; *Journal of Organic Chemistry,* **2000**, *65*, 8919 – 8923. 2. Katayama, H.; Taniguchi, K.; Kobayashi, M.; Sagawa, T.; Minami, T.; Ozawa, F.; *Journal of Organometallic Chemistry*, **2002**, 645 (1-2) 192 – 200. 3. Wojtyk, J.T.C.; Morin, K.A.; Boukherroub, R.; Wayner, D.D.M.; *Langmuir*, **2002**, 18, 6081 – 6087. 4. Wu, W.; Li, C.J.; *Chemical Communications*, **2003**, 14, 1668 – 1669. 5. Vilan, A.; Cahen, D.; *Advanced Functional Materials*, **2002**, 12, 795 – 807. 6. Campbell, I.H.; Rubin, S.; Zawodzinski, T.A.; Kress, J.D.; Martin, R.L.; Smith, D.L.; Barashkov, N.N.; Ferraris, J.P.; *Physical Review B*, **1996**, 54, 14321 – 14324. 7. Oldani, M.; Narducci, D.; Taffurelli, A.; *Surface Science*, **2007**, in press. 8. Narducci, D.; *European Patent*, **2006**, PCT/EP2006/001570.

SEZIONE

SPETTROSCOPIA E FOTOCHIMICA

I 2

Struttura e reattività di molecole isolate e clusters

Maurizio Becucci
Dipartimento di Chimica, Università di Firenze, v. Lastruccia 3, 50019, Sesto Fiorentino (FI), maurizio.becucci@unifi.it
LENS, v. Carrara 1, 50019 Sesto Fiorentino (FI)

Lo studio con metodi di spettroscopia laser di specie molecolari (sia molecole isolate che piccoli aggregati molecolari) raffreddati in jet supersonici permette di ottenere moltissime informazioni che riguardano sia la geometria d'equilibrio di questi sistemi che la dinamica di eventuali processi fotochimici.
La prima parte della comunicazione riguarderà la determinazione della struttura di diversi complessi che contengono molecole aromatiche. In particolare ci siamo interessati sia dei dimeri formati da queste molecole che i complessi bimolecolari formati per interazione con acqua, ammoniaca e metanolo. La topologia e la natura dell'interazione cambiano in maniera sostanziale nei diversi sistemi studiati. L'indagine è stata condotta sia per mezzo di spettroscopia elettronica (di ionizzazione multifotonica e LIF ad alta risoluzione in frequenza) che per mezzo di calcoli a diverso livello di teoria.
La seconda parte introdurrà i nuovi risultati che abbiamo ottenuto nel campo della dinamica di reazione chimica con l'uso di tecniche di *ion imaging*.[1] Si tratta di un metodo d'indagine particolarmente efficace nello studio dei processi unimolecolari di fotodissociazione. L'assorbimento di un primo fotone da parte della molecola d'interesse innesca la reazione di dissociazione. I frammenti così prodotti sono ionizzati selettivamente da un secodo fotone. Questi ioni sono poi proiettati su un rivelatore bidimensionale da un sistema di ottiche elettrostatiche. Il punto d'arrivo sul rivelatore è legato alla velocità acquisita dal frammento nella dissociazione. La misura del modulo della velocità dei frammenti e della loro distribuzione angolare ci permette di entrare nel dettaglio del processo reattivo. Come esempio mostreremo uno studio sulla fotodissociazione del N-metilpirrolo per eccitazione a 193 nm in cui si osservano due diversi meccanismi di reazione corrispondenti al distacco di frammenti metile con alta e bassa energia cinetica. La reattività osservata sarà discussa anche alla luce dei risultati pubblicati molto di recente sulla fotodissociazione del pirrolo.[2]

Nel corso di questo lavoro M.B. ha beneficiato di una Marie Curie fellowship (MTKD-CT-2004-BICAL-509761).

1. Bowen, M. S.; Becucci, M.; Continetti, R. E., J. Chem. Phys., **2006**, *125*, 133309. 2. Ashofold, M. N. R.; Cronin, B.; Devine, A. L.; Dixon, R. N.; Nix, M. G. D.; *Science*, **2006**, *312*, 1637.

O 2.1

Calculation of EPR parameters in solution by a recent integrated computational approach

Paola Cimino[&‡], Orlando Crescenzi[&] and Michele Pavone[&]
[&] *Università di Napoli, "Federico II", Complesso Universitario di Monte Sant'Angelo Via Cintia, I-80126 Napoli, Italy.*
[‡] *Permanent Address: Dipartimento di Scienze Farmaceutiche Università di Salerno Via Ponte Don Melillo 84084 Fisciano-Salerno, Italy*

Interpretation of structural properties and dynamic behaviour of molecules in solution is of paramount relevance for a better understanding of their stability, chemical reactivity, catalytic action. Information can be gained, in principle, by a variety of spectroscopic techniques, magnetic as well as optical. In particular, continuous wave electron spin resonance (cw-ESR) measurements are highly informative. However, the wealth of structural and dynamic information which can be extracted from ESR spectroscopy is, at present, limited by the necessity of employing computationally efficient models, which are increasingly complex for the need of taking into account diverse relaxation processes affecting the spectrum.
Here, we present selected examples where the role of stereo-electronic, environmental and short-time dynamic effects in tuning the hyperfine and gyromagnetic tensors of prototypical nitroxide spin probes has been investigated by an integrated computational approach based on molecular dynamics and discrete-continuum solvent models. The methods are based on a high-level DFT approach coupling the PBE0 hybrid functional with a tailored basis set, and with proper account of specific and bulk solvent effects.
The computed magnetic parameters are in satisfactory agreement with the available measured values, and allow for an unbiased evaluation of the role of different effects in tuning the overall EPR observables.

1. M.Pavone; P.Cimino; F. De Angelis; V.Barone;*, J. Am. Chem.Soc*., **2006,** *128*, 4338-4347.
2. M. Pavone; A. Sillampae; P. Cimino; O. Crescenzi; V. Barone, *J. Phys. Chem. B*, **2006,** *110*, 16189-16192.
3. P.Cimino; M.Pavone; V.Barone, *Chem. Phys. Lett*., **2006**, *409*, 106-110.**;**

O 2.2

Flexible nano-photo-electrochromic film

Giovanni De Filpo[a], Fiore P. Nicoletta[b], and Giuseppe Chidichimo
[a]*Dipartimento di Chimica, Università degli Studi della Calabria, 87036 Rende (CS), Italy, defilpo@unical.it*
[b]*Dipartimento di Scienze Farmaceutiche, Università degli Studi della Calabria, 87036 Rende (CS), Italy*

A flexible nano-photo-electrochromic PET-TiO_2-PO_4-Methylene Blue based film was obtained by the deposition of TiO_2 nanoparticles on a PET conductive substrate. A further covalent chemical bond of Methylene Blue (MB) molecules on the TiO_2 film by means of phosphate groups, ensures the photo-electrochromic properties of this device. Indeed, MB

molecules can change color both owing to the irradiation with red light, in the presence of electron donor molecules, and to the oxidation reaction with an oxidizing agent. Since the oxidation reaction of MB molecules occurs at the same electrode where the molecules are anchored, the film shows a very fast coloration time (600 ms).
The thermal stability of the film and the anchoring of MB molecules on TiO_2 nanoparticles was investigated by Differential Scanning Calorimetry (DSC) technique. Morphology of the surface and cross section of TiO_2 layer was studied by Scanning Electron Microscope (SEM). Moreover the device was characterized in terms of light absorption by UV-Visible spectroscopy and optical transmission by an optical line.

O 2.3

Role of excitonic interactions on the nonlinear absorption spectra of porphyrin J-aggregates

Elisabetta Collini, Camilla Ferrante, Renato Bozio
Dipartimento di Scienze Chimiche e UdR INSTM di Padova, Università di Padova, Via Marzolo 1, I-35131 Padova, Italy

Tetrasolphonatophenyl-porphyrin (TPPS) is a water soluble porphyrin capable to form J-type aggregates at pH < 4, when the diacid form is present. Dimension and shape of these aggregates depends on several factors such as: concentration, ionic strength of the solution, and solvent nature. The electronic properties of the TPPS molecule are strongly influenced by the aggregation process, as clearly shown by the linear absorption spectrum.[1]
We will present the two photon absorption (TPA) and the transient absorption (TA) spectra of diacid TPPS in water solution, both as a monomer and in the J-aggregate form. The spectra are measured with ultrashort laser pulses, employing the pump and probe technique. In particular TPA and TA differ for the wavelength employed for the pump pulse, being not resonant for TPA, and resonant for the TA. Therefore TPA is a coherent technique, investigating two photon allowed excited states, while TA investigates the incoherent population of the first excited state, followed by transient absorption towards higher two photon allowed states. The TPA cross section of TPPS in the J-aggregate form is thirty times more intense than in the monomer in the whole spectral range investigated (380-430 nm).[2] Such an enhancement can be exploited to build molecular devices with a high and fast nonlinear response. The TPA spectrum shows also a band at 410 nm, clearly visible in the aggregate spectrum, but apparently lacking in the one of the monomer. The TA spectra should display also a transient band in the NIR region, due to absorption from the Q-state of the TPPS towards the 410 nm state. Because of this, we have mainly investigated the TA of the monomer and J-aggregate in this spectral region and observed a clear TA band for the J-aggregate, while only residual TA and no clear band is present for the monomer. This is the first time, to our knowledge, that a state, falling at energies lower than the lowest two exciton band is observed in the TA spectrum of a molecular aggregate in solution. The nature of this state is discussed on the basis of the excitonic theory for molecular aggregates.

1. *J-Aggregates*; Kobayashi, T., Ed.; World Scientific: Singapore, **1996**.
2. Collini, E; Ferrante, C; Bozio, R; *J. Phys. Chem. B,* **2005, *109 (1),*** 2 -5.

O 2.4

Importance of the hydrogen bond in tautomeric equilibria and in molecular complex formation. Rotational spectroscopy in supersonic expansions

Sonia Melandri[a], Barbara Michela Giuliano[a], Assimo Maris[a], Biagio Velino[b], Laura Favero,[c] Walther Caminati[a]

[a] *Dipartimento di Chimica "G. Ciamician", via Selmi 2, I-40126 Bologna, sonia.melandri@unibo.it*
[b] *Dipartimento di Chimica Fisica e Inorganica dell'Università, Viale Risorgimento 4, I-40136 Bologna, Italy*
[c] *Istituto per lo Studio dei Materiali Nanostrutturati (ISMN, Sezione di Bologna), CNR, via Gobetti 101, I-40129 Bologna, Italy.*

The importance of weak interactions, especially inter and intramolecular hydrogen bonds, is recognized in all areas of chemistry and biology and the understanding of their role is essential to explain and model many phenomena.
In our studies the detailed nature of such interactions is revealed by high resolution spectral data on isolated molecules and molecular complexes observed in free jet expansions. The interpretation of these data is assisted by high level quantum chemical calculations and other models to help justify and rationalize the results.
We report microwave spectroscopy studies on molecules isolated in supersonic expansions: 4-hydroxypyrimidine,[1] methylsalycilate and erythritol, and show the importance of hydrogen bond formation on the shape of the tautomeric and conformational potential energy surface and on the geometry of the stable structures.
The study of small molecular hydrogen bonded complexes such as dimers or trimers is also very interesting and can be considered a starting point towards the understanding of bulk properties.
Weak and strong intermolecular hydrogen bonds (C-H...F, C-H...N, O-H...N) can be observed in the structures of the trimer of difluoromethane,[2] pyridine- CHF_3 or pyridine-water. These molecular complexes are stabilized by more than one hydrogen bond but they are also highly dynamical.

1. Sanchez, R.; Giuliano, B.M.; Favero ,L.B.; Caminati, W., *J. Am. Chem. Soc.*, **2007,** *129*, 6287-6290
2..Blanco, S.; Melandri, S.; Ottaviani, P.; Caminati, W.; *J. Am. Chem. Soc.*; **2007;** *129*(9), 2700 – 2703

O 2.5

Trehalose and glucose dynamics by low-frequency scattering techniques

A. Morresi,[a] M. Paolantoni,[a] P. Sassi,[a] M. E. Gallina,[a] D. Fioretto,[b] L. Comez,[b] F. Scarponi[b]
[a]*Dipartimento di Chimica, Università di Perugia, Via Elce di Sotto, 8, I-06123 Perugia, Italy*
[b]*Dipartimento di Fisica, Università di Perugia, Via Pascoli, I-06123 Perugia, Italy*

Studies of carbohydrates in aqueous solutions have been performed by different experimental techniques – molecular dynamics simulation, neutron scattering, time and frequency domain spectroscopies – in order to ascertain their important specific structural and dynamical properties, especially cryo-conservative ones. Nevertheless a definite molecular picture of the examined systems is not yet available.[1] Moreover, the different abilities of some important mono- and di-saccharides in long-term storage of biological materials have not been clarified so far.
Often it is suggested that the different hydrogen bond networks formed by the different sugars in water should be the principal responsible of their distinct bio-protective behaviour.
Concerning the water properties, they are among the most discussed and debated ones; in particular, different experimental measurements describe a complex picture with dynamical regimes following one upon the other: each experimental probe sheds light on a limited window of the whole dynamics, describing a single process, in a specific time range, within the femto- to milli-second region.
The water properties inside the solutions depend on the relative distance between solute and solvent molecules: the molecules in the immediate vicinity of the solute are called "biological water", in opposition to the rest, the bulk water, not influenced by the solute. It is also possible to distinguish inside the biological water, between bound and not-bound molecules, referred to the bonding with the solute molecules.[2]
The existence of different kinds of water in sugar solution has been recently evidence by terahertz spectroscopy results.[3] In the present contribution we show the low-frequency light scattering spectra of glucose and trehalose aqueous solutions, obtained with interferometric and dispersive experimental setups. Using the susceptibility representation of the recorded intensities, we are able to distinguish two different contributions of water molecules and to study the dependence of their amplitude and relaxation time on temperature and sugar concentration. Experimental and data manipulation approach are discussed and a physical interpretation of the estimated parameters is proposed.

1. Lee, S. L.; Debenedetti, P. G.; Errington, J. R.; *J. Chem. Phys.*, **2005**, *122*, 204511-10. 2. Nandi, N.; Bagchi, B.; *J. Phys. Chem. B*, **1997**, *101*, 10954 – 10961. 3. Heugen, U.; Schwaab, G.; Bründermann, M.; Heyden, M.; Yu, X.; Leitner, D. M.; Havenith, M; *PNAS*, **2006**, *103*, 12301 – 12306.

O 2.6

Photocatalytic activity of surface fluorinated and/or Au-modified titanium dioxide

Elena Selli
Dipartimento di Chimica Fisica ed Elettrochimica, Università degli Studi di Milano, Via Golgi 19, 20133 Milano, elena.selli@unimi.it

Titanium dioxide particles were modified either by gold nanoparticles deposition (Au/TiO_2) or by surface fluorination ($F\text{-}TiO_2$) and their photocatalytic activity was tested in the degradation of organic substrates in aqueous suspension, in order to assess the effects of noble metal deposition and of a hydrophobized oxide surface on the electron transfer processes occurring at the semiconductor – water interface under irradiation with light of different wavelength. The primary photocatalytic processes involving photopromoted conduction band electrons, e_{CB}^-, and valence band holes, h_{VB}^+, were investigated during the photodegradation runs, either by monitoring the evolution of hydrogen peroxide, formed through adsorbed dioxygen reduction by e_{CB}^-, or by EPR measurements of the DMPO-OH adduct produced by spin trapping of hydroxyl radicals formed through water or hydroxyl anions oxidation by h_{VB}^+, or eventually by other photoproduced oxygen species.
Surface fluorination of TiO_2 strongly modifies its surface properties. Indeed, the fast adsorption of fluoride anions on the semiconductor surface decreases the amount of surface hydroxyl groups, leading to the formation of ≡Ti-F species, which dominate at acidic pH [1], with an almost complete displacement of surface –OH groups at pH 3.7. Nanosized noble metal isles were deposited on TiO_2 particles mainly through the well established deposition-precipitation method [2], employing different pH adjusting media, or by immobilization of preformed metallic sols [3]. In this case a pre-irradiation step was necessary, to remove the organic species surrounding gold nanoparticles. This produced only a slight increase of the size of Au isles (from ca. 2 to ca. 5 nm, on average), as revealed by HRTEM analysis.
The photocatalytic degradation of aromatic moieties – containing substrates was markedly faster on $F\text{-}TiO_2$ than on unmodified TiO_2, in line with an enhanced hydroxyl radical formation. Indeed, EPR spin trapping measurements revealed that titanium dioxide surface fluorination leads to an increased concentration of the DMPO-OH adduct in the aqueous phase under irradiation [4]. By contrast, the photocatalytic degradation of formic acid was slower upon TiO_2 fluorination, but, at the same time, hydrogen peroxide concentration was much higher than on unmodified TiO_2. The peculiar role played by the $CO_2^{\bullet-}$ species, produced from formic acid oxidation, in H_2O_2 formation during the photocatalytic degradation of this latter on $F\text{-}TiO_2$. could thus be fully enlightened [5]. The main effect of surface fluorination thus appears to consist in its shielding effect at the semiconductor-water interface, which favours the desorption of photogenerated active species.
Gold nanoparticles deposition on TiO_2 produced much lower, though wavelength dependent, increases in the photocatalytic degradation rates of organic substrates. Maximum degradation rates were attained for different metal loadings, depending on the deposition procedure, allowing an optimum balance between the detrimental shielding effects of Au surface nanoparticles, which decrease the fraction of light absorbed by TiO_2, and their beneficial role in capturing photopromoted e_{CB}^-, thus decreasing the e_{CB}^- - h_{VB}^+ recombination rate [3].

However, a parallel increase of H_2O_2 production was always observed during the photocatalytic degradation runs, confirming the positive role of the noble metal in favouring the photopromoted electron transfer at the semiconductor oxide - water interface.
Finally, gold deposition on TiO_2 caused a marked increase of the DMPO-OH adduct concentration under irradiation. However, surface fluorination and gold deposition did not exhibit synergistic effects in the photocatalytic production of oxygen active species on the TiO_2 surface: in fact, the amount of DMPO-OH adduct detected under irradiation of fluorinated Au/TiO_2 water suspensions was lower than that detected with Au/TiO_2. Hydrogen peroxide, produced in relatively high amount on Au/TiO_2, may provide an extra source of $^{\bullet}OH$ radicals, parallel to water oxidation by valence band holes, by reacting with conduction band electrons, according to the surface process: $H_2O_2 + e^-_{CB} \rightarrow {}^{\bullet}OH + OH^-$. Such reaction is expected to be much less probable on the fluorinated surface, as demonstrated by the higher relative photostability of H_2O_2 on F-TiO_2 respect to naked TiO_2 [4].

1. Minero, C.; Mariella, G.; Maurino, V.; Vione, D.; Pelizzetti, E..; *Langmuir*, **2000**, *16*, 8964-8972. 2. Haruta, M.; *Gold Bulletin*, **2004**, *37*, 27-36. 3. Mrowetz, M.; Villa, A.; Prati, L.; Selli, E.; *Gold Bulletin*, **2007**, in press. 4. Mrowetz, M.; Selli, E.; *Physical Chemistry Chemical Physics*, **2005**, *7*, 1100-1102. 5. Mrowetz, M.; Selli, E.; *New Journal of Chemistry*, **2006**, *30*, 108-114.

O 2.7

Study on the adsorbate-substrate interaction between halogenated ethenes and TiO_2: IR spectroscopy and quantum-mechanical calculations.

Jessica Scaranto[a], Santi Giorgianni[a]
[a]*Università Ca' Foscari di Venezia, Dorsoduro 2137, 30123, Venezia, jeyscar@unive.it*

The study of the interaction between halogenated ethenes and TiO_2 is very important for the field of the heterogeneous photocatalysis. In a recent work[1] we have investigated the adsorption at room temperature of vinyl fluoride and chloride on powdered TiO_2 by IR spectroscopy. On the basis of the experimental data we have concluded that the adsorption occurs by one interaction between the halogen atom and the surface Lewis acid site (Ti^{4+}) and an H-bond between the CH_2 group and a surface Lewis basic site.
Here, we present the main results obtained from a periodic quantum-mechanical study on the vinyl fluoride adsorbed on the anatase (101) surface. All the calculations have been performed at DFT/B3LYP level using the CRYSTAL program[2,3]. In order to estimate the slab thickness to adopt for modelling the surface, the convergence with respect to the structural relaxation and the surface formation energy has been checked by taking into account slabs from 6 to 30 atomic layers. The adsorption study has been subdivided into two main steps: the first consists in the determination of all the possible adsorbate-substrate interactions arising from the adsorption through the halogen atom or the double C=C bond on a 12-atomic layers slab; this investigation has allowed to preventively verify that the experimental model represents an acceptable adsorbate-substrate structure. Then, this model has been used for performing a more detailed investigation adopting a 30-atomic layers slab and considering different surface coverages and periodicities. For both the two steps, the adsorption energetics have been evaluated by taking into account not only the binding energy but also the interaction and distortion ones. In this way, it has been possible to observe that the adsorbate-substrate interaction is bigger when the molecule adsorbs by the halogen atom than by the double C=C bond. A nearest and next-nearest neighbours model has been employed for evaluating the lateral effects between the CH_2CHF molecules and obtaining the energies in the limit of an isolated adsorbed molecule, i.e. when the lateral effects are negligible. Furthermore, the vibrational frequencies of the molecule have been determined and compared with the experimental ones: the good agreement between the calculated and observed values allows to conclude that the previously formulated model[1] provides a good description for the adsorption of vinyl halides on the anatase (101) surface.
In addition, the preliminary results obtained from infrared spectroscopy and quantum-mechanical studies on the adsorption of CH_2CFCl on TiO_2 are also presented.

1. Scaranto, J; Pietropolli Charmet, A.; Stoppa, P.; Giorgianni, S.; *Journal of Molecular Structure*, **2005**, *62*, 213 – 219. 2. Saunders, V.R.; Dovesi, R.; Roetti C., Orlando, R.; Zicovich-Wilson, C.M.; Harrison, N.M.; Doll, K.; Civalleri, B.; Bush, I.J.; D'Arco, P.; Llunell, M.; *CRYSTAL03 User's Manual*, Università di Torino, Torino (**2003**). 3. Dovesi, R.; Saunders, V.R.; Roetti C., Orlando, R.; Zicovich-Wilson, C.M.; Pascale, F.; Civalleri, B.; Doll, K.; Harrison, N.M.; Bush, I.J.; D'Arco, P.; Llunell, M.; *CRYSTAL06 User's Manual*, Università di Torino, Torino (**2006**).

SEZIONE

COLLOIDI ED INTERFASI

I 3

Aging and flow in a colloidal suspension

Giancarlo Ruocco

Dipartimento di Fisica e CRS SOFT-INFM-CNR, Università di Roma "La Sapienza", Piazza Aldo Moro 2, I-00185, Roma.

Understanding the physical mechanisms governing the interplay between aging dynamics and shear flow is crucial to both elucidating the nature of slow dynamics in soft materials and controlling their complex rheological behavior.

We investigate the evolution of the density autocorrelation function of an aging colloidal suspension subject to a steady shear flow (shear rate γ) . The competition between the structural relaxation time and the inverse shear rate gives rise to a complex dynamical behavior that we could quantitatively analyze studying the detailed shape of the particles density autocorrelation function.

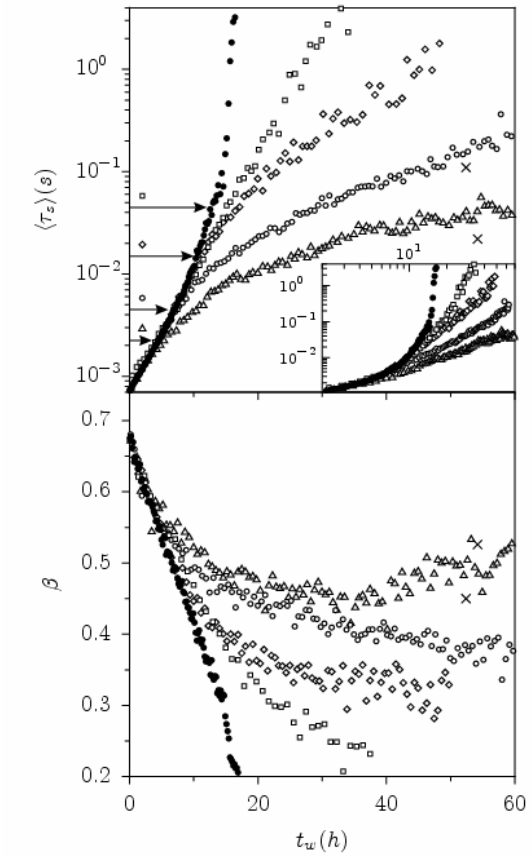

Figure 1. Average slow relaxation time $<\tau_s>$ and stretching exponent β as a function of waiting time t_w during aging under
different shear rates γ=446 (triangles), 223 (circles), 67 (diamonds), 22 (squares) s^{-1}. Solid symbols refer to aging without shear. Arrows in top frame indicate the γ^{-1} values corresponding to each curve. Inset in top frame shows the same data in a double-logarithmic scale (from [1]).

The sample is an aqueous suspension of Laponite, a highly thixotropic liquid which undergoes structural arrest on a timescale which strongly depends on concentration and ionic strength and that can be as long as few months. We found that the aging dynamics displays two different regimes whose boundary is marked by the condition $\tau\gamma$=1. As long as the characteristic relaxation time τ is small on the time-scale $1/\gamma$, aging is unaffected by the presence of shear. During aging dynamics slows down, and when τ becomes of the order of $1/\gamma$, the system enters a shear dominated regime where aging is strongly reduced and the structural relaxation time is very sensitive to γ. The intermediate scattering functions, characterizing the slow non-equilibrium dynamics of the sheared sample, are well described assuming an heterogeneous
scenario where the complex dynamics results from the superposition of relaxing units each one independently coupled to shear rate.

At the same time we monitor velocity profiles by means of heterodyne dynamic light scattering. Shear localization is observed at the lower rates of shear. An un-sheared gel band coexists with a uniformly sheared fluid band whose relaxation time is fixed by the shear rate.

We also study the aging process after rejuvenation of the sample with an high shear rate. The t_w dependence of τ after rejuvenation is substantially different from that observed in normal aging and follow a power law.

We discuss these results in relation to recent theoretical work and present a simple phenomenological model based on Langevin dynamics which is capable of reproducing many of the observed features.

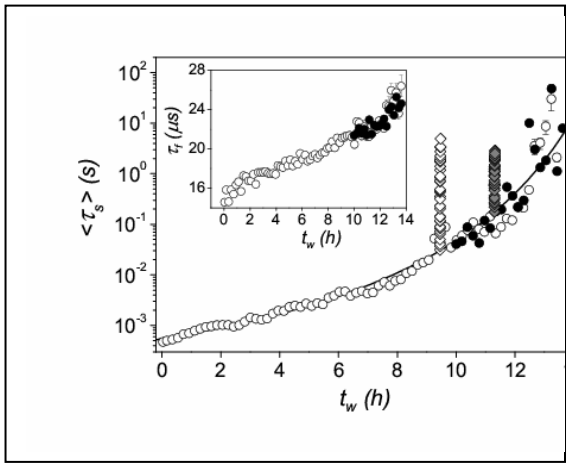

Figure 2. Complete rejuvenation of the Laponite sample in the slow aging regime, i.e. before gelation. Average slow relaxation time $<\tau_s>$ is plotted as a function of waiting time t_w for a sample aging soon after filtration (empty circles) and for the same sample aging after the application of a shear rate of 100 s^{-1} for 2 minutes, 13.4 hours after filtration (full circles). T_w is shifted in order to superimpose the first $<\tau_s>$ measured after the application of shear with the first aging curve (empty circles). The black line is a guide for the eye. In the inset the fast relaxation time is plotted as a function of t_w for the two aging evolution with the same shift in tw. The slow aging regime is also compared to the fast aging regime, which is observed after the shear rejuvenation of a gelled sample: white diamonds represent the evolution of the slow relaxation time after a shear rate γ = 0.5 s^{-1}, while grey diamonds are for γ= 100 s^{-1} (from [2]).

1. "*Aging under shear: structural relaxation of a non-Newtonian fluid.*" R. Di Leonardo, F. Ianni, and G. Ruocco. *Physical Review* **E71**, 011505 (2005).
2. "*Aging after shear rejuvanation in a soft glassy colloidal suspension: evidence for two different regimes.* " F. Ianni, R. Di Leonardo, S. Gentilini, and G. Ruocco. *Physical Review* **E75**, 011408 (2007).

O 3.1

Addressable DNA architectures anchored to Supported Lipid Bilayers

G. Caminati[a], *F. Gambinossi*[a], *D. Berti*[a], *M. Banchelli*[a], *P. Baglioni*[a], *T. Brown*[b], *B. Norden*[c]
[a]*Department of Chemistry and CSGI – University of Florence Via della Lastruccia 3, I-50019 Sesto Fiorentino (FI) Italy*
[b]*School of Chemistry, University of Southampton, Highfield, Southampton SO17 1BJ, UK*
[c]*Department of Chemical and Biological Engineering / Physical Chemistry, Chalmers University of Technology, SE-41296 Gothenburg, Sweden*

The quest for miniaturized arrays of addressable molecular structure has ignited the use of DNA sequences as building blocks for increasingly smaller self-assembly with molecular recognition properties[1]. Controlled immobilization of such nanostructures represents an additional bonus for many applications when tuning of surface density and directionality is required. Large spacing between immobilized upright DNA single strands is still a challenge in the search for efficient hybridization and surface-assisted construction of larger oligonucleotide (ON) architectures[2]. This issue was addressed using Supported Lipid Bilayer (SLB) as scaffold for cholesterol-oligonucleotide insertion. SLBs form a fluid two-dimensional space allowing free diffusion and rotation of lipid molecules and lipid-associated molecules directing the hybridization process. SLBs of Palmitoyl-2-Oleoyl-*sn*-Glycero-3-Phosphocholine (POPC) were prepared on gold surfaces by disruption of POPC liposomes.
The anchoring of cholesterol-TEG-DNA-18mers in the SLB was followed by means of a dissipative Quartz Crystal Microbalance (QCM) as a function of time and ON concentration. Insertion was studied both for the single- and the double-stranded oligonucleotide as a function of temperature. QCM data analysis provided the viscoelastic properties and the thickness of the resulting architectures whereas temperature cycling evidenced ds-ONs denaturation at the interface.
SLBs decorated with ds-ONs were also prepared by direct spreading of POPC vesicles hosting the desired cholesterol-ON. Excitation dependent emission of fluorescein covalently attached to the 5' terminus of one strand was used to trace the distribution of the ds–ON in the SLB matrix using spatially resolved Confocal Laser Scanning Microscopy (CLSM) with Dual Channel imaging.
Atomic Force Microscopy (AFM) revealed the morphology and the nanoscale organization of the DNA construct.

1. Feldkamp U.; Niemeyer C.M.; *Angew. Chem. Int. Ed*., **2006**, *45* 1856.
2. Opdhal A.;. Petrovyckh D.Y; Kimura-Suda H.; Tarlov M.J.; Whitman L.J.; *PNAS*, **2007**, *104* 9.

O 3.2

Structural Stability Against Disintegration by Anionic Lipids Rationalizes the Efficiency of Cationic Liposome/DNA Complexes

Giulio Caracciolo,[a] Daniela Pozzi,[a] Ruggero Caminiti,[a] Cristina Marchini,[b] Maura Montani,[b] Augusto Amici,[b] Heinz Amenitsch[c]
[a]*Department of Chemistry, University of Rome "La Sapienza", P.le A. Moro 5, 00185 Rome, Italy.*
[b]*Genetic Immunization Laboratory, Department of Molecular Cellular and Animal Biology, University of Camerino, Via Camerini 5, 62032 Camerino (MC), Italy.*
[c]*Institute of Biophysics and Nanosystems Research, Austrian Academy of Sciences, Schmiedelstrasse 6, A-8042 Graz, Austria.*

Non-viral gene delivery strategies have been receiving much attention since the ground-breaking studies by Felgner et al.[1] that had shown how complexes composed of cationic liposomes (CLs; self-closed lipid vesicles made of cationic and neutral lipids) and DNA, named lipoplexes, could serve as gene delivery vehicles in the targeting of extracellular DNA into cell nuclei. As with most synthetic transfection systems, the use of lipoplexes is limited by our insufficient understanding of formation mechanism, the structure, and the stability of the complexes and, most importantly, of the manner in which they cross cell membranes and how they are relieved of their genetic freight.[2]
More recently, the unbinding of DNA from a lipoplex after entering the cell, has been identified as one of the key steps in lipid-mediated DNA delivery (lipofection).[3] A number of investigators observed the release of DNA molecules from various lipoplexes after treatment with anionic lipids (ALs).[4-6] Experiments have clarified that the unbinding is a result of charge neutralization by cellular anionic lipids[5,7] and have also suggested that structural changes of lipoplexes may be a controlling factor in DNA delivery.[3]
To test this idea, we investigated the correlation between transfection efficiency (TE) and structural evolution of lipoplexes upon interaction with cellular (anionic) lipids. To this end, we used both binary and multicomponent (MC) lipoplexes.[8,9] MC lipoplexes, incorporating from three to six lipid species simultaneously, presented much higher transfection efficiency than binary lipoplexes, which are more commonly used for gene delivery purposes.[8,9] We applied small angle synchrotron X-ray diffraction (SAXD) to study the structural correlates of the lipoplex formulations and their mixtures with anionic lipids. Electrophoresis experiments were carried out to measure the extent of DNA unbinding.
We found evidence of the existence of three different regimes of stability related to interaction between complexes and anionic membranes. Both unstable (with low membrane charge density, σ_M) and highly stable lipoplexes (with high σ_M) exhibited low transfection efficiency while highly efficient multicomponent lipoplexes exhibited an 'optimal stability'. This intermediate regime reflects a compromise between two opposing constraints: protection of DNA in the cytosol and endosomal escape. Here we advance the concept that structural stability, upon interaction with cellular anionic lipids, is a key factor governing transfection efficiency of lipoplexes.[10]
Our results provide a physical basis for rational design of novel cationic lipid formulations. Future work will be made to confirm this hypothesis, and to check whether other effects, such as the specificity of lipid formulations and cell lines, may play a role in lipid-mediated gene

delivery. The future adoption of rationally designed lipoplexes offering protection against disintegration by anionic lipids would ensure that users definitely improve transfection efficiency of lipid carriers.

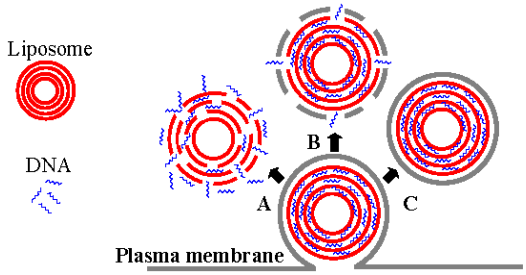

Figure1. Proposed mechanism of interaction of lipoplexes with the anionic plasma membrane of the cell. Electrostatic attractions let the lipoplex approach the anionic surface of the cell and attachment is followed by endocytosis resulting in endosomal entrapment. Solid grey line represents a portion of the plasma membrane separating inner and outer space of a cell. The less stable the lipoplexes the early the dissociation of DNA in the cytoplasm (A). When naked, DNA may be easily digested by enzymes the cytoplasm is rich in. Optimally stable lipoplexes (B) may release delivered DNA slowly in the cytoplasm, the event occurring through interactions with anionic proteins which readily form complexes with cationic vesicles. Too stable lipoplexes (C) do not fuse with the endosomes and do not allow for DNA release. Endosomal entrapment therefore results in a decrease in transfection efficiency.

1. Felgner, P. L.; Ringold, G. M. *Nature* **1989**, *331*, 461-462.
2. Ewert, K. K.; Ahmad, A.; Evans, H. M.; Safinya, C. R. *Expert. Opin. Biol. Ther.* **2005**, *5*, 33-53.
3. Koynova, R.; Wang, L.; Tarahovsky, Y.; MacDonald, R. C. *Bioconjug. Chem.* **2005**, *16*, 1335-1339.
4. MacDonald, R. C.; Ashley, G. W.; Shida, M. M.; Rakhmanova, V. A.; Tarahovsky, Y. S.; Pantazatos, D. P.; Kennedy, M. T.; Pozharski, E. V.; Baker, K. A.; Jones, R. D.; Rosenzweig, H. S.; Choi, K. L.; Qiu, R. Z.; McIntosh, T. J. *Biophys. J.* **1999**, *77*, 2612-2629.
5. Xu, Y. H.; Szoka, F. C. *Biochemistry* **1996**, *35*, 5616-5623.
6. Tarahovsky, Y.; Koynova, R.; MacDonald, R. C. *Biophys. J.* **2004**, *87*, 1054-1064.
7. Caracciolo, G.; Pozzi, D.; Caminiti, R., Marchini, C.; Montani, M; Amici, A.; Amenitsch, H. *Appl. Phys. Lett.* **2006**, *89*, 233903-3.
8. Caracciolo, G.; Pozzi, D.; Amenitsch, H.; Caminiti, R. *Langmuir* **2005**, *21*, 11582-11587.
9. Caracciolo, G.; Pozzi, D.; Caminiti, R.; Amenitsch, H. *Appl. Phys. Lett.* **2005**, *87*, 133901-3.
10. Caracciolo, G.; Marchini, C.; Pozzi, D.; Caminiti, R., Amenitsch, H.; Montani, M; Amici, A. *Langmuir* **2007**, *23,* 4498-4508.

O 3.3

Aggregation of triblock copolymers in water induced by chlorinated oils.

De Lisi R.[a], Gradzielski M.[b], Lazzara G.[a], Milioto S.[a], Muratore N. [a], Prevost S.[b,c]

[a]*Dipartimento di Chimica Fisica "F. Accascina", Università degli Studi di Palermo, Viale delle Scienze, Parco D'Orleans II, 90128 Palermo, Italy, g.lazzara@unipa.it.*

[b]*Stranski Laboratorium für Physikalische und Theoretische Chemie, Technische Universität Berlin, Straße des 17. Juni 112, 10623 Berlin, Germany.*

[c]*Hahn-Meitner-Institut Berlin, Glienicker Strasse 100, 14109 Berlin, Germany.*

We studied the solubilization of α,ω-dichloroalkanes in new aqueous nanostructured media which are composed of poly(ethylene oxide)-poly(propylene oxide)-poly(ethylene oxide) triblock copolymers (PEO-PPO-PEO). The thermodynamic study [1] allowed to determine the oil affinity to the aggregates through the evaluation of the standard free energy (ΔG°) and the volume (ΔV) for the oil-copolymer mixed aggregates formation. Fluorescence, SANS and DLS experiments [2] showed that even very low oil amounts added to unimeric copolymer solution lead to the formation of oil/copolymer mixed aggregates with a copolymer aggregation number which increases rapidly with the oil volume fraction. The oil enhancement of the aggregation process is less pronounced by decreasing the copolymer molecular weight.

1. De Lisi, R.; Lazzara, G.; Milioto, S.; Muratore, N.; *Journal Coll. Interface Sci.*, **2006**, *300*, 368. 2. Lazzara, G.; Milioto, S.; Gradzielski, M.: *Phys. Chem. Chem. Phys.*, **2006**, *8,* 2299.

O 3.4

Orientational order properties of nematic and smectic B phases of fluorinated liquid crystals by means of ^{13}C NMR, optical and dielectric studies

Alberto Marini[1,2], Marco Geppi[1], Carlo Alberto Veracini[1], Stanisław Urban[3], Joanna Czub[3], Roman Dąbrowski[4] and Wojciech Kuczyński[5]

[1] *Dipartimento di Chimica e Chimica Industriale, Università di Pisa, Via Risorgimento 35, 56126 Pisa, Italy*

[2] *Scuola Normale Superiore di Pisa, Piazza dei Cavalieri 12, 56126 Pisa, Italy*

[3] *Institute of Physics, Jagiellonian University, Reymonta 4, 30-059 Kraków, Poland*

[4] *Institute of Chemistry, Military University of Technology, 00-908 Warszawa, Poland*

[5] *Institute of Molecular Physics, Polish Academy of Sciences, Poznań, Poland*

In the past few years, liquid crystals displays (LCDs) have become a nearly inseparable part of our daily life. In this field fluorinated liquid crystals (FLC) represent an important class of materials with possible applications, especially thanks to their broad nematic mesophase ranges, low rotational viscosity and high dielectric anisotropy[1].

Structural and orientational order properties of **3Cy2CyBF2** [Cr-34.8°C-N-103.2°C-I] and of **5CyCy2BF2** [Cr-25°C-SmB-73.3°C-N-121.3°C-I] have been investigated by means of ^{13}C NMR, optical and dielectric spectroscopy methods.

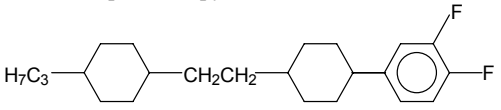

3Cy2CyBF2

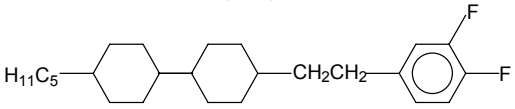

5CyCy2BF2

For both compounds ^{13}C-{^{1}H} NMR static spectra have been recorded by means of the Linear-Ramped Cross-Polarization technique, under SPINAL-64 decoupling[2]. The assignment of the ^{13}C resonances have been carried out thanks to the comparison with solution state spectra and with DFT calculations using Gaussian'03[3]. From the NMR point of view, the order parameters have been calculated analyzing all the ^{19}F-^{13}C dipolar couplings (D_{C-F}) by means of a least-square fitting procedure, according to the procedure described in ref. 4. The order parameters have been also obtained by fitting of all the experimental ^{13}C chemical shift anisotropies. Dielectric measurements were performed in a broad frequency range for two orientations of the nematic director with respect to the measuring field. At low frequencies a positive dielectric anisotropy ($\Delta\varepsilon$) was determined, which enabled the calculation of the order parameter[4]. At high frequencies the $\Delta\varepsilon$ changes its sign which can be useful in designing a dual addressing display. The optical birefringence $\Delta n = n_e - n_o$ was measured as a function of temperature which yielded the order parameter[4]. The nematic order parameter determined from the above cited techniques have been compared. The results so obtained have been discussed, also with reference to those previously reported for different fluorinated nematogens[4].

1. Kirsch, P.; Bremer, M.; *Angew. Chem. Int. Ed.*, 39, 4216, **2000**.
2. Fung, B. M.; Khitrin, A. K.; Ermolaev, K.; *J. Magn. Reson.* 142, 97, **2000**.
3. Gaussian 03, Revision B.05. M.J. Frisch et al., Gaussian, Inc., Pittsburgh PA, **2003**.
4. Catalano, D.; Geppi, M.; Marini, A.; Veracini, C. A.; Urban, S.; Czub, J.; Kuczynski, W.; Dabrowski, R.; *J. Phys. Chem. C*, 111, 5286, **2007**.

O 3.5

Magnetic properties of ultra-small nanoparticles: beyond the influence of particle size

D. Peddis[a], C. Cannas[a], D. Fiorani[b], A. Musinu[a], G. Piccaluga[a], S. Mørup[c]

[a]*Dipartimento di Scienze Chimiche, Cittadella Universitaria di Monserrato, bivio per Sestu, 09042 Monserrato (Cagliari), Italy. dpeddis@hotmail.com*

[b]*Istituto di Struttura della Materia-CNR. C.P. 10, 00016 Monterotondo Stazione (Roma), Italy.*

[c]*Department of Physics, Technical University of Denmark, DK-2800 Kongens Lyngby, Denmark*

The magnetic properties of nanosized particles are a subject of great interest both for application purposes (information storage,[1] ferrofluid technology,[2] biomedical application[3]) and for basic research to investigate, for example, how bulk properties transform as the size is decreased.[4] In this framework a lot of work has been focused on the study of the dependence of magnetic properties on particle size. Anyway, this approach is not completely exhaustive, because other factors affect the magnetic behaviour of nanoparticles. Magnetic interactions among nanoparticles play an important role in the physics of these system as well as the magnetic structure. The presence of non-collinear (canted) spin structures leads to modifications of the magnetic properties and for this reason "*spin canting*" may be, in some cases, a key point to understand the magnetic behaviour of nanoparticles.[5]

Besides, in the ferritic oxides $MeFe_2O_4$, where Me is a divalent cation, a further variant is given by the distribution of the cations in the tetrahedral and octahedral sites of the close packed oxygen structure, as it may affect the alignment of the moments of the various ions. The cation distributions are usually expressed in terms of the so-called inversion degree (γ), defined as the fraction of divalent ions in octahedral sites.[6]

In this communication two samples of $CoFe_2O_4$ nanoparticles dispersed in silica matrix with different abundance (10% and 5% by weight of $CoFe_2O_4$, called *N10* and *N5* respectively) and same mean particle size (~3 nm) are presented. Under these conditions the particle size effects should be similar in the two samples and this would make it possible to undertake a finer study of effects due to other factors. The magnetic properties of the nanoparticles are investigated through the combined use of classic magnetometry (*AC* and *DC* measurements) and Mössbauer spectroscopy (in zero and in high magnetic field).

In both samples the interparticle interactions are very weak, but through the combined use of Mössbauer spectrosocpy and magnetic measurements (*ZFC-FC*, *TRM*) some differences are highlighted.

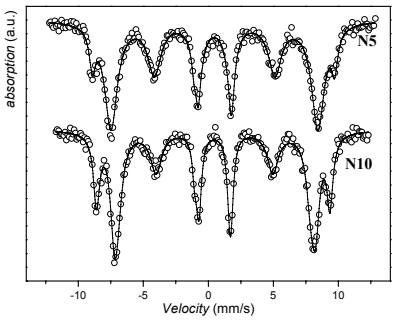

Despite the particles in the two samples have the same size, they show different values of saturation magnetization (M_s) and coercive field. In addition M_s is, for both samples, higher than the bulk value. From Mössbauer spectra in a magnetic field of 6T at low temperatures, 6K, (figure) the degree of spin-canting and the cationic distribution can be estimated. The best fit was obtained with three sextet assuming that some of the iron atoms are in perfect ferrimagnetic local environments and in accordance with this the relative areas of lines 2 and 5 were constrained to zero for two sextets corresponding to *A* (sextet 1, Fe^{3+} tetrahedrally coordinated) and *B* sites (sextet 2, Fe^{3+} octahedrally coordinated). A third sextet (sextet 3) was introduced to represent ions with canted spins, and in this component the ratio between the areas of the lines 2,5 and 3,4 was free. In all the three sextets the line widths and line intensities were constrained to be pair-wise equal.[7,8] In both samples, sextet 2 and sextet 3 show values of isomer shifts typical for octahedrally coordinated Fe^{3+} in spinel but larger than that of sextet 1, which is typical for tetrahedrally coordinated Fe^{3+}. This indicates that the canted spins are mainly located in the *B* sites.[7]

In the table, the values of the saturation magnetization (M_s), the inversion degree (γ), the anisotropy constant (K) and percentage of canted spins (N_c) for both samples are reported.

	M_s (A m^2 Kg^{-1})	γ	N_c (%)	K (J/m^3)
N5	109 (2)	0.22(2)	23 (3)	1.7×10^6
N10	89(2)	0.44(4)	17 (3)	1.6×10^6

Both samples show a considerable fraction of canted spins, highest in the more diluted nanocomposite. The magnetic anisotropy constants are much larger than that of bigger particles (> 7 nm),[7] presumably because of a large surface contribution to the anisotropy. A low inversion degree compared to bulk samples (γ bulk ~ 0.5) and other $CoFe_2O_4$ particles is observed. [9] This can be correlated with the surprisingly high values of saturation magnetization, especially for *N5* nanocomposite.
In conclusion, using magnetometry and Mössbauer spectroscopy in high magnetic field, a careful study of magnetic structure of nanoparticles has been performed and this allows explaining the difference in magnetic properties of the samples that do not depend on particle size.

1. Matsui, I.; *J. Chem. Eng. Jpn.*, **2005**, 38, 535. 2. Rosensweig, R. E.; *Chem. Eng. Prog.*, **1989**, 85, 53. 3. Tartaj, P.; Morales, M.P.; Vientemillas-Verdaguer, S.; Gonzales Cárreño, T.; Serna, C.J.; *J. Phys. D*, **2003**, 36, R182. 4. Dormann, J.L.; Fiorani, D.; Tronc E.; *Advances in Chemical Physics*, Wiley, New York, **1997**, Vol. XCVIII, p. 283. 5. Coey, J.M.D.; *Phys. Rev. Lett.*, **1971**, 27, 1140. 6. West, A.R.; *Solid State Chemistry*, Eds. Wiley &Sons. New York, 1984. 7. Cannas, C.; Musinu, A.; Piccaluga, G.; Fiorani, D.; Peddis, D.; Rasmussen, H.K.; Mørup, S.; *J. Chem. Phys.*, **2006**, 125, 16, 164714. 8. Anhøj, T.A.; Bilenberg, B; Thomsen, B.; Damsgaard, C.D.; Rasmussen, H.K.; Jacobsen, C.S.; Mygind, J.; Mørup S.; *J. Magn. Magn. Mater.*, **2003**, 260, 115. 9. Sawatzky, G.A.; Van der Woude, F.; Morrish, A.H.; *Phys. Rev.*, **1969**, 187, 747

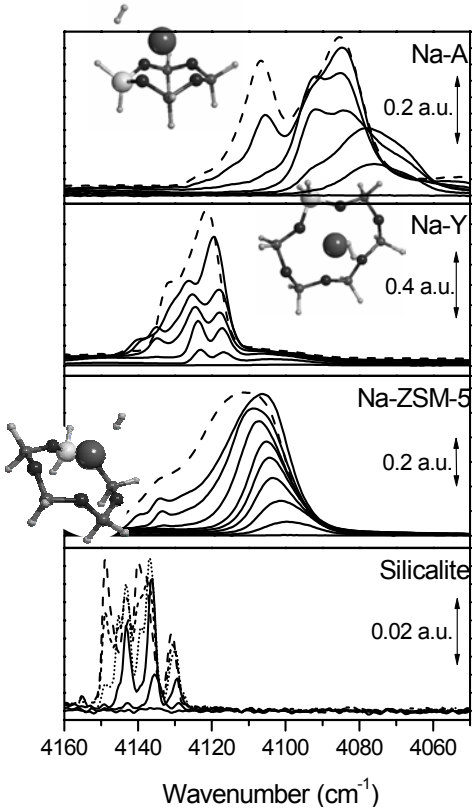

From top to the bottom: IR spectra of H_2 adsorbed at 20 K on NaA, NaY, Na-ZSM-5 and silicalite (the different curves correspond to increasing filling conditions).

O 3.6

Computational and spectroscopic screening of microporous materials for molecular hydrogen storage

Gabriele Ricchiardi, Jenny G. Vitillo, Giuseppe Spoto, Silvia Bordiga and Adriano Zecchina
Dipartimento di chimica IFM and Centro di Eccellenza NIS, Università di Torino, Via P. Giuria 7, 10125 TORINO, Italy, e-mail gabriele.ricchiardi@unito.it

Hydrogen storage by physisorption of molecular H_2 is a widely investigated option, and several classes of materials have been studied [1]. Among these, crystalline microporous materials like zeolites and metal organic frameworks, as well as several carbon structures, porous polymers and clathrates. Since several years we have addressed the problem of determining the nature and strength of the interactions of molecular H_2 with microporous materials by means of computational and spectroscopic techniques, aiming at understanding the key interactions involved and thus enabling an efficient screening of novel proposed materials for hydrogen storage, and the design of optimized adsorbents.
The interaction of H_2 with isolated cations, anions, and ion pairs modeling the adsorption sites of zeolites has been studied with accurate quantum methods (compared with a large set literature data) [2,3]. Relationships between the binding energies to anions and cations and the vibrational frequency of the molecule are determined, which show its peculiar nature as a "probe molecule" responding to polarizing fields of both signs. A breakdown of the interaction energies into its electrostatic and dispersion components is also obtained. This theoretical analysis has been extended to cations embedded in zeolite frameworks [4], in order to evaluate the strategy of functionalizing less-polar materials with polarizing ions. Giving the intrinsic limitations of zeolites ad hydrogen storage materials (see below), we have then addressed the theoretical description of adsorption on metal organic frameworks (MOFs), with careful analysis of the binding of H_2 to both the inorganic and organic sites of the structure [5]. The correct description of long range dispersive interactions, accounting for a significant fraction of the binding energy in microporous materials has stimulated the development of a nover molecular mechanics forcefield for MM simulations, obtained by fitting the ab-initio PES for the H_2-H_2 system and the eperimental dipole polarizability and quadrupole moment of the H2 molecule [6]. Finally, the problem of the maximal storage capacity of porous materials has been addressed using atomistic molecular dynamics simulations A method is devised for the prediction of the maximal capacity of a given microporous crystalline framework, and the method is applied to a variety of frameworks[7]. The obtained maximum capacities for zeolites are approximately 2.5% wt., well below the targets for mobile applications.
The interaction of H_2 with zeolite frameworks of variable polarity, topology and chemical composition, with several metal-organic framework, and with different porous polymers has been studied with low temperature IR experiments, which allow the measurement of heats of adsorption on specific sites, and with volumetric adsorption experiments [5,8,]. Low interaction energies are found in all cases (3-10 kJ/mol), in agreement with our calculations. However, calculations and experiments allow to highlight the desirable features, at the atomic scale, for better hydrogen adsorbers. In conclusion, the combined use of spectroscopic and theoretical methods allows a relatively fast and reliable screening of materials for their hydrogen storage potential, and provides guidelines for the functionalization of known porous structures with active sites with high hydrogen affinity.

1. A.Zuettel, *Naturwissenschaften* 91 (4): 157-172**, 2004**
2. Vitillo JG, Damin A, Zecchina A, Ricchiardi G, J.Chem.Phys. 122 (11): Art. No. 114311 **2005**
3. Vitillo JG, Damin A, Zecchina A, Ricchiardi G, J.Chem.Phys. 124 (22): Art. No. 224308, **2006**
4. Torres FJ, Vitillo JG, Civalleri B, Ricchiardi G, Zecchina A , J.Phys.Chem.C 111 (6): 2505-2513, **2007**
5. Bordiga S, Vitillo JG, Ricchiardi G, J.Phys.Chem.B, 109 (39): 18237-18242, **2005**
6. Gabriele Ricchiardi, **J**enny G. Vitillo, Donato Cocina, Evgueni N. Gribov and Adriano Zecchina *Phys. Chem. Chem. Phys.***, 2007,** DOI: 10.1039/b703409a
7. Vitillo JG, Ricchiardi G, Spoto G, Zecchina A, PCCP, 7 (23): 3948-3954 **2005**
8. Zecchina A, Bordiga S, Vitillo JG, Ricchiardi G, Lamberti C, Spoto G, Bjorgen M, Lillerud KP, J.Am.Chem.Soc., 127 (17): 6361-6366 **2005**

O 3.7

Luminescent Nanocrystals in PMMA Based Co-polymers: Novel Nanocomposite Materials for Nano Imprint Lithography.

Michela Tamborra[1,2], Maria Lucia Curri[1], David Mecerreyes[3], Juan Antonio Alduncin[3], Josè Adolfo Pomposo[3], Nikolaos Kehagias[4], Vincent Rebaud[4], Clivia M. Sotomayor Torres[4], Marinella Striccoli[1*]

[1]*IPCF, CNR, c/o Dept. Chemistry, University of Bari, Italy;*
[2]*Department of Chemistry, University of Bari, Via Orabona 4, 70126 Bari, Italy;*
[3]*CIDETEC, San Sebastian, Spain;*
[4]*Tyndall National Institute, University College Cork, Lee Maltings, Cork, Ireland.*

The design of new functional materials, able to join novel tailored physical and chemical properties with versatile and reliable processing capabilities, represents one of the most crucial challenges in modern material science. In this view, nanocomposite materials, based on thermoplastic polymers functionalized with inorganic nanoparticles, convey the unique size-dependent properties of nanosized particles into highly processable polymers.[1] The prepared materials then exhibit extraordinary optical and magnetic properties, as well as catalytic activity and mechanical strength. At the same time these functional materials are suitable for innovative fabrication process at micro and nano scale. Here the preparation of nanocomposites based on the incorporation of pre-synthesized CdSe@ZnS core-shell luminescent nanocrystals both in a curing resist polymer and into properly functionalized PMMA (poly-methyl methacrylate) co-polymers, is presented[2,3]. The spectroscopic and structural characteristics of the prepared materials are investigated in terms of chemical and physical interactions between the composite moieties to evaluate the nanocrystal interactions with the host matrix. In addition the well known excellent processability of both polymer matrixes in high resolution lithography has been exploited. Here, the fabrication of 2-D patterned photonic structures by Nanoimprint Lithography (NIL) has been demonstrated, showing a considerable enhancement in light extraction[3,4] (Fig.1).

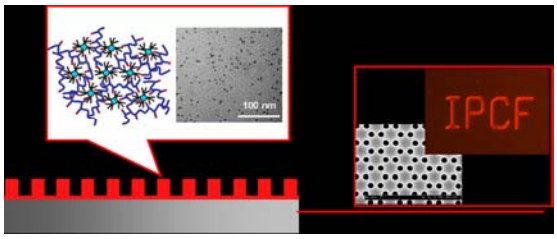

Fig.1: II-VI semiconductor nanocrystals in functionalized PMMA based co-polymers: highly homogeneous and luminescent composites for Nano Imprinting Lithography

The obtained results confirm the potential of the prepared luminescent functional materials for micro and nano fabrication, thus envisioning their development in permanent photonic applications.

Acknowledgments:

The support of the EC-funded project NaPa (contract no. NMP4-CT-2003-500120) and of MIUR Italian National Project no.232 is gratefully acknowledged. The content of this work is the sole responsibility of the authors.

References:

1 M. Tamborra, M. Striccoli, M. L. Curri, A. Agostiano "Hybrid Nanocomposites Based on Luminescent Colloidal Nanocrystals in PMMA: a Spectroscopical and Morphological Investigation" *Journal of Nanoscience and Nanotechnnology (2007) in press.*

2 M. Tamborra,, M. Striccoli, M. L. Curri, J. A. Alducin, D. Mecerreyes, J. A. Pomposo, N. Kehagias, V. Reboud, C. M. Sotomayor Torres, A. Agostiano "Nanocrystal-Based Luminescent Composites for Nanoimprinting Lithography" Small vol.3, Issue 5, pag.822-828 (2007)

3 V. Reboud, N. Kehagias, M. Zelsmann, M. Striccoli, M. Tamborra, M. L. Curri, A. Agostiano, M. Fink, F. Reuther, G. Gruetzner, C. M. Sotomayor Torres "Spontaneous emission control of colloidal nanocrystals using nanoimprinted photonic crystals" *Appl. Phys. Lett.* **2007**, *90*, 011115 selected for publication on the January 22, 2007 issue of *Virtual Journal of Nanoscale Science &Technology.*

4 V. Reboud, N. Kehagias, M. Zelsmann, M. Striccoli, M. Tamborra, M.L. Curri, A.Agostiano, D.Mecerreyes, J.A. Alduncín, C.M.S. Torres "Nanoimprinted photonic crystals for the modification of the (CdSe)ZnS nanocrystals light emission", *Microelectronic Engineering* (2007) *in press doi:10.1016/j.mee.2007.01.201.*

SEZIONE

CHIMICA FISICA DEI MATERIALI

I 4

Carbon Based Electron Donor Acceptor Hybrids for Solar Energy Conversion

Dirk M. Guldi
Institute for Physical Chemistry, University of Erlangen, 91058 Erlangen; e-mail: dirk.guldi@chemie.uni-erlangen.de

Carbon-based nanomaterials are currently under active investigations for producing innovative materials, composites, and electronic devices of greatly reduced size. Among the wide variety of carbon materials (i.e. fullerene, single and multi wall carbon nanotubes, carbon fibers, carbon nanoonions, and single wall carbon nanohorns), single wall carbon nanotubes (SWNT) and single wall carbon nanohorns (SWNH) are of particular interest.

The structure of SWNT is conceptualized by wrapping a one-atom-thick layer of a graphene sheet, that is, an interlinked hexagonal lattice of carbon atoms, into a seamless cylinder. The diameter of most SWNT is close to 1 nm, with a tube length that might be many thousands of times larger. Importantly, based on different arrangements, SWNT possess different electrical properties (i.e., semiconductor or metallic), which are the result of the electrons moving differently in the tube depending on the SWNT arrangement.
SWNH, on the other hand, are typically constituted by tubes of about 2-5 nm of diameter and 30 to 50 nm long, which associate with each other to give rise to round-shaped aggregates of 100 nm of diameter. SWNH are easily produced in large-scale quantities (i.e., up to 50 g/h) with an extraordinary purity (>90%) and, most importantly, are free of metal residue, since they are produced in the absence of any metal catalysts. Their large surface areas (1006-1464 m^2g^{-1}) and inner nanospaces (0.47-1.05 mL/g) are of great importance, since they ensure a great affinity with organic electron donors and make them promising candidates for electrical and chemical solar energy conversion.
In this respect, I will highlight the opportunities that rest on carbon nanostructures – much beyond the well-studied fullerenes – within the context of electron transfer reactions in novel chemical and light driven systems. In particular, I will survey our approaches to design, characterize, and examine the potential for practical applications of super- and supramolecular association of carbon-based nanomaterials with electron donors towards stable donor-acceptor nanohybrids and nanoconjugates within the context of light induced charge separation and solar energy conversion. Important are the impact, the benefits and some of the promises that evolve from electron transfer reactions with carbon nanostructures on i) the stabilization of radical ion pair states, ii) multi electron catalytic reactions and iii) photoelectrochemical / photovoltaic solar energy conversion.

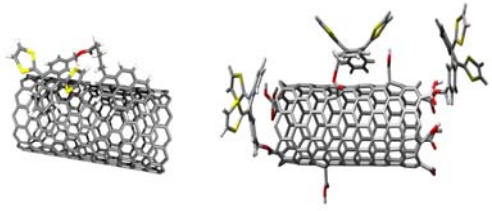

O 4.1

Stato dell'arte e Potenzialità del Solare Termico

Antonio Bee
COSTRUZIONI SOLARI, Zona PIP Cavallino, Lecce, c.s@ costruzionisolari.it

I pannelli solari piani, attualmente utilizzati, trasformano l'energia solare diretta e diffusa in calore. Questa tecnologia ha una buona efficienza per temperature fino agli 80° C. Ciò permette di coprire in modo efficace, una larga fascia di utilizzi: acqua calda sanitaria ad uso domestico e collettivo (alberghi, ospedali, ecc..), riscaldamento dell'acqua di piscine, riscaldamento d'ambiente (appartamenti, scuole, fabbriche), utilizzo del calore come acqua di processo nel settore industriale per temperature fino a 80°C.
La sfida che invece ci sta coinvolgendo ora e per i prossimi anni, è quella di ottenere tramite l'utilizzo del calore altre prestazioni oggi negate ai pannelli solari piani.
Lo studio che stiamo effettuando si sviluppa su alcuni tipi di macchine che devono lavorare con elevata efficienza a temperature costanti di 100°C, 250°C, 600°C.
Il raggiungimento dei 100°C dà la possibilità di utilizzare il calore prodotto dai pannelli solari nei gruppi frigoriferi ad assorbimento a bromuro di litio per generare freddo da utilizzare sia nel settore industriale che civile. Le macchine solari (paraboloidi non focalizzanti) che devono lavorare a temperature di 250°C servono per la produzione di vapore da utilizzare nel settore dell'industria alimentare e industriale. Infine le macchine che devono lavorare a temperature di 600°C servono per la produzione di energia elettrica mediante turbine; l'energia così prodotta può essere utilizzata anche per la produzione di idrogeno mediante il processo elettrolitico; questa è una delle vie più interessanti per la conservazione dell'elevatissima quantità di energia solare del periodo estivo, in tal modo è possibile utilizzarla in tutti i periodi dell'anno.

O 4.2

Role of defects and defect interactions on the photovoltaic properties of solar grade silicon

S. Binetti, M. Acciarri, J.Libal
Dipartimento di Scienza dei Materiali, Università di Milano-Bicocca, via Cozzi 53, I-20125 Milano, Italy simona.binetti@unimib.it

Nowadays silicon covers, as single crystal, multicrystalline (mc) almost the 90% of the photovoltaic (PV) market.
Currently the only commercial source for solar grade silicon (SoG-Si) is rejected and no-prime silicon from the semiconductor industry, but at the moment the shortage of Solar grade silicon is leading to high prices and a new supply of SoG-Si at reasonable costs is crucial for PV industry development.
One of the possible solutions is to produce SoG- silicon via a direct metallurgical route, followed by purification processes and by a final casting step to get multicrystalline (mc) silicon wafers. The material today available is however characterized by an high impurity content and relevant defectivity (dislocations,

precipitates). So the use of this material in solar cell production depends on the possibility of improve the electrical quality during the cell process in order to make it compatible in terms of solar conversion efficiency.
A deep understanding of the chemical physics of defects interactions and of the impurities segregation processes is the basic background needed to develop tools able to adapt the material to PV applications.
In this work it will be shown that the combined application of Photoluminescence and Infrared spectroscopy and Electron Beam induced Current (E.B.I.C) technique to study the recombination activity of extended defects in SoG-Si wafers succeeded in the identification of the nature of the defects which limit the quality of the base material and of the solar cell In the low temperature (T=12K) configuration, the PL technique was specifically adopted here for the study of SoG-Si multicrystalline ingots grown by the DS technique, by sampling wafers coming from different horizontal sections of the ingots, to follow the effect of impurity segregation at extended defects.
Furthermore, the level of impurity-contamination of dislocations has been systematically studied by EBIC contrast measurements at different temperatures. In order to improve the material quality, the samples have been also submitted to an ad hoc P-diffusion gettering process. As expected, the average lifetime increases after the P-diffusion process, which induces impurity gettering effects at the external surfaces. An increase of the local diffusion length was observed in defect-poor defective regions whereas the gettering efficiency is reduced in regions characterized by the presence of a high density of defects. An evident local increase of the electrical activity of some grain boundaries, after the P-diffusion process, was also observed. Furthermore, the PL spectroscopy mapping revealed the presence of as grown and process induced oxide precipitates. Apparently, a redistribution of impurities occurs at the processing temperature and impurities are captured at the deepest sinks. In fact, since grain boundaries act as heterogeneous segregation/ precipitation sites, some of them will compete with the external surfaces sinks, partly neutralising the effect of P-gettering.
This proves that extended defects represent a limiting factor for high efficiency solar cells but electrical properties in multicrystalline silicon of different quality can be improved if an appropriate cell process is applied.

This work has been carried out in the framework of the EU-founded Research Project "FOXY " (VI Framework Program).

O 4.3

Chiral recognition with enhanced sensing organic thin-film transistors

L. Torsi[a,b], G.M. Farinola[a], P. Iliade[a], M.C. Tanese[a], O. Hassan Omar[c], L. Valli[d], G. Giancane[d], F. Babudri[a,c], F. Palmisano[a], P.G. Zambonin[a,b] and F. Naso[a,c]
[a]*Dipartimento di Chimica Università degli Studi di Bari - Bari (Italy);*
[b]*Centro di Eccellenza TIRES - Università degli Studi di Bari - Bari (Italy);*
[e] *CNR ICCOM, Dipartimento di Chimica - Università degli Studi di Bari - Bari (Italy);*
[d] *Dipartimento di Ingegneria dell'Innovazione - Università degli Studi di Lecce - Lecce (Italy);*

Electronic detection with organic thin-film transistor (OTFT) sensors results in field-effect amplified responses repeatable within a standard deviation of few percentages [1]. Polycrystalline conducting polymers (CP) act both as transistor channel materials and sensitive layers and the CP side groups confer broad chemical selectivity but specificity and high sensitivity are yet open issues. Chiral discrimination is one of the hardest bench-test to prove sensors performance particularly in terms of selectivity and sensitivity. Here a OTFT gas sensor, bearing an amino-acid substituted CP active layer, is demonstrated to exhibit amplified sensitivity that allow to selectively detect β-citronellol enantiomers in the tens part per million (ppm) concentration range with highly repeatable responses. Markedly different sensitivities are seen for (S)- β-citronellol and (R)- β-citronellol and even in a racemic misture. The semi-conducting oligomers, which are designed to combine field-effect and enantiomeric recognition properties, are implemented in a novel sensing OTFT structure. Alkoxyphenylene-thienylene conjugated systems have been chosen for the active layer as they allow to covalently attach a wide variety of molecules as side groups, including bio-receptors [2-3], exhibiting also field-effect properties when deposited by the Langmuir-Schäfer (LS) procedure [4]. Chiral CP were synthesized already twenty years ago and differential detection of single enantiomers was performed with electrochemical, gravimetric and chemiresistor [5,6] sensors at part per thousand (ppth) concentrations. Our results demonstrate that combining field-effect amplified detection with chiral CP recognition properties allows enantiomeric discrimination at much lower concentration. This is a significant step further in the development of a highly-performing nanoscalable electronic sensing platform fully compatible with fast advancing organic electronic technologies.

[1] Torsi, L. and Dodabalapur, A. *Anal. Chem*. **70**, 381A (2005).
[2] Babudri, F., Farinola, G.M., Naso, F. *J. Mater. Chem.* **14,** 11 (2004).
[3] Naso, F., Babudri, F., Colangliuli, D., Farinola, G.M., Quaranta, F., Rella, R., Tafuro, R., Valli, L. *J. Am. Chem. Soc.* **125**, 9055 (2003).
[4] Tanese, M.C., Farinola, G.M., Pignataro, B., Valli, L., Giotta, L., Conoci, S., Lang, P., Colangiuli, D., Babudri, F., Naso, F., Sabbatini, L., Zambonin, P.G., Torsi, L, *Chem. Mat.* **18**, 778 (2006).
[5] Severin, E. J., Sanner, R. D., Doleman, B.J., Lewis, N.S. *Anal. Chem.* **70**, 1440 (1998).
de Lacy Costello, B.P.J., Ratcliffe, N.M., Sivanand, P.S. *Synth. Met.* **139**, 43 (2003)

O 4.4

Structural and physico-chemical studies of innovative layered Al-modified magadiite materials

Chiara Bisio[a], Guilherme Superti[b], Heloise O. Pastore[b], Leonardo Marchese[a]
[a] *DISTA, Università del Piemonte Orientale "A. Avogadro", 15053 Alessandria (Italy), chiara.bisio@mfn.unipmn.it*
[b] *Instituto de Quimica, Universidade Estadual de Campinas, Brasil*

Introduction

Magadiite is a crystalline hydrated sodium silicate, with an ideal unit cell of $Na_2Si_{14}O_{29}xH_2O$ [1], characterized by a layered structure, in which the negatively charged silicate layers are compensated by sodium ions. The crystal structure of magadiite is still unknown as no single crystals with suitable dimensions has never been obtained [2].

The intrinsic properties of this material can be exploited for applications as cation exchanger, adsorbent material, molecular sieve, catalysts support or polymer additive [3-5]. Nevertheless, more applications can be found by insertion of Al in the framework, leading to Brønsted acid surface centers that may be exploited in catalysis especially for the possibility to tune the surface hydrofobicity.

The synthesis strategy of Al-modified magadiite materials and the effects that such modifications have on the original surface properties of silicic magadiite will be illustrated in this work. In addition, details concerning the siliceous magadiite structure, obtained by combining experimental synchrotron XRPD and modeling techniques will be also discussed.

Experimental

Na-magadiite was prepared following procedure described in the literature [3]. The hydrothermal synthetic procedure was modified to introduce Al in the siliceous structure. Al-modified magadiite with different Si/Al ratio (15, 30 and 60) were then prepared using Al-isopropoxide as aluminum source. The so-obtained Na[Al]-magadiite were then fully-exchanged with NH_4^+ to prepare a precursor of H[Al]-magadiite. Acid magadiite samples were finally prepared by decomposing ammonium at high temperature in vacuum conditions.

Results and discussion

A detailed physico-chemical characterization of Na-magadiite and Al-derived solids were performed by using different experimental (XRDP analysis, TGA, IR and SS-NMR spectroscopy) and modeling techniques.

Several details on the magadiite structure, obtained by coupling synchrotron XRPD and computational models, will be illustrated.

XRD diffraction studies performed at increasing temperature (from r.t. to 1023 K) on all NH_4-[Al]-magadiite samples (Fig.1), showed that the thermal stability of the structure is similar to that of Na^+-magadiite.

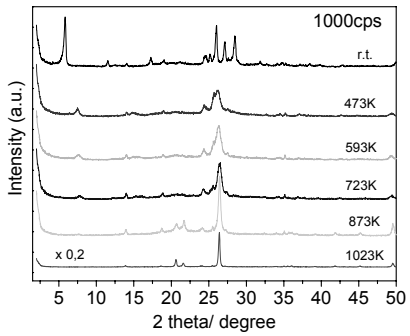

Fig.1: XRD pattern at increasing temperature of a NH_4-[Al]-magadiite with Si/Al ratio of 15

It was thus inferred that the introduction of Al ions does not affect the stability of the silica layers. Strong modifications of the XRD profiles occurred at T ≥ 473K, thus indicating that structural changes began at relatively low temperatures. The interlamellar space varied from 15.5 to 11.8 Å by heating at 473 K, due to desorption of water molecules. This process was also followed by IR and TGA studies, which suggested that, besides molecular water, silanol groups were eliminated at temperatures higher than 593K. A progressive collapse of the magadiite structure, which transforms into a dense phase, occurred from 723 to 1023 K.

The progressive condensation of silanols and elimination of water, allowed a coupling between adjacent silica layers, as suggested by the progressive intensification in the IR spectra of a specific band at *ca.* 704 cm^{-1} with increasing temperature [3]. Moreover, the silica rings also appeared irreversibly modified with the temperature (bands in the 650-500 cm^{-1}). Introduction of Al and subsequent Na^+ exchange with ammonium ions affected the hydrophilic properties of the materials. Indeed, TGA analysis showed that NH_4-[Al]-magadiite samples contained a much lower amount of water with respect to the parent Na-magadiite, as expected from the absence of Na^+ ions in interlamellar position. Decomposition of exchanged ammonium ions occurred at temperatures higher than 593K, and Brønsted acid sites were produced, as monitored by IR spectroscopy of CO adsorbed at 100K (Fig. 2).

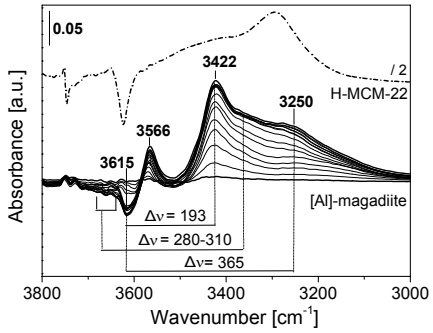

Fig.2: FTIR spectra evolution (in the 3800-3000 cm^{-1} range) of CO adsorbed at 100K on NH_4-[Al]-magadiite (Si/Al ratio =15)

IR data suggested that almost three different type of Brønsted acid sites were present in [Al]-magadiite samples, especially at higher Al content (see figure). The comparison with the results obtained on zeolite materials with similar Si/Al ratio allowed to evidence a higher heterogeneity of Brønsted acid sites in the case of Al-modified magadiite (dotted curve in the figure is related to a H-MCM-22 sample). The modification of the OH stretching vibration occurred after CO interaction ($\Delta\nu_{OH}$) indicates that [Al]-magadiite contains sites whose acidity is higher than for acid zeolites, being $\Delta\nu_{OH}\cong$ 280- 310 cm^{-1} for Al-OH groups and $\Delta\nu_{OH}\cong$ 365 cm^{-1} for Si(OH)Al sites, while $\Delta\nu_{OH}$ values associated to similar sites in zeolites are 200-220 and 300-320 cm^{-1}, respectively. These results indicated that the synthesis procedure allowed to introduce aluminum ions in tetrahedral coordination within the magadiite silica framework, in fully agreement with solid state ^{27}Al MAS-NMR studies. The presence of framework Al ions led to very strong Brønsted acid sites, which may be relevant for acid-catalyzed reactions.

References

1 Eugster H.P., Science 157 (1967) 1117- 2. A. Brandt, W. Schwieger, K.H. Bergk, Rev. Chim. Miner. 24 (1987) 564- 3. C. Eypert-Blaison,E. Sauzéat, M. Pelletier, L.J. Michot, F. Villiéras ad B. Humbert, Chem. Mater. 13 (2001) 1480; C. Eypert-Blaison,E. Sauzéat, M. Pelletier, L.J. Michot, F. Villiéras ad B. Humbert, Chem. Mater. **13** (2001) 4439- 4. S.T. Wong, S. Cheng, Chem. Mater. **5** (1993) 770- 5 J. S. Dailey, T. J. Pinnavaia, Chem. Mater. **4** (1992) 855

O 4.5

Preparation and optical properties of metal nanostructures.

Loredana Latterini, Matteo Amelia, Gian Gaetano Aloisi, Fausto Elisei
Dipartimento di Chimica and CENIM, Università di Perugia, Via Elce di Sotto 8, 06123 Perugia, Italy; (loredana@unipg.it)

Hybrid organic-inorganic nanostructures having a defined morphology and structure controlled at nanometric level represent a new and interesting class of materials for their biomimetic features and their versatility in many fields of high technologies.[1] Metal nanostructures have recently attracted attentions since they turned out to have interesting optical properties which can be tuned upon control of synthesis conditions.[2] In particular, the main resonance absorption peak of gold- and silver-spheres is centered at 520 and 430 nm, respectively and their spectral position and features are strongly affected by particle dimensions and shape[3] till they reach intense absorption in the near-infrared region (NIR) by emptying the interior of spherical nanoparticles to form hollow[4] or preparing Au-Ag alloys.[5] Furthermore, nanoshells convert absorbed light to heat with an efficacy and stability that far exceeds that of conventional dyes.[1]
Au and Ag (and their alloys) nanoparticles and nanoshells have been prepared by use of selective redox reactions and/or galvanic methods.

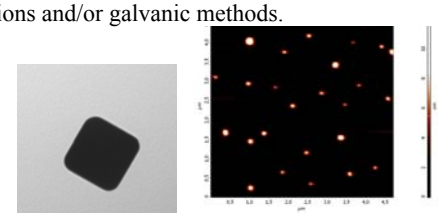

The statistical analysis of the particles dimensions obtained by TEM and AFM allowed to optimize the synthisis conditions to have full control of size and shaping.
Gold-nanoshell have been prepared upon deposition of gold clusters on silica dispersion or by galvanic exchange reactions. The preparation conditions were changed to tune the nanoshell resonance spectra to reach high absorption cross section in the NIR region. The thermal and photochemical stability of the nanoparticles has been tested and achieved by use of surfactants bearing substituent groups for further functionalization.
Au-nanosphere and nanoshell of about 20 nm diameter were conjugated to amminoacids and their interaction was quantitatively followed by spectrophotometric and AFM measurements.
These nanostructured materials having low toxicity and a large surface easily processable can be used as selective drug delivery systems and in photothermal treatments.

1. J.L. West, N.J. Halas, Curr. Opin. Biotech. **2000**, 11, 215-217. 2. P.K. Jain, K.S. Lee, I. El-Sayed, M. El-Sayed, J. Phys. Chem. B, **2006,** *110,* 7238-7248 3. C.A. Mirkin et al., *Science*, **1997**, 277, 1078. 4. J.L. West, N.J. Halas, *Annu. Rev. Biomed. Eng.*, **2003**, 5, 285. 5. D. P.O'Neala, L.R. Hirschb, N.J. Halas, J.D. Paynea, J.L. Westb, *Cancer Lett.*, **2004** 209, 171

O 4.6

Characterisation of highly dispersed gold on ZrO_2 catalysts active in the WGS reaction

Maela Manzoli[a], Flora Boccuzzi[a], Anna Chiorino[a], Floriana Vindigni[a], Francesco Pinna[b], Federica Menegazzo[b], Valentina Trevisan[b]
[a]*Dipartimento di Chimica I.F.M. and NIS Centre of Excellence, Via Pietro Giuria 7, 10125 Torino, Italy, maela.manzoli@unito.it*
[b]*Dipartimento di Chimica, Università di Venezia and Consorzio INSTM UdR Venezia, Venezia, 30123, Italy*

The most popular explanation for the variability of the catalytic properties of gold catalysts focuses on the amount of low-coordinated gold sites, whose concentration is usually related to the size of gold metallic particles.
High resolution transmission electron microscopy (HRTEM) can provide a particle size distribution from which a mean size can be obtained, but because of the hard detection of very small metallic particles (< 1 nm), this technique is not ideally applicable for samples containing highly dispersed gold.
In the present work, FTIR measurements of CO adsorbed at 120 K up to room temperature and quantitative CO chemisorption in the range 140-180 K were performed on differently prepared highly dispersed gold supported on zirconia.
The gold content was about 1 wt % for all samples and the metal has been loaded on the supports, previously calcined at 923 K, by deposition-precipitation at pH=8.6 with two different reagents: Na_2CO_3 and NaOH.
Both fresh and used (after 10 h in the water gas shift reaction mixture at 453-423) catalysts have been examined.
The aim was to determine quantitatively the amount of gold active sites by correlating the moles of chemisorbed CO with the integrated areas, normalized to the Au content, of the CO absorption bands on gold.
The results have been compared with those obtained (1) on the two reference samples provided by the World Gold Council, 1.51 wt% Au/TiO_2 and 4.48 wt% Au/Fe_2O_3, and with another low gold content catalyst, Au/Fe_2O_3 prepared by NaCN leaching of the parent sample.
The ratio mol_{CO}/mol_{Au} (0.32-0.36) and the I_{int}/ mol_{Au} (2.27-2.84) obtained for the fresh gold samples supported on zirconia are much larger than those related to the reference catalysts (0.028-0.033 and 1.05-1.10) indicating a gold dispersion at an atomic level.
On the contrary, the corresponding used samples showed analogous spectroscopic features to those of the reference catalysts, indicating an agglomeration of the metal after reaction as demonstrated by the appearance of metallic particles in the HRTEM images.

1. Menegazzo, F., Manzoli, M., Chiorino, A., Tabakova, T., Signoretto, M., Pinna, F., Perticone, N.; *Journal of Catalysis*, **2006**, *237*, 431 – 434.

O 4.7

Sostituzione cationica e proprietà in "bronzi di tungsteno"

V. Massarotti[a], D. Capsoni[a], M.Bini[a], M.C. Mozzati[b], C.B. Azzoni[b], P. Galinetto[b]
[a]*Dipartimento di Chimica Fisica "M. Rolla" dell'Università e IENI-CNR, Viale Taramelli 16, 27100 Pavia. e-mail: vincenzo.massarotti@unipv.it*
[b]*CNISM-Dipartimento di Fisica "A. Volta" dell'Università, Via Bassi 6, 27100 Pavia*

Alcune famiglie di ossidi misti consentono sostituzioni di cationi capaci di apportare significativi cambiamenti del comportamento chimico fisico del composto. Le variazioni di alcune proprietà fisiche possono così essere sfruttate per applicazioni in diversi campi, dall'elettronica alla catalisi, dall'elettro-ottica all'ottica non lineare. La famiglia dei bronzi di tungsteno, di formula $A_6B_2C_8O_{30}$, ha la struttura caratterizzata da tre differenti siti cationici [1] (Figura 1), sui quali opportune sostituzioni con elementi di transizione isovalenti o aliovalenti consentono l'ampia modulazione di proprietà elettriche e magnetiche richieste per applicazioni.

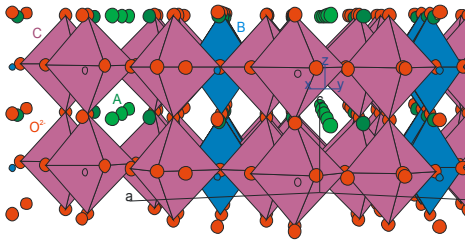

Figura 1 – Struttura di BZT con indicazione dei siti atomici.

Il reticolo ionico di $Ba_6Zr_2Ta_8O_{30}$ (BZT) [2], in cui Zr^{4+} e Ta^{5+} occupano i siti ottaedrici B e C, è stato paragonato ad un reticolo "vetroso", capace di ospitare cationi di transizione. Si può vedere che opportuni cationi M (Ni, Co, Fe, Mn, Cr) possono distribuirsi sui siti Zr e Ta assumendo diversi stati di valenza, determinabili con le misure EPR. Il sito A viene occupato esclusivamente dal grosso catione alcalino terroso, mentre la distribuzione di Zr o Ta sui siti B e C viene indagata con il metodo di Rietveld, cioè uno studio strutturale sulla base di misure di diffrazione da polveri. Nel composto BZT il sito C risulta occupato al 78% da ioni Ta^{5+} ed al 22% da ioni Zr^{4+}. Invece il sito B è occupato al 12.5% da Zr^{4+} ed all'87.5% da ioni Ta^{5+}.
Gli ioni droganti M sono selettivamente presenti sul sito C rispetto all'altro sito B. L'indagine strutturale suggerisce la maggiore deformazione dell'ottaedro C, caratterizzato da sei diverse lunghezze di legame comprese nell'intervallo 1.90-2.10 Å, rispetto all'ottaedro B, che presenta 4 legami equatoriali uguali di 1.98 Å e due legami apicali di 1.80 e 2.19 Å. Sulla base del valor medio delle distanze di legame l'ottaedro C risulta più dilatato dell'ottaedro B e la preferenziale sostituzione in C può quindi essere ricondotta alla maggiore deformazione del sito. Misure diffrattometriche e microscopiche (Figura 2) evidenziano, in campioni drogati con manganese e ferro, la formazione di cristalliti di dimensione media tre volte maggiore rispetto a quelli presenti nel campione puro o drogati con altri ioni (Ni, Co, Cr).

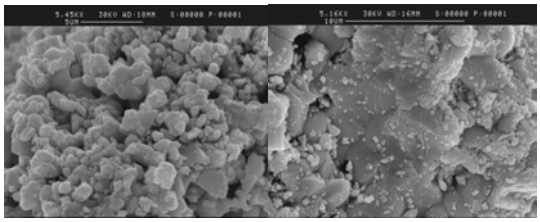

Figura 2 – Immagini SEM (5.5kX) del campione puro (sinistra) e drogato Fe (destra).

Informazioni sullo stato di valenza di ioni droganti e sulla loro distribuzione sui siti cationici possono essere ottenute dall'analisi dei segnali EPR attraverso un confronto con i risultati ottenuti sui campioni $Ba_6Ti_2Nb_8O_{30}$ (BTN) [3] di analoga struttura ma con Ti^{4+} e Nb^{5+} sui siti B e C (Figura 3).

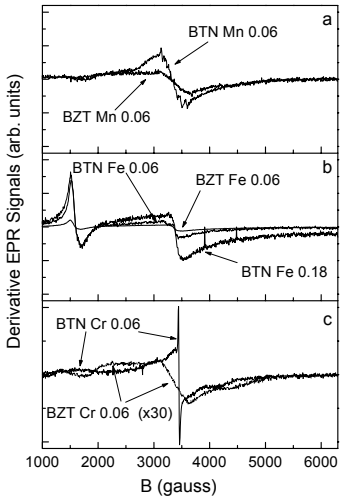

Figura 3 – Confronto dei segnali EPR dei campioni drogati BZT e BTN con differenti livelli di drogaggio.

I campioni drogati Mn e Fe mostrano segnali EPR tipici di ioni Mn^{2+} e Fe^{3+} in matrici disordinate o vetrose. Questo conferma che il sito ottaedrico C, preferenzialmente occupato dai droganti, è caratterizzato da una distribuzione di distorsioni.
Lo spettro micro-Raman del BZT ha alcune bande caratteristiche comuni a quello del BTN ma, nonostante le due strutture appartengano allo stesso gruppo spaziale tetragonale (*P4bm*), i loro spettri Raman mostrano differenze significative. Le larghe bande osservate nello spettro BTN trovano corrispondenza con picchi Raman stretti e ben definiti nelle stesse regioni spettrali. Il campione BTN mostra uno scattering allargato attorno a 250 cm^{-1}, praticamente assente in BZT dove si osserva un picco stretto a 295 cm^{-1}. Queste diverse caratteristiche possono essere imputate a diverso grado di simmetria, come si osserva in generale nel passaggio da struttura tetragonale a ortorombica. In effetti passando da BTN a BZT il comportamento degli spettri Raman è similare a quello osservato nel titanato di bario con l'abbassamento di temperatura, cioè con la transizione tetragonale → ortorombico → romboedrico. Il restringimento dei picchi Raman in BZT può essere giustificato dall'abbassamento di simmetria locale dovuto ad occupanza di Zr e Ta negli stessi siti precedentemente occupati da Ti e Nb in BTN. D'altra parte una distribuzione di distorsioni già rilevata da studi EPR e strutturali è più evidente in BZT che in BTN.

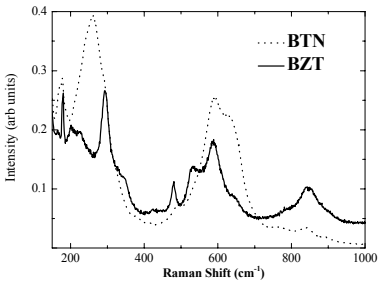

Figura 4 – Confronto fra spettri Raman di BZT e BTN puri.

1. Chi, E. O.; Gandini, A.; Ok, K. M.; Zhang, L.; Halasyamani, P. S. *Chem Mater*, **2004**, 16, 3616. 2. Massarotti, V.; Capsoni, D.; Bini, M.; Azzoni, C. B.; Mozzati, M. C.; Galinetto, P. *J. Phys. Chem. C*, **2007**, 111, 6857-6861. 3. Massarotti, V.; Capsoni, D.; Bini, M.; Azzoni, C. B.; Mozzati, M. C.; Galinetto, P.; Chiodelli, G. *J. Phys. Chem. B*, **2006**, 110, 17798.

O 4.8

Growth of neural cells on ultra thin organic semiconductors

E. Bystrenova[a], I.Tonazzini[a], P. Greco[a], S. Dutta[a], P. Stoliar[a], A. Lazar[a], C. Dionigi[a], M.G. Cacace[a], C. Martini[b], M. Jelitai[c], E. Madarasz[c] and F. Biscarini[a]

[a]*CNR, ISMN-Istituto per lo Studio dei Materiali Nanostrutturati,Via P. Gobetti 101, 40129 Bologna, I T A L Y, e.bystrenova@bo.ismn.cnr.it*
[b]*Department of Psychiatry, Neurobiology, Pharmacology and Biotechnology University of Pisa, Via Bonanno 6, 56126 Pisa, I TA L Y*
[c]*Laboratory of Cell and Developmental Neurobiology, Inst. of Experimental Medicine of Hungarian Academy of Sciences, Szigony u. 43,1083 Budapest, H U N G A R Y*

Many technological advances are currently being developed for nano- and micro- fabrication, offering the ability to create and control patterns of soft materials with sub micrometric precision[1].

In this work we report the deposition of cells on organic semiconductor ultra-thin films. This is a first step towards the development of active bio/non bio systems for electrical transduction that could be integrated directly in vitro. Thin films of pentacene molecules, whose thickness was systematically varied between 1 and 50 nm, were grown by high vacuum sublimation[2]. Human astrocytoma cells and NE-4C neural stem cells were grown and maintained in culture in standard condition (37^oC, 95% humidity, $5\%CO_2$) in medium supplemented. Small molecules (PL, laminine, APTES, dodecylamine, PEG etc.) were patterned onto the surface[3] by template-assisted deposition in order to spatially modulate the cell adhesion on the surface. Released pre-patterned multilayers were exposed to cell culture medium incubated at 37^oC for 70h.

Viability of cells in time was measured as a function of roughness and the characteristic morphology of ultra thin organic film, as well as the features of the patterned molecules. Optical fluorescence microscope coupled to atomic force microscope was used to monitor the presence, density and shape of deposited cells.

This work is supported by Project EU-NMP-STRP 032652 BIODOT.

[1] Ainslie KM, Bachelder EM, Borkar S, Zahr AS, Sen A, Badding JV, Pishko MV, Cell Adhesion on Nanofibrous Polytetrafluoroethylene (nPTFE), *Langmuir* **2007**, 23, 747.
[2] Dinelli F, Murgia M, Levy P, Cavallini M, Biscarini F, de Leeuw DM, Spatially correlated charge transport in organic thin film transistors. *Phys Rev Lett*., **2004**, 92, 116802.
[3] Bystrenova E, Facchini M, Cavallini M, Cacace M. G., Biscarini F, Multiple length scale patterning of DNA by stamp assisted deposition, *Angew. Chem. Int. Ed*., **2006**, 45, 4779.

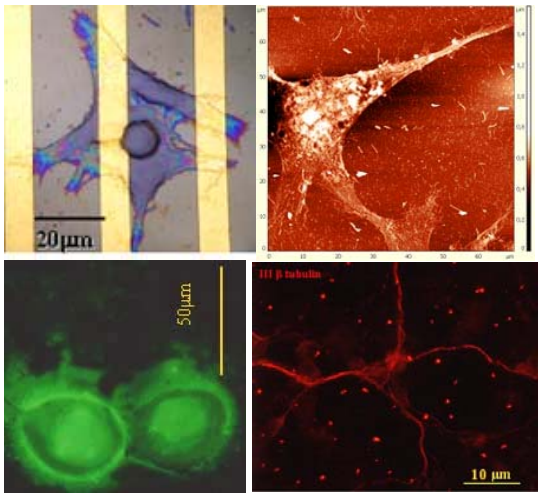

Fig.1: Optical micrograph, AFM in liquid and fluorescent images obtain on astrocytoma and neuronal cells growth on organic thin film.

SEZIONE

CHIMICA FISICA TEORICA E COMPUTAZIONALE

I 5

Ab-initio molecular dynamics of solute-solvent systems based on non periodic boundary conditions: applications to spectroscopic properties.

Nadia Rega[a]
[a]*Dipartimento di Chimica and INSTM, Universita' 'Federico II',Complesso Universitario di M.S.Angelo, via Cintia, I-80126 Napoli, Italy, nadia.rega@unina.it*

We employ ab-initio dynamics to simulate systems in aqueous solution.
The approach is based on the combination of QM/MM molecular dynamics techniques using localized basis sets and non-periodic boundary conditions, and a posteriori high-level quantum mechanical calculations.
This integrated methodology allows for a detailed analysis of the influence of stereoelectronic, microsolvation and short-time dynamic effects on the resulting spectroscopic parameters.
We present some pilot applications chosen as prototypes to treat solvent effects of strategical importance in biochemistry, with particular attention to the modulation of spectroscopic properties.
Such a model represents a valid alternative to the standard picture given by periodic boundary conditions for modeling condensed phase systems.

1. Rega N.; Brancato G.; Barone V.; *Chem. Phys. Lett.* **2006**, 422, 367.
2. Brancato G.; Barone V.; Rega N.; *Theor. Chem. Acc.*, **2007**, DOI:10.1007/s00214-006-0216-z .

O 5.1

On the active role of substrate reactivity in the context of enzymatic dehydrogenations: a theoretical investigation.

Gloria Tabacchi[a], Maria A. Vanoni[b], Aldo Gamba[a], Ettore Fois[a]
[a]*Dipartimento di Scienze Chimiche ed Ambientali and INSTM Università degli Studi dell'Insubria, Via Lucini 3, I-22100 Como (Italy), gloria@fis.unico.it*
[b]*Dipartimento di Scienze Biomolecolari e Biotecnologie Università degli Studi di Milano, Via Celoria 26, I-20133 Milano (Italy)*

Aim of the present study is trying to establish, by first principles calculations of physico-chemical properties of enzymatic dehydrogenation substrates, how the reactivity of specific substrates is related to the reaction mechanism adopted by the corresponding enzymes. Flavoenzymes, a class of oxidoreductases implicated in a variety of fundamental redox reactions of cell metabolism[1], have been chosen as test cases because they may accomplish substrate oxidation through different reaction paths.[2] For instance, in spite of the wealth of available experimental data, the dehydrogenation mechanism of α-hydroxyacids to the corresponding ketoacids is still debated.[2-3] The prototype enzyme flavocytochrome b_2 (Fcb2) catalyzes the oxidation of L-lactate to pyruvate.[3] According to the proton abstraction (PA) or carbanion mechanism (Scheme 1a), the lactate α-proton Hα is abstracted by an active site base with formation of an α-carbanion intermediate, which donates two electrons to the flavin and eliminates the α-hydroxyl proton in order to obtain pyruvate.[3a,b] In the hydride transfer (HT) mechanism (Scheme 1b), the active site base abstracts the lactate α-hydroxyl proton and Hα is transferred to the flavin as a hydride.[3c]

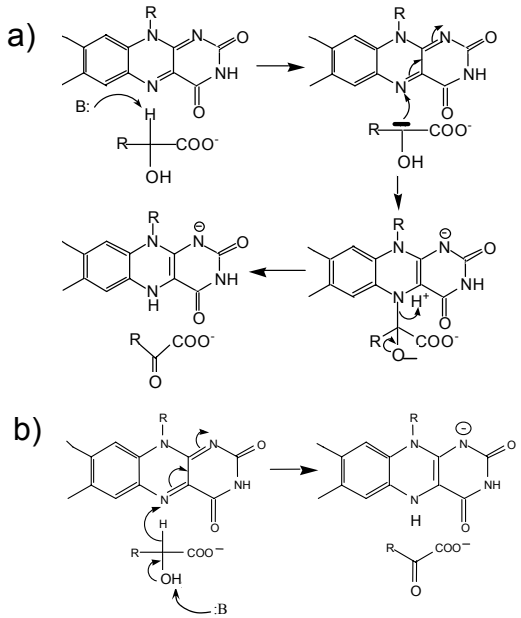

Scheme 1: L-lactate oxidation to pyruvate in Fcb2 *via:* a) PA mechanism; b) HT mechanism.

In order to help solving the Fcb2 mechanistic issue, we have addressed the question of the reactivity of lactate and of its deprotonated forms, i.e. the α-carbanion and the alkoxide, via ab initio calculations.[4] The geometries of the isolated species were optimized at the MP2/cc-pVTZ level, harmonic frequencies and atomic charges were calculated and the electronic structure investigated by NBO analysis. [5] In L-lactate, the Cα-Hα bond is longer and its stretching frequency lower with respect to the methyl C-H bonds. In the lactate alkoxide, which is more stable than the carbanion by 22.7 kcal mol^{-1}, the Cα-Hα bond is significantly longer than in L-lactate (0.039 Å) and is characterized by a large red shift of its stretching frequency (462 cm^{-1}); moreover an increase of electronic charge on Hα of ~ 0.2 e is found. NBO deletion analysis [5] indicated that such a significant Cα-Hα bond weakening is due to negative hyperconjugation, which implies electron density transfer from the lone pairs on the hydroxyl oxygen to the C-H σ* antibonding orbital.[6] The antibonding character of the Cα-Hα bond of lactate is greatly enhanced in the alkoxide, which is therefore poised for pyruvate conversion, while α-proton abstraction does not contribute to weaken the carbanion α-OH bond in order to obtain the reaction product. These results indicated the HT path as the oxidation mechanism favoured by the substrate.
The effect of the enzyme active site residues on the intrinsic reactivity was investigated on a model of the Fcb2- L-lactate Michaelis complex [7] using first principles molecular dynamics.[8] Simulation results indicated that the binding of the substrate with the active site residues enhances the n-σ* interaction responsible of the Cα-Hα bond weakening, already present in the isolated lactate. Therefore, the finite temperature behaviour in the model enzyme site also supports the HT mechanism and suggests that this enzyme may accelerate dehydrogenation by amplifying the lactate intrinsic

reactivity via hydrogen bonding interactions with the active site base.
In order to investigate whether a more general relationship may be established between the substrate intrinsic reactivity and the dehydrogenation mechanism operative in flavoenzymes, geometry optimizations, frequency calculations and NBO analysis were also performed on a series of substrates of other flavin containing enzymes for which the mechanism is well established.[1-3,7,9] For each isolated substrate, calculated bond elongations, frequency red shifts, and energetic contribution of n-σ* interaction are in line with the oxidation mechanisms occurring in the corresponding enzyme active sites, thus providing further support to the relevance of negative hyperconjugation in enzymatic dehydrogenations. On a general ground, from the present study it emerges that intrinsic substrate properties may drive the catalytic path in enzymes active sites.

1. De Colibus, L.; Mattevi, A. *Curr. Opin. Struct. Biol*. **2006**, *16*, 722-728.
2. Fraaije, M.W.; Mattevi, A. *Trends Biochem. Sci*. **2000,** *25*, 126-132.
3. Lederer, F. in: *Chemistry and Biochemistry of Flavoenzymes* **1991** (Müller, F., Ed.) pp.153-242, CRC Press, Boca Raton, FL.; b) Lederer,F.; Amar, D.; Ould Boubacar, A.K.; Vignaud, C. *in Flavins and Flavoproteins*, ed. T. Nishino, R. Miura, M. Tanokura and K. Fukui, ArchiTect Inc.,Tokyo**, 2005**, pp. 193-204; c) Fitzpatrick, P.F. *Bioorganic Chemistry* **2004**, *32*, 125-139.
4. Gaussian 98, Revision A.11.3, Frisch, M. J. et al., Gaussian, Inc., Pittsburgh PA, **2002**.
5. a) Reed, A.E.; Curtiss, L.A.; Weinhold, F. *Chem. Rev*. **1988**, *88*, 899-926; b) Glendening, E.D.;Reed, A.E.; Carpenter, J.E.; Weinhold, F. NBO 3.1; c) Goodman, L.; Sauers, R.R. *J. Comp. Chem.A* **2007**, *28*, 269-275.
6. a) DeFrees, D.J.; Bartmess, J.E.; Kim, J.K.; McIver, T.T.; Hehre, W.J. *J. Am. Chem. Soc*. **1977**, 99, 6451-6452; b) DeFrees, D.J.; Hassner, D.Z.; Hehre, W.J.; Peter, E.A.; Wolfsberg, M. *J. Am. Chem. Soc*., **1978**, *100*, 641-643; c) Lii, J.H.;.Chen, K.H.; Allinger, N.L. *J. Phys. Chem. A* **2004**, *108*, 3006-3015.
7. a) Vanoni, M.A.; Tabacchi, G.; Lederer, F.; Gamba, A.; Fois, E., in *Flavins and Flavoproteins*, ed. T. Nishino, R. Miura, M. Tanokura and K. Fukui, ArchiTect Inc.,Tokyo, **2005**, pp. 281-287; c) Tabacchi G., Vanoni, M.A.; Gamba, A.; Fois, E. *ChemPhysChem* **2007** in press.
8. a) Car, R.; Parrinello, M. *Phys. Rev. Lett*. **1985**, *55*, 2471-2474; b) CPMD V3.11 (www.cpmd.org) Copyright IBM Corp. 1990-2006, Copyright MPI für Festkörperforschung Stuttgart 1997-2001.
9) Tilocca, A.; Gamba, A.; Vanoni, M.A.; Fois, E.; *Biochemistry* **2002**, *41*, 14111-14121

O 5.2

Vibrational Corrections to Dipolar Coupling Constants: an Alternative for Determining Equilibrium Distances from Rotational Spectroscopy

Cristina Puzzarini[a], Thorsten Metzroth[b], Jürgen Gauss
[a] *Dipartimento di Chimica ``G. Ciamician", Università degli Studi di Bologna, Via Selmi 2, I-40126 Bologna, Italy, cristina.puzzarini@unibo.it*
[b] *Institut für Physikalische Chemie, Universität Mainz,D-55099 Mainz, Germany*

The main interaction between the spins of two nuclei is the dipole-dipole coupling between their magnetic moments. The importance of these interactions lies in the facts that

a) dipolar coupling constants should be considered for the proper analysis of the hyperfine structure in rotational spectra and
b) that dipolar-coupling tensors provide an alternative way for determining bond distances (based either on the analysis of rotational or NMR spectra).
In principle, the determination of the dipolar coupling constants just require knowledge of the molecular equilibrium geometry, though quantum-chemical investigations are necessary to evaluate the vibrational corrections. In this presentation we will compare computed dipolar coupling constants for several small to medium-sized molecules to experiment, and demonstrate the importance of including vibrational corrections for accurate predictions. In addition, we will show how experimental dipolar coupling constants together with computed vibrational corrections can be used to derive equilibrium bond distances.

O 5.3

Reazione di idrolisi della molecola di diborano in soluzione tramite simulazioni di dinamica molecolare ab initio

Elisa Di Pietro[a], Gianni Cardini[a,b], Vincenzo Schettino[a,b]
[a]*Dipartimento di Chimica, Univerista' di Firenze, via della Lastruccia 3, 50019 Sesto Fiorentino, Firenze, dipietro@chim.unifi.it*
[b]*European Laboratory for Nonlinear Spectroscopy (LENS), via Nello Carrara 1, 50019 Sesto Fiorentino, Firenze*

Tramite calcoli di dinamica molecolare ab initio di tipo Car-Parrinello[1] e' stata studiata la reazione di idrolisi del diborano in soluzione acquosa[2]. La reazione totale e' stata divisa in due parti, entrambe simulate nell'insieme Blue Moon[3] per ottenere informazioni sia sul meccanismo di reazione che sul profilo energetico.
La prima parte della reazione prevede la rottura della molecola di diborano in una molecola di H_2BOH, in un protone e in uno ione BH_4^-, che, successivamente diventa il reagente della seconda parte della reazione. L'energia libera di Helmoltz relativa al primo step reattivo e' di 13.00 kcal/mol.
Nella seconda parte della reazione lo ione BH_4^- reagisce con due molecole d'acqua dando luogo ad un'altra molecola di H_2BOH, uno ione ossidrile e due molecole di idrogeno.
Nel complesso emerge chiaramente che l'effetto del solvente sulla reazione e' piccolo, in particolare dallo studio della struttura elettronica di reagenti e prodotti e' possibile individuare solo lievi spostamenti dei doppietti elettronici relativi alla posizione dei centri di Wannier.
Infine, e' stata individuata l'esistenza di un addotto, $BH_3{\cdot}H_2$, il quale e' legato da un debole legame covalente a due elettroni e tre centri, che avviene tra gli elettroni nell'orbitale di legame della molecola di idrogeno e l'orbitale vuoto dell'atomo di boro nella molecola di BH_3. A 300 K il complesso e' rimasto stabile in soluzione per tutta la durata della simulazione (10 ps).

1. Car, R.; Parrinello, M.; P*hys. Rev. Lett.*, **1985,** *55*, 2471 – 2474. 2. Di Pietro, E.; Cardini, G.; Schettino, V.; *Phys. Chem. Chem. Phys.,* 2007, accepted. 3. Carter, E; Ciccotti, G.; Hynes, J.; Sprik, M..; *Chem. Phys. Lett.,* **1989**, *156*, 472.

O 5.4

From paratropic ring currents to closed-shell molecular magnets

Guglielmo Monaco, Riccardo Zanasi
Dipartimento di Chimica,Università di Salerno, via ponte Don Melillo, 84084 (SA) Fisciano, gmonaco@unisa.it

According to the laws of classical electromagnetism, the free electrons in a metallic ring are set in circulation by an external magnetic field and generate a magnetic field which is opposed to the external field. This phenomenon is common to the vast majority of closed-shell molecules. However quantum mechanics also allows the electrons to set in a paratropic circulation, which generates a field which adds to the external field, as happens in open-shell systems. Paratropic currents are generally too weak to dominate the magnetic behaviour of the molecule. Antiaromatic annulenes are a very interesting exception although they are generally unstable in the planar form with the most promising paratropic current. In the effort to design molecular systems which could exploit the characteristics of these systems, we demonstrated a novel theorem on the factorization of Kekulé counting, which guided us to design novel molecular systems ([8,5]-coronene and [12,5]-coronene), for which ab initio calculations gave a paramagnetic response along a molecular axis, which in [12,5]-coronene was so strong to dominate the isotropic magnetic behaviour of the molecule.[1] These coronenes are unique in that the two concentric rings of the molecular system both show a paratropic ring current, which is not a simple consequence of the fact that both rings have 4*n* pi electrons, but stems form the peculiar connectivity of the systems. The utility and the limitations of the factorization of Kekulé count as a useful tool for molecular design and for the interpretation of density currents have been investigated in several cases.

1. Monaco, G.; Zanasi, R.; Fowler, P. W.; Lillington, M.; *Angew. Chem. Int. Ed.*, **2007**, *46*, 1189-1192.

O 5.5

DFT-D study of the benzene dimer: structural minima, energies and molecular dynamics.

Michele Pavone[a]
Department of Chemistry Princeton University, 08540 Princeton NJ, USA; mipavone@unina.it

The benzene dimer is the simplest model for weak non-covalent interactions of the aromatic π–π type. Despite the small energy amount involved in the benzene-benzene binding (1-3 kcal/mol), the aromatic π–π interactions have been proven to play a crucial role as stabilizing forces in biological macromolecules, supramolecular self-assembly and molecular recognition. For these reasons, in the past decades there has been a great theoretical and experimental progress in a joint effort to characterize the structures and energetics of benzene clusters.[1]
Here we report the structures, the binding energies and the harmonic frequencies of the benzene dimer minima, computed at the well-known B3LYP density functional theory level, with the inclusion of a semiempirical correction term to properly account van der Waals forces, as recently proposed by Grimme.[2] Our results are in fair agreement with those obtained with expensive post-HF methods. Moreover, thanks to purposely tailored GTO basis set, that minimizes the BSSE and provides affordable computational costs, we performed first-principle molecular dynamics of the benzene dimer within the ADMP scheme[3]: average structures and computed frequencies will be dicussed.

a) Permanent address: Dipartimento di Chimica, Università di Napoli Federico II, Via Cintia I, 80126 Napoli, Italy
1. Muller-Dethlefs, K.; Hobza, P.; *Chem. Rev.*, **2000**, *100*, 143 – 167. 2. Grimme, S.; *J. Comput. Chem.*, **2006**, *27*, 1786 –1799.
3. Schlegel, H. B.; Iyengar, S. S.; Li, X.; Millam, J. M.; Voth, G. A.; Scuseria, G. E.; Frisch, M. J. *J. Chem. Phys.*, **2002**, *117*, 8694

O 5.6

Dynamics of the photodeactivation processes in DNA nucleobases

Fabrizio Santoro[a], Roberto Improta[b]
[a]*Istituto per i Processi Chimico Fisici del CNR, Via Moruzzi 1,I-56124 Pisa,f.santoro@ipcf.cnr.itr*
[b]*Roberto Improta, Istituto di Biostrutture e Bioimmagini del CNR, via Mezzocannone 8, I-80131 Napoli.*

Sunlight is essential to life but, as the other side of the coin, it is also a potential carcenogenic agent, and consequently evolution has selected highly photostable molecules to encode the genomic information. Their photostability is ensured by highly efficient decay pathways that transform the electronic excitation into vibrational energy and finally into heat [1].

The study of DNA and RNA photostability has been discouraged for a long time by the same reason that makes it so interesting: the extreme speed of the deactivation processes that is responsible for the very low quantum yields of fluorescence of the purine and pirimidine bases, traditionally considered as non fluorescent at all. Recently, the impressive progresses in time-resolved spectroscopies, up to the femtosecond regime, and the simultaneous advances in theoretical and computational methods, have allowed a true renaissance of the field. The deactivation mechanism of the single nucleobases after the UV π□ π* excitation has been recently extensively investigated by different experiments, from transient absorption to fluorescence up-conversion, in several solvents. It is now clear that the deactivation is ultrafast (from 200 fs in uracyl to some ps for the slower component in adenine) and can show mono- or bi-exponential features [1]. A reliable picture is now emerging for these processes, also thanks to the important help of theoretical and computational studies. They have allowed to locate the conical intersections (CI) [2-3], the funnels that drives back the system to the ground electronic state, to describe the minimum energy path (MEP) from the Franck-Condon (FC) to the CI regions, and to explore some portions of the excited potential energy surfaces (PES) [4-5]. Nonetheless, the description of the process remains static, and many issues are still to be clarified, concerning e.g. the solvent effect and the possible role of intermediate *n*□ π* states.

While the "static" computational study of the relevant PES and their topology is an important first step, there is no doubt that a full understanding of the mechanism may only come from a careful investigation

of the nuclear dynamics (including solvent modes). In fact, in presence of a large kinetic energy an excited wave packet may explore regions far from the MEP, while a given barrier along its way is more or less effective depending on the carried momentum distribution.

In this contribution we report our results, based on an extensive TD-DFT investigation of the excited energy surfaces of uracil and 5-fluorouracil in acetonitrile and aqueous solution, allowing the investigation of both the substituent and the solvent effect. We employ the PBE0 hybrid functional, while the solvent is described both at implicit level, by the polarizable continuum method, and by explicitly including the water molecules relevant for hydrogen bonds. We show strong static [5] and dynamical arguments in favour of a relevant role played by an intermediate $n\square\ \pi^*$ state in the decay of the initially excited $\pi\square\ \pi^*$ population, thus confirming the very recent experimental findings [6]. Our results further suggest that the solvent can drastically tune the $n\square\ \pi^*$ role in the deactivation process.

The understanding of the dynamics of isolated nucleobases is the necessary pre-requisite for a full comprehension of the deactivation processes in the real bio-polymers, where nonetheless inter-bases interactions might modify the efficiency of the single-base decays and open new competitive pathways [7-9]. As stated by Kohler, an expert in the field, in 2004 "the greatest future challenges concern excites dynamics in base multimers, including natural DNAs and RNAs" [1].

We present our TD-DFT results on adenine dimers and trimers pointing out a strong tendency to localize the Uv excitation on a single monomer but also, at the same time, the existence of minima on the first-exited state corresponding to dimer charge-transfers, confirming the existence of competitive decay pathways [10].

1. Crespo-Hernández, C. E. et al. ; *Chem. Rev*., **2004**, *104*, 1977.
2. Serrano-Andrés, L. et al.; *Proc Natl. Acad. of Science, USA* **2006**, *103*, 8691
3. Matsika, S; *J. Phys. Chem. A*, **2005**, *105*, 7538.
4. Markovitsi, D. et al. ; *J. Am. Chem. Soc*., **2005**, *127*, 17130.
5. Santoro, F.; Barone V.; Gustavsson, T.; Improta, R.; *J. Am. Chem. Soc.* **2006**, *128*, 16312
6. Hare, P. M. et al.; *Proc. Natl. Acad. Science, USA*, **2007,** *104*, 435
7. Crespo-Hernández C. E. et al ; *Nature*, **2005**, *436*, 1141; ibidem **2006**, *441*, E8.
8. Markovitsi, D.et al.; Nature, 2006, *441*, E7, (2006).
9. Kwok ,W.-M. et al. ; *J. Am. Chem. Soc.*, **2006**, *128*, 11894.
10. Santoro, F.; Barone V.; Improta, R *Proc Natl. Acad. of Science, USA*; **2007**, in press

O 5.7

A combined approach of theory and experiment for the study of platinum clusters derivatives

Gabriele Manca[a] , Alberto Albinati[b], Samantha Bruzzone[a], Fabrizia Fabrizi de Biani[c], Carla Guidotti[a], Piero Leoni[a], Lorella Marchetti[a], Piero Zanello[c]

[a] *Dipartimento di Chimica e Chimica Industriale, Università di Pisa, via Risorgimento 35, Pisa. Email:g.manca@dcci.unipi.it*

[b] *Dipartimento di Chimica Strutturale e Stereochimica Inorganica, via Venezian 21, Milano*

[c] *Dipartimento di Chimica,Università di Siena, via A. Moro, Siena.*

In the last years remarkable chemical and physical efforts have been addressed toward the realization and the study of composite compounds which can be employed in the technological field. In several cases the complexity of the observed phenomena makes very difficult an accurate knowledge of the underlying mechanisms through an experimental approach alone. On the other side, nowadays the ability of the density functional theory to reproduce the chemical and physical properties of large complexes is satisfactory. In this communication we report the synthesis and the spectroelectrochemical and computational characterization [1,2] of compounds 1-4 (Fig.1) containing one or two platinum clusters linked to an ethynylferrocene or to an ethynylbiferrocene , in which a MMCT is observed upon oxidation.

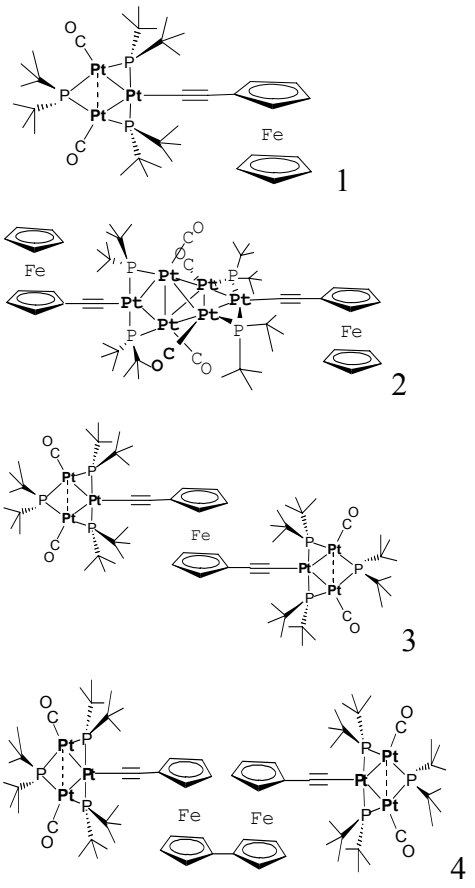

Figure 1

The aforesaid compounds have been studied using density functional methods with B3LYP functional and LANL2DZ as basis set with polarization d functions on P atoms

1. a) Tarraga, A.; Molina, P.; Curiel, D.; Velasco, M. D.; *Organometallics,* **2001,** *20*, 2145, b) Jiao, J.; Long, G. J.; Grandjean, F.; Beatty, A.M.; Fehlner, T. P.; *J. Am. Chem. Soc.,* **2003,** *125***,** 7522, 2. Long, N. J.; Martin, A. J.; Vilar, R.; White, A. J. P.; William, D. J.; Younus, M.; *Organometallics,* **1999**, *18*, 4261.

O 5.8

Insight into Elastic properties of binary alkali silicate glasses: prediction and interpretation through atomistic simulation techniques.

Alfonso Pedone,[a] Gianluca Malavasi,[a] Alastair N. Cormack,[b] Ulderico Segre[a] and M. Cristina Menziani.[a]
[a]*Dipartimento di Chimica, Università di Modena e Reggio Emilia, via G. Campi 183, 41100 Modena. apedone@unimo.it*
[b] Kazuo Inamori School of Engineering, New York State College of Ceramics, Alfred University, Alfred, NY 14802, USA

Molecular dynamics simulations and energy minimization techniques have been applied for the first time to determine the whole set of elastic properties (Young's modulus, shear modulus, bulk modulus and Poisson's ratio) of alkali silicate glasses with different ion modifiers (Li, Na and K) in the range 0 to 30% mol of alkaline oxide. The force-field recently developed by Pedone et al.[1] has been implemented in the DLPOLY package[2] which was used to create glass structures via a melt-quench process.[3] The static method included in the GULP package[4] was used to calculate the elastic properties. Excellent agreement has been found between the simulation results and the experimental data. The peculiar behaviour of the Li containing glasses with respect to the Na and K ones is discussed in terms of the glass structural features. It was found that the elastic properties variations as a function of alkali addition can be explained by three concurrent factors:[5] 1) the depolymerization of the silica network; 2) the establishment of alkali-Non-Bridging-Oxygen bonds which increase the cohesion of the glass; and 3) the increase of the glass packing density due to decreasing of the free volume.

1. Pedone, A.; Malavasi, G.; Menziani, M. C.; Cormack, A. N.; Segre, U., *J. Phys. Chem. B* **2006,** 110, 11780.
2. Smith, W.; Forester, T. R., *J. Mol. Graph.* **1996,** 14, 136.
3. Malavasi, G.; Menziani, M. C.; Pedone, A.; Segre, U., *J. Non-Cryst. Solids* **2006,** 352, 285.
4. Gale, J. D.; Rohl, A. L., *Mol. Simul.* **2003,** 29, 291.
5. Pedone, A.; Malavasi, G.; Cormack, A. N.; Segre, U.; Menziani, M. C., *Chemistry of Materials* **2007,** in Press.

CONTRIBUTI

POSTER

SEZIONE

CHIMICA FISICA BIOLOGICA ED AMBIENTALE

P 1.1

Nuclear Magnetic Resonance of ^{129}Xe and ^{1}H: structural characterization of hydrophobic cavities of Myoglobins

Roberto Anedda[1], Benedetta Era[2], Antonella Fais[2], Matteo Ceccarelli[3], Marcella Corda[2], Mariano Casu[1] and Paolo Ruggerone[3,4]

[1]Dipartimento di Scienze Chimiche, Università di Cagliari, 09042 Monserrato (CA), Italy.[2]Dipartimento di Scienze Applicate ai Biosistemi, Università di Cagliari,09042 Monserrato (CA), Italy.[3]CNR-INFM SLACS, Dipartimento di Fisica, Università di Cagliari,09042 Monserrato (CA), Italy.[4]CNR-INFM CRS DEMOCRITOS, SISSA, via Beirut 2-4, 34014 Trieste, Italy[a]

The relevance of an experimental technique relies on the possible manifold information that can be extracted but also on its complementing attitude. An example is the use of ^{129}Xe NMR as a powerful and attractive biomolecular probe for structural characterization of proteins. The chemical inertness of xenon, the polarizability of its electronic cloud, i.e. the sensitivity of its NMR parameters (chemical shift, line shapes, relaxation rates) toward non-bonded local environment and its hydrophobic character make this noble gas an ideal probe for the characterization of hydrophobic cavities within proteins[1].

Testing the ability of xenon as an efficient biomolecular probe of cavities in globular proteins and, particularly, in myoglobins (Mbs) is crucial to extract important information on their structure and function, but at the same time challenging due to the presence of different interaction sites besides the heme iron. However, the possibility to easily tune the oxidation state of the metal ion gives the unique opportunity to study interactions of different physical nature in the same protein, which are sensed by both the guest and the host itself.

Despite a number of progresses have recently significantly improved the technique, many issues concerning the molecular details of the binding process and on possible local distortions induced by xenon in the host structure are still unclear. Moreover, the scientific interest toward this technique is amplified by the possible use of xenon in clinical imaging and anesthesia.

Clearly, hints on the characterization of cavities and xenon-protein affinity can be achieved by comparatively studying myoglobins of different species or mutated myoglobins, as in a recent NMR investigation of the pig and horse metmyoglobins (MMbs)[2]. There, the combined use of the ^{129}Xe chemical shift and the ^{129}Xe spin lattice relaxation rate as a function of xenon and protein concentration has unraveled the influence of the structure and/or hydrophobicity of a cavity on its xenon occupancy. Horse and pig MMbs differ by 14 amino acids, mostly located on the protein surface. Only one difference involves the proximal cavity with the isoleucine 142 (Ile142) in horse Mb replaced by a methionine (Met142) in pig. The residues lining the proximal cavity (also called Xe1) in horse and pig Mbs are highlighted in the Figure. The study clearly supported the presence of xenon on the Xe1 site in pig MMb, which is, however, less populated than in the horse MMb, pointing out the existence of other binding sites besides Xe1.

Myoglobins from different species (horse, pig, sheep, rabbit) which differ for aminoacid composition of Xe1 cavity and for some external aminoacids, were studied in order to characterize the binding process. ^{1}H NMR studies on solutions of low-spin Cyano-MetMyoglobins (CNMb) from pig and horse pressurized with xenon gas show that, at a first approximation, the Xe1 cavity is the main binding site for xenon in horse Mb. A two-site thermodynamic model allows determining the binding constant, giving results in very good agreement with literature.

Moreover, by exploiting hyperfine interactions between the heme iron and the protons of residues surrounding the active site of horse CNMb, we collected evidences of local distortions caused by the guest xenon on the structure of the protein.

^{1}H and ^{129}Xe NMR measurements are in good agreement and it can be demonstrated that while the Xe1 cavity represents the principal binding site of xenon in horse Mb, a second cavity must be considered in pig Mb. The model adopted allows distinguishing between xenon-protein specific and non-specific interactions. The results undoubtedly show that binding of xenon to internal sites of the proteins is strongly influenced by the size and geometry of the cavity. The results are confirmed and substantiated by studying the myoglobins of sheep and rabbit.

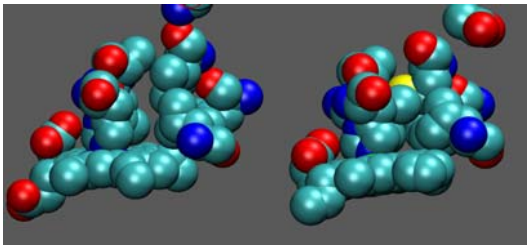

(a) **(b)**

Figure: Residues lining the Xe1 cavity in (a) horse (Leu89, Ala90, His93, Leu104, Phe138, Ile142, Heme) and (b) pig (Leu89, Ala90, His93, Leu104, Phe138, Met142, Heme) Mbs. The figures are obtained with the visualization program VMD (Humprey et al. 1996).

1. Goodson, B.M.; *J. Magn. Reson.* **2001**, *155*, 157 – 216. 2. Corda, M.; Era, B.; Fais, A. and Casu, M.; *Biochim. Biophys. Acta* **2004,** *1674*, 182 – 192.

P 1.2

Application of ISORROPIA and SOAP modules within CAMx model for PM simulation

Elena Chianese,[b] Guido Barone,[a] Angelo Riccio[b]

[a]Dipartimento di Chimica, Università di Napoli "Federico II", via Cintia, Napoli.

[b]Dipartimento di Scienze Applicate, Università degli Studi di Napoli "Parthenope", via De Gasperi 5, Napoli

CAMx[1] air quality model allows the study of emission, reaction and dispersion of gaseous pollutants emitted by anthropogenic and biogenic sources. Air quality problems are complicated by the presence of heterogeneous phases, particularly particulate matter. Atmospheric PM can be produced by gaseous precursors reactions, both from inorganic and organic species.

In this work we use ISORROPIA[2] and SOAP[3] modules for the study of inorganic and organic secondary aerosols from their precursors, for European and Italian domains;

particularly we present the comparison between simulated and observed data for 2001 year.

[1] Comprehensive Air quality Model with eXtension (see http://www.camx.com).
[2] Nenes, A.; Pilinis, C.; Pandis, S.N; *Aquatic Geochemistry,* **1998,** *4*, 123-152.
[3] Strader, R.; Lurmann, F.; Pandis, S.N.; *Atmos. Environ.,* **1999,** *33*, 4849-4863.

P 1.3

An application of OSAT probing tool in Southern Italy

Elena Chianese[b], Alessia Riccio[a], Guido Barone[a], Angelo Riccio[b].
[a]*Dipartimento di Chimica, Università di Napoli "Federico II", via Cintia, Napoli.*
[b]*Dipartimento di Scienze Applicate, Università degli Studi di Napoli "Parthenope", via De Gasperi 5, Napoli*

Air quality problems are related to many substances in the atmosphere directly generated by human activities or produced by reactions involving gaseous precursors.
Among them ozone, produced by VOC and NOx photochemical reactions, plays a key role in determining human health damages and monuments degradation.
Strategies for reduction of secondary atmospheric pollutants, as ozone, require the knowledge of many factors as: precursor emission, spatial location of sources, and so on.
All these parameters cannot be forecast by an air quality model; in this work we present the study of ozone formation in a summer period using CAMx model[1] with OSAT[2] probing tool, discussing results on ozone formation limiting conditions, sources and areas producing precursors.

P 1.4

PM INDOOR POLLUTION REDUCTION BY TiO_2 FILMS.

Elena Chianese[b], Giuseppina Pironti[a], Guido Barone[a], Angelo Riccio[b].
[a]*Dipartimento di Chimica, Università di Napoli "Federico II", via Cintia, Napoli.*
[b]*Dipartimento di Scienze Applicate, Università degli Studi di Napoli "Parthenope", via De Gasperi 5, Napoli*

Human exposure to urban atmospheric pollutants can determine health problems; different substances are responsible of these effects, particularly organic pollutants, nitrogen and sulphur oxides, ozone and fine particulate matter.
In the last years, it was established that these substances can determine harmful effects also in indoor ambient, specially in not well aerated conditions or in presence of source emission.
For that reason researches are devoted to the experimentation of materials[1] that can determine pollution reduction both for outdoor and indoor ambient.
In this work we present a testing made with TiO_2 paints for the reduction of PM2.5 produced form smoke activity.

1. O. Carp; C. L. Huisman; A. Reller; *Progress in Solid State Chemistry*, **2004**, *32*, 33-177.

P 1.5

Il metano ed il futuro del clima.

Elena Chianese[b], Giuseppina Pironti[a], Guido Barone[a], Angelo Riccio[b].
[a]*Dipartimento di Chimica, Università di Napoli "Federico II", via Cintia, Napoli.*
[b]*Dipartimento di Scienze Applicate, Università degli Studi di Napoli "Parthenope", via De Gasperi 5, Napoli*

Molti studi autorevoli sono concordi nell'attribuire alle attività umane l'incremento dell'effetto serra e le variazioni climatiche che ne conseguono [1] [2].
Le sostanze alle quali sono ascritti tali effetti sono sostanzialmente la CO_2 (il cui aumento in atmosfera è stato dimostrato mediante carotaggio ed analisi dei ghiacciai), gli ossidi di azoto (in particolare nella forma di N_2O), i CFC e gli HFC e FC (che hanno sostituito i primi in molte applicazioni; questi, e in particolare gli FC, hanno tempi di permanenza media molto lunghi in atmosfera). In realtà esiste un altro pericolo per l'aggravarsi dell'effetto serra da associare al gas CH_4, la cui concentrazione sta aumentando in associazione all'espansione delle risaie e degli allevamenti (in particolare di bovini) ai quali vanno aggiunti i processi fermentativi naturali che si hanno nelle paludi e nei termitai.
Oltre a queste fonti di metano "accertate" altre fonti possano contribuire (in particolare proprio a seguito di un incremento della temperatura, dunque come *feedback* positivo dell'effetto serra stesso) all'incremento delle emissioni di metano; in particolare può liberarsi il metano attualmente contenuto nei cristalli di gas idrati presenti in enormi depositi nel *permafrost* circumartico e nelle scarpate continentali [3].
In questo lavoro verranno dunque illustrate le caratteristiche salienti di queste strutture e verranno avanzate ipotesi sui possibili effetti che un loro scioglimento giocherebbe sul clima.

1. IPCC. Climate Change. The scientific basis. www.grida.no/climate/ipcc_tar/wg1/index.htm, 2001.
2. Crutzen P. J.; *Benvenuti nell'antropocene*. Mondadori, 2005.
3. Carroll J.; *Natural gas hydrates, a guide for Engineers*. Gulf Professional Publishing, Elsevier, 2003.

P 1.6

Conformational stability of a thermostable phosphotriesterase from the archaeon *Sulfolobus solfataricus* (SsoPox)

P. Del Vecchio[a], P. Carullo[a], G. Barone[a], L. Merone[b], M. Rossi[b], G. Manco[b]
[a]*Department of Chemistry, University "Federico II"of Naples,*
via Cintia, 80126 Naples, Italy, guido.barone@unina.it
[b]*Institute of Protein Biochemistry, via P. Castellino, 80131 Naples, Italy*

Organophosphate (OPs) degrading enzymes have become the focus of recent attention because of their potential

utility for the detoxification of chemical wastes, chemical warfare agents, and agricultural pesticides. Organophosphate compounds such as parathion constitute the largest class of insecticides currently used in the industrialized countries[1]. The lack of persistence of these pesticides in the soil has been attributed to their susceptibility to microbial transformation. Enzymes that catalyse the hydrolysis of the phosphoester bonds in OPs are known from several different bacterial species and are termed phosphotriesterases (PTEs). Among them, the homodimeric enzyme from *Pseudomonas diminuta* has received considerable attention on its use as a bioremediation agent and both functional and structural studies have been reported[2,3]. Recently, some of us, cloned a new gene from the hyperthermophilic archaeon *Sulfolobus solfataricus* MT4, coding for a putative protein reported to show sequence identity with the phosphotriesterase-related protein family (PHP), named *SsoPox*. This was the first phosphotriesterase to be reported from a hyperthermophilic archaeon[4].
Here we report a thermodynamic characterization of *SsoPox* performed by means of thermal and denaturant-induced unfolding, using circular dichroism (CD) and fluorescence measurements. *SsoPox* enzyme shows a very high denaturation temperature and a three-state mechanism on the GuHCl-induced unfolding. The results are compared with the literature data on the mesophilic enzyme from *Pseudomonas diminuta*[5].

1. Mulbry, W. W.; Karns, J. S. ; *Appl. Environ. Microbiol*, **1988,** *54,* 2566-2571. 2. Benning, M. M.; Shim, H.; Raushel, F.; Holden, H. M.; *Biochemistry,* **2001**, *40,* 2712-2722. 3. Dumas, D.P. ; Caldwell, S. R.; Wild, J. R.; Raushel, F. M.; *J. Mol. Biol.,* **1989,** *264,* 19659-19665. 4. Merone, L.; Mandrich, L.; Rossi, M.; Manco, G. ; *Extremophiles*, **2005***, 9,* 297-305. 5. Grimsley, J. K.; Scholtz, J. M.; Pace, C. N.; Wild, J. R.; *Biochemistry,* **1997**, *36,* 14366-14374.

P 1.7

Mn^{2+} in marmi bianchi antichi. Determinazione della cava con spettroscopia EPR tramite parametri magnetici

Alfonso Zoleo and Marina Brustolon
Dipartimento di Scienze Chimiche, Via Marzolo 1, 35131 Padova

La determinazione della cava di origine dei marmi bianchi antichi richiede l'uso di tecniche complementari, ma tra queste una delle più discriminanti è la spettroscopia EPR applicata al catione di Mn^{2+} (S=5/2), vicariante del Ca^{2+} e del Mg^{2+} nella calcite e nella dolomite. Il dintorno del Mn^{2+} infatti risente delle condizioni geochimiche di origine della cava, che determinano la simmetria del dintorno e la disomogeneità locale come segni identificativi della cava stessa.
Gli spettri EPR del Mn^{2+} nei marmi hanno caratteristiche fenomenologiche che dipendono dalla storia geochimica della cava. Grazie al database creato da D. Attanasio [1], è possibile usare queste caratteristiche (ampiezza dello spettro, distanze tra alcune coppie di righe) per attribuire la cava di origine con un margine di errore.
La simulazione numerica dello spettro, basata sui parametri dell'Hamiltoniano di spin (parametri di Zero Field Splitting, tensore di interazione iperfine, tensore quadrupolare) permetterebbe una maggiore precisione nella classificazione degli spettri rispetto all'osservazione delle caratteristiche fenomenologiche. Si illustreranno le problematiche di queste simulazioni, con alcuni esempi di marmi provenienti da cave antiche del Mediterraneo.

1. Donato Attanasio, *Ancient white marbles-Analysis and identification by paramagnetic resonance spettroscopy,* L'erma di Bretschneider, Roma 2003

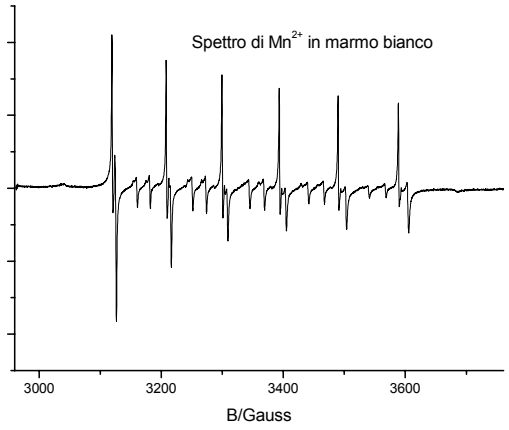

P 1.8

Osservazione diretta dell'effetto dell'associazione con la base complementare sul potenziale di ossidazione di guanosina e adenosina

Amedeo Capobianco [a], Tonino Caruso[a], Andrea Peluso[a]
[a]*Dipartimento di Chimica, Università di Salerno, Via Ponte Don Melillo, I-84085 Fisciano, SA* acapobianco@unisa.it

I potenziali di ossidazione di derivati della guanosina e dell'adenosina e dei loro complessi a ponte idrogeno con citidina e timidina sono stati determinati per via voltammetrica in $CHCl_3$ ed altri solventi organici.

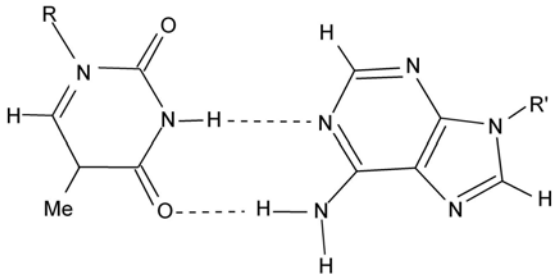

Per rendere solubili i nucleosidi in cloroformio, i gruppi OH sugli zuccheri sono stati protetti con terz-butil-dimetil-silile.
In $CHCl_3$, nel caso della guanosina, la formazione del complesso tipo Watson-Crick con la citidina comporta un abbassamento del potenziale di ossidazione di 0.34 V.[1] Allo stesso modo il potenziale di ossidazione dell'adenosina diminuisce di circa 0.28 V per effetto dell'interazione con la timidina.
Le costanti di autoassociazione[2] e quelle di formazione dei complessi guanosina-citidina e adenosina-timidina sono state ottenute da titolazioni NMR; i valori determinati sono simili a quelli riportati in letteratura per

le sole nucleobasi.
In figura è riportato il voltammogramma ciclico di una soluzione 1mM Guanosina – 1mM Citidina in $CHCl_3$. Il potenziale è riferito alla semicoppia ferrocene/ferrocinio.

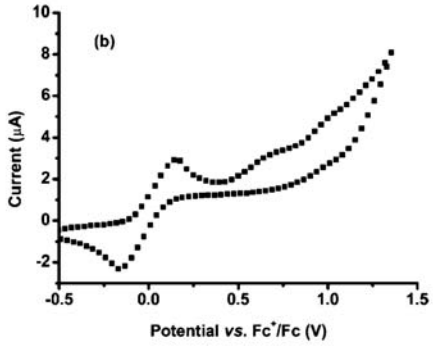

Calcoli teorici basati sul modello di Buckingham[3] in cui le molecole interagenti sono rappresentate come multipoli e polarizzabilità statiche e calcoli quantistici in cui la base purinica è trattata a livello B3LYP e la base pirimidinica è modellata come potenziale efficace di frammento, mostrano che l'abbassamento del potenziale di ossidazione della base purinica nel complesso è dovuto principalmente alla polarizzazione della base pirimidinica.
Infatti, la differenza tra il potenziale di ossidazione della base purinica e quello del complesso purina-primidina coincide con la variazione di energia di interazione del complesso a ponte idrogeno per effetto della ionizzazione.

1. Caruso, T.; Carotenuto, M.; Vasca, E.; Peluso, A.; *J. Am. Chem. Soc.*, **2005**, *127*, 15040 – 15041.
2. Kyogoku, Y.; Lord, R. C.; Rich A.; *J. Am. Chem. Soc*., **1967**, *89*, 496 – 504.
3. Buckingham, A. D.; *Adv. Chem. Phys.,* **1967**, *12,* 107 – 142.

P 1.9

Spectroscopic study of ochratoxin A and its interaction with cyclodextrins

R. Verrone[a], L. Catucci[a,b], P. Fini[b], P. Cosma[a,b], A. Agostiano[a,b], V. Lippolis[c], M. Pascale[c]
[a]*Dip. di Chimica, Università di Bari, Via Orabona 4, 70126 Bari, Italy catucci@chimica.uniba.it*
[b]*IPCF-CNR, Via Orabona 4, 70126 Bari, Italy*
[c]*ISPA-CNR, Via G. Amendola 122/O, 70126 Bari, Italy*

Ochratoxin A (OTA) is a mycotoxin produced by several *Aspergillus* species and by *Penicillium verrucosum*. OTA contaminates a wide range of foodstuffs, including cereals and their derivatives, coffee, beer, wine and cacao, and can represent a serious health threat both to humans and animals[1]. OTA can be also found in meat and milk because of carry-over by which the mycotoxin contained in feedstuffs can resist to metabolic processes and accumulate in the organism. It has been shown that OTA is neprhotoxic, hepatotoxic, teratogenic and immunotoxic to humans and several species of animals. Previous studies demonstrated that the presence of cyclodextrins (CDs) can affect OTA spectroscopic properties[2]. The ability of CDs to form inclusion complexes usually lead to variations in physico-chemical properties of the guest molecule, mainly enhancement of both solubility and fluorescence. In this work we investigated the effect of solvent properties on OTA spectroscopic behaviour and the interaction of OTA with different CDs. Dissolution of OTA in different solvents showed deviation of absorption and fluorescence maxima and variation of fluorescence quantum yields and of its detection limit. The presence of CDs influenced the protonated/deprotonated OTA equilibrium, as well as the toxin fluorescence intensity, depending from the nature of the solvent.

1. Ringot D., Chango A., Schneider Y., Larondelle Y., *Chemico-Biological Interactions*. 2006;159:18-46.
2. R. Verrone, L. Catucci, P. Cosma, P. Fini, A. Agostiano, V. Lippolis, M. Pascale, *J. Incl. Phen. and Macrocyc. Chem*. 2007;57:475-479.

P 1.10

Activity of photosynthetic membrane proteins of *Rhodobacter sphaeroides*: a possible role of cardiolipin

Vincenzo De Leo[a], Lucia Catucci[a,b], Francesco Milano[b], Angela Corcelli[b,c], Angela Agostiano[a,b]
[a]*Dip. di Chimica, Università di Bari, Via Orabona 4, 70126 Bari, Italy catucci@chimica.uniba.it*
[b]*IPCF-CNR, Via Orabona 4, 70126 Bari, Italy*
[c]*Dip. di Biochim. Medica e Biol. Medica, Univ. di Bari, P.zza G. Cesare, 70124 Bari, Italy.*

The levels of the anionic phospholipid cardiolipin have been found to increase upon exposition of the cells of the photosynthetic bacterium Rhodobacter sphaeroides to ipertonic solutions [1]. It is known that physical and chemical properties of the membrane proteins are critically determinated by the lipid matrix in which they are embedded. In the present work we performed investigation on the cardiolipin content on the photoactivity of chromatophores from *Rhodobacter sphaeroides* cells upon osmotic shock treatment. The presence of higher levels of cardiolipin enhances the thermal stability and the resistance to Q_B-site inhibitors of Reaction Centre in chromatophores, as indicated by charge recombination kinetics recorded after flash excitation. Moreover the resistance to photooxidative damages of Reaction Centre seems that is affected by cardiolipin content. Also the bc_1 complex activity increases in chromatophores obtained from osmotically shocked cells, as well as the stability of antenna complexes to alcohol-induced denaturation.

1. Catucci, L., Depalo, N., Lattanzio, V.M.T., Agostiano, A. and Corcelli, A *J.Biochem.* **2004**, 43, 15066-15072.

P 1.11

Photosystem II thermal stability and pigment photobleaching: Effect of membrane lipids

Andrea Ventrella[a], Lucia Catucci[a,b], Giuseppe Mascolo[c], Angela Corcelli[b,d], Angela Agostiano[a,b]
[a]*Dip. di Chimica, Università di Bari, Via Orabona 4, 70126, Bari, Italy. catucci@chimica.uniba.it.* [b]*IPCF-CNR, sez. Bari, Via Orabona 4, 70126, Bari, Italy.* [c]*IRSA-CNR, sez. Bari, Via F. De Blasio 5, 70123, Bari, Italy.* [d]*Dip. di Biochim. Medica e Biol. Medica, Univ. di Bari, P.zza G. Cesare, 70124, Bari, Italy.*

In this work, the effects of different exogenous phospholipids on spinach Photosystem II (PSII) complex activity were investigated: in particular, PSII thermal stability and resistance to strong illumination, leading to photobleaching, were studied in the presence of cardiolipin (CL) and phosphatidylglycerol (PG) by means of UV/Vis Absorption, Emission, Resonance Light Scattering and Oxygen Evolution Rate measurements. The phenomenon of PSII pigment photobleaching was studied by observing not only the effects of different phospholipids but also of other factors, such as the PSII aggregation state (monomers and dimers were tested) and the temperature. In both thermal stability[1] and photobleaching experiments, it was found that the presence of PG or CL helped the PSII activity to be better preserved.
Moreover, in order to gain information about the phospholipids directly surrounding the PSII complex, analyses of lipid extracts from spinach membrane fragments enriched in PSII and from spinach PSII dimers were carried out by means of Thin Layer Chromatography and Electro-Spray Ionization Mass Spectrometry. Isolation and characterization of CL found in association with PSII were obtained by mass and mass-mass analyses and evidences of CL structures with four unsaturated C18 acyl chains and variable saturation degrees were pointed out for the first time.

1. A. Ventrella, L. Catucci, G. Mascolo, A. Corcelli, A. Agostiano, BBA Biomembranes doi:10.1016/j.bbamem.2007.03.024

P 1.12

Studio sul metabolismo dell'arsenico attraverso spettroscopia NMR *in vivo*.

Marianna Aggravi[a], Claudia Bonechi[a], Claudio Rossi[a], Nadia Marchettini[b], Enzo Tiezzi[b], Alessandro Donati[a]
[a] *Università degli Studi di Siena, Dipartimento di Scienze e Tecnologie Chimiche e dei Biosistemi, Via Aldo Moro 2, 53100 Siena, Italia. alessandro.donati@unisi.it*
[b] *Università degli Studi di Siena, Dipartimento di Scienze e Tecnologie Chimiche e dei Biosistemi, Via della Diana 2/a, 53100 Siena, Italia.*

Il tema dell'interazione tra arsenico e organismi viventi è attualmente un argomento di intenso interesse scientifico. Ciò è dovuto alla recente scoperta che questo elemento, non sia caratterizzato solamente dalla sua ben nota tossicità acuta, ma anche da una tossicità cronica che si esplica anche a concentrazioni molto basse.
Il metabolismo dell'arsenico negli organismi viventi ha delle caratteristiche molto interessanti che coinvolgono variazioni cicliche del proprio stato redox, l'interazione con i gruppi tiolici di molte biomolecole, tra cui il glutatione (GSH) e l'emoglobina, e l'azione mimetica rispetto al gruppo fosfato. Purtroppo, nonostante i progressi fatti, il meccanismo di azione tossicologica non è stato ancora completamente chiarito. Ad esempio non è chiaro come l'arsenico venga trasportato all'interno delle cellule, come si esplichi l'azione tossica dei suoi metaboliti metilati e quale ruolo abbiano i processi redox.
Nel presente lavoro viene presentato uno studio NMR *in vivo* che mette in luce il comportamento di As nell'interazione con globuli rossi umani e di ratto, sia da solo che in presenza di glutatione e di altre molecole contenenti gruppi tiolici.
Tale indagine è stata effettuata parallelamente all'analisi strutturale e dinamica del complesso As-GSH effettuata attraverso tecniche 1H- e 13C-NMR e calcoli teorici.

1. Oremland, S. R., Stolz, J. F., *Science*, **2003**, *300*, 939 – 944. 2. Harvey, C. F., et al.,. *Science*, **2002**, *298*, 1602 – 1606.

P 1.13

Investigation of Self-Assembling Ionic Peptides

M. Alderighi[a], C. Duce[a], S. Monti[b], R. Solaro[a], M.R. Tiné[a]
[a] *Dept. of Chemistry & Industrial Chemistry, via Risorgimento 35, 56126 Pisa, Italy. celia@dcci.unipi.it*
[b] *Istituto per i Processi Chimico-Fisici (IPCF-CNR), Area della Ricerca, via G. Moruzzi 1, I-56124 Pisa, Italy*

The capability of self-assembling *in situ* into three dimensional scaffolds under physiological conditions together with the biocompatibility and the biodegradability are desirable features of biomaterials useful for tissue engineering and drug delivery applications.
The class of oligopeptides originally discovered by Zhang et al. [1-2] exhibits these properties and they can also be considered as a model system for studying insoluble macrostructures, which have been found in many neurological disorders such as Alzheimer diseases [3].
This class of oligopeptides consists of alternating hydrophilic and hydrophobic aminoacids; the hydrophilic surface of the molecule is constituted by alternating oppositely charged aminoacid residues. Several applicative studies on these systems are reported in the literature [1-3] but a systematic investigation of the physical-chemical features of the aggregation process is still lacking.
Central to mimicking biologically inspired self-assembly is the understanding of the forces that govern the thermodynamic stability and specificity of naturally occurring self-assembly events. The challenge is to rationally design building blocks amenable to self-assembly.
In this work, we investigate the self-assembly process of some tripeptides and pentapeptides characterized by an alternating sequence of negative and positive charges. KEK, KER, and RDKDR oligopeptides are in both the amidated (NH_2-KEK-$CONH_2$, NH_2-KER-$CONH_2$, and NH_2-RDKDR-$CONH_2$) and acetylated-amidated (AcNH-KEK-$CONH_2$, AcNH-KER-$CONH_2$, and AcNH-RDKDR-$CONH_2$) forms. A synergistic combination of Molecular Dynamics (MD) simulations, Atomic Force Microscopy (AFM), and Isothermal Titration Calorimetry (ITC) was used.
A series of classical molecular dynamics (MD) simulations were performed to investigate the aggregation properties of the short ionic tripeptide (KEK) in water solution [4]. The atomistic description of peptide and water molecules was based on the AMBER force field and the TIP3P water model. Possible aggregates were identified on the basis of potential inter-peptide hydrogen bonds and association/dissociation events were evaluated considering hydrogen bonds lifetime. The effects of different end groups on KEK peptide conformational self-assembling characteristics were evidenced through the analysis of structural microscopic and macroscopic parameters of the sampled aggregates. Ramachandran maps for the (φ,ψ) backbone dihedral

angles of the aminoacid residues and intramolecular as well as intermolecular hydrogen bonds were recorded.
To obtain a quantitative estimate of the aggregate size and shape, the ratio of the largest to the smallest principal moments of inertia ($r_I = I_{max}/I_{min}$), the eccentricity $\eta=1-I_{ave}/I_{max}$ where I_{ave} is the average of the three principal moments of inertia, and the radius of gyration Rg, were calculated.
AFM sample were prepared on mica by room temperature casting peptide water solutions at concentrations included between 6 μM and 5 mM. The images were recorded in tapping mode by a Multimode AFM Veeco instrument equipped with Nanoscope IV controller by collecting both topography and phase images.
AFM images of Ac–KEK–NH_2 cast on mica from 6 μM water solution showed the presence of 10–50 nm round clusters. The number of aggregates appreciably increased when 37 μM solution was used, although the aggregate size was almost unchanged. In both cases, the cluster height was about 5-10 Å, indicating that the aggregates consisted of oligopeptide monolayers. When AcNH–KEK–$CONH_2$ concentration was increased to 118 μM, 50-250 nm globular clusters 5–20 Å thick were detected, in agreement with the presence of multilayer aggregates.
Also the AFM images of NH_2-RDKDR-COOH pentapeptide cast from 1 mM solution evidenced the presence of globular aggregates, although their size was about 10 times bigger. On the other hand, images of the pentapeptide cast from 5mM solution evidenced the presence of a network of long branched fibrils about 50 nm wide and 2 nm thick (Fig. 1).

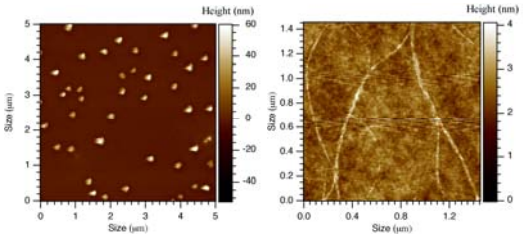

Fig. 1. AFM topography of NH_2-RDKDR-COOH cast from 1 mM (left) and 5 mM (right) water solutions.

Preliminary ITC experiments carried out in PBS buffer, at pH 7.4, and 25°C agree with AFM results. The calorimetric profile of tripeptide dilution curves revealed that aggregation process is not cooperative. The low cooperativeness causes the presence of protoaggregates even in dilute solution and results in non sigmoidal calorimetric dilution curve. On the contrary the enthalpogram of the pentapeptide AcNH-RDKDR-COOH shows a sigmoidal curve (Fig. 2) centered at 2.5 mM thus indicating the presence of a cooperative transition.

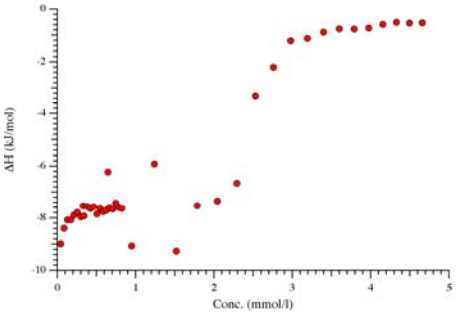

Figure 2. ITC enthalpogram of dilution of 12 mM AcNH-RDKDR-COOH solution in pH 7.4 PBS.

1. Zhang, S.; Holmes, T. C.; Lockshin, C.; Rich, A. *Proc. Natl. Acad. Sci. USA*. **1993**, *90*, 3334–3338. 2. Zhang, S., Lockshin, C.; Cook, R.; Rich, A. *Biopolymers* **1994**, 34, 663–672. 3. Fung, S. Y; Keyes, C.; Duhamel, J.; Chen, P. *Biophysical Journal* **2003**, 85 (1),537–548. 4. Duce, C.; Monti, S.; Solaro, R.; Tine, M. R. *J. Phys. Chem. B.* **2007**, *111*(5), 1165-1175.

P 1.14

Use of Cyclodextrins to Improve the Photostability of RB in Aqueous Solutions

P.Fini[a], A.E.Di Mauro[b], S.Rochira[b], P.Cosma[a, b], .Catucci[a, b], M.Castagnolo[b], , A.Agostiano[a, b]
[a]*Istituto per i Processi Chimico Fisici (IPCF) CNR, sez. Bari, Via Orabona 4, 70126 Bari, Italy;*
[b]*Dipartimento di Chimica, Universita' di Bari, Via Orabona 4, 70126 Bari, Italy*

Rose Bengal (3',4',5',6'- tetrachloro-2'- (2,4,5,7-tetraiodo -6- hydroxy-3-oxo-3H-xanthen-9-yl)benzoic acid, bis (sodium salt) is an alogenated xanthene widely exploited in many different fields. Almost all applications are based on the peculiar spectroscopic and photochemical properties of this dye. RB is often used as reagent for the production of singlet oxygen or reactive radicals and as standard for the evaluation of the quantum yield of singlet oxygen production of other photosensitizers. Therefore RB is often used in medicine, mainly in the photodynamic therapy to inactivate microorganisms and cause photodamage to target tissues. Other uses of RB in medicine are as photochemical tissue bonding to stitch wounds and to heighten damaged corneal and conjunctival cells. RB is also used for the waste water treatment and in the studies on solar energy conversion.
Major limits in applications are the high tendency of this dye in solution to aggregate with a consequent impairing of photoactivity and the necessity to prepare RB solutions just before the use or to keep them in the dark to avoid the photodegradation.
Our recent studies have shown that the presence in solution of cyclodextrin can be an efficient strategy to reduce the formation of aggregates. After a wide characterization of the interaction between RB and cyclodextrins in aqueous solutions [1-3], performed by measurements of vis absorbance, induced circular dichroism, calorimetry and electrochemistry, we have extended our studies on the effects of cyclodextrins on RB photostability in aqueous solutions. In this report we show the results of the study performed using a-cyclodextrin, hydroxypropyl-a-cyclodextrin, three β cyclodextrins (hydroxypropyl- β-cyclodextrin, the heptakis (2,6-di-O-metil)-β- cyclodextrin,the heptakis (2,3,6-tri-O-metil)-β- cyclodextrin) and the hydroxypropyl-g- cyclodextrin at a constant concentration. The obtained results indicate that the photostability of RB/CD complexes does not depend only on the stability of the formed complexes.

1. P.Fini, M.Castagnolo, L.Catucci, P.Cosma, A.Agostiano, Thermochimica Acta 418 (2004) 33.
2. P.Fini, F.Longobardi, L.Catucci, P.Cosma, A.Agostiano, Bioelectrochemistry 63 (2004) 107.
3. P.Fini, R.Loseto, L. Catucci, P. Cosma and A.Agostiano, , Bioelectrochemistry (in press)

P 1.15

Studio del meccanismo di degrado di vetri antichi rinvenuti nel parco archeologico di Siponto (Foggia)

A. Genga[a], M. Siciliano[a], L. Famà[a], D. Manno[a], T. Siciliano[a], A. Mangone[b], A. Traini[b], C. Laganara[c]
[a]Dipartimento di Scienza dei Materiali, *Università del Salento, via per Arnesano 73100 Lecce Italy, e.mail Alessandra.genga@unile.it*
[b]Dipartimento di Chimica, *Università degli Studi di Bari, via Orabona 4, 70126 Bari Italy*
[c]Dipartimento di Beni Culturali, *Università degli Studi di Bari, P.zza Umberto, 70100 Bari Italy*

Durante gli scavi archeologici vengono rinvenuti molti oggetti di interesse storico artistico caratterizzati dalla presenza di strati superficiali di corrosione. Il futuro stato di conservazione dipenderà dalle condizioni individuali di conservazione (p.e. umidità, temperature, concentrazione degli inquinanti atmosferici) e dalla conoscenza dei parametri chimico-fisici che influenzano i meccanismi di corrosione (p.e. cambiamento della composizione superficiale, stabilità chimica, meccanismi di lisciviazione e prodotti di alterazione).

Il degrado degli oggetti vitrei rinvenuti negli scavi archeologici è un processo molto complesso; dipende sia dalle caratteristiche chimico-fisiche dei vetri in oggetto (composizione chimica, trattamenti termici, morfologia superficiale) sia dalle condizioni esterne (microclima, temperatura, pH, composizione della soluzione acquosa, area superficiale per unità di volume del vetro in contatto con il suolo). Nel caso di reperti archeologici antichi gli strati di degrado possono avere spessore dalle decine di micron fino a 100 μm e presentano un effetto di iridescenza dovuti alle diverse proprietà ottiche degli strati superficiali e del bulk.

In questo studio vengono presentate le indagini preliminari sui meccanismi di degrado evidenziati in un gruppo di 16 campioni datati XII provenienti dalla stessa unità stratigrafica e rinvenuti nel parco archeologico di Siponto.

P 1.16

Uno studio combinato spettroscopico-teorico della struttura dell'ottasilicato di sodio RUB18

M. F. Iozzi, M. Cossi, C. Bisio, T. R. Macedo, L. Marchese
Università del Piemonte Orientale, Dipartimento di Scienze e Tecnologie Avanzate (DISTA), via Bellini 25G, 15100 Alessandria; francesca.iozzi@mfn.unipmn.it

I silicati stratificati (layered silicates, LS) riscuotono un interesse crescente grazie alla loro elevatissima area superficiale, che li rende utili come materiali di stoccaggio e di scambio in numerose applicazioni industriali: le proprietà chimico-fisiche delle superfici sono dominate dalla natura idrofobica/idrofila, dalla capacità di scambio ionico, e dalle proprietà molecolari conferite dagli adsorbiti organici con cui i silicati sono modificati. Benché la conoscenza della struttura dei LS a livello atomico sia di primaria importanza per interpretarne il comportamento, molte di queste strutture sono ancora sconosciute.

In particolare, l'ottasilicato RUB18 [$Na_8Si_{32}O_{64}(OH)_8$ * $32H_2O$] è stato recentemente analizzato dal gruppo di Gies e collaboratori, che ne hanno ipotizzato la struttura in base a misure di diffrazione (raggi X e neutroni), e a misure NMR: un aspetto determinante è costituito dalla presenza di network di legami idrogeno tra gli anioni silossano, i gruppi silanolici superficiali e le acque di solvatazione degli ioni Na^+.

In questo lavoro la struttura proposta in letteratura è stata verificata e dettagliata con un'analisi combinata sperimentale e teorica. Gli spettri IR di campioni di RUB18 sono stati accuratamente misurati a varie temperature, e confrontati con gli spettri simulati da calcoli *ab initio* ad alto livello; il confronto degli spettri simulati e misurati ha permesso di discriminare tra diverse possibili strutture atomiche delle regioni superficiali, e di identificare i più probabili network di legami idrogeno.

I calcoli teorici sono stati effettuati ottimizzando la struttura tridimensionale del RUB18 a livello semiempirico, selezionando la porzione più interessante della superficie e ricavandone un cluster finito: la struttura del cluster e lo spettro IR sono stati calcolati a livello DFT con un funzionale ibrido e un set di base esteso; l'effetto degli atomi più lontani è stato inserito nel calcolo con tecniche miste di tipo QM/semiempirico. Il livello della simulazione (e l'affidabilità dei risultati) sono tra i più alti disponibili con le tecniche di calcolo attuale. Il buon accordo tra gli spettri sperimentali e teorici dimostra la correttezza del modello adottato: si è anche dimostrato che è necessario considerare l'anarmonicità del potenziale di stretching e la presenza di risonanze di Fermi (tra la frequenza di stretching fondamentale e armoniche superiori o combinazioni di frequenze più basse) per assegnare correttamente gli assorbimenti legati al network di legami idrogeno.

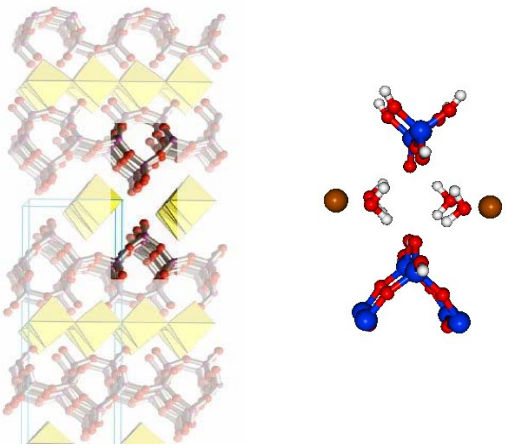

1. Vortmann, S.; Rius, J.; Siegmann, S.; Gies, H. *J. Phys. Chem. B.* , **1997**, *101*, 1292-1297
2. Borowski, M.; Kovalev, O.; Gies, H.; *Microporous & Mesoporous Materials*, in press

P 1.17

Influence Of Crowded/Confined Environments On Dynamics Of Amyloidogenic Protein Self-Assenbling

A. N. Lazar, E Bystrenova, C. Dionigi, P. Greco, S. Dutta, P. Stoliar, M.G. Cacace and F. Biscarini
CNR, ISMN-Istituto per lo Studio dei Materiali Nanostrutturati,Via P. Gobetti 101, 40129 Bologna, I T A L Y, a.lazar@bo.ismn.cnr.it

Proteins are the main essential active agents in biology and their geometrical characteristics are determinant for their functioning. Changes of the tertiary structure of proteins is known to have critical effect on functioning of cells and proteins self-assemblies are involved in a series of diseases like Alzheimer, Mad cow, Cystic fibrosis and even some types of cancers[1].

A complete understanding and control of the kinetics of the modifications in the tertiary structures of proteins under crowded/confined conditions may give the crucial information for developing efficient therapies or even for early diagnostic.

We propose new alternatives for understanding the dominant forces governing aggregation kinetics of amyloidogenic proteins[2] in crowded/confined environment – that mimics the dense environment in a living cell.

First of all we show that the characteristics of the environment like charge and hydrophilicity of substrates[3], molecular crowding associated to the macromolecules, are substantial parameters influencing the dynamic and self-structuring of the proteins.

Secondly, an evaluation of the aggregation mechanism of proteins[4,5] in a confined environment and not in a bulk continuous aqueous environment was performed. We succeeded in obtaining well-organized self-assemblies of proteins, with different characteristics (shape, molecular mass, tendency to aggregate) by the use of confined environments (bi-dimensional nano- and micro-channels and three dimensional cavities). This approach enables the understanding of the constrain-shape environment on proteins self-organization.

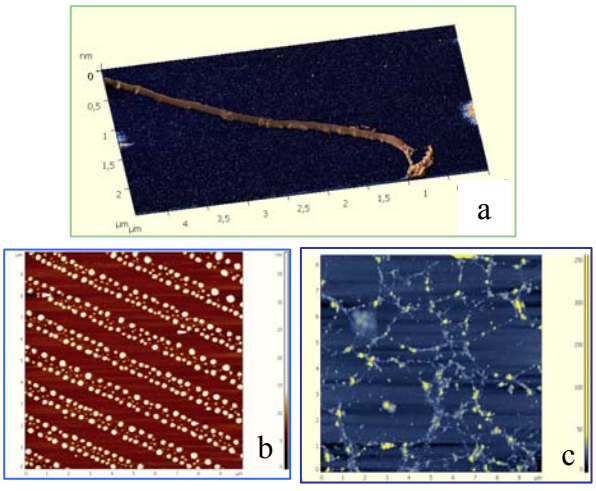

Figure 1: AFM images of self-assemblies of beta-amyloid peptide under different conditions: a – fibrils formed in bulk crowded environment; b,c – oligomers and fibrils formed in shape-constricted environments

All these results that represent a new approach in the elucidation of the problem of protein self-assembling could be of extreme importance for the clarification of the mechanism of amyloid aggregation.

This work is supported by Project EU-NMP-STRP 032652 BIODOT.

[1] Ferrone F, Methods Enzymol. 1999, 256-74
[2] Uversky VN, Fink AL., Biochim Biophys Acta, 2004, 131-53
[3] Schladitz C, Vieira EP, Hermel H, Mohwald H., Biophys J., 1999, 3305-10
[4] Giacomelli CE, Norde W., Macromol Biosci., 2005, 401-7
[5] Walsh DM, Tseng BP, Rydel RE, Podlisny MB, Selkoe DJ., Biochemistry., 2000, 10831-9.

P 1.18

Studio strutturale del processo di "unfolding" dell'albumina umana

Claudia LEGGIO, Luciano GALANTINI, Nicolae Viorel PAVEL
Dipartimento di Chimica, Università La Sapienza, P.le A. Moro 5, 00185 Roma, c.leggio@caspur.it

Le malattie da condensazione sono patologie eterogenee fra di loro ma caratterizzate da una iniziale perdita di solubilità di sostanze specifiche e da una conseguente formazione di fasi condensate [1]. Esempi tipici di tali malattie sono i calcoli renali, la cataratta, le nefriti, alcune patologie reumatiche, che sono spesso dovute alla denaturazione, all'aggregazione ed alla conseguente precipitazione di proteine. Poiché le molecole che condensano sono spesso proteine, gli agenti antidenaturanti potrebbero essere dei buoni candidati per il trattamento di queste malattie. La denaturazione delle proteine, seguita dal processo di aggregazione, può avvenire in fenomeni di infiammazione cronica in vivo. La denaturazione dell'albumina è stata osservata in pazienti con patologie reumatiche o lesioni infiammatorie. Per questo la stabilizzazione delle proteine in vivo è un problema di estrema rilevanza fisiologica. Molte sostanze esogene ed endogene proteggono le proteine dalla denaturazione. In questo senso ci sono numerose indicazioni di un effetto benefico della stabilizzazione delle proteine nel processo reumatico [2].

Nel nostro laboratorio è in corso uno studio mirato a determinare una correlazione tra la struttura e la stabilità dell' albumina di siero umano (HSA) in presenza di agenti endogeni ed esogeni. Sono stati effettuati studi preliminari (diffusione di raggi X a piccoli angoli, diffusione sia statica che dinamica della luce, misure di dicroismo circolare e di fluorescenza) allo scopo di discriminare la struttura dell'HSA monomerica e parzialmente denaturata dalla forma aggregata. Per quanto riguarda il processo di "unfolding", vi sono numerosi lavori con risultati in contrasto tra loro. Alcuni parlano della presenza di due soli stati, proteina nativa e denaturata, mentre studi più recenti prevedono la presenza di uno stato intermedio. Kamal et al. [3] hanno studiato la denaturazione dell'HSA a varie concentrazioni di guanidina, mediante misure di idratazione dinamica ed hanno proposto un possibile schema di apertura della proteina con la presenza di uno stato intermedio, nel quale rimane intatto esclusivamente il primo dominio.

Sono state quindi effettuate misure SAXS, SLS e DLS

per ottenere informazioni sulla conformazione che l'albumina assume all'aumentare della concentrazione di guanidina. Il grado di "unfolding" è stato monitorarto mediante misure di dicroismo circolare e di fluorescenza. I profili di intensità diffusa sono stati analizzati mediante la Trasformata di Fourier [4]. Inoltre, programmi basati su metodi statistici, quali il metodo Monte Carlo e algoritmi genetici [5, 6], consentono di ottenere una rappresentazione tridimensionale a bassa risoluzione delle diverse conformazioni che la proteina assume al variare della concentrazione di guanidina. I risultati mostrano che nel processo di "unfolding" sono presenti stati intermedi.

1. J. D. Sipe, A. S. Choen, J. Struct. Biol., **130**, 88 (2000).
2. L. Saso, B. Silvestrini, Medical Hypotheses, **56**, 114 (2001).
3. J. K. A. Kamal, L. Zhao, A. H. Zewail, Proc. Natl. Acad Sci. USA, **101**, 13411 (2004).
4. O. Glatter, J Appl. Cryst., **10**, 415 (1977).
5. P. V. Konarev, M. V. Petoukhov, V. V. Volkov, D. I. Svergun, J. Appl. Cryst., **39**, 277 (2006).
6. W. T. Heller, J. K. Krueger, J. Trewhella, Biochemistry, **42**, 10579 (2003).

P 1.19

Stabilità termodinamica del multimero del telomero umano ed energetica dell'interazione con la porfirina cationica

Luigi Petraccone[a], Luigi Martino[a], Bruno Pagano[b], Guido Barone[a], Concetta Giancola[a]
[a] *Dipartimento di Chimica, Università di Napoli "Federico II", via Cintia, 80126 Napoli, luigi.martino@unina.it*
[b]*Dipartimento di Scienze Farmaceutiche, Università di Salerno, via Ponte Don Melillo, 84084 Fisciano*

Il DNA telomerico umano, situato all'estremità dei cromosomi, termina con la sequenza nucleotidica d(TTAGGG), ripetuta n volte[1]. Questa sequenza, che in parte si presenta come un singolo filamento, è in grado di formare strutture a quadrupla elica di DNA. Queste strutture sono di particolare interesse per il loro ruolo biologico e come possibili target di molecole di interesse farmacologico implicate nella terapia anticancro. La maggior parte degli studi sulle proprietà termodinamiche e cinetiche della formazione delle G-quadruplex e delle loro interazioni con molecole di interesse farmacologico, sono stati condotti sulla sequenza telomerica umana formata da sole quattro unità ripetitive, $d(TTAGGG)_4$. Sono necessari, quindi, ulteriori studi per caratterizzare le proprietà di sequenze più lunghe di DNA telomerico (costituito da un numero di unità ripetitive superiore a quattro). Tali studi permetteranno di stabilire se i dati raccolti sulla sequenza telomerica corta sono utili per predire le propriertà della sequenza più lunga. A tal fine, è qui riportata la caratterizzazione sia della stabilità termodinamica che dell'energetica dell'interazine con la porfirina, della sequenza telomerica umana con otto unità ripetitive, $d(TTAGGG)_8$. I risultati sono stati confrontati con quelli ottenuti sulla sequenza telomerica corta $d(TTAGGG)_4$. Lo studio è stato condotto mediante tecniche microcalorimetriche (DSC, ITC) e spettroscopiche (CD).

1. Zakian, V. A.; *Science*, **1995**, *270*, 1601 – 1607.

P 1.20

ATPasi di tipo P in modelli di membrane biologiche: studio delle proprietà funzionali

M.R. Moncelli, G. Bartolommei, F. Tadini-Buoninsegni
Dipartimento di Chimica, Università di Firenze, BioElectroLab, via della Lastruccia 3, 50019 Sesto Fiorentino (FI); moncelli@unifi.it

Nel nostro laboratorio si studiano da diversi anni proteine di membrana in modelli sperimentali di membrane biologiche. In modo particolare si studiano ATPasi di tipo P con metodi chimico fisici. Recentemente abbiamo focalizzato la nostra attenzione sullo studio delle interazioni della Ca-ATPasi e della Na,K-ATPasi con alcuni farmaci.
Si illustreranno:
- le caratteristiche generali delle ATPasi;
- i metodi di indagine utilizzati: **a)** spettrofluorimetria con sonde stiriliche elettrocromiche e **b)** tecnica per salti di concentrazione su SSM (Solid Supported Membrane) [1-2].
Si presenteranno alcuni risultati:
- interazione della Ca-ATPasi con inibitori a differente affinità (clotrimazolo [3], tapsigargina, acido ciclopiazonico, curcumina);
- interazione della Na,K-ATPasi con clotrimazolo.

1. Tadini-Buoninsegni, F.; Bartolommei, G.; Moncelli, M.R.; Inesi, G.; Guidelli, R.; *Biophys. J*., 2004, *86*, 3671-3686. 2. Tadini-Buoninsegni, F.; Bartolommei, G.; Moncelli, M.R.; Guidelli, R.; Inesi, G.; *J. Biol. Chem*., **2006**, *281*, 37720-37727. 3. Bartolommei, G.; Tadini-Buoninsegni, F.; Hua, S.; Moncelli, M.R.; Inesi, G.; Guidelli, R.; *J. Biol. Chem.*, **2006**, *281*, 9547-9551.

P 1.21

Direct micelles as microreactors for the tuning of cobalt ferrite nanoparticle sizes

A. Ardu[a], C. Cannas[a], A. Musinu[a], D. Peddis[a], G.Piccaluga[a], D. Gatteschi[b], C. Sangregorio[b]
[a]*Dipartimento di Scienze Chimiche, Cittadella Universitaria di Monserrato, bivio per Sestu, 09042 Monserrato (Cagliari), Italy. musinu@unica.it*
[b] *Dipartimento di Chimica - Università di Firenze Via della Lastruccia, 3, 50019 Sesto F.no*

Synthesis and processing of fine magnetic particles have been the subject of extensive research due to their many technological applications including ferrofluids,[1] data storage[2] and biomedicine.[3] Most of these applications require particles of uniform size and shape distribution. In addition, for any particular application the magnetic nanoparticles must possess specific properties. For example, data storage applications require particles with stable, switchable magnetic states to represent bits of information, states not affected by temperature fluctuations. In biomedical applications, the nanoparticles must exhibit superparamagnetic behaviour at room temperature. A variety of methods have been developed to prepare these nanoparticles, however in most cases the resulting particles are poorly crystalline and calcination at high temperature is needed to induce highly crystalline structures.

Direct micelles (oil in water micelles) represent a good and quite simple method for synthetize magnetic crystalline nanoparticles with tunable particle size.[4] The microenvironment provides a template effect that controls the size and the particle shape. Cobalt (II) and iron (II) or iron (III) cloride and sodium dodecylsulphate (SDS) as surfactant are used as precursors for the formation of $Co(DS)_2$, $Fe(DS)_2$ or $Fe(DS)_3$. CH_3NH_3OH is added to the mixed micellar solution to induce the precipitation of nanosized magnetic particles. The size of the crystalline particles is controlled either by changing the micellar concentration or by increasing the temperature from 50 to 80°C. The effect of the surfactant concentration, in the investigated range, seems to be negligible.

In contrast to what is obtained with conventional precipitation method from homogeneous solution, cobalt ferrite particles can be obtained when the synthesis is performed at very low reactant concentration and at low temperature. Furthermore, when the synthesis is performed using Fe(II) salt as reactant, nanoparticles are obtained by micellar method whereas particles in the micrometer range are formed by homogeneous solution.

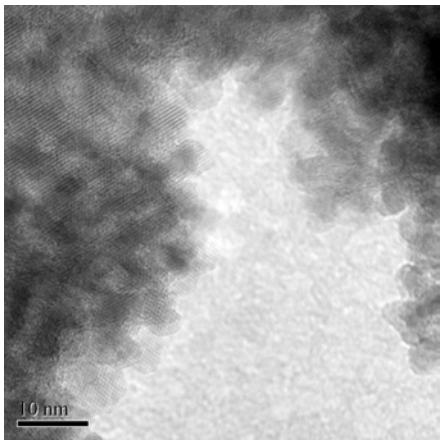

Figure: HRTEM of $CoFe_2O_4$ obtained form Fe(III) precursor.

Transmission electron microscopy in low and high resolution (figure) reveals that the particles are nanocubes with a narrow particle size distribution and average particle size ranging from 3 to 27 nm depending on the iron salt used, concentration and temperature. X-ray diffraction results indicate the typical spinel structure of $CoFe_2O_4$ and show the structural evolution as a function of temperature: cobalt ferrite phase is stable up to 1000°C and the particle size increases gradually up to 700°C and swiftly at higher temperatures.

Mössbauer Spectroscopy and nitrogen physisorption measurements are also performed in some specific cases in order to study the kinetic of the cobalt ferrite formation and the textural properties respectively. The materials are found to exhibit superparamagnetism. The blocking temperatures and coercivity are dependent on the size and on the iron salt used during the synthesis.

1.Rosensweig, R.E.; *Chem. Eng. Prog.*, **1989**, 85, 53. 2.Alivisatos, P.; *Science*, **1996**, 271, 933. 3.S. O' Brien, *Nature*, **2003**, 423, 968-971. 4.Vestal, C.R.; Zhang, Z.J.; *J. Of Nanotec.*, **2004**,Vol. 1, 240

P 1.22

Analisi termodinamica dell'interazione tra ligandi e quadruple eliche del DNA telomerico umano

Bruno Pagano[a], Antonio Randazzo[b], Gary N. Parkinson[c], Carlo A. Mattia[a], Concetta Giancola[c]
[a]*Dipartimento di Scienze Farmaceutiche, Università di Salerno, via Ponte Don Melillo, 84084 Fisciano, bpagano@unisa.it*
[b]*Dipartimento di Chimica delle Sostanze Naturali, Università di Napoli "Federico II", via D. Montesano 49, 80131 Napoli*
[c]*The School of Pharmacy, University of London, 29-39 Brunswick Square, WC1N 1AX London*
[d]*Dipartimento di Chimica, Università di Napoli "Federico II", via Cintia, 80126 Napoli*

Il DNA telomerico degli eucarioti è una doppia elica contenente brevi sequenze oligonucleotidiche identiche, ripetute migliaia di volte in tandem. Le sequenze ripetute del DNA telomerico variano a seconda degli organismi, ma in tutte si riscontra la presenza di un elevato numero di guanine. Inoltre, la parte 3'-terminale si presenta sempre come un singolo filamento in grado di ripiegarsi per formare inusuali strutture a quattro filamenti, le quadruple eliche.[1] Le quadruple eliche sono formate da unità strutturali dette G-tetradi, in cui quattro basi co-planari di guanine si dispongono secondo uno schema ciclico in cui ogni base accetta e dona contemporaneamente due legami idrogeno. La formazione delle quadruple eliche inibisce l'attività della telomerasi, suggerendo un loro potenziale utilizzo nella terapia anti-cancro. Diverse molecole si sono mostrate in grado di legare e stabilizzare questa struttura *in vitro*, amplificandone l'azione antitelomerasica.[2]
In questo studio è stata affrontata l'analisi chimico-fisica dell'interazione tra le quadruple eliche formate dalla sequenza ripetuta d(TTAGGG) del DNA telomerico umano ed alcune molecole di interesse farmacologico quali la distamicina e la porfirina cationica. I parametri termodinamici associati all'interazione tra le quadruple eliche di DNA ed i ligandi sono stati determinati, in maniera diretta, mediante calorimetria isoterma a titolazione (ITC). L'ITC ci ha permesso di studiare in dettaglio i processi che portano alla formazione dei complessi, ed inoltre, ci ha consentito di ripartire l'energia libera di legame nelle componenti entalpiche e entropiche, in modo da poter rivelare la natura delle forze che guidano la reazione.

1. Neidle, S.; Parkinson, G. N.; *Curr. Opin. Struct. Biol.*, **2003**, *13*, 275 – 283. 2. Cuesta, J.; Read, M. A.; Neidle, S.; *Mini Rev. Med. Chem*, **2003**, *3*, 11 – 21.

P 1.23

Sintesi stereoselettiva di 1,2,3-triaril aziridine e risoluzione strutturale via H^1-NMR di derivati con Pt(II)

E. Pindinelli, M. Fabio, L. Troisi
Università del Salento, Dipartimento di Scienze e Tecnologie Biologiche ed Ambientali, via Monteroni, 73100 Lecce, Emanuela.pindinelli@unile.it

L'elevata tenzione d'anello che caratterizza le aziridine conferisce a questo eterociclo un'elevata importanza sia

nel campo della sintesi organica[1], sia nel campo farmaceutico[2]. Con questa comunicazione riportiamo la sintesi stereoselettiva di alcuni 1,2,3-triaril aziridine attraverso la metodologia di Darzens.

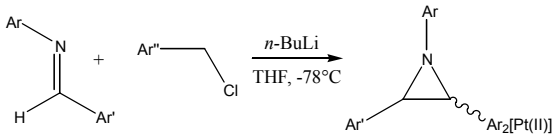

Alcune di queste aziridine , in particolare quelle di configurazione *cis* recanti sul C2 e C3 due eterocicli di cui almeno uno dei due possiede un gruppo *aza* in posizione α , si aprono nell'ambiente basico in cui viene condotta la reazione, riarrangiando in una struttura enamminica.
Saranno riportati i dati sulla stereoselettività della sintesi, sulla stabilità dell'anello aziridinico e sulla complessazione con il Pt(II) di alcune aziridine simmetriche (Ar'=Ar'') che ha permesso l'assegnazione della configurazione *cis/trans*, via H-NMR differenziando i protoni sul C2 e sul C3.

1. Yudin A. K., Wiley-VCH: Weinheim, Germany, *Aziridines and Epoxides in Organic Synthesis* **2006.**
2. Yudin A. K., and all, *Acc. Chem. Res*., **2006**, 39, 194-206.

P 1.24

Evidence for different routes of oxidation in the laccase-mediator system: a multifrequency EPR and DFT study.

R. Pogni[a], B. Brogioni[a], A. Sinicropi[a], M. C. Baratto[a], P. Giardina[b], G. Sannia[b], R. Basosi[a]
[a]*Chemistry Department, University of Siena, Via A. Moro, 53100 Siena, pogni@unisi.it*
[b]*Organic Chemistry and Biochemistry Department, University of Naples, via Cinthia 4, 80126 Napoli*

Laccases belong to the multicopper oxidase family and catalyse the oxidation of a wide variety of organic substrates with the concomitant reduction of O_2 to water. The use of low molecular weight compounds, called mediators, in combination with laccase, makes the enzyme suitable for the oxidation of "non-natural" non-phenolic substrates, hence significantly increasing the number of chemical structures that can be degraded. The role of the enzyme is to oxidise the mediator. The actual oxidation of the substrate is then carried out by the oxidized form of the mediator, in a non-enzymatic step. Mediators act as co-substrates, shuttling electrons between the enzyme and the substrate (1).
The understanding of the mechanisms of electron and proton transfer and the insight on the interactions of laccases with mediators can be of great help in designing more active laccase-mediator systems for biotechnological applications (2). In this view, we studied the interaction between a fungal laccase, POXC from *P. ostreatus*, and two chemically different redox mediators, violuric acid (VIO) (–NOH type) and 2,2′-Azino-bis(3-ethylbenzothiazoline)-6-sulfonic acid (ABTS). We observed that a radical intermediate species was formed on both synthetic mediators after the interaction with the enzyme. Both radicals were investigated by multifrequency EPR, X-band (9.4 GHz) and High Field (244GHz) (3). The X-band spectrum of ABTS was simulated with the program Bruker "X-Sophe" using a Simplex type iteration. The other experimental spectra were simulated using the program EasySpin (4) for fitting solid state EPR spectra with anisotropic g- and hf-tensors and for best fitting.
Experimental results were compared and discussed in the frame of theoretical calculations based on density functional theory (DFT) data. The agreement between experimental and calculated data confirms that two different routes of oxidations are possible for the two different type of mediators.
An important role in determining the mechanism of substrate oxidation may be played by the stability of the oxidized form of the radical mediator, as well as by its redox potential.

1. Galli, C.; Gentili, P.; *J. Phys. Org. Chem.*, **2004**, 17, 973-977.
2. Pogni, R.; Brogioni, B.; Baratto, M. C.; Sinicropi, A.; Giardina, P.; Pezzella, C.; Sannia, G.; Basosi, R.; *Biocat. and Biotransf.*, **2007**, in press.
3. Reijerse, E.; Schmidt, P.P.; Klihm, G.; Lubitz, W.; *Appl. Magn. Reson*. in press.
4. Stoll, S.; Schweiger, A.; *J. Magn. Reson.,* **2006**, 178 (1), 42-55.

P 1.25

Membrane insertion and bilayer perturbation by antimicrobial peptide

Sara Pistolesi[a], Jimmy B. Feix[b], Rebecca Pogni[a]
[a]*Dipartimento di Chimica, Università di Siena, Via A. Moro, 53100 Siena, Italy, pogni@unisi.it*
[b]*Department of Biophysics and National Biomedical EPR Center, Medical College of Wisconsin, 8701 Watertown Plank Rd., Milwaukee, Wisconsin 53226, U.S.A.*

Antimicrobial peptides (AMPs) are an important component of innate immunity, and have generated considerable interest as a potential new class of antibiotic (1-3). The biological activity of AMPs is strongly influenced by peptide-membrane interactions, however for many of these peptides the molecular details of how they disrupt and/or translocate across target membranes are not known. Our studies have focused on a linear, synthetic hybrid composed of the first seven residues of cecropin A and residues 2– 9 of the bee venom peptide mellitin. This 15-residue peptide, designated CM15, retains the two-domain structure of native cecropins (4), with a highly cationic N-terminal region and a mostly hydrophobic C-terminal region. CM15 displays potent, broad-spectrum antimicrobial activity, yet lacks the strong hemolytic activity of mellitin (5). Previously have been shown that CM15 folds into an α-helix upon membrane binding (6, 7), and that at low peptide/lipid ratios (i.e., under initial binding conditions) the helical axis is positioned ~ 5 Å below the hydrophobic interface of the membrane and aligned parallel to the bilayer surface (6). Osmoprotection studies with live bacteria indicate that cell killing by CM15 is mediated by the formation of membrane pores with a diameter of 2.2 – 3.8 nm (8), however nothing is known about the intermediate stages between initial binding and pore formation. In this study we have used site-directed spin labeling (SDSL) electron paramagnetic resonance (EPR) spectroscopy to investigate the behavior of a spin-labeled analog of CM15 as a function of increasing peptide concentration, and utilized phospholipid-analog spin labels to examine

the effects of CM15 binding and accumulation on physical properties of membrane lipids. We find that as the concentration of membrane-bound CM15 is increased, the N-terminal domain of the peptide becomes more deeply immersed in the lipid bilayer. Peptide binding dramatically increases interaction of the lipid-analog spin labels with the polar relaxation agent NiEDDA, indicating that there are significant changes in the physical state of the lipid bilayer that are not readily detected by methods that examine motional dynamics suggesting an increased permeability of the membrane to polar solutes. There was no evidence of peptide-peptide association, suggesting that transmembrane pores formed by the peptide are either transient, or that individual peptide monomers are separated by > 20 Å. Binding of CM15 to model membranes with a lipid composition mimicking the bacterial inner membrane caused only slight perturbations in membrane lipid dynamics, and changes in lipid dynamics were observed only for 5PCSL, suggesting that CM15 remains in a region of the bilayer near the hydrophilic interface even as the concentration of bound peptide is increased. Accessibility studies with both spin-labeled peptide and lipid-analog spin labels indicated an abrupt structural change at a lipid/peptide ratio of ~ 25:1. Overall, these results are most consistent with the toroidal pore model as the mechanism of bilayer disruption by CM15.

1. Boman, H.G.; *Ann. Rev. Immunol.*, **1995**, 13:61-92.
2. Hancock, R.E.W.; Chapple, D.S.; *Antimicrob. Agents Chemother.*, **1999**, 43:1317-1323.
3. Zasloff, M.; *Nature*, **2002**, 415:389-395.
4. Fink, J.; Merrifield, R.B.; Boman, A.; Boman, H.G.; *J. Biol. Chem.*, **1989**, 264:6260-6267.
5. Andreu, D.; Merrifield, R.B.; Steiner, H.; Boman, H.G.; *Biochemistry*, **1985**, 24:1683-1688.
6. Bhargava, K.; Feix, J.B.; *Biophys. J.*, **2004**, 86:329-336.
7. Sato, H.; Feix, J.B.; *Biochimica et Biophysica Acta.*, **2006**, 1758(9):1245-56.
8. Sato, H.; Feix, J.B.; *Biochemistry*, **2006**, 45:9997-10007.

P 1.26

The Fluorescence of Tryptophan in Monellin and Parvalbumin Resolved at the ab initio Multiconfigurational Perturbation Theory Level

Adalgisa Sinicropi[a], Sara Pistolesi[a], Rebecca Pogni[a], Riccardo Basosi[a], Massimo Olivucci[a,b]
[a]*Dipartimento di Chimica, Università di Siena, via Aldo Moro 2, I-53100 Siena, Italy*
[b]*Chemistry Department, Bowling Green State University, Bowling Green 43403, OH, U.S.A.*

The computer-aided design of unnatural proteins with specific optical properties, such as color and luminescence, represent a complex problem. In these cases, the quantum chemical method employed must be capable to describe both ground and electronically excited states of the protein chromophore. In particular, the computational description of a luminescent (e.g. fluorescent) protein implies the use of methodologies capable to predict the excited state equilibrium structure of fluorophores characterized, even for singlet states, by mixtures of open-shell and charge transfer characters. The ab initio (i.e. first-principle) complete-active-space self-consistent-field (CASSCF) method (1) is a multiconfigurational method offering maximum flexibility for an unbiased description (i.e. with no empirically derived parameters and avoiding single-determinant wavefunctions) of the electronic and equilibrium structure of the ground and excited states of a molecule. Furthermore, the CASSCF wavefunction can be readily used for subsequent multiconfigurational second-order perturbation theory (2) computations (CASPT2) of the dynamic correlation energy of each state ultimately allowing for a quantitative evaluation of energy gap between different electronic states. We show that a quantum-mechanics/molecular-mechanics strategy (3, 4, 5) based on ab initio (i.e. first principle) multiconfigurational perturbation theory can reproduce the spectral properties of a tryptophan residue in different protein environments within few kcal mol^{-1}. This result gives access to a detailed understanding of the molecular factors modulating the residue emission in different proteins as well as in mutants. We also show that that the same computational protocol can be used to simulate protein embedded tryptophan neutral and cationic radicals opening the way to the investigation of their redox properties.

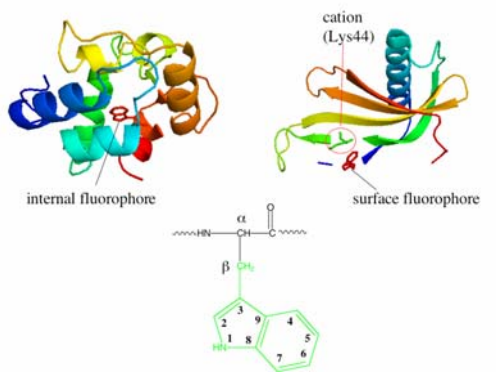

Top. View of parvalbumine (left) and monellin (right) highlighting the position of the 3-methylindole fluorophore (red). Bottom. Structure of the fluorophore 3-methylindole (in green).

1. Roos, B. O.; *In Advances in chemical physics: ab initio methods in quantum chemistry*, Lawley, K. P., Ed. Wiley: Chichester, UK, **1987**; Vol. 2, pp 399-445.
2. Andersson, K.; Malmqvist, P.-Å. ; Roos, B.O. ; Sadlej, A.J. ; Wolinsky, K.J.; *Journal of Chemical Physics*, **1990**, 94, 5483-5488.
3. Coto P.B.; Strambi A.; Ferré N.; Olivucci, M.; *Proc. Nat. Acad. Sci. USA*, **2006**, 103, (46), 17154-17159.
4. Andruniów, T.; Ferré, N.; Olivucci, M.; *Proc. Nat. Acad. Sci. USA*, **2004**, 101, 17908-17913.
5. Sinicropi, A.; Andruniow, T.; Ferré, N.; Basosi, R.; Olivucci, M.; *J. Am. Chem. Soc.,* **2005**, 127, 11534-11535.

P 1.27

Monitoring of the aggregation behaviour of a catalytic protein targeted by anticancer drugs through analysis of its intrinsic fluorescence

Stefania Ferrari[1], Maria Paola Costi[1], Monica Caselli[2] and Glauco Ponterini[2]
[1] *Dipartimento di Scienze Farmaceutiche and* [2]*Dipartimento di Chimica dell'Università di Modena e Reggio Emilia, via Campi 183, 41100 Modena, ponterini.glauco@unimore.it*

THIS WORK IS PART OF THE LIGHTS (LIGAND TO INTERFERE WITH HUMAN TS, LSHC-CT-2006-037852)

PROJECT (STREP FOUNDED BY THE FP6 PROGRAM) WWW.LIGHTS-EU.ORG.

Thymidylate synthase (TS) plays a key role in the intracellular synthesis of thymine, a building block of DNA. Its amount and activity depend on complex biochemical paths that may in principle be controlled by shifting the monomer (M) ↔ dimer (D) equilibrium in the cellular environment.

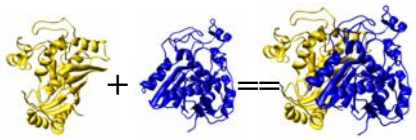

hTS monomer-dimer equilibrium.

In view of the promising therapeutical implications of the ability to control this equilibrium, we have been looking for spectroscopic and photophysical observables able to monitor M ↔ D interconversion of human TS.

In this contribution we will report on the results of our analysis of the intrinsic fluorescence of human TS and will show how such observables as emission and excitation spectra, quantum yield, anisotropy and lifetime distribution are affected by protein dimerization. A molecular interpretation of the observed changes will be finally attempted.

References:
Prasanna V. et al. *Biochem*. **1998**, *37*, 6883-93. ; Lovelace L. L. et al. *Biochem.* **2007**, *46*, 2823-30

P1.28

Multicomponent cationic liposome/DNA complexes: efficient vectors for gene delivery

G. Caracciolo[a], D. Pozzi[a], R. Caminiti[a], C. Marchini[b], M. Montani[b], A. Amici[b], H. Amenitsch[c]
[a]*Department of Chemistry, University of Rome "La Sapienza", P.le A. Moro 5, 00185 Rome, Italy.*
[b]*Genetic Immunization Laboratory, Department of Molecular Cellular and Animal Biology, University of Camerino, Via Camerini 5, 62032 Camerino (MC), Italy.*
[c]*Institute of Biophysics and Nanosystems Research, Austrian Academy of Sciences, Schmiedelstrasse 6, A-8042 Graz, Austria.*

Cationic lipid/DNA complexes (lipoplexes) are the best non viral carriers of DNA for gene delivery.[1] Here we report, for the first time, a synchrotron small angle X-ray diffraction (SAXD) study aimed at clarifying the correlation between transfection efficiency of lipoplexes and the structural changes occurring when lipoplexes interact with anionic membrane lipids (models of cellular membranes).[2-4] We showed that inefficient lipoplexes were unstable, rapidly fused and released DNA upon adherance to anionic vesicles. Conversely, formulations that were found to be efficient as DNA vectors in mouse fibroblast (NIH 3T3) and tumoral myofibroblast-like (A17) cell lines resisted solubilisation even in strong excess of anionic charge. These results implicate that structural stability upon interaction with cellular anionic lipids controls transfection efficiency of lipoplexes. Possible molecular mechanisms explaining experimental findings are discussed.[5] The adoption in the future of rationally designed lipoplexes stable against solubilisation by anionic lipids may allow increased transfection efficiency of lipoplexes.

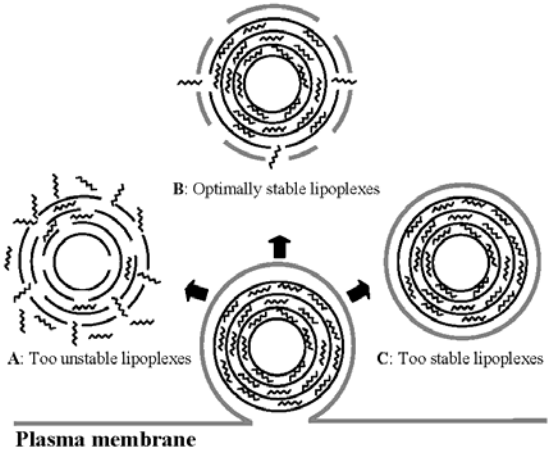

1. Felgner, P. L.; Ringold, G. M. *Nature* **1989**, *331*, 461-462.
2. MacDonald, R. C.; Ashley, G. W.; Shida, M. M.; Rakhmanova, V. A.; Tarahovsky, Y. S.; Pantazatos, D. P.; Kennedy, M. T.; Pozharski, E. V.; Baker, K. A.; Jones, R. D.; Rosenzweig, H. S.; Choi, K. L.; Qiu, R. Z.; McIntosh, T. J. *Biophys. J.* **1999**, *77*, 2612-2629.
3. Koynova, R.; Wang, L.; Tarahovsky, Y.; MacDonald, R. C. *Bioconjug. Chem.* **2005**, *16*, 1335-1339.
4. Caracciolo, G.; Pozzi, D.; Caminiti, R., Marchini, C.; Montani, M; Amici, A.; Amenitsch, H. *Appl. Phys. Lett.* **2006**, *89*, 233903-3.
5. Caracciolo, G.; Marchini, C.; Pozzi, D.; Caminiti, R., Amenitsch, H.; Montani, M; Amici, A. *Langmuir* **2007**, *23,* 4498-4508.

P 1.29

Aspetti dinamici su scala macroscpopica derivanti da organizzazione mesoscopica

Grazia Biosa, Marcus Hauser[a], Sandra Ristori[b], Eugenio Simoncini[c], Enzo Tiezzi[c] e Mauro Rustici
Università di Sassari, Dipartimento di Chimica, Via Vienna 2, 07100 Sassari, Italia
[a] *Otto-von-Guericke-UniversitÄat Magdeburg, Biophysics Group, UniversitÄatplatz 2, 39106 Magdeburg, Germany*
[b] *Universitµa di Firenze, Dipartimento di Chimica, Via della Lastruccia, 3, 50019 Sesto Fiorentino (FI), Italia*
[c] *Universitµa di Siena, Dipartimento di Scienze e Tecnologie Chimiche e dei Biosistemi, Pian dei Mantellini 44, 53100 Siena, Italia*

Le onde chimiche costituiscono degli esempi caratteristici per molte reazioni in cui sono presenti processi autocatalitici. Molti fenomeni come la propagazione di onde chimiche, treni d'onda o spirali possono essere descritte attraverso un meccanismo di reazione-diffusione. Per esempio l'osservazione di geometrie spiraliformi nei sistemi viventi ha importanti implicazioni nella salute umana.
In questo lavoro focalizziamo la nostra attenzione sulla caratterizzazione delle onde chimiche che si originano nella reazione di Belousov-Zhabotinsky (BZ) in una matrice fosfolipidica (DPPC). In questo caso la

propagazione di onde risulta influenzata dal contenuto di lipidico presente nel mezzo di reazione. In soluzioni acquose (0% DPPC) la reazione BZ conduce ad onde i cui "tips" si muovono seguendo traiettorie tipo "meandering" e la velocita di rotazione dell'onda spiraliforme diminuisce linearmente con il contenuto di DPPC nel mezzo di reazione in accordo con il generale aumento della viscosità del mezzo.
In contrasto rispetto alla velocitµa di propagazione dell'onda, altri parametri che descrivono le proprietµa cinematiche della spirale presentano un comportamento bimodale nel mezzo BZ/DPPC. La spirale ruota rigidamente attorno ad un centro di circa 0.3 mm quando la DPPC è compresa nell'intervallo tra 2.5 e 12% in peso, mentre il diametro aumenta drasticamente quando il contenuto fosfolipidico supera il 12%.
La dinamica del sistema che si osserva ad una scala macroscopica riflette pertanto un organizzazione interna originata a livello mesoscopico nei domini acquosi del sistema acqua/lipide.

P 1.30

Superstructural Organization of a G-Quadruplex Forming Homopuryne-Homopyrimidine Tract belonging to the Human Telomerase Reverse Transcriptase (H-Tert) Gene Promoter.

Maria Savino[a], Sabrina Pisano[b], Michela Varra[c], Emanuela Micheli[a], Teresa Coppola[c], Luciano Mayol[c], Pasquale De Santis[b]. [a]Dipartimento di Genetica e Biologia Molecolare and [b]Dipartimento di Chimica, Università di Roma "La Sapienza". [c]Dipartimento di Chimica delle Sostanze Naturali Università di Napoli "Federico II". maria.savino@uniroma1.it

The G-quartets structure has been proposed over four decades ago. In this arrangement four guanine can associate in a cyclic bulding-block, held together *via* Hoogsteen hydrogen bonds.
The G-quartets, in guanine-rich sequences, can organize complex-folded structures, the so-called "quadruplexes", stabilized by monovalent cations.
The understanding of quadruplex structures closely concerns two different research fields of increasing interest: the biological significance of G-rich sequences in genome organization and the development of biomaterials for nanotechnology applications (1,2).
In our research group, recently, we analyzed the sequence structural features of a homopurine/homopyrimidine tract, located about 100 bp upstream of transcription site within HTERT gene promoter, on account of its importance in chromatin organization and in transcriptional regulation (3).
Studying the structural organization of this homopurine oligonucleotide, (5'GGGGAGGGGAAGGAAAGG3'),HTP, by AFM imaging, we have found out that it can organize linear superstructures of different lengths on mica surface, characterized by the recurrence of single elements spaced every 14.2 nm. (See Fig.).
It is worth noting that the single units have height about 1.6 nm that are about twice with those of a duplex DNA, used as standard.
To highlight the structures involved, we have carried out electrophoretic mobility shift assays (EMSA) in different salt conditions. The obtained results suggest that the superstructures building blocks can be an intermolecular G-quadruplex structure, differently stabilized by Na+ and K+ cations. Surprisingly, the super-structural organization of G-quadruplex blocks appears regulated by the presence of negative phosphate charges at 5' sequence termini.
Circular dichroism studies support both the presence of intermolecular G-quadruplex and the different influence of Na+ and K+ cations on their thermodynamic stability.
Possible molecular models are under investigation.

1. T. Marsh, J. Vesenka and E. Henderson. NAR (1995) 23, 696-700
2. M. Batalia, E. Protozanova, R. Macgregor and D. Eric. Nano Letters (2002) 2 269-274
3. L Rossetti, G. D'Isa, C. Mauriello, M. Varra, P. De Santis, L. Mayol, and M. Savino: (submitted)

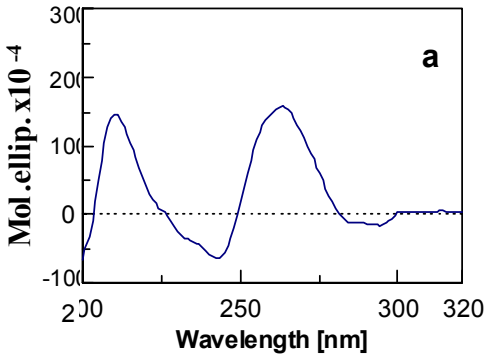

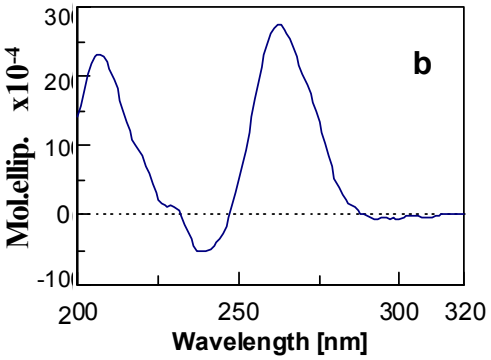

CD spectra of HTP
a) 50 mM NaCl, and 5 mM NaH_2PO_4 pH 7,5
b) 50 mM KCl, and 5 mM KH_2PO_4 pH 7,5

P 1.31

Analisi Emergetica dell'impatto ambientale delle faggete cedue lombarde

Alberto Schiraldi,, Thomas Epis
DISTAM Università di Milano, via Celoria 2 20133 Milano, alberto.schiraldi@unimi.it

Gli indicatori di di sostenibilità ambientale associata ad un ciclo produttivo, ad un prodotto o ad un territorio sono molti: Analisi del ciclo di vita (life cycle analysis).

- Analisi eMergetica (eMergy analysis).
- Impronta ecologica (ecological footprint).
- Valutazione del capitale naturale e dei servizi degli

ecosistemi (*natural capital*).

- Analisi exergetica (exergy analysis).
- Bilancio dei gas serra (greenhouse gas inventory).
- Analisi di dati dal satellite (remote sensing).
- Contabilità ambientale.

L'Analisi Emergetica si rifà alla memoria dell'energia lungo la catena di trasformazioni e usi:

Questa analisi richiede una procedura precisa:

1. Disegnare uno schema del sistema d'interesse
2. Definire i flussi emergetici tra i diversi elementi del sistema.
3. Quantificare gli input in termini energetici, monetari o di massa.
4. Determinazione dell'emergia di ciascun input, ottenibile moltiplicando gli input per i corrispondenti valori di transformity.
5. Somma dei singoli valori emergetici degli ingressi (R + N + F) per ottenere il valore emergetico del prodotto.
6. Calcolo della transformity del prodotto: emergia del prodotto / unità del prodotto (j,g,$).

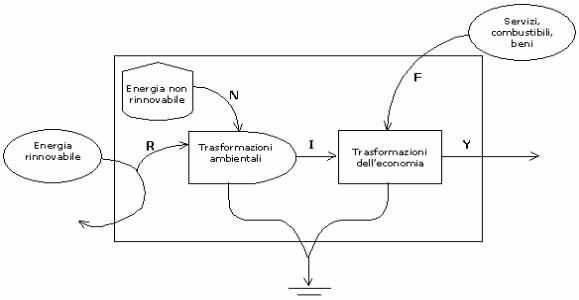

Per l'applicazione è stato utilizzato uno schema semplice in accordo con altre valutazioni emergetiche forestali:

a) Emergy evaluation of boreal spruce (Picea abies) and pine (Pinus silvestris) silvicultural production and timber extraction under 80 year rotation schedules in southern Sweden. (Doherty, 1995).
b) Emergy evaluation of slash pine (Pinus elliotti) silvicultural production and timber extraction under 25 year rotation schedules in north Florida. (Doherty, 1995).
c) Emergy evaluation fuelwood plantation production (Eucalyptus spp. And Melaleuca spp.) under 5 tear rotation schedules in south Florida. (Doherty, 1995).

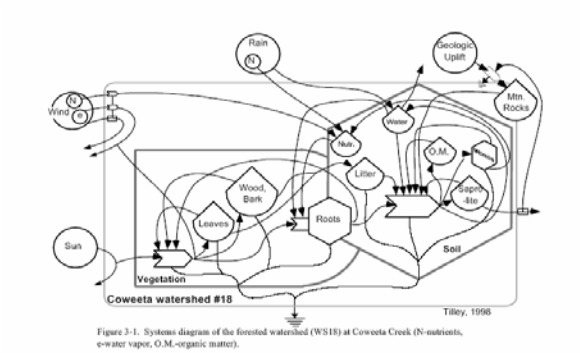

Figure 3-1. Systems diagram of the forested watershed (WS18) at Coweeta Creek (N-nutrients, e-water vapor, O.M.-organic matter).

Nel bilancio emergetico compaiono i diversi ingressi raggruppati secondo la tipologia che li identifica:
R: è stato considerata il solo input "Pioggia – evapotraspirazione" poiché l'energia solare e il vento sono i fenomeni che provocano la formazione delle precipitazioni.
F: i termini propri dell'emergia acquistata sono suddivisi in relazione alla tipologia.

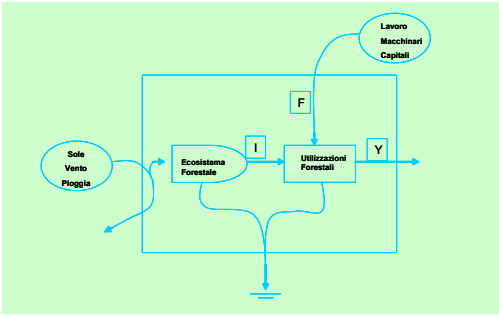

	Risorse (ha/anno)	Transformity (sej / unit)
R	Energia solare	1
	En. cinetica del vento	1500
	Pioggia- - evap	18200
F	Carburante	47900
	Lubrificante	54000
	Macchinari forestali	6700000000
	Manodopera	10900000
	Progettazione	10900000
	Capitale investito	1500000000000

Applicata ad una faggeta cedua, l'analisi emergetica porta ai seguenti risultati

	Risorse	Emergia (sej /ha anno)
R	Energia solare	2,85988E+13
	En. cinetica del vento	4,36379E+13
	Pioggia- - evap	8,09172E+14
F	Carburante	2,67382E+14
	Lubrificante	258336
	Macchinari forestali	2,16306E+13
	Manodopera	2,55513E+14
	Progettazione	3,06616E+13
	Capitale investito	7,96264E+13
Y	Prodotto	1,46399E+15

Rapporto d'impatto ambientale, (N+F)/R = 0,809
Rendimento emergetico,Y/F = 2,236
Investimento emergetico, F/(N + R) = 0,809

P 1.32

Scuola Nazionale Di Metodologie Chimico Fisiche Per Lo Studio Dei Sistemi Biologici

Alberto Schiraldi
DISTAM Università di Milano, via Celoria 2 20133 Milano, alberto.schiraldi@unimi.it

La Scuola Nazionale vuole essere un riferimento comune per i gruppi di ricerca italiani che si occupano dello studio di sistemi e sostanze di interesse biologico con metodologie chimico-fisiche, sperimentali e teoriche.
La Scuola è rivolta a laureandi, dottorandi, borsisti, ricercatori dell'università, degli enti pubblici e dell'industria, che operano o intendono operare nel campo delle scienze della vita. Le lezioni saranno dedicate alla presentazione delle tecniche sperimentali e degli aspetti teorici dello studio dei sistemi biologici, con specifico riferimento alle macromolecole biologiche (proteine, carboidrati, acidi nucleici) e alle strutture supramolecolari di origine naturale e sintetica di interesse fisiopatologico, farmacologico e alimentare.
La scuola si propone di trattare un ventaglio ampio di tecniche Chimico-fisiche applicate ai sistemi biologici fra le quali: NMR, EPR, Raman, Metodi ottici stazionari e risolti nel tempo, Microscopia (AFM, STM, SNOM), Metodi teorici e computazionali, Cristallografia a raggi X (anche supportata da sorgenti al Sincrotrone), Spettrometria di massa, Elettrochimica, Calorimetria, ecc. la domanda di partecipazione dovrà essere inviata all'indirizzo della segreteria marco.signorelli@unimi.it.
La quota d'iscrizione è € 350.
Sono disponibili un numero limitato di borse di partecipazione a copertura totale o parziale delle spese d'iscrizione a favore di giovani non strutturati. Le domande, corredate da una lettera di accompagnamento del supervisore, dovranno pervenire alla Segreteria della Scuola.

P 1.33

Peptides with regular enantiomeric sequences as self-assembling nanotubes for nanotechnology.

A. Scipioni[a], S. Morosetti[b], P. De Santis[b]

[a]Dipartimento di Chimica, La Sapienza Università di Roma, P. le A. Moro5, 00185 Roma; anita.scipioni@uniroma1.it
[b]Dipartimento di Chimica, La Sapienza Università di Roma, P. le A. Moro5, 00185 Roma

The wide interest in the nanoscience and nanotechnology of carbon and inorganic nanotubes raised a renewed attention to organic tubular assemblies. In fact, organic trans-annular assemblies constitute an expanding class of structures with promising applications in supramolecular chemistry and realistic perspectives for the design of nanotechnological devices for molecular electronics and membrane separation technology. Among the strategies developed for the design and engineering of organic nanotubes, those characterized by regular alternating enantiomeric amino acid sequences have been proven particularly useful. The basic principles that regulate the conformational stability of enantiomeric sequences were formulated by De Santis and coworkers about thirty years ago (1). Amino acid sequences with alternating configurations have the propensity to form self-assembling trans-annular nanotubes (or helical channels) stabilized by multiple hydrogen bonds with different inner radius and quantized lengths. These can be further stabilized by suitably designed amino acid sequences, which provide cross-links between the adjacent cyclic DL-peptides (or helical spires).
On the basis of the theoretical predictions, more than twenty years ago, long time before nanotubes were conceived, we synthesized and investigated the properties of poly(DL-proline) as an ion channel and found regular current fluctuation events due to a single channel molecule in bilayer membranes, doped with the polypeptide (Figure 1) (2-5).
We are at present investigating the possibility to obtain self-assembling nanotubes using different amino acids and adopting suitable strategy of stabilization. In particular, DL-cysteine and DL-lysine seem to be promising. In fact, DL-cysteine could be stabilized by vulcanization of adjacent annular peptides (Figure 2) while DL-lysine nanotubes could be obtained by formation of metal complexes between their salycilaldimine derivatives (Figure 3) (7-8).
In all cases, it is possible to separate nanotubes with differently sized lengths. Such nanotubes are characterized by high rigidity and modularity and provide the possibility to build ion single molecule conductors, nanomemory for electronics obtained by the quantized states of a suitable cation confined in a nanotube. Self-assembled nanotubes with peptide architecture can be used for casting metal nanowires, for example to be used as tips for Atomic Force Microscopy and improve the resolution power. The peptide nanotubes coated with suitable metal complexes of lysine derivatives are easily oriented under magnetic field on suitable surfaces and could be used as rigid linear building blocks for spintronic devices.

1. De Santis P.; Morosetti S.; Rizzo R.; *Macromolecules*, **1974**, *7*, 52-58. 2. De Santis P.; Palleschi A.; Savino M.; Scipioni A.; Sesta B.; Verdini A.; *Biophys. Chem*., **1985**, *21*, 211-215. 3. De Santis P.; Palleschi A.; Savino M.; Scipioni A; *J. Phys. Chem*., **1988**, *92*, 4759-4765. 4. De Santis P.; Scipioni A.; Palleschi A.; Savino M.; *Biopolymers*, **1989**, *28*, 285-296. 5. De Santis P.; Palleschi A.; Scipioni A.; Camalli M.; Spagna R.; Zanotti G.; *Biopolymers*, **1998**, *45*, 257-267. 6. Ascoli F.; De Angelis G.; Del Bianco F.; *Biopolymers*, **1975**, *14*, 1109-1114. 7. Dentini M.; De Santis P.; Savino M.; *Macromolecules*, **1980**, *13*, 1308-1311. 8. De Santis P.; Morosetti S.; Scipioni A; *Journal of Nanosciences and Nanotechnology*, **2007**, *7*, 1-9 *(invited paper)*.

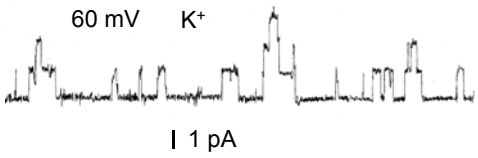

Fig.1

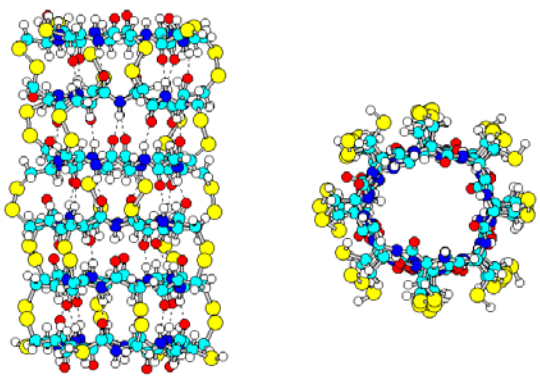

Fig.2

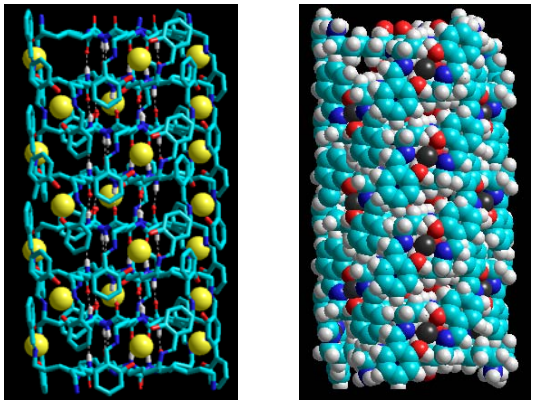

Fig.3

P 1.34

Isotopic effect on the kinetics of the Belousov-Zhabotinsky reaction: Cerium-Malonic subsystem.

Simoncini E.[a], Rossi F.[b], Rustici M.[c], Marchettini N.[a]
[a]*Dipartimento di Scienze e Tecnologie Chimiche e dei Biosistemi, via della Diana, 2/a, 53100 Siena. Simoncini7@unisi.it*
[b]*Dipartimento di Chimica Fisica, Università di Palermo.*
[c] *Dipartimento di Chimica, Università di Sassari, Via Vienna 2, Sassari.*

In this work we present results about the Deuterium isotopic effect on Ce(IV) oxidation of Malonic Acid and its influence on the global behaviour of the Belousov-Zhabotinsky reaction.
In the oscillating chemical reactions field the Belousov-Zhabotinsky (BZ) reaction, i.e. the catalytic oxidation of Malonic Acid (MA) by bromate ions, in the presence of ceric ions, represents one of the most known and studied examples[1,2]. The study of the system in deuterated environment allowed us to stress the relevance of the enolization step in the bromine-MA reaction[3].
The BZ reaction in deuterated environment presents a slower global kinetics, as happens for the single Ce(IV) – MA reaction[4,5]. In the present work, the kinetic constant of MA oxidation by Ce(IV) in D_2O was experimentally calculated, and the reaction mechanism was characterized. Furthermore, a BZ reaction simulation was performed using MBM kinetic model and COPASI package, introducing the kinetic constants found for Ce(IV) – MA and bromine – MA reactions; we finally compare simulation results with experimental data.

1. Belousov B. P.; *Ref. Radiat. Med*., **1959**, 145. 2. Zhabotinsky, A.; *Biofizika*, **1964**, *9* (3), p. 306. 3. Rossi F.; Rustici M.; Rossi C.; Simoncini E.; Tiezzi E.; **2006,** *XXII Congresso della Società Chimica Italiana, Atti del Congresso*, p. 249. Sessione Poster. 4. Hsu M.-C.; Jwo J.-J.; *Int. J. Chem. Kinet*., **1999,** *31*, p.455-461. 5. Jwo J.-J.; Noyes R. M.; *J. Am. Chem. Soc*., **1975**, *97*, 5422-5431.

P 1.35

Theoretical Studies on the Structure of Polycyclic Aromatic Hydrocarbons (PAHs) and Soot Platelets and Their Oxidative Functionalization

Anna Giordana,[a] Andrea Maranzana,[a] Giovanni Ghigo,[a] Mauro Causà,[b] G. Tonachini[a]
(a) Dipartimento di Chimica Generale e Organica A., Università di Torino, Corso Massimo D'Azeglio 48, I-10125 Torino, Italy, e-mail: glauco.tonachini@unito.it; (b) Dipartimento di Chimica, Università di Napoli "Federico II", ComplessoUniversitario di Monte Sant'Angelo, Via Cintia 1, I-80126 Napoli, Italy

At the outset, we aimed to define appropriate PAH-like or periodic models for a soot platelet, and then examined the gas-solid interaction of some small species (H, NO, NO_2, and NO_3) by which soot functionalization can take place.[1] Subsequently, we considered soot oxidation operated by ozone, and compared its features with some experimental studies.[2] Finally, we have explored the nature of the oxidized soot surface through the theoretical study of the desorption mechanisms of a variety of polar groups from different systems, and attempted to give a contribution to the interpretation of Temperature Programmed Desorption (TPD) spectra.[3]

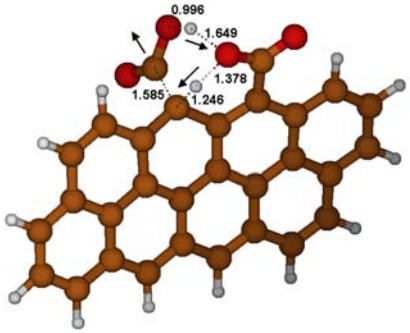

The investigation is now being extended to different model systems, which can be reasonably assumed to form during combustion. These are made up by an even or odd number of carbon atoms, such as the PAH systems detected in flames (where they are almost equally important), and can contain 5-membered rings. For these systems, we compare the reactivity of both internal and peripheral positions toward ozone [4] as well as hydroxyl and nitrogen oxides.[5,6]

1. Ghigo, G.; Maranzana, A.; Tonachini, G.; Zicovich-Wilson, C. M.; Causà M. *J. Phys. Chem. B* **2004**, *108*, 3215–3223. **2**. Maranzana, A.; Serra, G.; Giordana, A.; Tonachini, G.; Barco, G.; Causà M. *J. Phys. Chem. A* **2005**, *109*, 10929–10939. **3**. Barco, G.; Maranzana, A.; Ghigo, G.; Causà M.; Tonachini, G. *J. Chem. Phys.* **2006**, *125*, 184706. **4**. Giordana, A.; Maranzana, A.; Ghigo, G.; Causà M.; Tonachini, G., *to be submitted*. **5**. Ghigo, G.; Causà M.; Maranzana, A.; Tonachini, G. J. Phys. Chem. A 2006, 110, 13270-13282. **6**. Maranzana, A.; Ghigo, G.; Tonachini, G., *to be submitted*.

P 1.36

Vapor pressures, sublimation and vaporization enthalpies using isothermal and non-isothermal thermogravimetry

S. Vecchio
Dipartimento di Ingegneria Chimica Materiali Ambiente, Sapienza, Università di Roma, Via del Castro Laurenziano, 7, 00161 Roma, stefano.vecchio@uniroma1.it

Thermogravimetry under both isothermal and non-isothermal (linear heating) condition is used in this study to determine apparent values of the vapor pressure of pure substances. To this end, some substances whose vapor pressures, vaporization and sublimation enthalpies are known in suitable ranges of temperatures are considered with the aim to test the reliability of the method. The rate of mass loss, $\Delta m/\Delta t$ (kg s^{-1}), due to free evaporation under either isothermal and non-isothermal conditions is correlated with the vapor pressure P (kPa) exerted by the examined compounds tested, through the Langmuir equation [1,2]:

$$p = \left(\frac{\Delta m}{\Delta t} \cdot \frac{1}{S} \cdot \sqrt{\frac{T}{M}} \right) \cdot \frac{\sqrt{2\pi R}}{\alpha'} \quad (1)$$

where T is the temperature (K), M is the molar mass (kg mol^{-1}), R is the gas constant (R=8.3145 J mol^{-1} K^{-1}) and α' is the vaporization constant. Using a linear regression analysis the enthalpies of vaporization and sublimation were obtained from the slope of the modified Clausius-Clapeyron plot $\ln[(\Delta m/\Delta t)\cdot(1/S)\cdot(T/M)^{0.5}]$ *vs*. $1/T$ for the two reference compounds at the mean temperature of the experimental temperature range. These values were subsequently corrected for the standard state at 298 K using the difference $C_p(g) - C_p(s)$ recommended from literature [3,4]. The results obtained for benzoic acid and ferrocene are reported in Tables 1 and 2, as an example.

Table 1 Molar standard enthalpies of benzoic acid derived using the proposed TG techniques. Literature enthalpy value for comparison purpose is $\Delta_{sub}H°$(298 K)=89.7±1.0 kJ·mol^{-1} (ref. 5).

		ΔT	$\Delta_{sub}H°$(298 K)[c,d]	
technique	process	K	kJ·mol^{-1}	
I-TG	sublim	333 – 356	87.7	± 1.5
NI&I-TG[a]	sublim	361 – 393	89.1	± 1.0
NI&I-TG[aa]	vaporiz	396 – 458	90.3	± 2.0

[a] mean of three experiments (one I-TG and two NI-TG ones).
[aa] mean of five experiments (one I-TG and four NI-TG ones).

Table 2 Molar standard enthalpies of ferrocene derived using the proposed TG techniques. Literature enthalpy value for comparison purpose is $\Delta_{sub}H°$(298 K)=89.7±1.0 kJ·mol^{-1} (ref. 5).

		ΔT	$\Delta_{sub}H°$(298 K)[c,d]	
technique	process	K	kJ·mol^{-1}	
I-TG	sublim	313 – 353	73.6	± 1.7
I-TG	sublim	396 – 436	74.1	± 2.2
NI&I-TG[a]	sublim	357 – 403	73.7	± 0.8

[a] mean of three experiments (one I-TG and two NI-TG ones).

An excellent agreement was found between the obtained molar standard enthalpies and those found in literature [5] as well as those recommended by the IUPAC [6], thus confirming the reliability of the proposed method.
Finally, the following average equations, which describe the temperature dependence of vapor pressure, were derived by applying a linear regression analysis to Eq .(1):

benzoic acid (s): $\ln P$(kPa)=(15.52±0.38)–(10287±155)/(T/K) (from 333 to 393 K)
benzoic acid (l): $\ln P$(kPa)=(10.22±0.41)–(8130±141)/(T/K) (from 396 to 458 K)
ferrocene (s): $\ln P$(kPa)=(11.50±0.45)–(8547±178)/(T/K) (from 313 to 447 K)
naphthalene (s): $\ln P$(kPa)=(13.41±0.46)–(8423±139)/(T/K) (from 333 to 353 K)

The results obtained in this study confirm that thermogravimetry offers several advantages over the conventional techniques (Knudsen, torsion effusion, gas saturation and transpiration methods): simple experimental set-up, limited amounts of sample, short time analysis, absence of pretreatment of the sample. Even if its accuracy and precision are not so high compared to the above-mentioned techniques it allows a preliminary screening of the vapor pressure and a rapid estimation of sublimation enthalpy of pure substances [7,8].

1. Vecchio, S.; Brunetti, B.; *J. Chem. Eng. Data*, **2005**, 50, 666 – 672. 2. Jones, H.A.; Langmuir, I.; Mackay, M.G.; *Phys. Rev*., **1927**, 30, 201 – 214. 3. De Kruif, C. G.; Blok, J. G.; *J. Chem. Therm*. **1982**, 14, 201 – 206. 4. Torres, L.A.; Barreiro-Rodriguez, G.; Galarza-Mondragon, A.; *Thermochim. Acta* **1988**, 124, 229 – 233. 5. Sabbah, R.; Xu-wu, A.; Chickos, J. S.; Leita, M. L. Planas; Roux, M. V.; Torres, L.A.; *Thermochim. Acta* **1999**, 331, 93-204. 6. Marsh, K. N.; IUPAC-Recommended Reference Materials for the Realization of Physicochemical Properties, Blackwell Scientific Publications, Oxford, UK, 1987. 7. Price, D.M.; *Thermochim. Acta*, **2001**, 367-368, 253 – 262. 8. Chatterjee, K.; Hazra, A.; Dollimore, D.; Alexander, K. S.; *Eur. J. Pharm. Biopharm*., **2002**, 54, 171 – 180.

P 1.37

Vaporization study of acetaminophen and three of its derivatives using isothermal and non-isothermal thermogravimetry

V. Rossi[a], M. Tomassetti[b], S. Vecchio[a]
[a]*Dipartimento di Ingegneria Chimica Materiali Ambiente, Sapienza, Università di Roma, Via del Castro Laurenziano, 7, 00161 Roma, stefano.vecchio@uniroma1.it*
[b]*Dipartimento di Chimica, Sapienza, Università di Roma, P.le A. Moro, 5, 00185 Roma.*

The knowledge of vapor pressure is important in several fields of application, ranging from the pharmaceutical and the environmental to the separation and purification ones. Even if thermogravimetry (TG) under both isothermal and non-isothermal (linear heating) condition is less accurate than conventional methods, it can be used to determine apparent values of the vapor pressure of pure substances with sufficient precision. On the other hand, the relatively small amount of substance, the simplicity of the experimental set-up and the short experimental times represent the advantages of TG over the more conventional techniques. Therefore, some substances (whose vapor pressures, vaporization and sublimation enthalpies are known in suitable ranges of temperatures) can be considered to test the reliability of the method. In the present study, benzoic acid, ferrocene, and naphthalene were used for this purpose measuring the rate of mass loss $\Delta m/\Delta t$, due to free evaporation under both isothermal and non-isothermal conditions through the TG apparatus. This quantity can be correlated under vacuum condition with the vapor pressure P exerted by the examined compounds tested, through the Langmuir

equation [1]. Price and Hawkins [2] used this relation with a TG equipment and affirmed that the vaporization rate of the sample is not significantly affected by the flow rate of the used purge gas. By contrast, Pieterse and Focke [3] proposed a revised vaporization equation justified by the fact that the rate of vaporization is limited by diffusion. However, recently it was demonstrated that in some cases the difference between the results obtained using the two mentioned approaches is negligible [4].

On the other hand, the atmospheric accumulation of toxic compounds such as pesticides and pharmaceuticals is essentially due to the use of substances having low vapor pressure at room temperature [5]. Consequently, the vaporization pathway of these substances is a crucial phenomenon that is worth investigating. As far as pharmaceuticals is concerned, their amount in a tablet dosage form may vary due to evaporation during the tableting process, hence depleting its specific properties in the solid mixture. Furthermore, for a given formulation of a drug it is important to determine and quantify the evaporation characteristics of each individual component. To this end, in the present investigation acetanilide and three of its para- substituted derivatives, namely the para-hydroxyacetanilide (PHA), the para-ethoxyacetanilide (PEA) and the para-bromoacetanilide (PBA), were selected, taking into account that the thermal behavior and the vaporization kinetics of these drugs was already studied in a previous paper [6]. Moreover, in this study their vaporization enthalpies as well as their temperature dependences of vapor pressure were derived over their melts in suitable ranges of temperatures using both the methods proposed by Price and Hawkins [2] and the one proposed by Pieterse and Focke [3]. The results obtained were compared and discussed with a particular view to establish if vaporization of these substances is limited by diffusion. Furthermore, the experimental vapor pressure data obtained in this study with both the two methods for acetanilide were also compared with those values reported in literature [7] in the same temperature range. In addition, the vaporization enthalpies calculated at the mean of the experimental temperature ranges were subsequently corrected for the standard state at 298 K using the difference in the heat capacity of solid and vapor proposed by Chickos et al [8]. In conclusion, the results obtained in this study enable us to confirm that the TG technique is a useful tool to define the vaporization characteristic of pure drugs with a sufficient precision, providing a rapid response with a small amount of sample and very short experimental time compared with the conventional techniques used for this purpose.

1. Jones, H.A.; Langmuir, I.; Mackay, M.G.; *Phys. Rev*., **1927**, 30, 201 – 214. 2. Price, D.M.; Hawkins, M.; *Thermochim. Acta*, **1998**, 315, 19 – 24. 3. Pieterse, N.; Focke, W. W.; *Thermochim. Acta*, **2003**, 406, 191 – 198. 4. Vecchio, S.; *J. Therm. Anal. Cal.,* **2007**, 87, 79 – 83. 5. Lyman, W.; Environmental Exposure from Chemicals, vol 1, Chapter 2, CRC Press, Boca Raton, 1985. 6. Vecchio, S.; Catalani, A.; Rossi, V.; Tomassetti, M.; *Thermochim. Acta*, **2004**, 420, 99 – 104. 7. Yaws, C. L.; Handbook of vapor pressure, vol 3, Gulf Publishing Company, Houston (TX) , 10th ed., 1994. 8. Chickos, J. S.; Hosseini, S.; Hesse, D. G.; Liebman, J. F.; *Struct. Chem.*, **1993**, 331, 261 – 269.

P 1.38

Monitoring peptide folding by Time-Resolved Spectroscopies: the effect of a single Gly to Aib susbtitution

Mariano Venanzi,[a] Emanuela Gatto,[a] Gianfranco Bocchinfuso,[a] Antonio Palleschi,[a] Lorenzo Stella,[a] Chiara Baldini,[b] Fernando Formaggio,[b] Claudio Toniolo[b] and Basilio Pispisa[a]

[a]*Department of Chemical Sciences and Technologies, University of Roma Tor Vergata, 00133 Rome, Italy, venanzi@uniroma2.it*

[b]*Department of Chemistry, University of Padua, 35131 Padua, Italy*

We have recently reported[1] on a new fluorescent analog of trichogin GA IV, a natural peptide showing interesting antimicrobial activity. The primary structure (and acronym) of the peptide investigated is:

Fmoc-Aib-Gly-Leu-Aib-Gly-Gly-Leu-TOAC-Gly-Ile-Leu-OMe (F0T8)

The double substitution of an energy donor (Fmoc) and an acceptor (TOAC) pair in the trichogin chain enabled us to make use of time-resolved optical spectroscopies, spanning from the nanosecond to the microsecond time regime, to investigate the conformational propensity and the dynamical features of F0T8. Experimental and computational results indicated that the structural and dynamical properties of F0T8 were determined by the transition from an elongated helical conformation to a compact structure mimicking a helix-turn-helix motif. To further investigate the role of the Gly^5-Gly^6 central motif we have synthesized a new trichogin analog having the Gly^6 residue substituted by Aib, i.e.

Fmoc-Aib-Gly-Leu-Aib-Gly-Aib-Leu-TOAC-Gly-Ile-Leu-OMe (F0A6T8)

Time resolved spectroscopy measurements show that the conformations actually populated by F0T8 are not significantly perturbed by the Aib vs. Gly substitution in F0A6T8, as also confirmed by preliminary molecular mechanics calculations. This finding emphasizes the structural rigidity of the peptides investigated. By contrast, the Aib insertion affects the peptide dynamical properties in the microsecond time scale. Important differences in the binding of Ca(II) and Gd(III) by the two peptides have been also observed.

[1]*M.Venanzi, E. Gatto, G. Bocchinfuso, A. Palleschi, L. Stella, C. Baldini, F. Formaggio and C. Toniolo J. Phys. Chem. B 2006, 110, 22834-22841.*

P 1.39

Antimicrobial peptides chelating lanthanide ions: the case of Trichogin GAIV analogs and Terbium(III)

Mariano Venanzi,[a] Emanuela Gatto,[a] Lorenzo Stella,[a] Gianfranco Bocchinfuso,[a] Antonio Palleschi,[a] Fernando Formaggio[b] and Claudio Toniolo[b]

[a]*Department of Chemical Sciences and Technologies, University of Roma Tor Vergata, 00133 Rome, Italy, venanzi@uniroma2.it*

[b]*Department of Chemistry, University of Padua, 35131 Padua, Italy*

Lanthanide chelates are actively explored for potential applications in medical diagnostics, bioimaging and bioanalytical assays. One major problem to be faced for the utilization of lanthanides is their insertion and vehicolation through the membrane phase. Specifically designed oligopeptides, due to their ability to fold into specific structures, to bind membranes or proteins, and to transport ions and small organic molecules, represent promising novel smart materials to be investigated.
We report on the ion binding properties of two fluorescent analogs of trichogin GA IV, a natural peptide showing interesting antimicrobial activity. Primary structures (and acronyms) of the peptides investigated are:
Fmoc-Aib-Gly-Leu-Aib-Gly-Gly-Leu-Aib-Gly-Ile-Leu-OMe (F0)
nOct-Aib-Gly-Leu-Aib-Gly-Gly-Leu-Aib-Gly-Dab(Fmc)-Leu-OMe (F10)
where Aib is α-aminoisobutyric acid, Fmoc is fluoren-9-ylmethyloxycarbonyl and Fmc fluoren-9-ylmethylcarbonyl.

CD titration experiments with Tb(III) revealed that, upon ion binding, both F0 and F10 undergo a conformational transition, forcing the peptide chain to attain folded, non-helical structures. Upon ion binding the fluorescence of Tb(III) markedly increased, due to an energy transfer process from the fluorene excited state to Tb(III). The occurrence of a Förster energy transfer (FRET) mechanism is made possible by the spectral overlap between the emission spectrum of the donor molecule (fluorene) and the absorption of the acceptor species [Tb(III)]. The excitation spectrum carried out at the acceptor emission wavelength confirmed the transfer of excitation energy in the Fluorene→Tb(III) direction. From FRET experiments we found that the donor-acceptor distance in the F0-Tb(III) complex is 12Å, while in the F10-Tb(III) it is 5.8Å. These results suggest that the ion binding site is close to the C-terminus of the peptide chain. Molecular mechanics calculations are currently underway, to obtain structural information on the ion-peptide complex.

.

P 1.40

Effect of aggregation and membrane-water partition on peptide antimicrobial activity: a lesson learned from spectroscopic studies.

L. Stella[a], C. Mazzuca[a], G. Bocchinfuso[a], F. Formaggio[b], E. Gatto[a], K. S. Hahm[c], A. Palleschi[a], B. Pispisa[a], C. Toniolo[b], M. Venanzi[a]
[a]*Dipartimento di Scienze e Tecnologie Chimiche, Università di Roma Tor Vergata, 00133 Roma, Italy. Stella@stc.uniroma2.it*
[b]*Dipartimento di Chimica, Università di Padova, 35131 Padova, Italy.*
[c]*Research Center for Proteineous Materials, 501-759 Gwangju, Korea.*

Notwithstanding the great potential of antimicrobial peptides as new antibiotic agents, the rational design of new analogues with improved activity, selectivity and bioavailability properties remains challenging. In a series of studies on different antibiotic peptides (trichogin GA IV, alamethicin, PMAP-23), we combined several spectroscopic techniques to obtain a detailed quantitative characterization of their physico-chemical behavior (aggregation in water and in the membrane, membrane-water partition, position and orientation in the bilayer, translocation across the membrane). These studies allowed us to discriminate between different models for the mechanism of action, showed that simple modifications in the peptide sequence (e.g. lipidation) perturb peptide partition and aggregation equilibria, and helped us to explain why these changes can lead either to an increase or to a reduction in the overall membrane perturbing activity, depending on the specific case. In addition, experiments on giant unilamellar vesicles (GUVs) provided a direct view of the peptide-induced leakage process. Finally, molecular dynamics simulations starting from a random mixture of water, lipids and peptide, showed in atomic detail the process of bilayer formation, and provided a prediction of the peptide location inside the bilayer in perfect agreement with experimental data. Data on trichogin GA IV are reported here, as a typical test case.

1. Con il contributo del Ministero degli Affari Esteri.

P 1.41

A novel method for detection of Se-Met inclusion into protein crystals *via* Raman microscopy

Alessandro Vergara,[a, b,c] Antonello Merlino,[a] Elio Pizzo,[d] Giuseppe D'Alessio,[d] and Lelio Mazzarella[a,b,c]
[a] *Dipartimento di Chimica, Università degli Studi di Napoli "Federico II", Complesso Monte S. Angelo, Via Cinthia, I-80126. Napoli, Italia, avergara@unina.it*
[b] *Istituto di Biostrutture e Bioimmagini, CNR, via Mezzocannone 6, I-80134 Napoli,*
[c]*Consorzio Bioteknet, University of Naples "Federico II", 80126 Naples, Italy.*
[d]*Dipartimento di Biologia strutturale e funzionale,, Università degli Studi di Napoli "Federico II", Complesso Monte S. Angelo, Via Cinthia, I-80126. Napoli, Italia*

Multiwavelength anomalous dispersion (MAD) is the most widespread approach in structural biology to determine the crystal structure of a novel protein. Mass spectrometry is currently used to evaluate the Se-Met content in solution, but a routine method to check the Se-Met inclusion and storage in the crystal state is not yet available. Raman microscopy is having increasing application into molecular biology, ranging from studies on ligand binding [1] and secondary structure analysis [2]. Here we present a novel tried-and tested methodological development to conduct, via Raman microscopy, analysis on Se-Met labelled protein crystals to be used for MAD crystallography. The method is described, and is supported by validation and application to two novel proteins (a βγ-crystallin-like protein and a DNA-binding protein). Markers of the Se-Met residues are in the range from 570-600 cm^{-1}, where proteins usually do not show any Raman band.

1. P. R.Carey, J. Dong, *Biochemistry* **2004**, *43*, 8885-8893.
2. P. R. Carey, *Ann. Rev. Phys. Chem*. **2006**, *57*, 527-554.

P 1.42

Nanovoid-structured TiO_2 encapsulating $(I_2)_n$ molecules: a way to tune the photoactivity in the visible region

A. Zecchina, G. Ricchiardi, S. Usseglio, A. Damin, D. Scarano, C. Lamberti, S. Bordiga
[a]*Centro di Eccellenza NIS, Dipartimento di di Chimica IFM, Via Giuria 7, 10125 Torino, gabriele.ricchiardi@unito.it*

Among all the semiconductors used in photocatalysis, TiO_2 is essentially the best material for environmental remediation. The only drawback of TiO_2, is that its band gap lies in the near UV of the electromagnetic spectrum: 3.2 eV (285 nm) and 3.0 eV (410 nm) for anatase and rutile respectively. As a consequence, only UV light is able to create electron-hole pairs and to initiate photocatalytic process. As UV light constitutes only 5% of the solar spectrum , 95% of the solar photons are useless for TiO_2 photocatalysts. It is therefore evident that any modification of the TiO_2-based photocatalysts resulting in a lowering of its band gap, or in the introduction of stable optical sensitizes, will represent a breakthrough in the field.

A new strategy to synthesize a TiO_2 characterized by the presence of internal nanovoids is presented. It consists in the hydrolysis at room temperature of pure $Ti(OC_3H_7)_4$ in air (30-40% humidity), according to Equation: $Ti(OC_3H_7)_4 + 2H_2O \rightarrow TiO_2 + 4\ C_3H_7OH$. After 36 hours the white powder obtained was dried at 373 K in an oven and then calcined in air at 773 K for 6 hours.

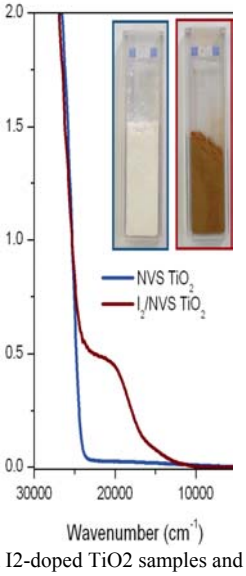

Fig. 1 pure and I2-doped TiO2 samples and their UV-Vis Diffuse Reflectance spectra.

The walls of the internal cavities are populated by adsorbed molecular species derived form the partial combustion of isopropoxide groups. Addition of iodine as dye molecule in the synthesis procedure results in a new nanovoid structured titanium oxide characterized by $(I_2)_n$ adducts encapsulated inside the cavities that in this way are protected from degradtion. The resulting material is able to absorb visible photons of the solar light and to photodegrade methylene blue. Thus surface area of the nanovoid structured TiO_2 is about one order of magnitude lower that that of the P25 commercial TiO_2 photocatalyst, but its ability to degrade methylene blue is comparable. This implies that the surface specific degradation efficiency of this new material is about ten times higher than that of the P25.

P 1.43

MeCAL-2: New catalysts for methane combustion

G. A. V. Martins [a], G. Berlier [a], M. Straussc, S. Coluccia[a], L. Marchese[b], Heloise O. Pastore[c], A. Scarpa[d], R. Pirone[d]
[a]*Dipartimento di Chimica IFM, Università di Torino, Turin I-10125 Italy, gesley.martins@unito.it,* [b]*Dipartimento di Scienze e Tecnologie Avanzate, Università del Piemonte Orientale, Alessandria I-15100, Italy* [c]*Instituto de Química, Universidade Estadual de Campinas, Campinas-SP, Brasil.* [d]*Istituto di Ricerche sulla Combustione IRC-CNR, Napol, Italia. e-mail: gesley.martins@unito.it.*

The search for clean energy sources is the object of study of many research groups. Catalytic combustion is an environmentally friend alternative for heat and power generation using fossil fuels, since it is possible to obtain very efficient burning at concentrations below the flammability limits and at lower temperatures than in the conventional flame combustion, without undesired by-products such as UHC (unburned hydrocarbons), CO and NOx [1]. The present work describes the characterization of a new kind of microporous materials containing transition metal ions, the MeCAL-2, active for hydrocarbon combustion.

[1] M. Zwinkels, S.G. Jaras, P.G. Menon, in: A. Cybulski, J. Moulijn (Eds.), Structured Catalysts and Reactors, Marcel Dekker, New York, 998, p. 149.

P 1.44

Pt-Ba/Al_2O_3 LNT catalysts: TRM and FT-IR analysis of the reduction of stored NO_x in different model atmospheres

F. Frola[1], F. Prinetto[1], G. Ghiotti[1], I. Nova[2], L. Lietti[2], P. Forzatti[2]
[1]*Dipartimento di Chimica IFM, and NIS Centre of Excellence, Università di Torino, Via P. Giuria 7, 10125 Torino. francesca.frola@unito.it*
[2]*Dipartimento di Chimica, Materiali e Ingegneria Chimica "Giulio Natta", Centro NEMAS—Nano Engineered Materials and Surfaces, Politecnico di Milano, Piazza Leonardo da Vinci 32, 20133 Milano.*

Introduction

"Lean NO_x Trap" (LNT) systems, constituted by a NO_x-storage component (alkaline or earth-alkaline metal oxide) and by a noble metal (Pt) which operates the NO_x

reduction, represent the most promising solution to satisfy the demand for new catalytic systems efficient in reducing NO_x emissions by engines working under "lean" conditions [1]. Although used at commercial scale in Japan, a common agreement on the mechanistic aspects of the storage of NO_x species and of their reduction is still lacking [1]. Our previous studies showed that the NO_x storage process occurs through two parallel ways, the "nitrite" and "nitrate" routes (the former occurring only when stored NO_x originated from NO/O_2 mixtures, the latter both in the cases of storage of NO/O_2 mixtures or NO_2) [2, 3]; in this study we used again FT-IR spectroscopy and the transient response method (TRM) as complementary techniques with the aim of providing new insights on the reduction by hydrogen of stored nitrates over Pt-Ba/Al_2O_3.

Experimental

Reduction of NO_x stored on Pt-Ba/Al_2O_3 model catalyst (Pt=1% w/w, Ba=16% w/w) at 350°C by imposing a rectangular step feed of NO (1000 ppm) in flowing He + 3% v/v O_2 (TRM experiments) or admitting NO/O_2 1:4 mixture (FTIR experiments, pNO=4mbar) was studied at different temperatures, in the range 100-350°C, by imposing a stepwise change in the H_2 concentration (2000 ppm) (TRM) or admitting pure H_2 pH_2=5 mbar (FTIR) The effect of the presence of CO_2 and/or water during the reduction phase was also analysed.

Results and discussion

TRM regeneration procedures following NO_x adsorption at 350°C were performed at different temperatures in the range 100-350°C. At temperatures below 150°C the NO_x reduction was very slow and delayed with respect to hydrogen admission, and NH_3 was the main reaction product. In the range of temperatures 150-300°C the reduction process was very fast, but higher ammonia formation and a not complete removal of the stored NO_x was observed. At 350°C, H_2 was immediately consumed with an immediate selective formation of N_2; small amounts of NO were also detected in the gas phase at the beginning of the reduction process. Then, when hydrogen appeared into the gas phase, the concentration of nitrogen decreased and after H_2 breakthrough, evolution of ammonia was observed. Similar experiments were also performed in the presence of water or CO_2: data showed that water favoured the rate of NO_x reduction, whereas CO_2 had an adverse effect. No significant effects on the nitrogen selectivity were observed. A parallell FT- IR study was carried out during which the evolution of stored NO_x with the temperature in the different atmospheres was analyzed. In the case of pure H_2 the results were in line with the TRM experiments: nitrate reduction started at 150 °C and was completed at 250°C. The presence of CO_2 inhibits the NO_x reduction, as also pointed out by TRM data. No reaction intermediates or reaction products are detected by IR spectroscopy using pure H_2. At variance, using the H_2/CO_2 mixture, starting from 100°C weak absorptions between 2070 and 2020 cm^{-1} were detected, due to CO linearly adsorbed on $Pt^{\delta+}$ or Pt^0. This shows that the reversed water shift reaction takes place and CO adsorbed on Pt inhibits the NO_x reduction. Moreover, weak bands at 2242 and 2164 cm^{-1} appeared starting from 150°C, reasonnably due to the presence of surface cyanate and/or isocyanates. As in the case of CO_2, FT-IR experiments performed with H_2/H_2O mixture were in agreement with TRM data, confirming a benefical effect of water on the reduction of stored nitrates, i.e lowering the temperature at which the reduction starts. Since TRM data show that NH_3 is the main product at temperature up to 150 °C, dedicated FT-IR experiments were involving reduction of the stored NO_x in pure H_2 at 150°C followed by cooling the catalyst in the reaction mixture down to RT in order to detect the adsorbed NH_3 possibly formed. When the sample is cooled to RT, no traces of adsorbed NH_3, but hydroxyls, small amounts of coordinated water and of nitrites were detected. With the aim to understand the origin of the nitrite formation a new series of FT-IR analysis was performed: NO_x species were first stored at 350°C at different coverage, sample was cooled down to RT and increasing amount of H_2O or D_2O were adsorbed up to the vapor saturated pressure. Nitrites are always observed to form in increasing amounts on increasing the H_2O or D_2O coverage, showing that their formation is a peculiar results of the interaction of water at RT with a surface not satured with nitrates. Both TRM and FT-IR data are consistent with a reaction pathway in which H_2 is dissociated on Pt sites, followed by spillover of the atomic H towards the stored nitrates leading to their destabilization/decomposition and to their reduction. CO_2 inhibits the reaction due to CO adsorption on Pt whereas water would favour the process by enhancing the H spillover. In this light, the selectivity of the process (*i.e.* NH_3 *vs.* N_2 formation) might be governed by the NO_x/H ratio, i.e on the relative abundance of NO_x surface species and of the split H. Besides, the participation of NH_3 by-product in the reduction of stored NO_x cannot be excluded.

Conclusions

The reduction of the stored NO_x over a model Pt-Ba/Al_2O_3 catalysts under different atmospheres at different temperatures was investigated by TRM and FT-IR spectroscopy, showing that the NO_x reduction pathway and the selectivity of process strongly depend on operating conditions. Further TRM and FT-IR analyses are currently in progress which analyse ammonia formation and its possible involvement as intermediate species in the mechanism governing the reduction of NO_x adsorbed specie by H_2.

References

[1] Epling W.S, Campbell L.E., Yezerets A., Currier N.W.,.Park II J.E, Catal.Reviews, 46(2) (2004) 163

[2] Nova I., Castoldi L., Prinetto F., Ghiotti G., Lietti L., Tronconi E.,.Forzatti P, J.Catal, 222/2 (2004) 377

[3] Nova I., Castoldi L., Lietti L., Tronconi E.,.Forzatti P, J.Catal, 239 (2006) 244

SEZIONE

SPETTROSCOPIA E FOTOCHIMICA

P 2.1

Small, Infrared, Luminescent Type II Semiconductor Nanocrystals for Animal Imaging

Matteo Amelia, Loredana Latterini, Gian Gaetano Aloisi and Fausto Elisei
Dipartimento di Chimica and Centro d' Eccellenza Materiali Innovativi Nanostrutturati (CEMIN), Università degli Studi di Perugia, Via Elce di Sotto 8, 06123 Perugia, ameliamat@libero.it

Recently introduced Type II quantum dots[1] possess both the valence and the conduction band with higher, or lower, energy than the core ones. As a result, one carrier is mostly confined to the core, while the other is mostly confined to the shell. Consequently two different classes of Type II QDs can be assembled, one class where the shell presents both the valence and the conduction band at a lower energy with respect to the core, which has holes mostly confined in the core and electrons mostly confined in the shell. Despite, the second class possesses a shell with both the valence and the conduction band at higher energy compared to those of the core, bringing to confine mostly the electrons in the core and the holes in the shell.
Type II quantum dots provide access to wavelength not previously available with a single material, especially in the spectral NIR region (700-1000 nm). This is highly desirable for *in vivo* imaging because of the enhanced contrast resulting from the separation of the nanocrystal photoluminescence from the autofluorescence background and of the increased penetration of both excitation and emission light through tissues[2]. The applicability of NIR type II quantum dots to biomedical *in vivo* imaging has been already proved with the employment of CdTe/CdSe for limph-node mapping in both mice and pigs animal models[3]. Moreover, the spatial charge separation delays the hole-electron recombination bringing to an extremely long fluorescence lifetime. One of the applicative field that can be improved by the introduction of Type II heterostructures is the building up of photovoltaic devices. In fact, in Type I systems photogenerated electrons and holes are concentrated in the core region and their effective separation requires additional excitation into the matrix material, which may suppress the effectiveness of photovoltaic devices, but in Type II systems such barriers are absent, at least for one type of carriers.
In the present work, the CdTe shell deposition on a CdSe core template building a "reverse" Type II CdSe/CdTe heterostructure is reported. The particles synthesized are highly monodispersed and show new optical properties. The almost featureless absorption spectrum possesses a NIR band (detected by PLE spectroscopy) allowing excitation where the light is more penetrative through the tissues. The emission spectrum has been proved to emerge from the two materials interband and to change in the NIR region with the number of shell layers deposited on the template core structure. The system has a high fluorescence quantum yield (up to 20%) comparable with the Type I core/shell QDs and a long lifetime (about 70 ns) that ensures the obtained spatial charge separation. The employment of Successive Ion Layer Adsorption and Reaction (SILAR) has been revealed to be crucial in order to achieve an improvement in the radiative process and in the quality and the homogeneity of the particles. The Type II nanocrystals can be further build up, with minor modifications to the original synthetic scheme, and render water-soluble and bio-compatible. They also result stable under long term irradiation with UV-Vis light. The described properties render the prepared NCs good candidates for animal imaging and for photovoltaic devices applications.

1. Kim, S.; Fisher, B.; Eisler, H. J.; Bawendi M.; *J. Am. Chem. Soc.* **2003**, 125, 11466-11467. 2. Sevick-Muraca, E. M.; Houston, J. P.; Gurfinkel M.; *Curr. Opin. Chem. Biol.* **2002**, 6, 642-650. 3. Kim, S.; Lim, Y. T.; Soltesz, E. G.; Grand, A. M. D.; Lee, J.; Nakayama, A.; Parker, J. A.; Mihaljevic, T.; Laurence, R. G.; Dor, D. M.; Cohn, L. H.; Bawendi, M. G.; Frangioni, J. V. *Nat. Biotechnol.* **2004**, 22, 93-97.

P 2.2

Doped Nanocrystals: Coupling Optical and Magnetic Properties

Matteo Amelia, Loredana Latterini, Gian Gaetano Aloisi and Fausto Elisei
Dipartimento di Chimica and Centro d' Eccellenza per i Materiali Innovativi Nanostrutturati (CEMIN), Università degli Studi di Perugia, Via Elce di Sotto 8, 06123 Perugia, ameliamat@libero.it

Cadmium based semiconductor nanocrystals have been intensively studied in the past three decades due to their enormous advantages versus organic dyes, such as broad excitation profile and by a narrow (FWHM = 25-35 nm) and tunable, accordingly to size, photoluminescence spectrum[1]. However, recently, many concerns have been moved against those systems for the intrinsic toxicity of Cd^{2+} that can compromise the future of cadmium chalcogenide nanocrystals in biological applications, especially *in vivo* (animal models and human body). Within this picture it has been appeared necessary move toward the synthesis and characterization of greener systems.
Manganese doped nanocrystals seems to be the most attractive systems because of their Stokes's shift of about 150 nm and of their red and strong quantum efficiency[2]. In the present Chapter, a decoupling nucleation strategy for doped nanocrystals synthesis is reported[3]. The main innovative aspect, with respect to the already described methods, is the possibility to get the core/shell nanosystem in a easy way by using only one shell precursor and one shell deposition temperature.
The synthesized manganese-doped nanocrystals show a strong photoluminescence intensity (quantum yield of about 30%) centred at 590 nm. The PL peak is slightly affected by size effects opening new possibilities to the employment of nanocrystals in bio-imaging. For instance, it is possible to keep the same emission profile changing the hosting materials and the sizes. Moreover, nanoparticles with same size and hosting materials but with different photoluminescence peaks, might be prepared just exchanging the impurity atoms (e.g. Cu for green PL and Eu for NIR PL) in the same host.
A secondary shell was deposited on the nanocrystals to enhance the persistency of the emission intensity, generally related to the ability of manganese atoms to diffuse at the nanocrystal surface during the purification, irradiation and ageing processes. The latest synthetic step brought to nanocrystals with robust and stable emission properties.
MnSe/ZnSe/ZnS NCa posses an absorption spectrum close to the bare ZnSe NCs (which is the absorbing species) and a PL spectrum linked to the atomic emission

between d states belonging to the manganese doping atoms. They have an high quantum yield and a short lifetime (4 ns). The samples are fairly monodispersed being mainly constituted by one size, as proved by TEM imagines and analysis. Their dimensions may widely range from 2 to 10 nm.
The bioactivation of the ZnS, realized via peptide-coating[4], affected mainly the QY that drops to 3-4%. That low value was proved to be to due to an incomplete surface coverage, so that it can be raised up by a secondary water stabilizer (such as thioglycerol).
Magnetic properties of the doped nanocrystals arising from the manganese have also been demonstrated by Superconducting Quantum Interferometer Devices SQUID measurements. The coupling of optical and magnetic properties in one marker might be tremendously advantageous in biomedicine due to the double imaging mode.

1. Michalet, X.; Pinaud, F. F.; Bentolila, L. A.; Tsay, J. M.; Doose, S.; Li, J. J.; Sundaresan, G.; Wu, A. M.; Gambhir S. S.; Weiss S.; *Science* **2005**, 307, 538-544. 2. Bhargava, R. N.; Gallagher, D.; Hong X.; Nurmikko A.; *Phys. Rev. Lett.* **1994**, 72, 416-419. 3. Pradhan, N. ; Goorskey, D.; Thessing J.; Peng X.; *J. Am. Chem. Soc.* **2005**, 127, 17586-17587.4. Pinaud, F.; King, D.; Moore H. P.; Weiss S.; *J. Am. Chem. Soc.* **2004**, 126, 6115–6123.

P 2.3

Magnetic Resonance investigations on Cultural Heritage materials.

Alfonso Zoleo[a], Marco Ruzzi[a], Lorenzo Franco[a], Daria Confortin[a], Marina Brustolon[a]
[a]*Department of Chemical Sciences, University of Padova, via Marzolo 1, 35131 Padova, marinarosa.brustolon@unipd.it*

Modern spectroscopic techniques for the investigations of art works and archeaeological materials can give a fundamental contribution for a deeper knowledge of the techniques of production, provenance, conservation status and degradative processes of a broad range of materials and objects.
We applied magnetic resonance methods, mainly Electron Spin Resonance spectroscopy and Nuclear Magnetic relaxation methods to the analysis of several materials such as ancient paper and marbles, with the aim to develop a reliable method for the provenance and the evaluation of the conservation status.
Several samples of paper dating from the XV to the XX century have been investigated using CW-EPR spectroscopy. Ancient paper specimens were characterized by apparent signals from radicals, Mn(II), Cu(II) and Fe(III). The relative intensity among the signals was found dependent on the samples, with interesting correlations, e.g., strong Cu(II) signals are detected in deteriorated samples, quite independently of the age of the sample. Furthermore, a comparison among several paper samples from ancient books showed that EPR Mn(II) signal could possibly be used as a marker of the paper origin. We also investigated the photoinduced generation of radicals in ancient paper composed of pure cellulose and in modern paper, which is composed also of lignin and other components. By conventional and pulsed EPR spectroscopy we identified several UV-induced radicals in the cellulose and in the lignin components, and measured their decay kinetics in air and anoxic conditions. The effects of photodegradation of paper has also been investigated using a magnetic resonance technique such as NMR relaxometry, using a single-sided low-field NMR instrument. Our aim is to develop a fast and non-invasive method for the evaluation of the degree of cellulose depolimerization and the water content in paper by means of the analysis of ^{1}H nuclear relaxation times [1].
A further interesting research regards the assessment of the quarry of ancient white marbles. We have studied by EPR spectroscopy the Mn(II) spectra in a series of white marble samples coming from a local archaeological excavation site of roman age (Montegrotto; Padova) and from Museo degli Eremitani, Padova. Mn(II) EPR spectra allow the identification of the provenance of white marble [2], thanks to a database collecting the Mn(II) EPR parameters of most of the ancient quarries.

1. Blumich, B.; Anferova, S.; Sharma, S.; Segre, A.L.; Federici, C.; *J. Mag. Reson.* **2003**, *161(2)*, 204 – 209. 2. Attanasio, D.*;Ancient White Marbles-Analysis and Identification by Paramagnetic Resonance Spectroscopy*- Ed. <<L'Erma> **2003**

P 2.4

The triplet of DCM observed for the first time: a TR-EPR study of the dye inclusion in a KH Phthalate single crystal.

Marina Brustolon[#], Roberto Zanré[#], Antonio Barbon[#], Kristin L. Wustholz[§], Bart Kahr[§]
#Department of Chemical Sciences, Via Marzolo 1, 35131-I, Padova, (Italy)
§ Department of Chemistry, University of Washington, Box 351700, Seattle, WA 98195-1700 (USA)

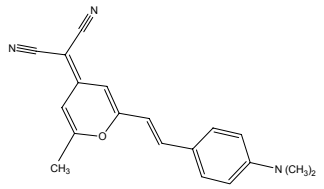

DCM

Colourless crystals of simple salts grown from solution in presence of a dye can be stained by molecules many times larger than those of the host. They are called Dyes Inclusion Crystals (DIC) [1] . Time Resolved EPR is a convenient technique to study some of their singular properties, as e.g. the orientations of the included dyes, breaking often the bulk symmetry of the host [2]. 4-dicyanomethylene-2-methyl-6-(*p*-(dimethylamino)styryl)-4*H*-pyran (DCM) is a laser dye with a push-pull structure. It has many interesting properties arising from the charge transfer that occurs in the excited state. Its photophysical behaviour has been investigated by numerous authors, with different spectroscopies. Its triplet state had never been observed till the present study. We have investigated DCM in a single crystal of KAP (Potassium Acid Phthalate) by Time-Resolved EPR. In this rigid matrix we have been able to observe for the first time the photoexcited triplet of DCM. Its ZFS parameters have been compared with computations sensitive to the conformation of the excited state.
Moreover, we have obtained interesting results on the orientations of the dye giving rise to the triplet state,

which is included only in {11-1} growth sector. We have isolated two sub-volumes from this sector, cutting the fragment along the *c* axis. We have found that the DCM molecules giving the triplet spectrum are present in each sub-sector in an unique orientation, and with slightly different ZFS parameters. The two orientations are not symmetry related, despite the fact that the two sub-sectors are mirror images one of the other. The breaking of the crystal symmetry may be explained as a consequence of intrasectoral zoning via the vicinal faces of growth hillocks. Intrasectoral zoning is here observed for the first time by EPR.

1. B. Kahr, R. W. Gurney, Chem. Rev. 2001, **101**, 893.
2. A. Barbon, M. Bellinazzi, J. B. Benedict, M. Brustolon, S. D. Fleming, S.-H. Jang, B. Kahr, A. L. Rohl, , *Angew. Chem. Int. Ed. Engl.,* 2004, 43, 5278-5286; M. Bellinazzi, A. Barbon, B. Kahr, J. B. Benedict, M. Brustolon , 2006, PCCP, 8, 379-385.

P 2.5

Laser Ablation-Inductively Coupled Plasma Mass Spectrometry for the Determination of Heavy Metals in Airborne Pariculate Matter (Pm10)

Ameriga Fanigliulo, Giuseppe E. De Benedetto
Laboratorio di Analisi Chimiche per i Beni Culturali e per l'Ambiente, Dipartimento dei Beni delle Arti e della Storia, Università del Salento, viale San Nicola, 73100 Lecce. e-mail: giuseppe.debenedetto@unile.it

The coupling of Laser Ablation (LA) with Inductively Coupled Plasma Mass Spectrometry is applied for the qualitative and quantitative determination of heavy metals suspended in airborne inhalable particulate matter, sampled with an impactor high volume air sampler on quartz fiber filters. The easy, rapid, non-destructive method is proposed as a rapid screening procedure for this peculiar environmental specimen. The un-necessity of a preparative/extracting or diluting step and the absence of the stressing conditions generally included in that step (temperature, microwave power, strong acids...) dramatically reduces the probability of interferences or understimating errors [1, 2]. On the other hand, a major statistical study is needed in planning instrumental conditions and data collecting, in order to ensure valuable and reproducible numerical data. We propose a cross-calibration procedure which uses the results obtained on some of the specimens of the sample batch, analysed after acidic digestion and interpolated on a acqueos standard solution calibration curve, as reference points for the direct quantification of the remaining samples, analysed under laser ablation. Real samples from a traffic city site and a rural site, taken as blank, were analysed and compared with acidic digestion analysis. The method was proved to be affordable, reliable and rapid to set.

Wang, C.-F.; Chin, C.-J.; Luo, S.-K.; Men, L.-C; *Anal. Chim. Acta,* **1999**, *389*, 257-266. 2. Rauch, S.; Lu, M.; Morrison, G. M.; *Environ. Sci. Technol.* **2001**, *35,* 595-599

P 2.6

Spectral studies of Nicotinamide and Zinc phthalocyanine complexes

R. Del Sole[a], M. R. Lazzoi[a], A. De Luca[a], G. Vasapollo[a]
Dipartimento di Ingegneria dell'Innovazione, Universita' Degli Studi di Lecce, via per Monteroni, km1, 73100, Lecce, roberta.delsole@unile.it.

Phthlocyanines (Pcs) and metallo phthalocyanines (MPcs) are nowdays considered very attractive materials for their technological applications such as gas sensors, solar cells, homogeneous and/or heterogeneous catalysts, photodynamic therapy and so on [1]. It is well known that the properties of these compounds depend strongly on the nature of the metal, substituents and coordinated ligands [2]. Generally, the presence of alkyl or aryl groups as peripheral substituents or coordinated ligands in the molecules can improve the solubility but also can influence the physical and photo-physical properties.
Nicotinamide (NAM) is an important molecule widely diffused in nature as a form of vitamin B3. NAM is also part of nicotinamide adenine dinucleotide (NAD) and nicotinamide adenine dinucleotide phosphate (NADP) coenzymes and consequently it is involved in various redox processes into the human body [3].
For long time we have been interested in the synthesis of new phthalocyanines and in the study of their coordinating properties with particular molecules [4]. So that, continuing our research in this area, we report here spectral studies and job plot analyses which provide evidence of complexes formation of zinc phthalocyanines and zinc naphthalocyanines complexes with nicotinamide (NAM) and with its isomers isonicotinamide (iNAM) and picolinamide (PAM). To validate complexes formation some of them have been also isolated and fully characterized by FT IR and NMR spectroscopic techniques.

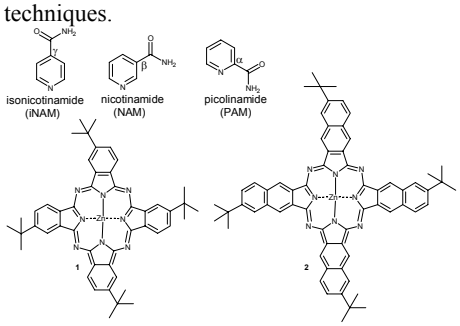

1. a) McKeown, N. B.; Phthalocyanine *Materials: Synthesis, Structure and Function*, Cambridge University Press: Cambridge, **1998**; b) De La Torre, G.; Claessens, C. G.; Torres, T.; *Eur. J. Org. Chem.*, **2000,** 2821-2830.
2. a) Barthel, M.; Dini, D.; Vagin, S.; Hanack, M.; *Eur. J. Org. Chem.,* **2002**, 3756; b) Tomachynski, L. A.; Chernii, V.Y.; Volkov, S. V.; *J. Porphyrins Phthalocyanines*, **2001**, 5, 731.
3. Williams, A.; Ramsden, D.; *Parkinsonism Relat. Disorders*, **2005**, 11, 413.
4. Del Sole, R.; De Luca, A.; Mele, G.; Vasapollo, G.; *J. Porphyrins and Phthalocyanines,* **2005**, 9 (7), 519.

P 2.7

Studio degli ioni Mg^{2+} e Ca^{2+} in metanolo liquido attraverso dinamica molecolare *ab initio* Car-Parrinello

Cristian Faralli[a], Marco Pagliai, Gianni Cardini[a,b] e Vincenzo Schettino[a,b]
[a]*Laboratorio di Spettroscopia Molecolare, Dipartimento di Chimica, Università di Firenze, via della Lastruccia 3, 50019, Sesto F.no, Firenze, Italia, cristian.faralli@unifi.it*
[b]*European Laboratory for Nonlinear Spectroscopy (LENS), via Nello Carrara 1, 50019, Sesto. Fno, Firenze, Italia*

Le proprietà di solvatazione degli ioni Mg^{2+} e Ca^{2+} in soluzione di metanolo completamente deuterato sono state indagate attraverso simulazioni di dinamica molecolare *ab initio* Car-Parrinello al fine di comprendere meglio gli effetti di polarizzazione che insorgono per la presenza dello ione. E' stato analizzato l'effetto delle dimensioni del campione sul comportamento delle molecole della prima sfera di solvatazione senza trovare una particolare influenza sulle proprietà strutturali. Calcoli di trasferimento di carica e di momento di dipolo sono stati esaminati per descrivere dettagliatamente il ruolo della riorganizzazione elettronica e comprendere l'influenza sulla stabilità della prima sfera di solvatazione. I dati ottenuti sono stati confrontati con i risultati delle precedenti analisi per i metalli alcalini (Li^+, Na^+ e K^+).

P 2.8

Low-frequency Raman scattering from aqueous solutions of carbohydrates

S. Perticaroli, P. Sassi, A. Morresi, M. Paolantoni
Dipartimento di Chimica, Università di Perugia, Via Elce di Sotto, 8, I-06123 Perugia, Italy

Understanding the dynamics of water molecules in aqueous solutions of complex biological systems is a subject of considerable interest, due to the fundamental role played by the water in determining the properties of these systems.
Raman and depolarized Rayleigh scattering (DRS) techniques are powerful probes in the study of structural and dynamical properties of carbohydrates aqueous solutions.[1,2] In our laboratory, with regard to glucose and trehalose, we have shown that the contribution of the sugar dynamics is well separated from that of water molecules; moreover, we probed the presence of different components for the relaxation process of bulk and hydrating water[3].
In the present work, the study of sugar-water systems is extended to the analysis of different mono- and polysaccharide solutions. DRS spectra of glucose, fructose, trehalose and dextran aqueous solutions have been analyzed in terms of water and sugar relaxation processes, together with damped harmonic oscillators describing the bending (~50 cm^{-1}) and stretching (~180 cm^{-1}) of O-H···O structures in the low-frequency Raman spectrum. The comparison of the effect of different carbohydrate systems on the properties of water dynamics and structure is performed and discussed.

1. Gallina, M. E.; Sassi, P.; Paolantoni, M.; Morresi, A.; Cataliotti, R. S.; *J. Phys. Chem. B,* **2006,** *110*, 8856 – 8864. 2. Fioretto, D.; Comez, L.; Gallina, M. A.; Morresi, A.; Calmieri, L.; Paolantoni, M.; Sassi, P.; Scarponi, F.; *Chem. Phys. Lett.* in press. 3. Morresi, A.; Sassi, P.; Paolantoni, M.; Gallina, M. E.; Fioretto, D.; Comez, L. in preparation.

P 2.9

Competitive photoisomerization pathways of 1,2-diarylethenes and related compounds

G. Bartocci, S. Ciorba, G.Ginocchietti, U. Mazzucato and A. Spalletti
Dipartimento di Chimica and Centro di Eccellenza Materiali Innovativi Nanostrutturati (CEMIN), Università di Perugia, 06123 Perugia, Italy; faby@unipg.it (Spalletti, A.)

The interest of our laboratory in the internal rotation around the double bond in 1,2-diarylethenes and related compounds has been recently focused on the geometric photoisomerization occurring on a unique potential energy surface by an adiabatic mechanism, i.e. giving rise to an electronically excited photoproduct. The main factors responsible for this behaviour are the nature and energy of the lowest excited states of singlet (S_1) or triplet (T_1) multiplicity of these flexible molecules and the relative position of the energy levels of the excited twisted configuration (^{1,3}perp*) with respect to the quasi-planar (^{1,3}trans* or ^{1,3}cis*) excited forms. In fact, the common diabatic mechanism of the geometric (cis/trans) photoisomerization of 1,2-diarylethenes, implying rotation to the ^{1,3}perp* configuration, followed by internal conversion to the twisted ground state (^{1}perp) and equipartitioning to the ground trans and cis forms, can compete with (or to be completely replaced by) the adiabatic process from one to the other quasi-planar excited states when the twisted form is at a maximum in the potential energy surface describing the isomerization process. This generally (not always) occurs in non-polar solvents when a one-way cis $\rightarrow$ trans photoisomerization is operative.

The cross-road between the competitive pathways would depend on the energy of the twisted geometry: when ^{1,3}perp* is at a flat position or shallow minimum, some molecules undergo $S_1 \rightarrow S_0$ internal conversion there, but others may continue on the same surface towards the excited planar isomer. On the other hand, when the ^{1,3}perp* is at higher energy with respect to at least one of the planar geometries, particularly ^{1,3}trans*, the photoisomerization may really occur on a unique potential energy surface, without crossing (or avoided crossing) with the descendent curve of an upper excited state of the same multiplicity.

The present contribution will describe some typical examples of adiabatic photoisomerization recently evidenced by fluorimetric, flash photolytic and photochemical techniques and confirmed by theoretical calculations. A speculative hypothesis that the mixed mechanism may involve two distinct pathways since the beginning of the twisting process from the starting (planar) geometry is under investigation.

Internal rotation around the quasi-single bonds between the aryl groups and the ethenic carbons is also investigated since it can play a role in the geometric

isomerization. When the arylolefins exist in solution as mixtures of equilibrated conformers, an interesting selectivity in the adiabatic photoisomerization of a specific conformer of the cis compounds can be often evidenced; in particular, the adiabatic formation of the excited ^{1,3}trans* isomer is peculiar to the *s-trans* rotamers whereas the *s-cis* rotamers are prompted to photocyclize. Also the interconversion among different rotamers in the excited states was observed in some cases against the NEER (non equilibration of excited rotamers) principle.

P 2.10

FTIR spectroscopy and thermodynamics of hydrogen adsorbed in a cross-linked polymer

Olena Zavorotynska, Giuseppe Spoto, Jenny Vitillo, Alessandro Damin, Francesca Bonino and Adriano Zecchina.

Dipartimento di Chimica IFM and NIS Centre of Excellence, Via Giuria 7, I-10125 Torino E-mail: giuseppe.spoto@unito.it

Singling out of safe and efficient storage methods still represents an open problem which needs to be solved in view of the widespread use of hydrogen as energetic vector. Among the envisaged technologies [1] reversible adsorption on microporous solids is in principle simple and inexpensive, although yet inadequate to meet the stringent DOE (U.S. Department of Energy) targets for on board hydrogen storage systems. The method is based on dispersive interaction between the H_2 molecule and the surface of the adsorbent, and its effectiveness is essentially depending on (i) the energetic of interaction, which influences the optimal storage temperature, and (ii) the surface extension, which relates to the amount of stored gas. Among the investigated materials polymers of induced (by post-synthesis crosslinking procedures) or intrinsic porosity (because of the use of proper monomeric units) have attracted recent interest because of promising adsorptive properties (up to 3 H_2 wt%) [2]. Noteworthy, the data published up to date present only gravimetric analysis of the amount of hydrogen stored in these materials, while the information on the physical nature and the thermodynamics of the interaction between hydrogen molecules and polymer is copletely missing. With the aim of contributing to fill this gap in this work we have investigated by means of infrared spectroscopy at temperature variable between 300-20 K (VTIR method) the interaction of H_2 with commercial crosslinked polymer (St-DVB poly(styrene-co-divinylbenzene) from Aldrich). VTIR can in fact allow to evaluate the adsorption energy from the optical isobars [3] and to investigate the nature of the interaction from the pertrubation of the vibrational modes of adsorbed H_2 with respect to gas phase.

Surface area, pore volume and pore size distribution of St-DVB were obtained by N_2 adsorption measurements carried out at 77 K. The calculated BET surface area results to be 920 m^2 g^{-1} with a broad pore size distribution covering the 6 – 40 Å range and centred at about 16 Å. The gravimetric analysis of H_2 adsorption at 77 K over the 0 – 10 bar pressure range shows that St-DVB can reversibly adsorb at 77 K up to *ca.* 1.3 H_2 wt% at 1 bar and 1.8 wt% at 10 bar (Fig.1) in good agreement with literature data for other hypercrosslinked polymers [2].

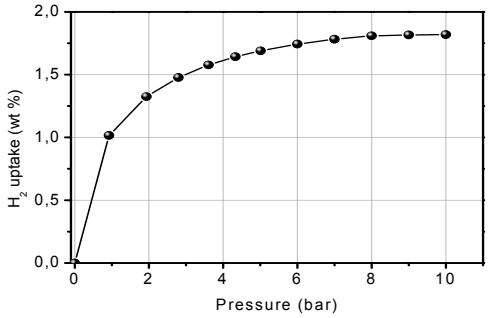

Fig. 1. Gravimetric H_2/St-DVB adsorption isotherm at 77 K

IR experiments consisted of three steps. In the first step (spectra 1-7 on the Fig.2a) H_2 (typically 30 mbar) was dosed at 300 K and spectral series recorded upon gradually decreasing the temperature down to 20 K while simultaneously monitoring the gas phase equilibrium pressure. Following this procedure, bands first appear at 70 K at 4112, ca. 4680 cm^{-1} , and ca. 4445 cm^{-1} which shift at higher frequency (9.5-9.7 cm^{-1}) with lowering the T to 20K. We assign the first two manifestations to the Q(1) (pure vibrational) and S (1) (roto-vibrational) transitions of adsorbed ortho-molecules and the third very weak component at 4445 cm^{-1} to the S(0) mode of the less abundant para-H_2 species. The aproximate ratio in the intensities of two strong bands and the weak one (3:1) reflects the natural ratio of ortho and para species in hydrogen gas. The site-specific adsorption enthalpy, calculated from these VTIR measurements, is *ca.* 2.5 kJ mol^{-1}. This weak interaction is the result of the specific physisorption of H_2 on the the aromatic part (phenyl rings) inside the St-DVB micro-cavities of the polymer. This interaction is also responsible for the infrared activation of ν (H-H) mode (Q_1) and its shift about - 40 cm^{-1} with respect with hydrogen gas. In the second step (8-12, Fig.2a) spectra were recorded at fixed time intervals while keeping constant the temperature (20 K) and the H_2 equilibrium pressure of the H_2/St-DVB system. This procedure allowed to investigate the change in composition of the adsorbed phase in terms of ortho- and para-H_2. In the last step (Fig. 2b) the H_2/St-DVB system was progressively outgassed at constant temperature (20 K). H_2 adsorption on St-DVB is fully reversible at 20 K, as demonstrated by the fact that all the above manifestations readily disappear upon decreasing the H_2 equilibrium pressure.

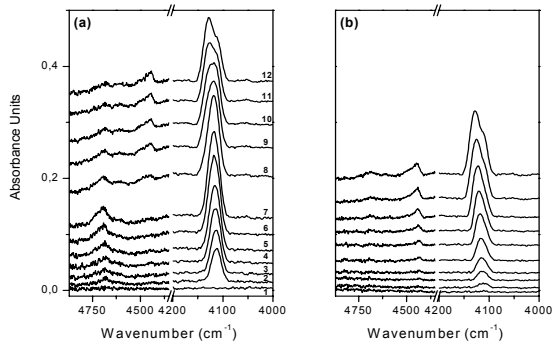

Fig. 2. Infrared spectra of H_2 adsorbed on St-DVB

To further supports the hypothesis of a specific adsorption of the H_2 molecules on the phenyl groups inside the St-DVB micropores we have performed theoretical calculations concerning the interaction of dihydrogen with the benzene ring. Good correspondence between the calculated shift of the anharmonic frequency of the ν(HH) mode of the H_2/C_6H_6 adducts (-33 cm^{-1}) and the experimental value for the H_2/St-DVB interaction (-37 cm^{-1} for the $Q(0)$ band) was obtained. The calculated energy of interraction (4.2 kJ mol^{-1}) slightly overstimated with respect to the experimental value of 2.5 kJ mol^{-1} observed.

Thus, VTIR technique, applied in this study shows that the H_2/St-DVB interaction primarily involves specific weak (adsorption energy *ca.* 2.5 kJ mol^{-1}) adsorption of the H_2 molecule on the phenyl rings and gives rise to well defined vibrational and vibration-rotational IR manifestations never reported before for the hydrogen adsorption on polymeric materials.

1. Züttel A.. *Naturwiss*. 2004, 91, 157-172.
2. McKeown N., Budd M.P., and Book P. *Macromol. Rapid Commun.* 2007, 28, 995-1002.
3. Spoto G., Bordiga S., Zecchina A., Cocina D., Gribov E.N., Regli *Catal. Today* 2006, 113, 65-80.

P 2.11

Quinol re-oxidation in the Reaction Center photocycle in vitro

Nicola De Nicolò, Péter Maróti, László Nagy, Massimo Trotta, Francesco Milano and Angela Agostiano.
Istituto per i Processi Chimico Fisici – sede di Bari, c/o Dipartimento di Chimica – Via Orabona, 4 – 70124 Bari, f.milano@ba.ipcf.cnr.it

The energy associated to the solar radiation is converted in chemical energy available for living organisms during the photosynthesis. The main actor in this process is the so called photosynthetic reaction centre (RC), a membrane-bound pigment-protein complex in which the absorption of a photon promotes a charge separation reaction that would be otherwise energetically unfavourable. In the photosynthetic bacterium *Rhodobacter sphaeroides* the net reaction after the absorption of two photons is the double reduction of a loosely bound ubiquinone-10 (UQ_{10}) and the oxidation of two molecules of ferrocytochrome c_2. Another transmembrane protein, the cytochrome bc_1 complex, catalises the reaction between the products quinol and ferricytochrome, restoring the initial situation, with the net result of proton translocation and gradient formation across the membrane that will be used to drive the ATP synthesis from ADP and phosphate.

RCs are readily extracted and purified form the their native environment, the so called intracytoplasmatic membrane. The result is a micellar solution in which the RC photocycle can be realised adding external pool of electron donors and acceptors in the appropriate redox state. A commonly used electron donor is the ferrocene, an organometallic compound containing a ferrous ion, with a midpoint potential of 400 mV capable of reducing the oxidised primary donor (E_m = 450 mV) in the millisecond timescale. The widespread use of such chemical is due to 1) the stability of reduced form in aqueous solution, 2) the lack of proton uptake or release upon redox, 3) the negligible absorption changes upon oxidation in the visible spectrum. The oxidised form of ferrocene, the ferrocenium ion, and the quinol produced after double light activation of the RC, undergo to a short-circuit reaction in which the quinone is restored. The mechanism of this reaction has been investigated using either the native UQ_{10} or its water-soluble analogue ubiquinone-0. In the latter case the reaction is mediated, at physiological pH, by the mono-deprotonated form of the quinol, and the reactant diffuse and equilibrate in the solution bulk before the reaction. The situation is less straightforward in the case of the UQ_{10}, where the reaction takes place in an heterogeneous system, namely the micellar phase for the quinol and RC and the aqueous phase for the ferrocenium. Is such system the neutral form of the quinol appears to be involved in the redox reaction and the surface charge of the RC modulates the rate of the redox reaction.

F. Milano, L. Gerencsér, A. Agostiano, L. Nagy, M. Trotta, and P. Maróti, *"Mechanism of Quinol Oxidation by Ferricenium Produced by Light Excitation in Reaction Centers of Photosynthetic Bacteria"* **J. Phys. Chem.**, Web Release Date: 30-Mar-2007
A. Agostiano, F. Milano and M. Trotta, *"Investigation on the detergent role in the function of secondary quinone in bacterial reaction centers"*, (1999) **Eur. J. Biochem.,** 262, 358±364

P 2.12

Studio di processi di binding a carico di cellule batteriche mediante spettroscopia ATR-FTIR differenziale

Livia Giotta[a], Disma Mastrogiacomo[a], Francesca Italiano[b], Angela Agostiano[b,c], Francesco Milano[b], Massimo Trotta[b]
[a]*Dipartimento di Scienza dei Materiali, Università del Salento, Strada Provinciale per Monteroni - 73100 Lecce, livia.giotta@unile.it*
[b]*CNR - Istituto per i Processi Chimico-Fisici, Sezione di Bari, c/o Dipartimento di Chimica, via Orabona, 4 - 70124 Bari*
[c]*Dipartimento di Chimica, Università degli Studi di Bari, via Orabona, 4 - 70124 Bari*

Diversi microrganismi presentano interessanti capacità bioassorbenti nei confronti di sostanze tossiche e risultano pertanto interessanti per lo sviluppo di tecniche di risanamento di siti inquinati (bioremediation)[1,2]. In particolare è stato dimostrato che una ampia varietà di

ceppi batterici è in grado di immobilizzare metalli pesanti sulla superficie cellulare esterna. La parete cellulare e la membrana esterna (per i Gram-negativi) presentano infatti una struttura chimica molto complessa, ricca di gruppi funzionali che manifestano elevata affinità per i protoni e per diversi cationi metallici tossici. Allo scopo di selezionare i ceppi più versatili ed eventualmente realizzare un miglioramento dei microrganismi basato sull'ingegneria genetica, è fondamentale identificare i siti di binding maggiormente coinvolti nell'immobilizzazione dei metalli pesanti..
Le transizioni energetiche nell'ambito dei livelli vibrazionali delle molecole, promosse dalla radiazione elettromagnetica infrarossa, sono fortemente influenzate dall'intorno chimico risultando sensibili ad eventi di binding. La spettroscopia infrarossa in riflettanza totale attenuata (ATR) è stata dunque utilizzata con successo per delucidare la natura chimica dei gruppi funzionali protonabili, responsabili dell'immobilizzazione di Co^{2+} e Ni^{2+} sulla superficie esterna di *Rhodobacter sphaeroides*[3], un microrganismo fototrofo Gram-negativo, appartenente alla famiglia dei batteri rossi non sulfurei. L'utilizzo di una cella in flusso e la modalità differenziale di acquisizione degli spettri ha permesso di sviluppare un protocollo altamente efficace per l'analisi di sottili biofilm batterici e di rivelare con estrema sensibilità gli eventi di binding a carico delle strutture cellulari esterne.

1. Malik, A.; *Environment International*, **2004**, *30*, 261 - 78. 2. Munoz, R.; Alvarez, M.T.; Munoz, A.; Terrazas, E.; Guyesse, B.; Mattiasson, B.; *Chemosphere*, **2006**, *63*, 903 – 11. 3. Buccolieri, A.; Italiano, F.; Dell'Atti, A.; Buccolieri, G.; Giotta, L.; Agostiano, A.; Milano, F.; Trotta, M.; *Annali di Chimica*, **2006**, *96*, 195 - 203

P 2.13

Does the lipid environment influence the spectral and kinetic properties of semiquinones in bacterial photosynthetic reaction centres?

F. Milano[a], E. Altamura[b], A. Agostiano[a,b], L. Giotta[c], L. Nagy[d], P. Maroti[d] and M. Trotta[a].

[a]CNR – Istituto per i Processi Chimico Fisici, and [b]Dipartimento di Chimica Università di Bari; [c]Dipartimento di Scienza dei Materiali - Università di Lecce; [d]Department of Biophysics – University of Szeged – Szeged (Hungary)

Quinones perform a key role in the energy conversion of biological systems, coupling oxydation/reduction reactions to proton uptake or release across membranes. In bacterial photosyntesis a cyclic electron flow occurs between the Reaction Centrer (RC), the bc_1 complex and the cytochrome c_2; this movement of electrons is accompanied by a net flow of protons from the periplasmic to the cytoplasmic space. Electrons are shuttled beteween the membrane-spanning RC and bc1 complex by the hydrophobic ubiquinone-10 (UQ_{10}). In the RC crystal structure two molecules of UQ_{10} are found in distinct binding sites, termed Q_A and Q_B. The quinone in the Q_A pocket acts as a single electron carrier and is firmly associated to the protein, while the one in the Q_B pocket can undergo to double reduction and protonation and is loosely bound. When isolated RC are hit by a light flash, the charge separated state $D^+Q_B^-$ (or $D^+Q_A^-$ in the presence of Q_B inhibitors) is produced. Here D is the primary donor, a bacteriochlorophyll dimer. In the presence of a suitable electron donor to D, a relatively stable semiquinone is formed. The properties of the two semiquinones are mainly modulated by the protein environment, but fine adjustments are achieved by the interaction with the protein surrounding, namely the lipidic bilayer. We have reconstituted the RC in liposomes made by different and physiologically important phospholipids and recorded the spectra of the semiquinones with the aim of study protein-lipid interactions that are involved in the fine tuning of these key intermediates.

P 2.14

The hydrophobic chain length of phospholipids influences the functioning of photosynthetic Reaction Centres reconstituted in proteoliposomes.

M. Trotta[a], F. Milano[a], N. De Nicolò[b], L. Giotta[c], L. Nagy[d], P. Maroti[d] and A. Agostiano[a,b]

[a]CNR – Istituto per i Processi Chimico Fisici, and [b]Dipartimento di Chimica Università di Bari; [c]Dipartimento di Scienza dei Materiali - Università di Lecce; [d]Department of Biophysics – University of Szeged – Szeged (Hungary)

The photosynthetic Reaction Centre (RC) is a transmembrane pigment-protein complex where the energy associated to the electromagnetic solar radiation is converted into chemical energy in the form of a charge separated state. Following absorption of a photon the bacteriochlorophyll dimer (D) reaches its singlet excited state (D*) and then transfers an electron through a chain of cofactors to the final electronic acceptor Q_B. In absence of electron donors to D, a charge recombination reaction occurs with a lifetime in the seconds timescale, strongly influenced by the protein environment. The membrane-spanning portion of the RC is about 35 Å long and is normally embedded in the intracytoplasmic membrane where the most representative phospholipid is palmitoyl-oleoyl-phosphatidylcholine (POPC) with side chains of 16 (saturated) and 18 (monounsaturated) carbon atoms (n_c) forming a 44 Å thick bilayer. To assess the effect of a complete or partial covering of the transmembrane portion, RC have been reconstituted in liposomes formed by 1,2 diacyl – phosphatidylcholine with n_c spanning from 9 to 14, ensuring that the bilayers formed are in the liquid-crystalline phase. RCs embedded in POPC proteoliposome, showing a charge recombination lifetime of 2.2 s, was taken as a reference system. A discontinuity in the charge recombination reaction lifetime was found between $n_c = 12$ and $n_c = 14$ corresponding to a bilayer thickness of 32 and 37 Å respectively.

P2.15

New Sol-Gel Hybrid Materials for High Energy Applications in Nonlinear Optics

I.Fortunati[a]; R.Signorini[a]; R.Bozio[a]; G.Brusatin[b]; M.Guglielmi[b]; S.Dirè[c]
[a]Dip. di Scienze Chimiche, *Univ. di Padova, via Marzolo 1, I-35131, Padova, Italy, ilaria.fortunati@unipd.it*
[b]*Dip. di Ing. Mecc.-Sett. Materiali, Univ. di Padova, via Marzolo 9, I-35131, Padova, Italy*
[c]*Dip di Ingegneria dei Materiali e Tecnologie Industriali, Univ. di Trento, via Mesiano 77, I-38050 Trento, Italy*

Organic-inorganic hybrid materials, composed of inorganic oxide structures and interpenetrated cross-linked organic polymers, are promising candidates for electro/optical applications, combining the most important glass-like and polymer-like properties. This is particularly true when large laser power density is used, in fact these materials show high laser damage resistance compared with that of polymeric systems.
To our knowledge, a deep study of the effects and causes of hybrid materials laser damage has never been done. The mechanisms of optical damage depend on a multiplicity of factors both on the laser source experimental parameters, such as pulse duration, beam size and wavelength, and on the material microstructural characteristics and defects.
The hybrid sol-gel synthesis is an attractive, simple, cheap and very versatile way to produce materials with desired shapes and properties. The wide possibility to vary the process parameters, like precursors, type of catalysis and chemical route of synthesis, permits one to control also the microstructure and the macroscopic properties of final samples.
The use of Glycidoxypropyltrimethoxysilane (GPTMS) and silica-based Nanobuilding Blocks (NBB) allows preparing materials with good optical properties, controlled heterogeneity and scratch and abrasion resistance.
Different sol-gel matrices, based on GPTMS and NBB, have been prepared in order to study their laser damage resistance. The possibility of varying the catalyst and precursors or the synthesis procedure allows obtaining materials with similar chemical composition but different microscopical properties. By this way, it is possible to study the laser damage threshold of these samples, understand effects and causes of the damage and find the way to enhance and optimize the laser damage resistance, useful in non-linear optics.

SEZIONE

COLLOIDI ED INTERFASI

P 3.1

THERMAL ANALYSIS CHARACTERIZATION OF SOME CATIONIC LIPOSOMES

Bonicelli M. G.[a], Giansanti L.[b], Mancini G.[c], Pascale F.[d]

[a,d] *Dipartimento Ingegneria Chimica, Materiali, Ambiente, Sapienza Università di Roma, Via del Castro Laurenziano 7, 00161 Roma, Italy*

[b,c] *Dipartimento Chimica Organica, Sapienza Università di Roma, Piazzale Aldo Moro5, 00161 Roma, Italy*

Differential scanning calorimetry (DSC) is a rapid simple thermodynamic technique which may be used to study lipid thermotropic phase behaviour in biological membranes and in their model systems, such as closed lipid bilayers entrapping an internal aqueous phase (liposomes) formed by phospholipid. The structure, fluidity, transport properties, surface potential of these model systems can be systematically investigated at the aim of understanding the more complex biomembrane systems.[1]

We have determined the gel to liquid crystalline phase transition temperature, calorimetric ΔH and the cooperativity of the process in mixed liposomes composed by 1,2-dimyristoyl-*sn*-glycero-3-phosphatidylcoline (DMPC) and synthetic cationic surfactants **1**, (1S,2S)-N-hexadecyl-N-methylprolinolinium bromide, **2**, (1R,2S)-N-hexadecyl-N-methylprolinolinium bromide, **3**, N-hexadecyl-L-prolinolinium bromide, and **4**, N,N-dihexadecyl-L-prolinolinium bromide.[2]

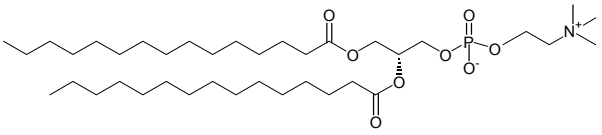

DMPC

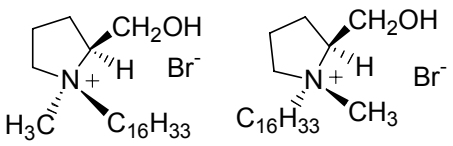

1 **2**

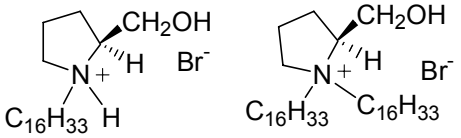

3 **4**

Mixed binary systems composed of DMPC and cationic surfactants at different molar ratios (8/2, 7/3, 6/4, 5/5) have been calorimetrically characterized at the aim of correlating the mo

lecular structure of the components to the physicochemical features of the aggregates. The deconvolution analysis of DSC data to obtain bilayer partition function based on the method described by Freire and Biltonen [3] provided information about lipid organization and fluidity of hydrocarbon chains.

Furthermore, with careful analysis and interpretation, calorimetric experiments can directly yield fundamental thermodynamic information about the processes involved, such as phase separation and domain formation.

[1] Leidy C., Wolkers W.F., Jorgensen K., Mourtisen O.G., Crowe J.H., *Biophysical Journal*, 80 (**2001**), 1819-1828

[2] S. Borocci, F. Ceccacci, L. Galantini, G. Mancini, D. Monti, A. Scipioni, M. Venanzi, *Chirality*, 15(5) (**2003**), 441-447

[3] E. Freire, R. Biltonen, *Biochimica et Biophysica*, 514 (1978), 54-68 (**1978**)

P 3.2

Effect of dopant (Nd, Er, Eu and Ce) amount on yttrium aluminum garnet nanoparticles structure

Eugenio Caponetti[a], Delia Chillura Martino[a], Maria Luisa Saladino[a], Stefano Enzo[b], Giulio Ibba[b]

[a]*Dipartimento di Chimica Fisica "F. Accascina", Università di Palermo and INSTM-Udr Palermo,Parco d'Orleans II, Viale delle Scienze pad.17, Palermo 90128,caponett@unipa.it*

[b]*Dipartimento di Chimica, Università di Sassari and INSTM-Udr Sassari, Via Vienna 2, Sassari 07100*

Hydroxides precursors synthesized by co-precipitation method, were calcined at different temperatures from 900

to 1100°C for one hour to produce the YAG nanopowders. Further, to obtain information on the degree of solubility of some lanthanide ions, YAG powders with different doping amounts of Nd^{3+}, Er^{3+}, Eu^{3+} and Ce^{3+} have been prepared.

All samples were characterized by Field Emission Gun-Scanning Electron Microscopy, Thermo-Gravimetry and Differential Thermal Analysis, X-Ray Diffraction and Surface Area Analysis. The effect of thermal treatment on the powders structure was systematically inspected.

TG and DTA experiments were performed from room temperature up to 1500 °C; the presence of exo- and endo-thermal events was found to accompany phase transformation phenomena.

FEG-SEM observations showed the presence of aggregation features in the powders with a rounded morphology.

Analysis of XRD patterns confirmed the formation of YAG phase. The lattice parameter of garnet phase depends on the specific doping, its amount and temperature treatment.

For each dopant there is not a regular trend. In all case at low concentration lanthanide ions substitute for yttrium ions in the dodecahedral sites of the garnet structure. On increasing the temperature a reduction of the YAG cell parameter is observed probably due to defect release in the garnet structure. In addition to this, the formation of other crystalline phases such as YAH, YAM and YAP are observed.

P 3.3

Studio strutturale di polimeri supramolecolari host-guest

Luciano GALANTINI[a], Claudia LEGGIO[a], Nicolae Viorel PAVEL[a], Massimiliano ANSELMI[a], Alfredo DI NOLA[a], Aida JOVER[b], Francisco MEIJIDE[b], Victor Hugo SOTO TELLINI[b], José VÁZQUEZ TATO[b]

[a]*Dipartimento di Chimica, Università La Sapienza, P.le A. Moro 5, 00185 Roma, l.galantini@caspur.it*

[b]*Departamento de Química Física, Facultad de Ciencias, Universidad de Santiago de Compostela, Avda. Alfonso X El Sabio s/n, 27002 Lugo, Spain*

Il recente sviluppo della chimica supramolecolare ha ravvivato la possibilità di ottenere polimeri per mezzo di associazioni reversibili, ovvero polimeri supramolecolari realizzati attraverso l'associazione di monomeri mediante interazioni non covalenti. Il principale vantaggio di questi polimeri rispetto a quelli covalenti risiede nel fatto che in essi il processo di polimerizzazione è rappresentato da equilibri che, essendo funzione di variabili termodinamiche, possono essere facilmente condizionati, fornendo la possibilità di governarne le proprietà dall'esterno. In particolare polimeri supramolecolari host-guest, alcuni dei quali mostrano interessanti applicazioni potenziali, sono stati ottenuti utilizzando le proprietà ospitanti della ciclodestrina [1-4]. Con opportuni guests queste molecole danno origine a composti di inclusione molto stabili che, impiegati nella polimerizzazione, dovrebbero garantire il raggiungimento di elevati gradi di polimerizzazione. Tuttavia, molto spesso sembrano formarsi strutture cicliche o complessi chelati che prevengono la formazione di polimeri lunghi [3,4]. Sebbene una grossa mole di lavoro sia stata dedicata alla preparazione di nuovi polimeri supramolecolari host-guest, manca ancora una descrizione dettagliata della loro struttura in soluzione e alcuni aspetti del quadro piuttosto complesso, rappresentato dalle proprietà di aggregazione di questi sistemi, restano oscuri. Per questa ragione è stato effettuato uno studio strutturale su un copolimero supramolecolare formato da dimeri di β-ciclodestrina (β-CD_2) e dimeri di Adamantano (Ad_2), combinando esperimenti di small angle X-ray scattering e light scattering con simulazioni di dinamica molecolare (MD) e Monte Carlo (MC). Dapprima sono state studiate le soluzioni dei monomeri attraverso le sole misure di scattering. Successivamente, è stato analizzato il complesso generato da una molecola di Ad_2 e due molecole di β-ciclodestrina correlando risultati di scattering e simulazioni di MD, per caratterizzare la connessione host-guest. Infine, una interpretazione dettagliata dei dati di scattering del polimero è stata realizzata attraverso simulazioni MC. Quest'ultime sono state condotte su un singolo aggregato supramolecolare e, vista la forma peculiare della catena polimerica, utilizzando la struttura molecolare completa, senza ricorrere a modelli semplificati di catena polimerica. Il confronto delle simulazioni, con e senza interazioni di volume escluso, indicano che il polimero è vicino alla

condizione teta. Minimizzazioni mediante metodi di Reverse MC mostrano che il polimero presenta una forma ripiegata ma non si chiude in strutture cicliche, come generalmente ipotizzato per questo tipo di oligomeri. Tuttavia, è stato stimato un grado di polimerizzazione di circa 8 (4 Ad_2 e 4 β-CD_2) che non manifesta alcuna dipendenza dalla concentrazione.

1. Y. Liu, H. Wang, P. Liang, H.-Y. Zhang, Angew. Chem., Int. Ed., **43**, 2690 (2004**).**
2. V. H. Soto, A. Jover, J. Carrazana, L. Galantini, F. Meijide, J. Vázquez Tato, J. Am. Chem. Soc., **128**, 5728 (2006).
3. Y. Hasegawa, M. Miyauchi, Y. Takashima, H. Yamaguchi, A. Harada, Macromolecules, **38**, 3724 (2005).
4. K. Ohga, Y. Takashima, H. Takahashi, Y. Kawaguchi, H. Yamaguchi, A. Harada, Macromolecules, **38**, 5897, (2005).

P 3.4

Physico-Chemical and Structural Properties of hydrogels formed by Chitosan, in the Presence and Absence of Poly(vinylpyrrolidone) and Sodium decylsulfate

Gaetano Mangiapia[a] , Luigi Paduano[a], Henrich Frielinghaus[b], Gerardino D'Errico[a], Ornella Ortona[a], Roberto Sartorio[a]

[a]*Università degli Studi di Napoli Federico II, Dipartimento di Chimica, via Cinthia, 80126 Napoli, luigi.paduano@unina.it; CSGI – Consorzio interuniversitario per lo sviluppo dei Sistemi a Grande Interfase*

[b]*Institut für Festkörperforschung, Forschungszentrum Jülich, D-52428 Jülich, Germany; JCNS – Jülich Centre for Neutron Science.*

Chitosan is a polycationic biopolymer obtainable from partial enzymatic or alkaline deacetylation of chitin, a natural and abundant polysaccharide, occurring in crustaceous shells and insect exoskeletons, often in association with proteins and minerals [1,2].

The good biocompatibility, natural availability, and the excellent physical, chemical and mechanical properties shown by chitosan, make it a good candidate for using in drug delivery systems, medical field, as component in cosmetic products, agriculture and water treatment [3-6].

One of the most attractive features of chitosan that has cap-tured the attention of researchers from both academic and industrial areas, is the capability to form semirigid films and hydrogels with good swelling properties [1]. This characteristic, together with its protonable nature, has allowed to form pH-sensitive swellable chitosan gels, used as stomach-targeted drug delivery systems [7,8], and chitosan complexes useful in gene delivery applications [9].

In order to formulate new biomaterials with more appealing characteristics, chitosan is often used in blend with other polymers or in combination with surfactant substances. The use of polymer blends allows, in principle, having new gels with properties which are different from those of the single components [10,11], whereas polymer-surfactant complexes, where present, can significantly modify the characteristics of solutions and hydrogels (for instance improving swelling properties) opening new possibilities of applications [12].

Among the polymers, poly(vinylpyrrolidone) is recognized to be a good candidate due to its good biocompatibility.

On these bases, the structure of chitosan and chitosan/poly(vinylpyrrolidone) (PVP) hydrogels, chemically crosslinked, has been investigated by means of the combined use of small angle neutron scattering (SANS), electron paramagnetic resonance (EPR), intradiffusion and swelling degree measurements. According to the SANS results, the structure of these hydrogels may be described in terms of an inhomogeneous structure composed by polymeric-rich and polymer-poor regions. The polymer rich region, whose correlation distance ζ is ranged between ~ 600 Å and ~ 850 Å, are in turn characterized by the presence of a network formed by the chemical crosslinks (see figure 1), with a mean correlation distance $\xi \sim 90$ Å .

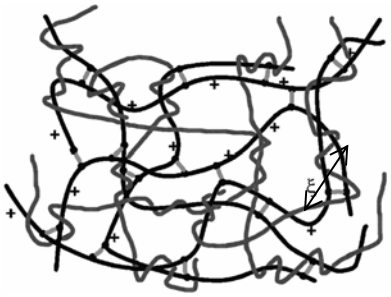

Figure 1 – Schematic representation of the polymer rich region of Chitosan/PVP hydrogels. Mean mesh size ξ of the network is also indicated.

The structure of chitosan and chitosan/PVP hydrogels has also been analyzed in the presence of sodium decylsulfate (C10OS) micelles that could provide a multidomain system useful, in principle, for drug delivery applications. Both SANS and EPR measurements have shown that sodium decylsulfate (C10OS) micelles do not significantly interact with both the gels, being free to move inside the polymer networks. Finally, intradiffusion and swelling degree measurements, have shown an improved hydrophilicity of chitosan/PVP gels, further magnified by the presence of C10OS surfactant.

In light of the results obtained, chitosan and chitosan/PVP hydrogels appear as possible matrices for building up systems for drug delivery of both hydrophilic and hydrophobic active molecules. These matrices can be attained by simple addition to the gel of an appropriate amount of amphiphilic substances, such as a surfactant, forming a swellable multi-domain system able to be used as lipophilic and hydrophilic reservoir for the releasing of small molecules.

1. Ravi Kumar, M. N. V.; Muzarelli, R. A. A.; Muzzarelli, C.; Sashiwa, H.; Domb, A. J.; *Chemical Reviews*, **2004,** *104*, 6017.

2. Hudson, S. M.; Smith, C. Polysaccharides: chitin and chitosan: chemistry and technology of their use as structural materials. In *Biopolymers from Renewable Resources*; Kaplan, D. L., Ed.; Springer: Berlin, Germany, 1998; pp 96.

3. Sakkayawong, N.; Thiravetyan, P.; Nakbanpote, W.; *Journal of Colloid and Interface Science*, **2005,** *286*, 36.

4. Yan, W. L.; Bai, R.; *Water Research*, **2005,** *39*, 688.

5. Shi, X. Y.; Tan, T. W.; *Journal of Bioactive and Compatible Polymers*, **2004,** *19*, 467.

6. Ham-Pichavant, F.; Sebe, G.; Pardon, P.; Coma, V.; *Carbohydrate Polymers*, **2005,** *61*, 259.

7. Siegel, R. A.; Falamarzian, M.; Firestone, B. A.; Moxley, B. C.; *Journal of Controlled Release*, **1988,** *8*, 179.

8. Anandan, R. N., P. G. V.; Mathew, S.; *Journal of Pharmacy and Pharmacology*, **2004,** *56*, 265.

9. Borchard, G.; *Advanced Drug Delivery Reviews*, **2001,** *52*, 145.

10. Sionkowska, A.; *Journal of Photochemistry and Photobiology, B: Biology*, **2006,** *82*, 9.

11. Kim, S.; Nimni, M. E.; Yang, Z.; Han, B.; *Journal of Biomedical Materials Research, Part B: Applied Biomaterials*, **2005,** *75B*, 442.

12. Sagnella, S.; Mai-Ngam, K.; *Colloids and Surfaces, B: Biointerfaces*, **2005,** *42*, 147.

P 3.5

Self-assembly of starch stabilized Ag nanocrystals into ribbon-like and globular agglomerate structures for biosensors application.

A. Serra, D. Manno, E. Filippo, T. Siciliano, A. Tepore

Dipartimento di Scienza dei Materiali – Unità CNISM
Università del Salento – Via Monteroni, 73100 Lecce

Metal and semiconductor nanoparticles are of great importance due to their potential applications in emerging areas of nanoscience and technology. Size, shape, and surface morphology play pivotal roles in controlling the physical, chemical, optical, and electronic properties of these nanoscopic materials[i]. Preparation of nanoparticles generally involves the reduction of metal ions in solutions or in high temperature gaseous environments.

Most of the synthetic methods reported to date rely heavily on organic solvents. This is mainly due to the hydrophobicity of the capping agents used. There have been approaches reported for the synthesis of H_2O-soluble metal nanoparticles. The majority of methods reported to date use reducing agents such as hydrazine, sodium borohydride ($NaBH_4$), and dimethyl formamide (DMF). All of these are highly reactive chemicals and pose potential environmental and biological risks.

In this work we propose a preparation method of silver nanoparticles and nanowire based onto hydrothermal

synthesis that uses solvent medium, reducing agent, and capping agent that are all environmentally benign and nontoxic material.

In the present approach, H_2O is utilized as the environmentally benign solvent throughout the preparation. The sugar, β-D-glucose, is used as the reducing agent. With gentle heating, this system is a mild, renewable, inexpensive, and nontoxic reducing agent. The final, and perhaps most important, issue in the preparation of nanoparticles is the choice of starch as the capping material used to protect or passivate the nanoparticle surface.

The resulting nanocomposites were investigated using structural, optical and morphological methods. XRD spectra of the nanocomposites confirmed the presence of nanostructured silver (cubic phase) in the matrix. High Resolution Transmission Electron Microscopy (HREM) methods showed that the nanoparticles are mostly spherical in shape and aggregate in nano-ribbon and globular formation (figure 1).

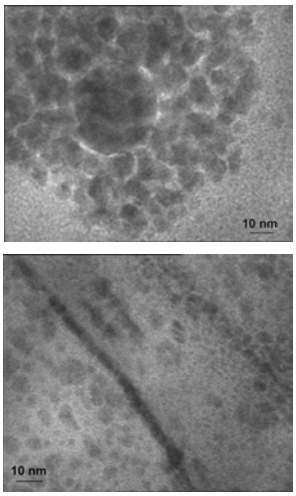

Figure 1 (a) A typical globular agglomerate of Ag nanocrystals; (b) nanoparticles spherical in shape and aggregate in nano-ribbon.

X-ray diffraction (XRD) measurements were performed on a Rigaku miniflex X-ray diffractometer (Cu Kα1/2 radiation, λ = 0.154 nm). Figure 2 shows the XRD spectrum of the silver- starch nanocomposite.

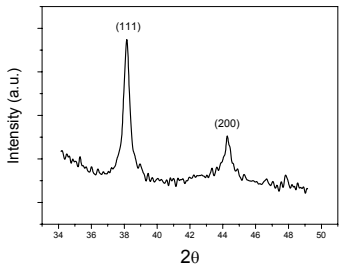

Figure 2 XRD pattern of Ag-starch nanocomposite.

The peaks correspond to 111 and 200 planes of the cubic phase of metallic silver

Analyses of the optical properties of the silver nanocomposite aqueous dispersions have been performed by UV-Vis spectroscopy.

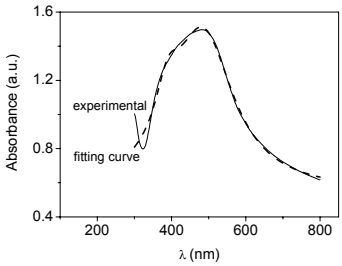

Figure 3 UV-Vis spectrum obtained onto the solution Ag-starch nanocomposite

In Figure 3 is visible a broad peak in the 400-500 nm spectral range. This is due to surface plasmon resonance phenomena of the electrons in the conduction bands of silver and also indicate the formation of silver colloids with nanometer-sized dimensions. To interpret the absorption spectrum of silver nanoparticles, we used the light scattering theory of Mie[ii] and free electron theory of Drude[iii]. The experimental absorption coefficient vs. wavelength plots have been fitted with modified Mie theory, taking into account the finite size distribution of the particles in colloidal solution. The reported fit has been obtained for a volume fraction of 84 % of nanoparticles having mean size of 20 nm.

The silver nanostructures were electrodeposited onto suitable substrates with gold interdigital electrodes. The obtained amperometric biosensors showed an high sensitivity to hydrogen peroxide.

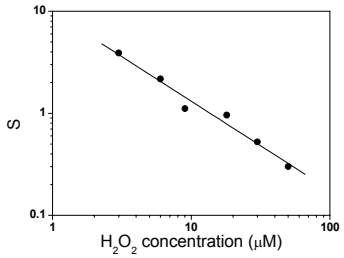

Figure 4 Sensitivity (S) as function of hydrogen peroxide concentration.

To evaluate the faculty of a sensor to detect a particular chemical species[iv] by a variation of its resistance, we introduced the sensitivity *S* defined as the absolute value of the ratio

$$S = \frac{\Delta R}{R} \Big/ \frac{\Delta C}{C}$$

where ΔR is the resistance variation due to chemical species concentration variation ΔC. This ratio gives a measurement of the electrical response of the sensor in a close relation to the response phenomena. As evident the sensitivity decreases as the concentration increases too.

P 3.6

Kinetics of Gelation of Aqueous Laponite Dispersions in the Presence of Tri-block Copolymers and their Homopolymers. Rheological and Dynamic Light Scattering Studies

R. De Lisi,[a] M. Gradzielski,[b] G. Lazzara,[a] S. Milioto[a] and N. Muratore[a]

[a] *Dipartimento di Chimica Fisica "F. Accascina", Università degli Studi di Palermo, Viale delle Scienze, Parco D'Orleans II, 90128 Palermo, Italy, nicola.muratore@unipa.it*

[b] *Stranski Laboratorium für Physikalische und Theoretische Chemie, Institut für Chemie, Technische, Universität Berlin, Straße des 17. Juni 124, 10623 Berlin, Germany*

Laponite is a low cost highly pure synthetic clay frequently used as thickener agent of water-based products (drilling fluids, personal care products, pharmaceutics, building materials, paper coaters, paints, etc.). Aqueous dispersions of such a clay contains monodisperse nanometric disks which undergo to a sol-gel transition.

Within this topic adsorption of homopolymer and copolymers on clay particles is relevant because polymers can inhibit the gelation process by steric hindrance [1]. Moreover, coated particles may have advanced features generating novel materials like clay-polymer nanocomposites. Particularly, tri-block copolymers offer the great advantage to be properly tuned by modulating the length of the constituent blocks or by changing their architecture.

Therefore, we believed that it would be interesting to perform small amplitude oscillatory shear and dynamic light scattering studies on gelation kinetics of aqueous laponite dispersions in the presence of poly(ethylene oxide)-poly(propylene oxide)- poly(ethylene oxide) tri-block copolymers and their homopolymers. To this aim, the effect of the polymer hydrophilicity, the copolymer molecular weight keeping constant the hydrophilic/hydrophobic ratio, and the architecture was investigated. The findings on the homopolymers confirm our earlier unexpected results obtained by means of high shear viscosity experiments [2]. Namely, the gelation process is speeded up in the presence of low molecular weight polymer and it is slowed down for higher molecular weights. The results in the presence of copolymers are also unusual. As a general feature, the copolymer slow down the kinetics of gel formation the effect being more important the lower the molecular weight is.

1. De Lisi, R.; Lazzara, G.; Lombardo, R.; Milioto, S.; Muratore, N.; Turco Liveri, M. L.; *Phys. Chem. Chem. Phys.,* **2005,** *7*, 3994 - 4001. 2. De Lisi, R.; Gradzielski, M.; Lazzara, G.; Milioto, S.; Muratore, N.; *Langmuir* (submitted)

P 3.7

The aggregative behavior of hydrophobically modified chitosans of 10% level substitution

Ornella Ortona[a,b], G. D'Errico[a,b], G. Mangiapia[a,b], L. Paduano[a,b]

[a]*Università degli Studi di Napoli "Federico II" – Dipartimento di Chimica. Via Cinthia, 80126 Napoli, e-mail:ornella.ortona@unina.it*

[b]*CSGI – Consorzio interuniversitario per lo sviluppo di Sistemi a Grande Interfase.*

Nowadays chitosan, obtained from partial deacetylation of chitin, is becoming one of the most interesting row material for the actual and potential applications in several fields such as waste water and drinking water treatment, food processing, biotechnology, medical application, agriculture. Being chitin obtained from the crustacea carapace, chitosan is very abundant and ecologically friendly. This is the reason why attention is paid on its properties from both a technological and a basic science viewpoint.

In the past, a quantitative reductive amination reaction of the amino groups present in the gluco-pyranose units of chitosan, CHIT, allowed to graft to chitosan a lot of pendants such as aliphatic chains, ethoxylic groups, sugar residues and so on, modulating at will both the substitution entity and the water affinity of the grafted polymer, C_n-CHIT.

This work is devoted to the study of the intra and inter-aggregation properties in acidic water of modified chitosan by the insertion of aliphatic chains on its backbone.

Chitosan has been modified with reductive amination by inserting aliphatic chains of different length, namely: C_5, C_6, C_8, C_{10}, C_{12} at 10% of molar substitution degree. The physico-chemical properties of the acidic solutions of the polymers have been studied through Newtonian viscosity and by the aid of the pyrene fluorescence.

Viscosity showed that while for CHIT and C_5-CHIT the viscosity behavior is quite similar highlighting that the insertion of this short aliphatic chain does not modify the rigidity and /or the interaction with the solvent, for C_6, C_8, and C_{10}-CHIT, the increasing length of the pendant promote a more and more efficient auto-association of the polymer as shown by the reduction of its hydrodynamic radius.

Converging evidences are obtained by the analysis of the fluorescence spectra of pyrene, used as probe, in the aqueous solutions of the grafted polymers and evidencing how different is the environment in which pyrene is located if short or long chained polymers are analyzed. In fact, the spectra in CHIT, C_5-CHIT and C_6-CHIT solutions are quite similar among them and also similar to the pyrene spectrum in water. These evidences confirm the scarce ability of these aliphatic substituents to tune hydrophobic aggregation. In contrast, pyrene in the presence of C_8-CHIT, C_{10}-CHIT, and C_{12}-CHIT solutions, gives rise to a progressive and evident modification of the spectra resembling that of this fluorescent probe in a hydrocarbon solvent.

P 3.8

Modeling of H_2 adsorption and spectroscopic observation of the ortho-para conversion on the ETS-10 titanosilicate

G. Ricchiardi, J. G. Vitillo, D. Cocina, G. Spoto, A. Zecchina

Dipartimento di Chimica IFM and NIS Centre of Excellence, Università di Torino, INSTM UdR Università, Via Pietro Giuria 7, 10125 Torino, Italia. Phone: +39 011 6707845. Fax: +39 011 6707855. E-mail: gabriele.ricchiardi@unito.it

INTRODUCTION

The titanosilicate ETS-10 is a zeotype having chemical formula $(Na,K)_2TiSi_5O_{13}$. Its structure is characterized by 12- and 7-ring channels. Only the channels formed by 12-rings are permeable to diatomic molecules. In the as-synthesized material [1] two alkali-metal cations are incorporated for every titanium atom. Four sites (I -IV) can be recognized which have an occupancy factor of 1.0 in ETS-10: among them, only the Na(III) is fully exposed [2].

Infrared spectroscopy has been used to study the adsorption of hydrogen on the ETS-10, in the 300-15 K

temperature range. A molecular mechanics (MM) study has been employed in order to evaluate the steric constraints to H_2 interactions with Na+ sites and to predict coordination shells.

EXPERIMENTAL

The ETS-10 sample was supplied by Engelhard (Iselin, NJ, USA). The infrared spectroscopic measurements were performed by using an home made cryogenic set-up (for a detailed description see Ref. 3). Thin self-supported wafers of the zeolite sample were prepared and activated in high vacuum at 773 K for 2 h. The H2 was dosed at 15 K on the activated sample. Once the equilibrium has been reached, the H2 gas was gradually outgassed.

Calculations were performed by using MM methods. A novel forcefield for H2-H2 and H2-Na+ interactions has been fitted to experimental electrostatic properties and ab initio PES. Periodic models with P1 symmetry have been used. The complete filling of the channels has been evaluated following a procedure described in the literature [4].

RESULTS AND DISCUSSION

The spectra of H_2 adsorbed on ETS-10 at 15 K depend on two parameters: the H_2 pressure and the contact time. As far the dependence of the pressure is concerned. at low H2 coverage, two ν_{H-H} peaks are observed at 4107 and 4113 cm^{-1}. Their separation and relative intensities (3:1) allow to assign them to ortho- (4107 cm^{-1}) and para-H_2 (4113 cm^{-1}) (ortho:para ratio 75:25) adsorbed in $Na^+\cdots H_2$ 1:1 complexes. With respect to free H_2 these peaks are downward shifted of -47 cm^{-1}. Upon increasing the coverage, the original peaks are consumed and a new one appears at 4111 cm^{-1} with a shoulder at 4118 cm^{-1}. In our opinion, this behavior is due to the transformation of the 1:1 $Na^+\cdots H_2$ adducts into $Na^+\cdots(H_2)_2$ complexes. Further increase of the hydrogen pressure leads to the appearance of additional bands in the 4150-4120 cm^{-1} interval, as shown in Fig. 1 (dashed line). These bands are assigned to aspecific interactions of H_2 with the ETS-10 walls (4130-4120 cm^{-1}) and to the formation of a liquid-like phase in the cavities (4150-4130 cm^{-1}). The possible formation of $Na^+\cdots(H_2)n$ complexes with n>2 can been discarded on spectroscopic as well as on a theoretical ground basis: MM simulations show in fact that their

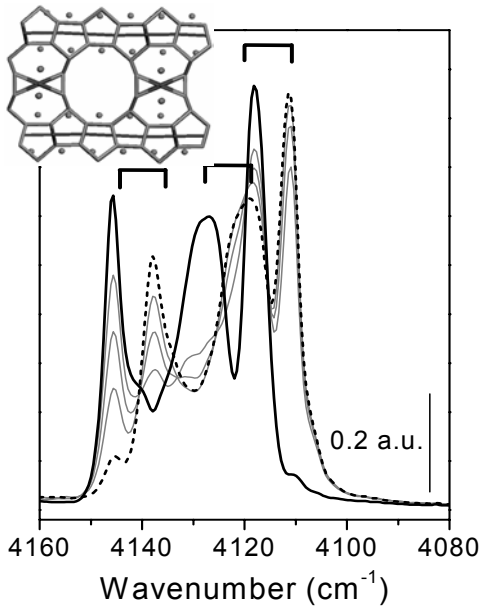

Fig. 1 FTIR spectra recorded at 15 K of H_2 adsorbed on ETS-10 (dashed line) and after a period of 18 h (solid line). Gray lines refer to intermediate elapsed times. A representation of ETS-10 is also reported.

formation is hindered on a steric basis. The simulated Na-H radial distribution function of hydrogen shows three well separated adsorption regimes: the formation of the 1:1 adduct, its evolution into a 1:2 adduct and a further disordered layer filling all the available pore volume. The time evolution of the spectra over a period of 18 h is shown in Fig. 1 (solid line): it consists in the gradual disappearance of the triplet described above and the parallel formation of a new triplet upward shifted of about 7 cm^{-1}. It is noticeable the presence of clear isosbestic points in Fig. 1. We think these facts can be interpreted on the basis of an ortho to para conversion process involving adsorbed H_2 and due to the combination of single-site reactions catalyzed by the zeolite involving the whole family of adsorbed species. This is the first direct in situ observation of the catalyzed ortho-para conversion of H_2 on adsorbed molecules.

REFERENCES

(1) S. M. Kuznicki, *US Patent* 4853202, **1989**.

(2) A. Zecchina, C. Otero Areán, G. Turnes Palomino, F. Geobaldo, C. Lamberti, G. Spoto, S. Bordiga, *Phys. Chem. Chem. Phys*, **1999**, *1*, 1649.

(3) G. Spoto, E. N. Gribov, G. Ricchiardi, A. Damin, D. Scarano, S. Bordiga, C. Lamberti, A. Zecchina, *Prog. Surf. Sci.*, **2004**, *76*, 71.

(4) J. G. Vitillo, G. Ricchiardi, G. Spoto, A. Zecchina, *Phys. Chem. Chem. Phys.* **2005**, *7*, 3948.

P 3.9

Structure and nuclearity of active sites in Fe-zeolites: comparison with iron sites in enzymes and homogeneous catalysts.

Gabriele Ricchiardi, Mickaël Rivallan, Gloria Berlier, Carlo Lamberti, Adriano Zecchina

Università di Torino, Dipartimento di Chimica Inorganica, Fisica e dei Materiali, and NIS Centre of Excellence, Via P. Giuria 7, 10125 Torino, Italy. *Gabriele.ricchiardi@unito.it*

Fe-ZSM-5 and Fe-silicalite zeolites efficiently catalyse several oxidation reactions which find close analogues in the oxidation reactions catalyzed by homogeneous and enzimatic compounds [1,2]. The iron centres are highly dispersed in the crystalline matrix and on highly diluted samples, mononuclear and dinuclear structures are expected to become predominant. The crystalline and robust character of the MFI framework has allowed to hypothesize that the catalytic sites are located in well defined crystallographic positions. For this reason these catalysts have been considered as the closest and best defined heterogeneous counterparts of heme and non heme iron complexes and of Fenton type Fe^{2+} homogeneous counterparts [3]. On this basis, an analogy with the methane monooxygenase has been advanced several times. The examination of the structure, nuclearity and catalytic activity of the iron species obtained with various characterization techniques already reported in literature, we conclude that Fe-ZSM-5 and Fe-silicalite are not the ideal samples conceived before and that many types of species are present, some active and some other silent from adsorptive and catalytic point of view. The relative concentration of these species changes with thermal treatments, preparation procedures and loading. Only at lowest loadings the catalytically active species become the dominant fraction of the iron species.

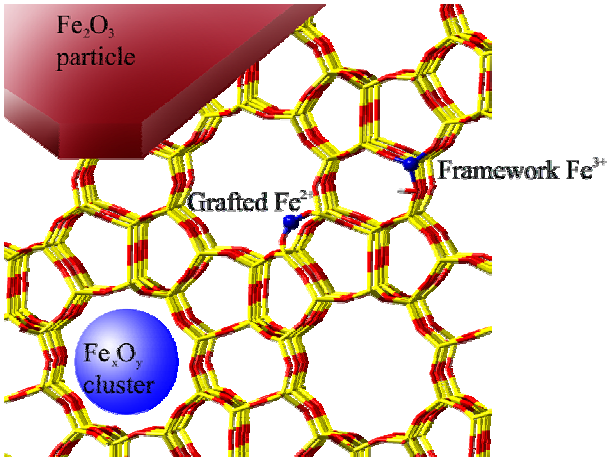

Fig. 1 Diferent classes of iron sites in Fe zeolites.

On the basis of the spectroscopic titration of the active sites by using NO as probe [1,2,4,5], we conclude that the active species on very diluted samples are isolated and highly coordinatively unsaturated Fe^{2+} grafted to the crystalline matrix. Indication of the constant presence of a smaller fraction of Fe^{2+} presumably located on small clusters is also obtained. The nitrosylic species have been analyzed in detail and the similarities and differences with the cationic, heme and non heme homogeneous counterparts have been evidenced. The same has been done for the oxygen species formed by N_2O decomposition on isolated sites [7,8], whose properties are more similar to those of the iron in cationic complexes [3] (included the $[(H_2O)_5FeO]^{2+}$ "brown ring" complex active in Fenton reaction) than to those of ferryl groups in heme and non heme counterparts.

1. G. Berlier, G. Spoto, S. Bordiga, G. Ricchiardi, P. Fisicaro, A. Zecchina, I. Rossetti, E. Selli, L. Forni, E. Giamello and C. Lamberti, *J. Catal.,* 208 (2002) 64; **2**. G. Berlier, A. Zecchina, G. Spoto, G. Ricchiardi, S. Bordiga and C. Lamberti, *J. Catal*., 215 (2003) 264; **3**. A. Wanat, T. Schneppensieper, G. Stochel, R. van Eldik, E. Bill and K. Wieghardt*, Inorg. Chem*., 41 (2002) 4; **4**. A. Zecchina, M. Rivallan, G. Berlier, C. Lamberti and G. Ricchiardi, *Phys. Chem. Chem. Phys*., invited paper, submitted (2007); **5**. M.T. Nechita, G. Berlier, G. Ricchiardi, S. Bordiga and A. Zecchina, *Catal. Lett.,* 103 (2005) 33; .**6**. G. Mul, J. Perez-Ramirez, F. Kapteijn and J.A. Moulijn, *Catal. Lett*, 80 (2002) 129; **7**. L. Kiwi-Minsker, D.A. Bulushev and A. Renken,

Catal. Today, 91-92 (2004) 165; **8**. A. Heyden, N. Hansen, A.T. Bell and F.J. Keil, *J. Phys. Chem. B*, 110, (2006) 17096

P 3.10

FT-IR Study of the State of Iron(III) Chloride Clusters Confined in AOT Reverse Micelles

V. Turco Liveri[a], R. Biancheri[a], L. Ceraulo[b], S. Fanara[b], C. Giordano[a], A. Ruggirello[a]

[a]*Dipartimento di Chimica Fisica, Università di Palermo,Viale delle Scienze Parco d'Orleans II, 90128 Palermo, turco@unipa.it*

[b]*Dipartimento di Chimica e Tecnologie Farmaceutiche, Università di Palermo, via Archirafi 32, 90123 Palermo*

Recently, it has been shown that large amounts of some hydrophilic organic and inorganic substances can be entrapped in almost dry reverse micelles forming small size aggregates stabilized by a monolayer of opportunely oriented surfactant molecules. Thus, through a simple procedure and using mild experimental conditions, supramolecular clusters of urea, cyanamide, cobalt nitrate and ytterbium nitrate confined in the core of sodium bis(2-ethylhexyl) sulfosuccinate (AOT) reverse micelles and suspended in an apolar organic solvent have been obtained [1-5]. In any case, experimental results emphasized that, due to confinement and interfacial effects, these clusters show physicochemical properties different from those in the bulk state or isolated molecules whereas, due to the increase of the amount of hydrophilic compound confined in the micellar cores, the structural properties of the reverse micellar aggregates are more or less significantly affected. Moreover, a comparison of the maximum attainable value of the solubilizate-to-surfactant molar ratio in reverse micellar solutions suggests that it critically depends on the nature of solubilizate, surfactant and apolar solvent showing frequently marked supersaturation effects.

Here we report on the entrapment and FT-IR characterization of iron(III) chloride clusters in AOT/CCl_4 micellar solutions as a function of the salt-to-surfactant molar ratio R at fixed surfactant concentration. Interestingly, while the confinement of many water-soluble inorganic salts in AOT reverse micelles needs preliminarily the presence of significant amounts of water within the micellar core, solubilization of $FeCl_3$ occurs without the need to add water in the micellar solution reaching the very high solubility value, expressed as the maximum salt-to-surfactant molar ratio, of 1.30. The analysis of the FT-IR spectra of the investigated samples leads to hypothesize that iron(III) chloride is secluded within the reverse micellar core as small size melted clusters of ionic species arising from the reactions

$$FeCl_3 + FeCl_3 \rightarrow FeCl_2^+ + FeCl_4^-$$

$$FeCl_3 + FeCl_4^- \rightarrow Fe_2Cl_7^-$$

followed by a strong structural rearrangement of the AOT head group region surrounding the micellar core and a shift of the sodium counterion from the micellar core surface to its interior. This picture has been further corroborated by conductivity measurements of $FeCl_3$/AOT/CCl_4 solutions as a function of the salt-to-surfactant molar ratio.

1. Giordano, C.; Longo, A.; Turco Liveri, V.; Venezia, A. M.; *Colloid & Polymer Science*, **2003**, *281*, 229 – 238. 2. Caponetti, E.; Chillura-Martino, D.; Ferrante, F.; Pedone, L.; Ruggirello, A.; Turco Liveri, V.; *Langmuir*, **2003**, *19*, 4913 – 4922. 3. Calandra, P.; Longo, A.; Ruggirello, A.; Turco Liveri, V.; *Journal of Physical Chemistry B*, **2004**, ***108***, 8260 – 8268. 4. Ceraulo, L.; Filizzola, F.; Longo, A.; Ruggirello, A.; Turco Liveri, V.; *Colloid & Polymer Science*, **2006**, *284*, 1085 – 1095. 5. Longo, A.; Ruggirello, A.; Turco Liveri, V.; *Chemistry of Materials*, **2007**, *19*, 1127 – 1133.

P 3.11

Investigation of the adsorption of PEG1500-12-acyloxystearate surfactants into phospholipids bilayers: An Ellipsometry and Cryo-TEM study.

Mauro Vaccaro[a,c], Christian von Corswant[b], Olle Söderman[c].

[a]*Università degli Studi di Napoli Federico II, Dipartimento di Chimica, via Cinthia, 80126 Napoli, mauro.vaccaro @fkem1.lu.se; CSGI – Consorzio*

interuniversitario per lo sviluppo dei Sistemi a Grande Interfase.

[b]*AstraZeneca R&D Mölndal, SE 431 83 Mölndal, Sweden.*

[c]*Physical Chemistry 1, Lund University, Box 124, 22100 Lund, Sweden.*

In this communication, we present a study of a new class of surfactants denoted as PEG1500-12-acyloxystearate [1], which has potential use as pharmaceutical solubilizers. These amphiphilic molecules present interesting properties with regard to cell damage effects. PEG1500-12-acyloxystearates with C14 to C16 acyloxy chains display little or no damage to red blood and intestinal cells, whereas the surfactants with shorter chains, from C8 to C12, exhibit a measurable damage. To understand the underlying mechanism, systematic studies of adsorption properties of the surfactants into phospholipid bilayers were carried out by the use of ellipsometry. The measurements revealed that the kinetic for the adsorption process varies considerably with respect to the length of the acyloxy chain. The rate of incorporation of the surfactants in the lipid membrane becomes slower upon increasing the length of the acyloxy chain. Cryo-TEM images have confirmed the ellipsometry results, by showing that the dissolution of the phospholipid bilayer is slower for the surfactants of the series having longer chains.

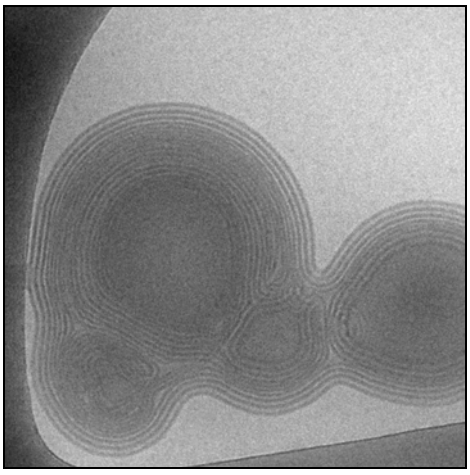

Figure 1: Cryo-TEM image of DOPC vesicles incubated with PEG1500-C18C12 for half hour.

[1] McNamee, C., M. Nilsson, C. von Corswant, and O. Söderman. 2005. Physicochemical Characterization of PEG1500-acyloxy-stearate Micelles and Liquid Crystalline Phases. *Langmuir*. 21: 8146-8154.

P 3.12

Characterisation of new gold catalysts supported on mixed ceria-titania oxides for the water-gas shift and preferential CO oxidation reactions

Floriana Vindigni[a], Maela Manzoli[a], Anna Chiorino[a], Tatyana Tabakova[b], Vasko Idakiev[b], Flora Boccuzzi[a]

[a]*Department of Chemistry IFM, University of Torino and NIS Centre of Excellence, via P. Giuria 7, 10125 Torino, Italy. Floriana.vindigni@unito.it*

[b] *Institute of Catalysis, Bulgarian Academy of Sciences, Acad. G. Bonchev str., bl. 11, 1113 Sofia, Bulgaria.*

Introduction

Gold catalysts, due to their high catalytic activity, particularly in CO oxidation at low temperature [1], are promising candidates both for H_2 production, through methanol decomposition and water gas shift (WGS) reactions, and purification, through the preferential CO oxidation (PROX). The nature of the support on which gold is dispersed plays a crucial role in determining the catalytic activity. When Au nanoparticles are supported on ceria, the systems are very stable and exhibit a high activity for the WGS reaction [2] over a wide temperature range, at different space velocity and H_2O/CO ratios [3]. We observed recently that the addition of ceria is effective on the stability and on the activity of other catalysts in WGS reaction [4]. A TEM, FTIR and UV-Vis characterisation has been undertaken on new gold catalysts supported on CeO_2-TiO_2 mixed oxides with different ceria loadings (20% - $AuCe_{0.2}Ti_{0.8}$ and 50% - $AuCe_{0.5}Ti_{0.5}$) to get an interpretation of the positive effect of ceria and to test the ability in the PROX reaction. All the catalysts were prepared by deposition-precipitation method and subsequent calcination at 670 K, to generate strong contact between the metal and the oxide support. The effect on the gold dispersion and on the catalytic

activity of different calcining temperature of the supports before the deposition has also been investigated.

Results and discussion

HRTEM measurements evidenced that the two oxides, ceria and titania, are easily recognizable (ceria appears darker than titania) and that they do not give rise to a solid solution or to a new mixed phase. The diffraction fringes show highly defective oxide phases in both cases. Figure 1 shows the FTIR spectra of CO adsorbed at room temperature on oxidized catalysts.

In addition to the usual bands related to CO weakly bonded to the metallic gold step sites and to the uncoordinated support cations, a new absorption band, at 2166 cm^{-1}, is present. This band is completely irreversible to the outgassing at room temperature, giving an evidence of a strong bond between the CO and the involved adsorption sites [5]. On the basis of its frequency and its behaviour it has been assigned to cationic gold clusters [6] stabilized on the structural and/or electronic defects. The activity in the PROX reaction in presence of CO, O_2 and H_2 has also been studied in situ by FTIR. CO_2 production is very fast, and the large intensity of the related band indicates a high activity also in the presence of an excess of hydrogen.

Conclusions

The FTIR data have evidenced positive gold clusters, stabilized by the mixed oxide surface, where CO is strongly bonded and remains adsorbed up to the temperatures useful in PROX for PEM fuel cells applications.

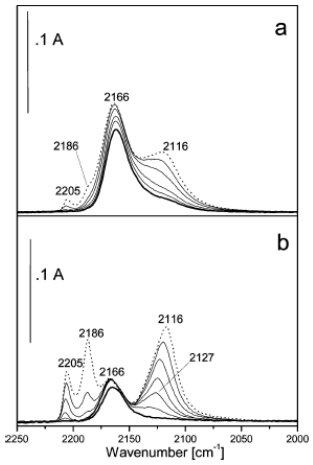

Figure 1. FTIR spectra of AuCe0.5Ti0.5 (a) and AuCe0.2Ti0.8 (b) oxidized at 673 K after the adsorption of 15 mbar of CO at RT (dashed line), at decreasing pressures (fine lines), and under outgassing at RT (bold line).

References

1. Haruta M.; Tsubota S.; Kobayashi T.; Kageyama H., Genet M.J.; Delmon J.; *J. Catal,* **1993,** *114*, 175-192
2. Tabakova T.; Boccuzzi F.; Manzoli M., Andreeva D.; *App. Catal. A*, **2003**, *252,* 385-397.
3. Andreeva D.; Idakiev V.; Tabakova T.; Ilieva L.; Falaras P.; Bourlinos A.; Travlos A.; *Catal. Today*, **2002**, *72*, 51-57.
4. Boccuzzi F.; Chiorino A., Tabakova T.; Manzoli M.; Idakiev V.; Vindigni F.; *Catalysis: a key to a richer and cleaner society Proceedings of Europacat VII*, 28 August-1 September 2005, Sofia, Bulgaria.
5. Vindigni F.; Manzoli M.; Chiorino A.; Tabakova T.; Boccuzzi F.; *J. Phys. Chem. B*, **2006,** *110*, 23329-23336.
6. Wu X., Senapati L., Nayak S.K., Selloni A., Hajaligol M., *J. Chem. Phys.,* **2002**, *117,* 4010-4015.

P 3.13

Gas-phase photocatalytic reduction of NO_x onto immobilized colloidal TiO_2 nanocrystals: a preliminary study

P. Ielpo[1], G. Lasorella[2], R. Comparelli[2], A. Panniello[1], M. Striccoli[2], M. Caselli[1], A. Agostiano[1,2], M. L. Curri[2]

[1] *Dipartimento di Chimica, Università di Bari, Via Orabona 4, 70126 Bari, Italy*

[2] *CNR IPCF, sez. Bari, c/o Dip. Chimica, Università di Bari, Via Orabona 4, 70126 Bari, Italy; lucia.curri@ipcf.ba.cnr.it*

Nanostructured materials have been increasingly investigated in the recent years due either to the fundamental interest in their physical and chemical properties and to the numerous application in different scientific and technological fields. The possibility of performing a kinetic control of the dimensions by using suitable synthetic techniques has allowed the use of such nanomaterial in optoelectronics, energy photoconversion and photocatalysis. In the case of nanosized material, the atoms residing at the surface represents a not negligible

fraction of the total number of atoms, and this fact dramatically affects the free energy of the crystalline material, and makes size-dependent the NC chemical-physical properties.

The photocatalytic degradation assisted by semiconductors under UV irradiation represent an appealing and promising method to scale up gas pollutant remediation by means of low cost processes. In particular, numerous studies have been carried out in the field of heterogeneous catalysis by using immobilized catalysts. However a significant loss of performances has been recorded in the case of deposited bulk semiconductors due to the decreasing of the surface active area. In this perspective nanocrystalline semiconductors could be able to minimize this drawback thanks to their extremely high surface to volume ratio. For this purpose the deposition technique and the choice of a proper substrate play a very important role.

Nanostructured semiconductors have been successfully employed in the removal of organic and inorganic pollutants in gas phase by means of photocatalytic techniques. In this work a possible application of the colloidal TiO_2 nanocrystal (NC) photocatalytic process has been investigated to perform a gas phase reduction of nitrogen oxide (NO_2). For this purpose a suitable apparatus has been designed and set up by using a cylindrical photoreactor carrying an UV-vis lamp able to illuminate the TiO_2 NC immobilized onto spherical glass beads while the gas carrier (O_2) containing NO_2 has been made flowing through the system, in order to perform the catalytic reduction. The gas mix is then bubbled in an absorbing solution, acting as a trap for the residual, not reduced, nitrate the residual, not reduced, NO_2.

An ion chromatographic analytical procedure has been then developed, validated and applied to quantify the nitrate amount after the reduction cycle.

The proposed approach thus offer a valuable tool to monitor the NO_2 reduction yield of the gas phase catalytic process, and to perform a kinetic study which allows an evaluation the efficiency of the system, as a function of different experimental parameters, such as catalyst composition (colloidal TiO_2 NCs vs TiO_2 P25 Degussa), deposition route, gas flow, etc.

Acknowlegment

This work has been partically supported by the Explorative Project PE_049 funded by Apulia Region.

SEZIONE

CHIMICA FISICA DEI MATERIALI

P 4.1

Nuclear Magnetic Resonance of ^{129}Xe used as a probe for the characterization of void space in crystalline microporous dipeptides: thermodynamics and molecular details of sorption.

Roberto Anedda,[a] Dmitriy V. Soldatov,[b] Igor L. Moudrakovski,[c] Mariano Casu[a] and John A. Ripmeester[c]

[a] *Department of Chemical Sciences, University of Cagliari, Monserrato (CA), Italy. aneddar@unica.it*
[b] *Nikolaev Institute of Inorganic Chemistry, Russian Academy of Sciences, Novosibirsk, Russia*
[c] *Steacie Institute for Molecular Sciences, National Research Council, Ottawa, Canada, John.Ripmeester@nrc.ca*

The suitability of ^{129}Xe NMR in characterizing voids comprised within porous materials and/or biomolecules has recently given to this technique a widespread diffusion. Among the reasons for this popularity are the chemical inertness of Xe and the remarkable sensitivity of its NMR parameters (chemical shift, line shape, relaxation rate) toward non-bonded local environment[1].
A wealth of information has been extracted so far on a number of very different systems both in solution and in solid state: for instance, Xe NMR has been used for the characterization of ligand binding sites in proteins, to distinguish protein conformation changes and detecting blood oxygenation level. Moreover, in the solid state, due to the sensitivity of ^{129}Xe NMR parameters, the size and shape of pores within some crystalline and amorphous materials and the dynamics of sorption process have been investigated.
Despite a number of progresses have recently significantly improved the technique, many questions concerning the molecular interaction of xenon with the host structures and on the correlation between ^{129}Xe NMR parameters and size/shape of cavities still remain unanswered. Moreover, the scientific interest toward this technique is amplified by the possible use of xenon in clinical imaging, anesthesia and to generate isomorphous heavy-atom derivatives in structure determination by single-crystal XRD.
In order to deepen the understanding of the inclusion process, we concentrate on model systems which allow a systematic study on thermodynamics and molecular details of sorption of xenon in solid porous materials and xenon binding to proteins in solution. This presentation summarizes latest achievements on ^{129}Xe NMR characterization of solid microporous materials.
^{129}Xe NMR has demonstrated its validity in characterizing porous materials with large pores (d > 1nm)[1], where xenon NMR parameters are mediated by exchange processes. Moreover, previous calculations have shown that the ^{129}Xe chemical shift anisotropy observed in many microporous materials is related to size and shape of the cavities/channels where xenon atoms are sorbed. We studied a series of eight microporous dipeptides: Ala-Val (AV), Val-Ala (VA), Leu-Ser (LS), Ala-Ile (AI), Val-Val (VV), Ile-Ala (IA), Ile-Val (IV), Val-Ile (VI). The sorbents belong to the group of *biozeolites* and are formed by helical self-assembly of H-bonded dipeptides to generate isolated 1D chiral nanochannels in the final crystalline material[2]. The sorption of xenon was characterized with solid-state continuous-flow ^{129}Xe NMR. The isosteric heat of sorption (q_{st}) and entropy factors were determined in the range 173-343K within two independent models based on the analysis of ^{129}Xe NMR signal intensities and isotropic chemical shifts variations observed in variable-temperature experiments. Additionally, studying the pronounced chemical shift anisotropy and line shapes as a function of temperature made it possible extracting information on the structure of xenon-cavity complex, on the flexibility of the nanopores and on molecular-scale details of sorption process. The presented procedure is suggested as an express method that allows obtaining quantitative
thermodynamic parameters and molecular level peculiarities of sorption in microporous materials. This method may be particularly suitable for the characterization of soft materials, where the flexibility of the framework that might lead to permanent structural changes (aging) and/or phase transitions do not allow the application of standard analyses such the acquisition of adsorption isotherms.

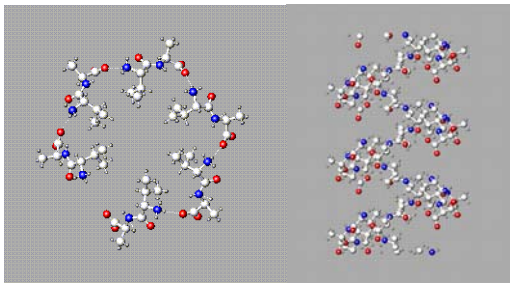

Figure. *Fragment of the crystal structure of VA (hexagonal, space group P6$_1$) showing H-bonding helical assembly of the dipeptide molecules surrounding the channel: a view along the channel (left) and side view (right).*

1. Ratcliffe, C. I.; *Annu. Rep. NMR Spectrosc.*, **1998**, *36*, 124 – 208. 2. Soldatov, D. V.; Moudrakovski, I. L.; Grachev, E. V.; Ripmeester, J. A.; *J. Am. Chem. Soc.* , **2006**, *128*, 6737 – 6744.

P 4.2

SiO_x and SiN_x layers with improved barrier effect and tribological properties

E. Angelini[1], R. d'Agostino[2], S. Grassini[1], F. Palumbo[3], F. Rosalbino[1]
[1]*Department of Materials Science and Chemical Engineering, Polytechnic of Turin, Turin, Italy*
[2]*Department of Chemistry, University of Bari, Bari, Italy*
[3]*Institute for Inorganic Metodologies and Plasmas, CNR, Bari, Italy*

SiO_x coatings deposited by PECVD of organosilicons, can improve the corrosion resistance of metals in different aggressive environments. Silicon based materials including more or less C, O, N and H show high potential for corrosion protection essentially because they are dense (low permeability to water and gases), amorphous, chemically inert and show a low electrical conductivity or can be insulator depending on their composition. Moreover, the coating promotes no galvanic

coupling deleterious to the uncoated metallic surface. From the mechanical point of view, SiO_x coatings are know to be rather brittle, therefore, the substitution of oxygen by nitrogen should allow to get higher improved tribological properties keeping the insulating nature, that is one of the parameters responsible for corrosion protection.
In this study an investigation of the tribological and electrochemical behavior of SiO_x and SiN_x thin films has been undertaken. Moreover, the deposition of multilayers, such as SiN_x/SiO_x or $SiO_x/SiN_x/SiO_x$, as well as of $Ti/TiN/SiO_x$ and $Cr/CrN/SiO_x$ has been investigated, too.
SiO_x and SiN_x have been deposited on stainless steel and aluminium alloys in an RF parallel-plate reactor starting from different organosilicon precursors (HMDSO, TEOS, HNDSN, etc.) in mixture with argon and/or oxygen, with different plasma pre-treatments, performed in H_2, O_2 and NH_3 containing plasmas. Ti/TiN and Cr/CrN films have been deposited by magnetron sputtering, using Ti and Cr targets at 200°C, $3{,}0 \cdot 10^{-2}$ Torr and input power ranging from 150 to 300W; N_2 and Ar gases were used as a reactive source and a sputtering gas, respectively.
The chemical characterisation of coatings has been carried out by means of X-Ray Photoelectron Spectroscopy (XPS) and Infrared Spectroscopy (FT-IR).
The barrier effect properties of deposited films have been assessed by means of Electrochemical Impedance Spectroscopy in aerated 0.1 M NaCl solution at room temperature. Impedance spectra have been recorded at the open circuit potential by applying a sinusoidal signal of 10 mV amplitude in the frequency range 100 kHz -10 mHz. The experimental data interpreted on the basis of an equivalent circuit model allow to obtain the charge transfer resistance, R_{ct}, and the coating capacitance, C_c, which can be directly related to the protective properties of the coatings.
The mechanical and tribological properties of mono and multilayers has been assessed by means of Vickers microhardness measurements and sliding wear resistance test (pin-on-disc).
Morphological characterization of deposited films has been performed, before and after the tribological and electrochemical tests, by means of scanning electron microscopy (SEM).
The tribological and electrochemical behaviour of the coatings increases with the power density of the discharge, and with the oxygen content of the feed gas. When the deposition process is preceded by a proper plasma treatment, which depends on the metal under study, a marked increase of the protective properties is detected.
Moreover, a marked increase of the barrier effect , without affecting their mechanical properties, has been observed for $Ti/TiN/SiO_x$ and $Cr/CrN/SiO_x$ coated steel in comparison to magnetron sputtered ones.

P 4.3

Synthesis and characterization of hybrid organic/inorganic mesoporous photoactive nanoparticles

Bertolino, C.A., Caputo, G., Gianotti, E.
Dipartimento di Chimica IFM e NIS Centre of Excellence, Via P. Giuria 7, 10125 Torino, chiara.bertolino@unito.it

In this contribution, the synthesis and the characterisation of photoluminescent hybrid organic-inorganic mesoporous nanoparticles (NPs) are described. Highly fluorescent organic dyes of the indocarbocyanines family, namely IRIS 3, have been embedded within the pores of MCM-41[1].
The host-guest interaction between the inorganic framework and the organic dyes is extremely effective in protecting the dye and enhancing its emitting performances, with no structural modification of the inorganic material.
The bulk material, obtained by impregnation of the mesoporous host with dyes solution, was nano-sized by sonication, preserving the features of both the organic dye and the mesoporous structure. A complete physical chemical characterization of the bulk material and the NPs was performed by X-Ray Diffraction (XRD), High Resolution Transmission Electron Microscopy (HRTEM), UV-Vis and Photoluminescence spectroscopy.
NPs spectra were recorded by analyzing NPs suspensions at different pH values of phosphate buffer saline solutions (pH=3.60; pH=5.50; pH=7.40; pH=9.00), corresponding to the environment in different cellular compartments. One of the application of this new material is in the field of diagnostics and molecular imaging[3], thus the bio-compatibility and cytotoxicity of silica nanoparticles were assessed in mastocytes-like RBL cells, using a confocal microscope.

1.Gianotti, E.; Bertolino, C.A.; Caputo, G.; Coluccia, S.; *Microporous and Mesoporous Materials* (submitted)
2. J.Bujdák, N.Iyi, T.Fujita, *Colloids and Surfaces A*, **2002**, *207,* 207-214.
3. Santra, S.; Liesenfeld, B.; Bertolino, C.A.; Dutta, D.; Cao, Z; Tan, W.; Moudgil, B.M.; Mericle, R.A.; *Journal of Luminscence*, **2006**, *117*, 75-82.

P 4.4

THERMAL ANALYSIS CHARACTERIZATION OF SOME PROCESSES RELATED TO DISPROPORTIONATION OF STANNOUS OXIDE

Bonicelli M. G.[a], Ceccaroni G.[b], Gauzzi F [c]., Mariano G.
[a] *Dipartimento Ingegneria Chimica, Materiali, Ambiente, Sapienza Università di Roma, Via del Castro Laurenziano 7, 00161 Roma, Italy*
[b,c] *Dipartimento di Scienze e Tecnologie Chimiche, Università di Roma Torvergata,Via O.Raimondo, 00173 Roma, Italy*

The disproportionation products of SnO are Sn and either SnO_2 or an intermediate oxide (IO) Sn_xO_{1+x} depending on the reaction temperature. A dispersion of Sn droplets into the oxides results from this process. In a previous work [1], the disproportionation products of pure SnO were investigated by DSC with the aim of examining the fusion and solidification behaviour of Sn droplets and the catalytic nucleation of solid or liquid Sn on tin oxides. As a subsequent development, SnO disproportionation has been now carried out directly in the calorimeter: so that heating and cooling rates we applied could vary over larger intervals and their values were more exactly

measurable. It was also possible to obtain and analyze the complete thermograms of disproportionation at various temperatures. As far as the solidfication and fusion of metallic Sn is concerned, the results are substantially in agreement with those reported in [1]. Furthermore, the deconvolution of the solidification thermograms of metallic Sn in the presence of IO allows to estimate the quantity of Sn that solidifies in correspondence of every value of supercooling.

[1] Bonicelli M.G. ;Ceccaroni G. ;Gauzzi F. ; Mariano G.: *Thermochimica Acta* **2005** , 430, 95–99

P 4.5

Surface Chemistry Effects on the Early Growth Stages of Pentacene Films from a Soluble Precursor on Silicon-Based Materials

C. Musumeci[ζ,ξ], C. Cascio[ζ,ξ], A. Scandurra[ζ,ξ], G.F. Indelli[ζ,ξ], C. Bongiorno[Γ], S. Ravesi[ζ,Б] and B. Pignataro[ζ,*]
[ζ]*PLAST_ICs, Stradale Primosole 50, 95121, Catania*
[ξ]*Superlab -Consorzio Catania Ricerche, Stradale Primosole 50, 95121, Catania*
[Γ]*Istituto per la Microelectronica e Microsistemi (IMM), Stradale Primosole 50, 95121, Catania*
[Б]*ST-Microelectronics, Stradale Primosole 50, 95121, Catania*
[*]*Dipartimento di Chimica Fisica F. Accascina, V.le delle Scienze – Parco D'Orleans II, 90128 Palermo, bruno.pignataro@unipa.it*

To date among conjugated molecules pentacene showed very promising transport properties which makes it a good candidate for the build up of organic thin films transistors (OTFT). Thin films of pentacene are usually prepared by evaporation under vacuum since it is scarcely soluble in organic solvent, especially in the green ones. However, the developing of solution processes is in several cases desirable as for the fabrication of low-cost and large- scale plastics devices.

Here we show an innovative solution approach which leads to the formation of pentacene thin films via a retro Diels-Alder reaction by heating a thin film of a soluble pentacene precursor (13,6-N Sulfinylacetamidopentacene) transferred on solid interfaces through spin-coating. Our study is centred on the early growth stages of pentacene crystals on both hydrophilic and hexamethyldisilazane-treated hydrophobic silicon-oxide materials. Such interfaces are of relevant interest for OTFT as for instance the electron mobility under field-effect has been demonstrated to occur at the very first layers in direct contact with silicon-based dielectrics. In order to have a precise thickness control of the films we employed for their preparation the Langmuir-Blodgett method in addition to spin-coating. By combining Atomic Force Microscopy, Transmission Electron Microscopy and X-Ray Photoelectron Spectroscopy, we found that the thermal treatment leads to the complete conversion of the precursor and that the early growth stages of pentacene crystals are strongly influenced by the interface-chemistry. In particular almost flat-lying molecules first nucleate in islands made of molecules almost normal to the surface which then develop in crystals up to some microns in diameter. Compact and holed micro-crystals have been observed respectively on the hydrophobic and hydrophilic surfaces. The structural data provide important inside for the understanding of the field-effect transport properties along with the conduction mechanisms of the above films.

P 4.6

New advances in the high temperature decomposition of H_2SO4

S. Brutti[a], L. Bencivenni[a], V. Barbarossa[b], G. De Maria[a]
[a] *Dipartimento di Chimica, Università di Roma "La Sapienza", P.le A. Moro 5, 00185 Roma, Italy*
[b] *ENEA- Research Center "Casaccia" – 00060 S. M. Di Galeria, Roma, Italy*

The sulphur-iodine cycle is one of the most promising thermochemical cycle for hydrogen production. Its coupling with a solar energy primary source is a great challenge to achieve an efficient and economically competitive H_2 production. Within this cycle the decomposition of sulfuric acid plays a key role being this process the most energy-demanding reaction step. Here a combined computational and experimental study of the decomposition at high temperature of H_2SO_4 to SO_2 is presented. From a computational point a view the role of the hydrated gaseous coordination adducts of SO_3(g) and H_2SO_4(g) in the dissociation-decomposition process has been evaluated. A first principles study of the gaseous coordination complexes $SO_3(H_2O)_n$ (n=1-3) and $H_2SO_4(H_2O)_m$ (m=1-2) has been carried out deriving equilibrium ground state structures, vibrational frequencies and energetic stabilities. These results have been used to derive the enthalpy of formation at 0 K and the Gibbs energy functions of these molecules. A new thermodynamic modeling of the decomposition of H_2SO_4(g) has been therefore performed considering the effect of temperature, pressure and initial composition of the gas (hydration conditions).The experimental investigation of the high temperature decomposition of H_2SO_4 by using a standard electrical furnace and a concentrated solar power furnace without catalysts or using a Fe_2O_3-based catalyst was carried out. The computational and experimental results obtained are discussed together with the available literature.

P 4.7

Lithium Order-Disorder in Superionic LLTO: Theory and Experiment

M. Catti
Dipartimento di Scienza dei Materiali, Università di Milano Bicocca, 20125 Milano, catti@mater.unimib.it

LLTO ($Li_xLa_{2/3-x/3}\square_{1/3-2x/3}TiO_3$) is one of the materials with the highest lithium ion electrical conductivity (about 10^{-3} S cm^{-1} for x=0.3) at room temperature, of interest as solid electrolyte or cathode in lithium batteries.[1] Structural studies of the x=0.3 term, performed by TOF neutron powder diffraction on samples with different thermal history, showed tetragonal perovskite superstructures with $\sim\sqrt{2}a_p\times\sqrt{2}a_p\times 2a_p$ unit-cells (a_p ~ 3.87 Å for cubic perovskite).[2,3] By Rietveld refinements in the *P4/nbm* (unquenched) and *I4/mcm* (quenched

sample) space groups, the main findings were: anti-phase octahedral tilting $a^0a^0c^-$, partial La-Li ordering in two independent (001) layers for the unquenched sample, and lithium atoms located in two distinct disordered sites with fourfold oxygen coordination within the A-type dodecahedral cage of ABO_3 perovskite. The short Li-Li' distances account for the high ionic mobility and suggest a mainly (001) two-dimensional mechanism of ion hopping among Li sites.

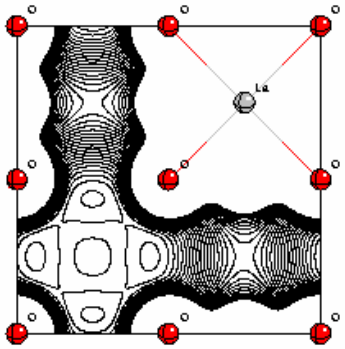

An *ab initio* periodic quantum-mechanical simulation of possible locally ordered structures was then performed, by use of the B3LYP hybrid functional and of an all-electron basis set of atomic orbitals (CRYSTAL06 code[4]). The compositions $Li_{0.5}La_{0.5}TiO_3$ and $Li_{0.3125}La_{0.5625}\square_{0.125}TiO_3$ were considered, with 4 to 16 formula-units of LLTO per primitive unit-cell, and with symmetry lowered to monoclinic *Pm*. Several different La-Li-□ ordering patterns within the (001) layers of A-cages were devised. The structures were fully optimized by energy minimization, so as to localize the preferred lithium sites for each ordering scheme. Maps of the electrostatic potential were also computed in ionized Li-free model structures, in order to study the electric field acting on Li^+ ions (cf. the figure). It was found that the anti-phase octahedral tilt is reproduced only for layers with mixed La-Li composition, and not for full La-Li ordering in different layers. Further, the positions adopted by lithium depend significantly on the locally ordered environment, so that the two sites appearing in the experimental average structure can be assigned to specific ordered configurations on the basis of the theoretical results obtained. The most populated Li site, close to the O_4 windows separating adjacent A cavities in the layer, corresponds to La-poor local configurations, and is actively involved in the ion migration process. The other one, closer to the cage centre, is related to La-rich local environments, and is a trapping location less favourable to the transport mechanism.

1. Inaguma, Y.; Chen, L.; Itoh, M.; Nakamura, T.; Uchida, T.; Ikuta, H.; Wakihara, M.; *Solid State Commun.,* **1993**, *86*, 689. 2. Sommariva, M.; Catti, M.; *Chem. Mater.*. **2006**, *18*, 2411. 3. Catti, M.; Sommariva, M.; Ibberson, R.M.; *J. Mater. Chem.*, **2007**, *17*, 1300.
4. Dovesi, R.; Saunders, V.R.; Roetti, C.; Orlando, R.; Zicovich-Wilson, C.; Pascale, F.; Civalleri, B.; Doll, K.; Harrison, N.M.; Bush, I.J.; D'Arco, Ph.; Llunell, M.; CRYSTAL06: *User's Manual*; http://www.crystal.unito.it

P 4.8

Tuning of chemical and physical properties of Poly(methyl metacrylate)- TiO_2 nanocrystals based nanocomposites for sensing applications

A. Convertino[1], G. Leo[1], M. Striccoli[2], M. Tamborra[3], C. Sciancalepore[3], M. L. Curri[2]
1 CNR ISMN, Via Salaria Km 29.300, 00016 Monterotondo St. (Roma), Italy
2 CNR IPCF, sez. Bari, c/o Dip. Chimica, Università di Bari, Via Orabona 4, 70126 Bari, Italy
3 Dipartimento di Chimica, Università di Bari, Via Orabona 4, 70126 Bari, Italy; : annalisa.convertino@ismn.cnr.it

The growing demand of our society to detect and monitor gases and vapors for safety, health and environmental issues requires a high degree of innovation in sensor technology, which includes both the research development of novel sensing materials and the integration of original sensor architectures. Particular attention has been devoted to polymers as sensing materials for devices exploiting various transduction signals, such as optical, mechanical, electrical and thermal. Some recent results show that the presence of inorganic nanoparticles (NPs) causes a further modification of the sorption processes in a polymer matrix [1]. Indeed the interaction between the NP surface and the gas molecules can control the selectivity, rate and efficiency, of molecule adsorption in the nanocomposite. In addition, the high surface-to-volume ratio of NPs increases the number of active sites for interaction with the analytes. Hence, NP based polymer composites can address an innovative generation of chemical sensors combining the sensing abilities and the possibility of a versatile tailoring of the physical properties of the NP with the mechanical and/or optical responses related to the gas sorption processes of the polymers. In this work the sensing properties of Poly(methyl metacrylate) (PMMA) based nanocomposite have been investigated as a function of the shape (dot or rod), concentration and surface ligands (oleic and phosphonic acid) of the embedded TiO_2 colloidal nanocrystals (NCs). Colloidal chemical routes have been used to synthesize the TiO_2 NCs with a high control on size, shape and crystal phase. The surface chemistry of the NCs has been modified by exploiting ligand exchange techniques.
Thin films of TiO_2 NC-PMMA nanocomposite deposited by spin coating on Si and glass substrates, have been investigated by Vis-NIR spectrophotometry in presence of organic vapors (acetone, ethanol). Films of PMMA composites based on commercial TiO_2 NCs have also been prepared as comparison. The effects of the surrounding vapors on the nanocomposite thin films have been tested by reflectance measurements in the visible. The vapor sensing behavior of the PMMA nanocomposite have been estimated by measuring the degree of swelling, $\Delta t/t$, where t is the thickness of the film and Δt is the relative thickness variation, from the reflectance spectra measured before and after the vapor exposure [2]. Indeed, when the organic vapors are adsorbed by the polymer host matrix, a reversible shift of the fringe pattern has been observed in the reflectance spectra for the nanocomposite films due to the reversible film swelling. The overall results have indicated that, the different shape of the embedded NCs and the presence of the organic molecule layer coordinating the surface of the TiO_2 NCs appear to be critical in the sensing process, by enhancing or inhibiting the swelling phenomenon of the nanocomposite, and by modifying the response time of the PMMA.

[1] A. Convertino et al. *Adv. Mater.* 13, 1103, (2003).
[2] A. Convertino et al. *Sensors and Actuators B*, (2007) doi:10.1016/j.snb.2006.11.043.

Acknowlegment
This work was financially supported by the EC-funded Project NOVOPOLY (Contract no. STRP 013619).

P 4.9

A computational multiscale approach to the modelling of 45S5 Bioglass®

M. Corno[a], A. Pedone[b], B. Civalleri[a], M.C. Menziani[b] and P. Ugliengo[a]
[a]*Dipartimento di Chimica IFM Università di Torino, via P. Giuria 7, 10125 Torino, marta.corno@unito.it*
[b]*Dipartimento di Chimica Università di Modena e Reggio Emilia, via G. Campi 183, 41100 Modena*

The Hench Bioglass® 45S5 of 48.1% SiO_2, 25.9% CaO, 22.2% Na_2O and 3.7% P_2O_5 composition is of great interest in medical applications since in the presence of body fluids, and depending upon the rate of ion release and resorption, it creates chemical gradients which promote the formation of a layer of biologically active bone-like hydroxyapatite at the implantation interface. Osteoblasts can preferentially proliferate on the apatite layer, and differentiate to form new bone that binds strongly to the implant surface.
Its simulation has been undertaken in a multiscale approach in which molecular dynamics simulations based on classical force fields have been carried out on a unit cell containing 78 atoms with $Na_{12}Ca_7P_2Si_{13}O_{44}$ composition and P1 symmetry. Molecular mechanics minimization was then run on a representative quenched structure, to relax fully the system which is subsequently passed to the CRYSTAL06 code as a starting structure to perform a full ab-initio periodic geometry relaxation using the hybrid B3LYP functional with Gaussian basis sets of double-ζ quality. The hybrid B3LYP has been chosen because it has recently proved to be very successful in the treatment of complex silicate crystals. The full IR and RAMAN spectra of the Bioglass® have been computed ab-initio and compared to experimental results.
Some important points can be highlighted from the comparison between the molecular mechanics and B3LYP optimized structures (Figure 1) of the Bioglass 45S5.

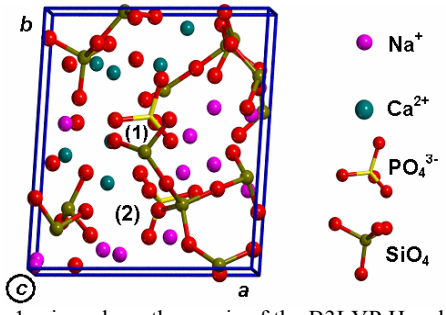

Figure 1: view along the *c* axis of the B3LYP Hench 45S5 bioglass optimised unit cell

B3LYP optimized structures show a slightly higher density than the one computed with the molecular mechanics approach, this latter being also in good agreement with the experimental one. This is due to a known weakness of many GGA and hybrid functionals which overestimate the Si-O bonds and underestimate the Si-O-Si and Si-O-P angles, respectively. Ca and Na distributions are in very good agreement between the two approaches, as it is the local environment around the two PO_4 groups.
The B3LYP calculations provide Mulliken net charges which are close to the formal ionic charges showing the ionic nature of the bioglass, whereas the large band gap of 6.5 eV shows its strong insulating character.
As for vibration frequencies, in spite of great complexity due to the large number of active modes, a good agreement with experimental data was found, confirming the reliability of the present model. Spectroscopic data were compared also with simulated vibrational spectra of pure amorphous silica, to highlight the role of phosphorus and network modifiers cations.
The present attempt is the starting point of a more general multiscale approach in which molecular mechanics calculations will provide initial structures for ab-initio simulation. This latter, in turn, will provide electronic features of complex materials and can also be used to refine, in a fully self consistent way, the force field parameters derived empirically. Present DFT functionals (hybrid ones in particular) have been proved excellent tools for the simulation of static and dynamic properties of silica-based materials.

P 4.10

Structural and chemical properties of the hydroxyapatite surface. A computational *ab initio* and a microcalorimetric/IR spectroscopic characterization

M. Corno[a], L. Bertinetti[a], V. Bolis[b], C. Busco[b], G. Martra[a] and P. Ugliengo[a]
[a]*Dipartimento di Chimica IFM Università di Torino, via P. Giuria 7, 10125 Torino, marta.corno@unito.it*
[b]*Dipartimento DiSCAFF Università del Piemonte Orientale "A. Avogadro", via Bovio 6, 28100 Novara*

Bioactive glasses, when implanted in the body or simply immersed in simulated body fluids (SBF), develop a biologically active hydroxyapatite (HA) layer which in turn does promote the bone-tissue formation. In fact hydroxyapatite, which exhibits strong similarities to the mineral phase of the mammalian bones and teeth, does play a key role during the bioactive glasses integration processes, in that it facilitates adhesion and subsequent proliferation of the osteocytes, so allowing the damaged bone tissues to be repaired. The first step of these processes is the adsorption of biomolecules at the active surface of HA. Therefore, studies aimed at quantitatively describing the structural and chemical properties of the HA surface are of greatest interest, in the attempt to elucidate at nano-level the interfacial processes involved in the biological fixation of inorganic materials to the living tissues.
In the present study, *ab initio* methods and experimental techniques have been used to characterize the adsorption features of HA surfaces using H_2O and CO as molecular probes. Periodic *ab initio* B3LYP calculations using CRYSTAL06 code have run to characterize the (001) and (010) bare surfaces for both hexagonal and monoclinic HA phases. On the geometrically relaxed surfaces the adsorption of H_2O and CO has been simulated, from low to high coverage. Energies of adsorption and the vibrational features of H_2O and CO have been computed as a function of coverage and compared with the corresponding microcalorimetric data and infrared spectra.

The main conclusions from the simulations are that both H_2O and CO adsorb on the exposed Ca^{2+} ions which are characterized by rather strong local electric fields, although not strong enough to dissociate H_2O. The (001) surface is more active than (010) when considering CO as a probe.
H_2O adsorption studies on the (010) are, at the moment, still in progress. For the CO case, comparison between the computed and the measured CO stretching frequencies confirms that the exposed Ca^{2+} ions behave as a Lewis acidic sites, in that bathochromic shifts have been measured and computed. Microcalorimetric data for the CO adsorption are still in progress, whereas the RT adsorption of H_2O on a nanosized HA specimen has already been investigated.
In Figure 1 the heat of adsorption of H_2O vapour is reported as a function of the adsorbed amount. The energy of interaction is quite high not only in the early stage of the process but also at high coverage (correspondent to the formation of a second shell of coordinated H_2O). The interaction energies computed at B3LYP level are in fair agreement with the experimental heats, confirming that the interaction (which is also partially irreversible upon evacuation) is quite strong (see Figure 1).
It is suggested that the strong, but still molecularly coordinated H_2O on the *cus* Ca^{2+} cations at the HA surface has likely an implication in the adsorption of proteins at the hydrated layer interface. Indeed, if reactive Ca-OH groups were formed at the surface upon contact with H_2O, denaturation of proteins would occur hampering cells adhesion.

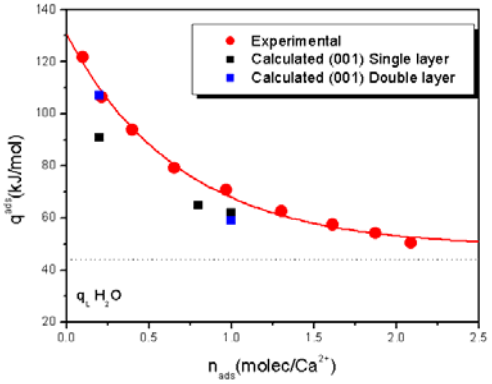

Figure 1: differential heats and B3LYP energies of adsorption of H_2O *vs* coverage on nanosized HA

In conclusion, the joint use of experimental and computational approaches has been found extremely fruitful to elucidate the molecular events which are responsible of the adsorption processes occurring at the HA surfaces.

P 4.11

Tailored functionalization of luminescent colloidal nanocrystals for selective 2/3D assembly

M.Corricelli[a], R. Comparelli[a], N. Depalo,[b] M. Striccoli[a], V. Saadhu,[c] J. Huskens,[c] M.L. Curri[a]

[a] *CNR-IPCF Sede Bari, c/o Dip. Chimica – Via Orabona 4, Bari, I-70126, Italy; r.comparelli@ba.ipcf.cnr.it*
[b] *Università di Bari – Dip. Chimica, Via Orabona 4, Bari, I-70126, Italy*
[c] *Laboratories for Supramolecular Chemistry and Technology MESA+ Institute for Nanotechnology, University of Twente P.O. Box 217, 7500AE, Enschede (TheNetherlands)*

The functionalization of colloidal nanocrystals (NCs) is a fundamental goal to exploit NCs as building-blocks for the realization of ordered architectures in 2 and 3 dimensions.[1]
A plethora of approaches have been exploited in assembling nanoparticles, such as fluid-aligned, surfactants-interacted, DNA-directed, electrostatic-interaction oriented, and recognition-mediated organization.[2]
In this work, luminescent semiconductor NCs of different chemical composition (CdS and CdSe@ZnS) have been synthesized by colloidal chemistry routes and functionalized by means of silanol groups. The silanization procedure, typically used to make water-soluble and biocompatible NCs,[3] consist of the growth of a thin silica shell on the NCs surface allowing to introduce suitable functional groups on the surface of the silica network. Herein, we modified the silanization approach to confer tailored functionality (amine, thiol, and phosphonate moieties) to CdS and CdSe@ZnS NCs. The obtained water soluble silanized NCs have been extensively investigated by means of optical (UV-Vis, PL, PL time-resolved, FTIR), structural (HRTEM) and electrophoretic techniques.
The functional groups of silanized NCs have been exploited to direct the electrostatic interaction driven assembly of such luminescent NCs onto patterned silicon substrates functionalized with amino-alkyl SAM (5x3μm)[4]. The obtained assembly has been investigated by means of microscopic techniques (fluorescence microscopy and AFM) which confirm the selective binding of the silanized NCs to the SAM molecules.
Acknowledgment. The partial support of the EC-funded project NaPa (Contract no. NMP4-CT-2003-500120) is gratefully acknowledged. The content of this work is the sole responsibility of the authors.

1. Shipway, A.N.; Katz, E.; Willner, I; ChemPhysChem. **2000**, 1, 18-52 2. Depalo, N.; Comparelli, R.; Striccoli, M.; Curri, M.L.; Fini, P.; Giotta, L.; Agostano, A.; *Journal of Physical Chemistry B* **2006**,110,17388-17399 and reference therein 3. Gerion, D.; Pinaud, F.; Williams, S. C.; Parak, W. J.; Zanchet, D.; Weiss, S.; Alivisatos, A.; *Journal of Physical Chemistry B*; **2001**, 105, 8861-8871. 4. Maury, P; Escalante, M; Reinhoud, D. N.; Huskens, J; *Advanced Materials*, **2005**, 17, 2718-2723.

P 4.12

Physical properties of the magnetic superconductor Ru – 1222 obtained from Ru–1212 and $Ce_{0.6}Gd_{0.4}O_{1.8}$ powders

G. A. Costa [a], C. Artini [a], M. M. Carnasciali [b], R. Masini [c] and A. Ubaldini [d]

[a] *INFM and DCCI, Via Dodecaneso 31, 16146 Genova*
[b] *INSTM and DCCI, Via Dodecaneso 31, 16146 Genova*
[c] *CNR-IMEM, Via Dodecaneso 33, 16146 Genova*

[d] *NIMS, 1-1 Namiki, Tsukuba, Ibaraki, 305-0044, Japan*

The ruthenocuprates $RuSr_2RECu_2O_8$ (Ru – 1212) and $RuSr_2(RE_{1-x}Ce_x)_2Cu_2O_{10}$ (Ru – 1222) are very attractive compounds, as they present at the same moment superconductivity and many complex magnetic orderings [1, 2]. While, on one hand, the synthesis of these materials is apparently simple, the reported values of the transition temperatures are critically dependent on the sample preparation conditions [3]. Classical solid state route requires a preliminary calcination of the precursors in argon and then many subsequent annealings in oxygen. Previous results have shown that at the end of the first step in argon the system is formed in the case of Ru – 1212 by $RuSr_2GdO_6$ and Cu_2O, and in the case of Ru – 1222, in addition to these, also by $(RE_{1-x}Ce_x)O_{2-x/2}$. In flowing oxygen these phases react to form the ruthenocuprate [4]. For the Ru – 1222 the presence of three different phases makes the reaction more complex. Actually, it is possible to detect the presence of Ru – 1212 in samples of Ru – 1222 prepared at low temperature.
In this work, polycrystalline Ru – 1222 synthesised by a different route was studied with the aim of preparing samples with higher degree of purity. This compound was obtained from the reaction between Ru – 1212 and $Gd_{0.4}Ce_{0.6}O_{1.8}$ previously prepared. The former was synthesised following the classical procedure [5] and the latter using a co-precipitation method [6]. They were mixed and calcined in flowing oxygen in several subsequent steps.
The structural, electrical, magnetic and spectroscopic characterisations of the so formed $RuSr_2Gd_{1.4}Ce_{0.6}Cu_2O_{10}$ are reported.

1. Jorgensen, J. D.; Chmaissem, O.; Shaked, H.; Short, S.; Klamut, P.W.; Dabrowski, B.; Tallon, J.L.; *Physical Review B* **2001** *63* 054440-1/5. 2. Butera, A.; Fainstein, A.; Winkler, E.; Tallon, J.L.; *Physical Review B* **2001** *63* 0544420-1/5. 3. Artini, C.; Cimberle, M. R.; Costa, G.A.; Carnasciali, M.M.; Ferretti, M.; Masini, R.; *Ruthenate and rutheno-cuprate materials: theory and experiments*, Springer Verlag LNP series, ed.: C. Noce, A. Vecchione, M. Cuoco, A. Romano, **2002** *603* 222-238. 4. Artini, C.; Ubaldini, A.; Firpo, F.; Carnasciali, M.M.; Bruzzone, G.; Costa, G.A.; Masini, R.; Cimberle, M.R.; Tropeano, M.; *Applied Superconductivity 2003*, Proceedings of the 6th European Conference on Applied Superconductivity, Sorrento, 14-18/9/2003 **2004** 1167-1173. 5. Artini, C.; Carnasciali, M.M.; Costa, G.A.; Ferretti, M.; Cimberle, M.R.; Putti, M.; Masini, R.; *Physica C*, **2002** *377* 431-436 .6. Mele, P.; Artini, C.; Masini, R.; Costa, G.A.; Hu, A.; Chikumoto, N.; Murakami, M.; *Physica C* **2003** *391* 49-54

P 4.13

Fluorination of TiO_2: effects on surface hydroxyl groups and photoreactivity

M.G. Faga[a,c], M. Minella[b], V. Maurino[b], G. Martra[a], C. Minero [b], E. Pelizzetti[b], S. Coluccia[a]
[a]*Dipartimento di Chimica IFM e Centro di Eccellenza NIS, Università di Torino, Via Pietro Giuria 7, 10125 Torino, Italy.*
[b]*Dipartimento di Chimica Analitica e Centro di Eccellenza NIS, Università di Torino, Via Pietro Giuria 5, 10125 Torino, Italy.*
[c]*CNR-ISTEC, Strada delle Cacce 73, 10135 Torino*

Titanium oxide plays and important role in the field of photocatalysis. Several studies related to the photodegradation of a wide number of organic compounds can be found in literature. Since there is almost unanimous agreement that the photocatalytic reactions occur at the surface of the TiO_2 particles, specific adsorption of ions can affect the performance of the system. For instance, the influence of several anions, such as halides, on the photocatalytic processes involving some target organic molecules were considered. In particular, the beneficial effect of fluorination of TiO_2 P25 on the photocatalytic production of H_2O_2, during phenol degradation was studied by Minero and coworkers [1,2]. Tough such influence was well assessed, no detail information about the surface states of fluorinated titania was obtained. Moreover, studies on different kind of commercial titania powders, namely Merck and P25 Degussa, have highlighted remarkable differences in their surface structure [3].
Based on these reasons, this work is aimed to compare the effect of fluorination on both TiO_2 Merck and P25 powders. Different levels of fluorination were attained by OH^-_{surf}/F^- exchange at various pH (Figure 1).

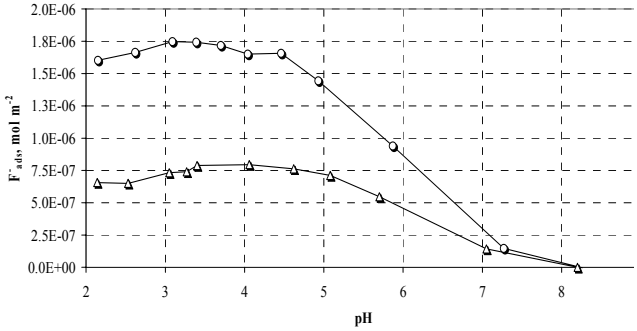

Figure 1: Amount of F^- adsorbed on TiO_2 P25 (10 g L^{-1}) as a function of pH and of the concentration of HF in the exchange solution: (○) HF 1.0 mM, (Δ) HF 0.5 mM

In the case of the P25, significant differences were observed for the bare and fluorinated TiO_2 powders. Conversely, TiO_2 Merck in both the bare and fluorinated forms exhibited similar performances in the photoproduction of H_2O_2, that, in turn, appeared close to the behaviour of TiO_2 P25 with a higher amount of fluoride.
The bare TiO_2 and the derived fluorinated samples were studied by infrared spectroscopy: i) after outgassing at room temperature, when the titania surface is still retains hydroxyl groups and water molecules coordinated to surface cations, and ii) after outgassing at 150° C, when water from the extended faces is usually removed [3]. As for the powders simply outgassed at r.t., the IR spectrum of the bare sample showed a series of components in the 3800–3600 cm^{-1} range, due to the stretching mode (νOH) of different types of free hydroxyl groups, and an intense and broad absorption in the 3600–3200 cm^{-1} range, due to hydroxyls and water molecules bonded via hydrogen bond. In this region a maximum at 3418 can be observed, arising from the superposition of the νOH mode of bonded hydroxyl groups and of the symmetric and antisymmetric νOH modes of molecular water coordinated to four coordinated Ti^{4+}ions, typically exposed on (1 1 0) faces. The variety of components in the 3800–3600 cm^{-1} region is consistent with a large heterogeneity of hydroxyl groups, arising from the different kinds of planes exposed at the surface of the TiO_2 P25 microcrystals and from the presence of sites in defect position [3]. At lower wavenumbers, the spectrum is characterised by a main band located at ca. 1630 cm^{-1}, due to the bending of water molecules. In the case of the samples containing different amount of fluoride, a higher

relative intensity of the δ_{H2O} mode, proportional to the amount of F^-, was found, indicating and increased hydrophylicity of the materials. Some slight difference in the spectral pattern of isolated hydroxyls was also observed. Even after outgassing at 150 °C the fluorinated powders still exhibited a higher hydrophilicity, retaining higher amount of adsorbed water. Furthermore, the spectral pattern related to isolated hydroxyl groups underwent significant changes (Figure 2). In the case of the bare sample, four main partially resolved components at 3730, 3690, 3670 and 3650 cm^{-1}. Passing to the sample with a low amount of fluoride (prepared at pH = 6), the peak located at 3670 cm^{-1} became the dominant feature, while the 3690 cm^{-1} one almost disappeared and the 3730 cm^{-1} component appeared stronghly decreased in intensity. In the case of the titania with a higher level of fluorination, an even more simplified ν_{OH} pattern was obtained, characterized a main component at 3670 cm^{-1}, with an unresolved shoulder at 3650 cm^{-1}. Interestingly, this pattern appeared quite similar to that of the bare TiO_2 Merck, that exhibited similar photoproduction of H_2O_2.

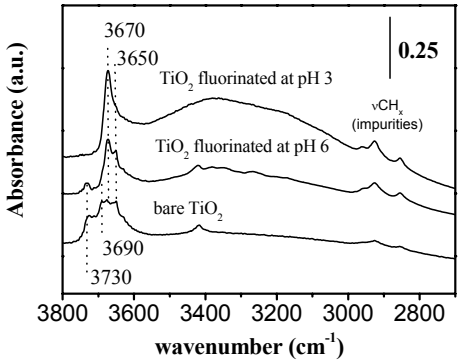

Figure 2: IR spectra, in the νOH region, of TiO_2 P25 in the bare form and after fluorination at pH= 6 and pH=3. All samples were outgassed at 150 °C.

The results clearly put in evidence a dependence of the surface hydrophilicity on the fluorination degree for the P25 powder.
Furthermore, the evolution of the spectral pattern in the hydroxyls stretching region indicated that fluoride ions replaced hydroxyls present at the surface of the TiO_2 P25 in peculiar positions only. From a morphological point of view, HR-TEM images of TiO_2 P25 evidenced the presence of relevant amount of corner, edge and kink surface terminations, absent in the case of TiO_2 Merck. The similarity of the νOH pattern of the TiO_2 P25 with a higher fluoride content with that of the bare TiO_2 Merck makes then allowance to propose that such "peculiar position" are coordinatively defective surface sites.

References
1. Minero, C.; Mariella, G.; Maurino, V.; Pelizzetti, E.; *Langmuir,* **2000,** *6,* 2632-2641.
2. Minero, C.; Mariella, G.; Maurino, V.; Vione, D.; Pelizzetti, E.; *Langmuir,* **2000,** *16,* 8964-8972.
3. Martra, G.; *Applied Catalysis A: General, 200,* **2000,** 275-285 and reference therein

P 4.14

Transient Absorption properties of the monomer and dimer of TTF radical cation

Eleonora Garbin, Elisabetta Collini, Camilla Ferrante, Renato Bozio
Dipartimento di Scienze Chimiche e UdR INSTM di Padova, Università di Padova, Via Marzolo 1, I-35131 Padova, Italy

Ultrafast Transient Absorption (TA) experiments performed on tetrathiafulvalene perchlorate ($TTF^{+\cdot}ClO4^-$) in solution and polymer films are presented.
In DMSO solution and in polymer matrices the $TTF^{+\cdot}$ radical forms dimers, characterized by a first excited singlet state with a strong charge transfer (CT) character, falling at 770 nm.[1,2] In the TA experiments the pump beam is resonant with the CT transition of the dimer while the probe is tuned between 675 nm and 1100 nm. The transient decay curves show a double exponential behavior with characteristic time constants of 220 ± 90 fs and 3.0 ± 1.3 ps. When the probe wavelength is smaller than 875 nm, both components appear as bleaching features, while when it is larger than 875 nm, the first component is still a bleaching, and the longer decay appears as photo-induced absorption (PIA). We attribute the 220 fs bleaching feature to a spectral diffusion effect, while the 3.0 ps component is attributed to the lifetime of the lowest CT state. The latter component appears as a bleaching when the ground state absorption is stronger than the excited state one (under 875 nm), and it turns into PIA when the opposite happens (above 875 nm).
In acetonitrile solution, instead, only the monomer form is present. TA experiments are performed with the pump beam set at 403 nm while the probe beam is tuned in the 425-625 nm range. The transient decay curves show a double exponential behavior with characteristic time constants of 1.4 ± 0.7 ps and 21 ± 7 ps.

1. Torrance, J. B.; Scott, B. A.; Welber, B.; Kaufman, F. B.; Seiden, P. E.; *Physical Review B*, **1979**, *19*, 730
2. R. Bozio and C. Pecile, in *Spectroscopy of Advanced Materials*, Eds. R.J.H. Clark and R.E. Hester**, 1991**, J. Wiley & Sons, Chichester

P 4.15

Squaraine dyes as powerful nonlinear absorbers in the NIR region

Elisabetta Collini1, Ilaria Fortunati1, Luca Ciaffoni1, Camilla Ferrante1, Renato Bozio1, Luca Beverina2, Alessandro Abbotto2, Giorgio A. Pagani2
1Dipartimento di Scienze Chimiche e UdR INSTM di Padova, Università di Padova, Via Marzolo 1, I-35131 Padova, Italy
2 Dipartimento di Scienze dei Materiali e Unità di Ricerca INSTM, Università di Milano-Bicocca, Via Cozzi 53, I-125 Milano, Italy

Squaraine dyes have always attracted attention for their peculiar electronic structure and for the possibility to exploit them as sensitive materials in electro-photography and as singlet oxygen sensitizers. 1,2 Furthermore these dyes are capable to give rise to various kind of aggregates, depending on the solvent or solid state matrix in which they are embedded.3
Very recently some of us have also shown that squaraine derivatives, suitably substituted with electron-withdrawing or electron-donating groups, are endowed

with extremely high two photon absorption (TPA) coefficients in the NIR region.4
In this communication we will present the linear and non linear optical characterization of a class of highly conjugated pyrrole containing squaraine dyes in solution. In particular the linear absorption and resonance Raman spectra will be presented, together with the TPA spectra. The latter have been recorded with the Z-scan technique, employing ~ 150 fs long pulses in the wavelength range 750-1100 nm, as well as the two-photon induced fluorescence technique, exciting the samples with an ultrafast laser source delivering 150 fs long pulses in the 750-900 nm range. The results show that some of these dyes are characterized by TPA cross section of the order of thousands of Göppert-Mayer (1GM = 1×10-50 cm4 photon s-1 molecule-1).
Singlet oxygen production of these molecular systems has also been investigated through luminescence experiments detecting the 1270 nm emission of singlet oxygen.

1. Law, K.Y.; Chem. Rev., **1993,** *93*, 499
2. R. Bonnet, "Chemical aspects of Photodynamic Therapy", Gordon and Breach, **2000**.
3. Chen, H.; Farahat, M. S.; Law, K. Y.; Whitten, D. G.; J. Am. Chem. Soc., **1996**, *18*, 2584.
4. a) Beverina, L.; Abbotto, A.; Landenna, M.; Cerminara, M.; Tubino, R.; Meinardi, F.; Bradamante, S.; Pagani, G.A.; *Org. Lett.* **2005**, *7(19)*, 4257-4260. b) Chung, S-J; Zheng, S.; Odani, T.; Beverina, L.; Fu, J.; Padilha, L.A.; Biesso, A.; Hales, J.M.; Zhan, X.; Schmidt, K.; Ye, A.; Zojer, E.; Barlow, S.; Hagan, D.; Van Stryland, E.; Yi, Y.; Shuai, Z.; Pagani, G.A.; Bredas, J-L; Perry, J. W.; Marder, S.R.; *J. Am. Chem. Soc.* , **2006**, *128(45)*, 14444.

P 4.16

TPA Absorption properties of octupolar metal complexes

Simone Mazzucato [1], Ilaria Fortunati [1], Sara Scolaro [1], Michele Zerbetto [1], Camilla Ferrante [1], Raffaella Signorini [1], Danilo Pedron [1], Renato Bozio [1], Danika Locatelli [2], Stefania Righetto [2], Dominique Roberto [2], Renato Ugo [2], Alessandro Abbotto [3], Graziano Archetti [3], Luca Beverina [3], Sergio Ghezzi [3]
[1]*Dipartimento di Scienze Chimiche e UdR INSTM di Padova, Università di Padova, Via Marzolo 1, I-35131 Padova, Italy*
[2] *Dipartimento di Chimica Inorganica, Metallorganica e Analitica and Centro di Eccellenza CIMAINA dell'Università di Milano, UdR INSTM di Milano, via Venezian 21, 20133 Milano, Italy.*
[3] *Dipartimento di Scienze dei Materiali e Unità di Ricerca INSTM, Università di Milano-Bicocca, Via Cozzi 53, I-125 Milano, Italy*

The second order non linear response of multipolar metal coordination compounds has been thoroughly investigated in recent time [1,2] with the aim to incorporate them in solid state matrices as active materials for photonic devices. Only in the last couple of years the third order non linear response of these complexes has also started to be investigated, since they appear to be promising candidates as multiphoton absorber in optical switches and optical limiting devices; a large multiphoton absorption cross section, coupled with a good luminescence quantum yield, is also required in the field of bio-imaging and up-converted lasing. [3,4] In this work we present an investigation of the non-linear optical (NLO) properties of two octupolar chromophores: $[Zn(4,4'\text{-bis(dibutylaminostyryl)-}[2,2']\text{-bipyridine})_3]^{2+}$ and $[Zn(4,4'\text{-bis((E)-2-(N-(TEG)pyrrol-2-yl)vinyl)-}[2,2']\text{-bipyridine})_3]^{2+}$ with Zn(II) as the coordination center, using two-photon induced fluorescence technique (TPF) in fs-pulse temporal regime. Compared to the free ligands, our results do not show a net increase in the two-photon absorption (TPA) cross-section for the octupolar complexes, once normalized to the ligand unit. This result is in partial disagreement with theoretical studies investigating the former complex where a significant increase of the TPA cross-section is predicted.[5,6]

1. Sénéchal, K.; Maury, O.; Le Bozec, H.; Ledoux I.; and Zyss, J.; *J. Am. Chem. Soc.* , **2002**, *124*, 4560.
2. Maury O.; and Le Bozec, H.; *Acc. Chem. Res.*, **2005**, *38,* 691.
3. Zheng, Q.; He G.S.; and Prasad, P.N.; *J. Mater. Chem.,* **2005**, *15*, 579.
4. Coe, B. J.; Samoc, M.; Samoc, A.; Zhu, L.; Yi Y.; and Shuai, A. Z.; *J. Phys. Chem. A*, **2007**, *111*, 472.
5. Liu, X. J.; Feng, J. K.; Ren, A. M.; Cheng, H.; and Zhou, X.; *J. Chem. Phys.,* **2004**, *120*, 11493.
6. Zhang, X-B; Feng, J-K; Ren, A-M; *J. Chem. Phys. A,* **2007**, *111,* 1328.

P 4.17

EFFECT OF GRAIN SIZE ON THE MAGNETIC PROPERTIES OF $La_{1-x}Ca_xMnO_3$ MANGANITES NANOPARTICLES

C. Castellano[1], M.R. Cimberle[2], M. Ferretti[1,3], A. Martinelli[1] and R. Masini[2]
[1]*LAMIA-INFM-CNR, Corso Perrone 24, 16152 Genova, Italy*
[2]*CNR-IMEM sezione di Genova c/o Dipartimento di Fisica, Via Dodecaneso 33, 16146 Genova, Italy*
[3]*Dipartimento di Chimica e Chimica Industriale, Universita' di Genova, Via Dodecaneso 31, 16146 Genova, Italy*

Manganites $La_{1-x}Ca_xMnO_3$ are objects of an intense study due to the complexity of their phase diagram (1). They present, as a function of the doping x, magneto-conductive phase transitions, charge ordering (CO) of the ions Mn^{3+}/Mn^{4+} in sub-lattices and above all the so-called colossal negative magnetoresistance also greater than 90 %. Only in the last years, beside theoretical models based on the double exchange mechanism and on a strong electron-phonon coupling as a Jahn-Teller polaron at high temperature ($T > T_{Curie} \approx 270$ K), several evidences of nanophase inhomogeneities at low T between a metallic-ferromagnetic component and an insulating Jahn-Teller distorted one have been obtained for $0.2<x<0.5$ (2-4). The nature of this last insulating phase is still uncertain but it is probably a CO component with a very low coherence length and then not visible by diffraction or conventional spectroscopy measurements (5). Then recent developments of research have discovered new aspects that insert the study of manganites in the context of natural or self-assembled nanostructured materials and not only in that of strongly correlated electron systems (2).

The mesoscopic and nanoscopic phase texture of manganites allows to continue to miniaturize transistors and electronic components useful for computer engineering and spintronics applications, in particular providing a potential alternative to the conventional Si lithography top-down and bottom-up syntheses techniques. This result, which goes beyond silicon limitations, should be due to the possibility to alter the magnetic and electronic structure of a manganite on a nanoscopic scale (6,7).

For these reasons we have investigated the effect of nanometric grain size on magnetic and electronic properties of different $La_{1-x}Ca_xMnO_3$ nanocrystalline samples obtained by two different techniques: high-energy ball milling and sol-gel route (Pechini process, ref. 8).

In the first case the samples were prepared by a conventional solid state reaction at high temperature and high-energy ball milling was subsequently carried out for different time.

In the second case, after calcinations of the dried gel, the oxides were submitted to various thermal treatments to obtain different grain sizes in a range of 10-30 nm.

All samples have been characterized by X-ray powder diffraction (XRD) and High Resolution Transmission Electron Microscopy (HRTEM). Electric properties have been investigated by impedance spectroscopy measurements (EIS) carried out as a function of temperature and composition of the nanostructured manganites. Magnetic properties have been investigated by means of dc and ac magnetic measurements in the temperature range 5-350 K**.**

We evidence that the grain of our samples reach dimensions also much below the values already reported in literature (about 10 nm instead of 15-20 nm (9)). Therefore we suppose that our smaller grain powders can give rise to a superparamagnetic phase when their sizes are lower than a critical threshold (9). This result is due to the gradual reduction of the grain core size respect to the non-magnetic outer grain shell and is strongly related to the spin-polarized transport of conduction electrons at the grain boundaries. The ac magnetic measurements (Fig. 1) seem to confirm this hypothesis evidencing a broadening and relevant shift of the ferromagnetic transition only in powders of smaller grain dimensions, probably due to such superparamagnetic disorder.

Moreover we observe a similar dc magnetic behaviour in Mn-substituted samples (e.g. $La_{0.25}Ca_{0.75}Mn_{0.92}Cr_{0.08}O_3$, see Fig. 2). In these samples we induce chemical defects determining a random impurity effect and therefore a disordered Jahn-Teller distortion (5). In the framework of manganites nanophase inhomogeneity this effect favours the appearance of ferromagnetic nano-clusters in the long range insulating matrix, whose magnetic behaviour is very similar to that of a superparamagnetic system, as can be deduced comparing Figs. 1 and 2.

In conclusion we suppose that both in nanometric grain powders and in manganese substituted manganites (Figs. 1 and 2 respectively) the magnetic structure is characterized by a nanometric distribution of defects that below a definite dimension threshold gives rise to superparamagnetic effects.

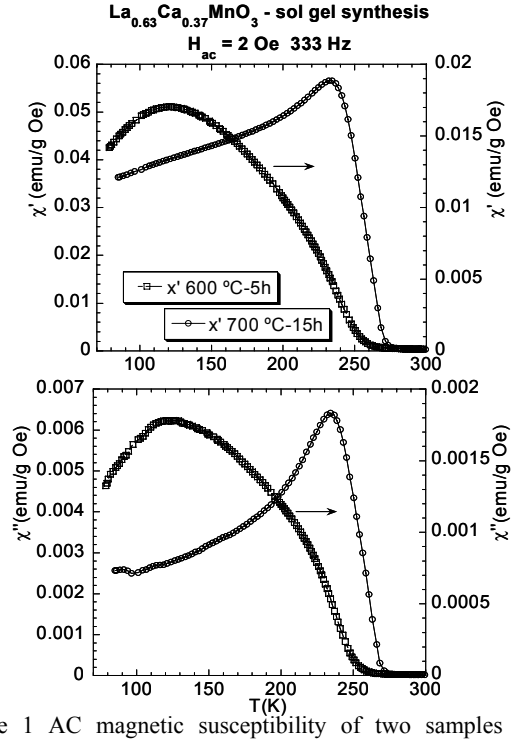

Figure 1 AC magnetic susceptibility of two samples characterized by different grain size: ~10 nm (600°C-5h) and ~30 nm (700°C-15h).

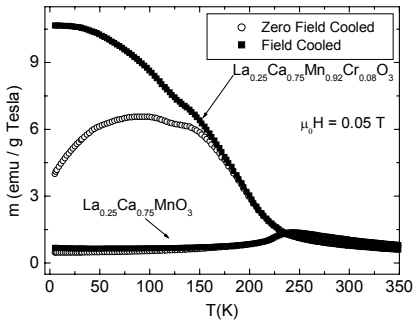

Figure 2 DC magnetic measurements of unsubstituted and Mn-substituted samples

(1) P. Schiffer *et al.*, Phys. Rev. Lett. **75**, 3336 (1995).
(2) A. Moreo, S. Yunoki, E. Dagotto, Science **283**, 2034 (1999).
(3) M. Fäth *et al.*, Science **285**, 1540 (1999).
(4) S. J. L. Billinge *et al.*, Phys. Rev. B **62**, 1203 (2000).
(5) C. Castellano *et al.*, Solid State Commun. **136**, 244 (2005).
(6) N. Mathur *et al.*, Nature Mat. **3**, 207 (2004).
(7) P. Levy *et al.*, Phys. Rev. B **65**, 140401 (2002); Hueso and Mathur, Nature **427**, 301 (2004).
(8) M. Gaudon *et al.*, Solid State Sciences **4**, 125 (2002).
(9) P. Dey *et al.*, Phys. Rev. B **73**, 214425 (2006).

P 4.18

A multi-frequency EPR study on TiO_2 colloidal nanocrystals: a closer insight on the catalytic activity

M. Fittipaldi[1], C. Sangregorio[1], D. Gatteschi[1], N. Grassi[2], M. L. Curri[3], R. Comparelli[3], M. Striccoli[3], A. Agostiano[3,4]

[1]*INSTM - Dipartimento di Chimica, Università di Firenze, via della Lastruccia 5, 50019 Sesto Fiorentino, Italy*

[2]-INFN sezione di Firenze, via B. Rossi 1, 50019 Sesto Fiorentino (FI)
[3]CNR-IPCF Sez. Bari c/o Dipartimento di Chimica, Università di Bari, via Orabona 4, 70126 Bari, (Italy)
4Dipartimento di Chimica, Università di Bari, via Orabona 4, 70126 Bari, (Italy); maria.fittipaldi.unifi.it

TiO_2 nanocrystals (NCs) have attracted much attention due to their remarkable photocatalytical activity [1]. It has been widely demonstrated the dependence of the catalytic activity of TiO_2 NCs on the synthetic route and, accordingly on the surface chemical status [2]. For this purpose a deeper characterization has been carried out on the TiO_2 NCs by means of a multifrequency EPR study, in order to achieve a deeper understanding of the catalytic systems. Here, we report on EPR measurements performed at X-band (9 GHz), Q-band (35 GHz), and W-band (95 GHz) at various temperatures with and without UV irradiation. Differently shaped NCs, nanorods (NRs) or nanodots (NDs), obtained by using two distinct synthetic routes, namely hydrolytic and non.hydrolytic and carrying diverse capping molecules at the surface, oleic acid (h-TiO_2) and TOPO (nh- TiO_2), respectively, have been investigated in order to evaluate a possible relation between the structural properties and the specific catalytic activity of the NCs. The EPR study presented, carried out by using a multi frequency approach, has demonstrated to be an extremely valuable tool for the elucidation of the structural properties of the investigated systems. At low temperature, UV excitation of this semiconductor promotes electrons from the valence band to the conduction band. The generated electrons in the conduction band, as well as the holes in the valence band, can be trapped either at the Ti sites or at the surface oxygen sites, giving rise to paramagnetic species that are detectable by EPR. The EPR spectra enable the identification of the different sites at which the charges are trapped.
Moreover, an extensive elemental analysis has been performed on the NC samples by using Particle Induced X-ray Emission (PIXE) analysis. Such measurements have allowed to carefully characterize, either qualitatively and quantitatively, the composition of the amount of purity of the samples. The obtained results well agree with the picture that comes out form the EPR investigation, providing useful insight for the elucidation of the (photo)catalytic behaviour of the systems.
[1] O. Carp, Progress in Solid State Chemistry (2004) 32, 33.
[2] R. Comparelli, E. Fanizza, M. L. Curri, P. D. Cozzoli, G. Mascolo, R. Passino, Agostiano Applied Catalysis B: Environmental (2005) 55, 81.

Acknowlegment
This work was financially supported by the EC-funded Project NOVOPOLY (Contract no. STRP 013619) and MIUR.

P 4.19

Correlation between transport properties and lattice effects in the $NdCoO_3$ based catalysts and sensor materials

G. Flor[a], C. Tealdi[a], L. Malavasi [a], F. Gozzo[b], G. Chiodelli[c]
[a]Dipartimento di Chimica Fisica "M.Rolla", Università di Pavia, Viale Taramelli 16, 27100 Pavia, Italia, flor@unipv.it
[b]Paul Scherrer Institute, Swiss Light Source, 5232 Villigen PSI, Switzerland
[c]CNR - IENI Sede di Pavia, Viale Taramelli 16, 27100 Pavia, Italia

Rare earth cobaltates of general formula $Ln_{1-x}A_xCoO_3$ (Ln = rare earth, A=alkaline or alkaline earth metal) show interesting structural, magnetic and transport properties, which are sensitive to the average ionic radius of the A-site cations and are closely related to the availability of different oxidation and spin states for the Co ion.
The research interest in cobalt containing oxides ranges over a wide variety of fields, from sensor devices and catalysts that oxidize CO and CH_4 or reduce NO [1,2] to components in solid oxide fuel cells [3], from the unusual thermoelectric behaviour [4,5] to the peculiar magnetic properties [6], up to the latest discovery of superconductivity in layered systems such as $Na_{0.3}CoO_2{\cdot}1.3H_2O$ [7].
In this study we aimed at clarifying the effect of aliovalent cation doping on the structural and transport properties of $NdCoO_3$ as a function of temperature by covering a temperature range of applicative interest for catalyst and sensor activity, i.e. the high-temperature region.
A previous computational study on the effect of aliovalent doping in $NdCoO_3$ has pointed out that on the Nd site, Ca^{2+} and Sr^{2+} are predicted to be the most favourable dopants; for alkaline earths, the solution energies strongly depend on the dopant size and Na is in this case the most favourable dopant.[8] Therefore, powder samples of composition $NdCoO_3$, $Nd_{0.9}Na_{0.1}CoO_3$ and $Nd_{0.8}Ca_{0.2}CoO_3$ were prepared by conventional solid state reaction. The amount of the two dopant ions has been chosen in order to ensure the same oxygen vacancies concentration for the two compositions, in agreement with the different oxidation state of the aliovalent dopants.
Neutron and x-ray powder diffraction data have been combined to carefully determine lattice constants and atomic positions while four probe direct current conductivity and thermoelectric power measurements allowed us to follow the thermal evolution of the transport properties of these compounds.
The dramatic improvement of the room temperature conductivity of $Nd_{0.8}Ca_{0.2}CoO_3$ with respect to the pure and the Na-doped compound is explained in terms of a different spin-state for the Co ions within this structure. The experimental data and the Co environment analysis here discussed, in particular bond lengths distortion and bending angles, are fully consistent with a spin state (low to intermediate) transition in $NdCoO_3$. The higher conductivity and the absence of anomalies in the thermal expansion makes the Ca-doped compound more attractive than the pure $NdCoO_3$ in view of possible applications.

1. L. Forni, I. Rossetti, *Appl. Catal. B* **2002**, *38*, 29.
2. L. Malavasi, C. Tealdi, G. Flor, G. Chiodelli, V. Cervetto, A. Montenero, M. Borella, *Sens. Actuators* B **2005**, *105*, 407.
3. B.C.H. Steele, *Solid State Ionics* **1996**, *86-88*, 1223.
4. A. Maignan, D. Flahaut, S. Hebert, *Eur. Phys. J. B* **2004**, *39*, 145.
5. R. Robert, S. Romer, A. Reller, A. Weidenkaff, *Adv. Eng. Mater.* **2005**, *7*, 303.
6. J. Androulakis, P. Migiakis, J. Giapintzakis, *Appl. Phys. Lett.* **2004**, *84*, 1099.
7. K. Takada, H. Sakurai, E. Takyama-Mutomachi, F. Izumi, R.D. Dilanian, T. Sasaki, *Nature*, **2003**, *422*, 53.

8. C. Tealdi, L. Malavasi, C.A. J. Fisher, M. S. Islam, *J. Phys. Chem. B* **2006,** *110,* 5395.

1. Farkye N. Y.; *International J. Dairy Technology* , **2004**, *57, (2-3)*, 91.
2. Hu et al., *Biotechnol. J.*, **2006**, *1,* 75.
3. Hearn et al., *J. Biochem. Biophys. Methods,* **1996**, *31,* 165.

P 4.20

Challenges In Biocatalysis: Immobilization Of Porcine Pepsin In Mesoporous Silicas

Haresh G. Manyar[a]*, Simonetta Tumbiolo[a,b], Enrica Gianotti[a], Salvatore Coluccia[a], Osamu Terasaki[b]
[a]*Dipartimento di Chimica IFM and NIS - Centre of Excellence, University of Torino, via P. Giuria 7, 10125 Torino, Italy . E-mail: hareshmanyar@rediffmail.com*
[b]*Structural Chemistry, Arrhenius Laboratory, Stockholm University, S-10691 Stockholm, Sweden*

Pepsin, an acidic protease has high commercial importance in cheese manufacture from milk with global sales value of cheese amounting to 34000 US $ per annum [1]. There have been many attempts to immobilise pepsin however its bulky nature hinders its diffusion inside the porous systems, and hence its fixation is restricted to covalent binding on synthetic and natural polymers and inorganic oxides. In this regard large pore mesoporous silica molecular sieves are highly favoured materials due to their high surface area and well defined pore geometry. We herein report a successful, simple and convenient methodology for encapsulation of Porcine Pepsin into the pure silica MCM-41 and SBA-15 by physical adsorption. MCM-41 and SBA-15 were chosen as suitable hosts because their channel-pores with uniform diameter are arranged in the two dimensional hexagonal p6mm symmetry. The enzyme amount that can bind to these mesoporous supports (94 mg/g for MCM-41 and 169 mg/g for SBA-15) is much higher than for other inorganic supports [2,3]. Pepsin adsorption followed Langmuir adsorption isotherm. The maximum equilibrium adsorption amount of Pepsin into SBA-15 mesopores is ≈ 179 mg/g and maximum equilibrium adsorption amount of Pepsin into MCM-41 mesopores is ≈ 119 mg/g. The dissociation constant values for Pepsin/SBA-15 (0.48) and Pepsin/MCM-41 (0.28) indicate fairly strong interaction of Pepsin with the surface. The hybrid materials were subsequently modified by functionalisation with Aminopropyl Triethoxy Silane (APTES) to encapsulate the Pepsin inside the mesopores. This functionalisation has reduced the diameter of the pore, preventing the loss of enzyme from the surface in the reaction medium.

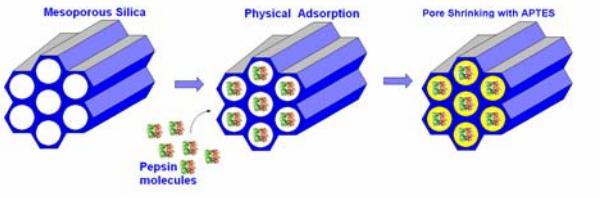

The hybrid materials were characterised by XRD, TEM, Volumetric (N_2 sorption), FT-IR and DR-UV-Vis techniques. The physico-chemical characterization of these materials has confirmed the presence of the pepsin inside the pores of the inorganic materials. The catalytic activity of Pepsin/MCM-41 and Pepsin/SBA-15 was evaluated by peptic hydrolysis of a dipeptide, Z-L-glutamyl-L-tyrosine. The immobilized pepsin exhibited high catalytic activity in hydrolysis of Z-L-glutamyl-L-tyrosine.

P 4.21

Luminescent nanocrystal modified epoxy photoresist for the fabrication of 3-D high aspect-ratio microstructures

C. Ingrosso[1], V. Fakhfouri[2], M. Striccoli[3],A. Voigt[4], G. Gruetzner[4], M. L. Curri[3], J. Brugger[2]
[1]*Dipartimento di Chimica, Università di Bari, via Orabona 4, 70126 Bari, (Italy)*
[2]*Microsystems Laboratory, Ecole Polytechnique Fédérale de Lausanne (EPFL), Station 17, CH-1015 Lausanne, Switzerland.*
[3]*CNR-IPCF Sez. Bari c/o Dipartimento di Chimica, Università di Bari, via Orabona 4, 70126 Bari, (Italy)*
[4]*Micro resist technology GmbH, Koepenicker Str. 235, Haus 2111, 12555 Berlin Germany*
E-mail: lucia.curri@ba.ipcf.cnr.it

Recently many efforts have been directed towards the fabrication of nanocomposite materials based on an organic matrix combined with nanometer sized inorganic nanoparticles, due to its high impact to transfer the unique size dependent properties of the nanoparticles into highly processable materials.[1] Specific electrical, magnetic, mechanical, chemical and optical properties can be thus added to the organic moiety, preserving at the same time its intrinsic properties.[2] Epoxy based photo-resists are excellent candidates for novel composite materials, since they possess superior lithographic properties. This class of materials can provide homogeneous layers over a wide range of thicknesses and patterns having structures with high aspect-ratio and nearly vertical sidewalls can be obtained by using standard near ultra violet (UV) optical lithography. In the past, this class of photosensitive materials have revolutionized the manufacturing of Microsystems,[3] while later they have been used for micromechanical applications and microsystems as microfluidic systems,[4] packaging,[5] scanning probes,[6] and, thanks to the convenient optical properties, for optical waveguides[7] and near-field optical probes.[8] At present, one of the key points in these materials comes from the lack of any inherent complex functionality; hence the current challenge is to add new properties to the photo-resist matrix by means of nanocrystals (NCs) maintaining the structurability of the photosensitive resist by UV lithography. In this perspective, only few examples are reported in literature on the use of nanoparticle modified photostructurable composites.[9-16]
Several routes can be followed for the preparation of a NC based polymer nanocomposite. For instance the choice of a suitable ligand for NCs can ensure a proper interaction between NCs and the host matrix and consequently a homogeneous dispersion. Alternatively the organic component can be properly functionalized with suitable chemical groups, which enable an effective interface with nanoparticles.[17]
Luminescent nanocrystals (NCs) have a great potential as single photon sources and lasers and may be implemented in integrated optical devices.[18] Such NCs have also numerous advantages, such as controlled size-dependent electronic and optical properties, large optical gain, intense fluorescence ompared with other visible

fluorophores, i.e. organic dyes, and immunity from photobleaching.
Our approach has generally intended to handle NCs and host polymer (photoresist etc.) as separate entities, being the nanocomposite preparation decoupled from the "ex situ" NC synthesis very flexible and prone to be largely customized. Such scheme allows also a wider choice of the two components, since: i) on one side a wide range of high quality NCs can be afforded by using the more advanced synthetic routes to carefully control size and size dispersion, ii) the same flexibility can be attained on the definition of type and formulation of the host polymer composition. This procedure appears to be very convenient in the case of photostructurable composites, which could be influenced by chemical modification procedures of the photosensitive moiety, or by the specific reactivity of the NC surface toward the host environment both resulting detrimental for the final structurability of the material.
We present a novel approach to further advance this field by combining light emitting NCs with a negative tone photosensitive epoxy based resist. Colloidal methods have been used to synthesize luminescent cadmium selenide NCs with tuneable size coated by a shell of zinc sulfide (CdSe@ZnS) exhibiting size-dependent optoelectronic properties. In this work the NC incorporation relies on the selection of a common solvent able to safely disperse pre-synthesized organic capped nanoparticles into the host photoresist. The media used for dispersion have been demonstrated to play a significant role on the photoluminescent (PL) efficiency of emitting NCs, in addition to the synthetic parameters.[19] A combined effort has been made both on the resist formulation and on the NC solubility investigation, in order to define such solvent effective for the single resist component and to enable a homogeneous dispersion of the NCs in the final photoresist formulation. The original spectroscopic characteristics of the obtained composite material have been studied as a function of the solvent characteristics and described in terms of physical interaction with the solvent itself. Then, films of NC modified photoresist have been patterned and the overall UV-structuring capability of the final material has been demonstrated. The preservation of the NC distinctive optical properties of the fabricated microstructured patterns has been finally confirmed. The morphology of the patterned structures have been also investigated and compared with those of the unmodified photoresist. Finally, the presented results open new perspectives toward the micro/nano patterning of original functionalized photosensitive materials tailored for the fabrication of highly integrated, functional MEMS/NEMS with inherent photonic characteristics and activities.

Acknowlegment
This work was financially supported by the EC-funded Project NOVOPOLY (Contract no. STRP 013619).

1. Balazs, A. C.; Emrick, T.; Russell, T. P.; *Science* **2006**, *314*, 1107. 2. Kickelbick, G.; *Prog. Polym. Sci*. **2003**, *28*, 83. 3. McDonald, S. A.; Cyr, P. W; Levina, L.;. Sargent, E. H; *Appl. Phys. Lett*. **2005**, *85*, 2089. 4. Jenke, M.G.; Schreiter, C.; Kim, G.M.; Vogel, H.; Brugger, J.; *Microfluidics and Nanofluidics* **2006** published on line. 5. Krassow, H.; Campabadal, F.; Lora-Tamayo, E.; *Sen. and Act., A: Physical* **2000**, *82*, 229. 6. Genolet, G.; Brugger, J.; Despont, M.; Drechsler, U.; Vettiger, P.; de Rooij, N. F.; Anselmetti, D.; *Rev. Sci. Instr.* **1999**, *70*, 2398. 7. Kim, J.-S.; Kang, J.-W.;. Kim, J.-J; *Jap. J. Appl. Phys*. **2003**, *42*, 1277. 8. Kim, G. M.; Kim, B. J.;. Ten Have, E. S.; Segerink, F.; Van Hulst, N. F.; Brugger, J.; *J. Microscopy-Oxford,* **2003**, *209*, 267. 9. Wiche, G.; Goettert, J.;. Song, Y; Hormes, J.; Kumar, C. S. S. R.; *Int. J. Comput. Eng Sci.* **2003**, *4*, 525. 10. Zhang, N.; Xie, J.; Guers, M.; Varadan, V. K.; *Smart Mater. Struct*. **2003**, *12*, 260. 11. Damean, N.; Parviz, B. A.; Lee, J. N.; Odom, T.; Whitesides, G. M.; *J. Micromech. Microeng.* **2005**, *15*, 29. 12. Jiguet, S.;. Bertsch, A; Hofmann, H.; Renaud, P.; *Adv. Func. Mater.* **2005**, *15*, 1511. 13. Jiguet, S.; Bertsch, A.; Hofmann, H.; Renaud, P.; *Adv. Eng. Mater.* **2004**, *6*, 719. 14. Xu, X.; Thwe, M.; Shearwood, C; Liao, K; *Appl. Phys. Lett.* **2002**, *81*, 2833. 15. Cho, J. - D.; Ju, H.- T.; Park, Y. –S.; Hong, J.-W.; *Macromol. Mater. Eng.* **2006**, *291*,1155. 15. Jiguet, S.; Bertsch, A.; Hofmann, H.; Renaud, P.; *Adv. Eng. Mater,* **2004**, *6*, 719. 16. Liu, H.; Edel, J. B.; Bellan, L. M.; Craighead, H. G.; *Small* **2006**, *4,* 495. 17. Thang, Z.; Kotov, N. A.; *Adv. Mater.* **2005,***17*, 951. 18. Zhang, C. L.; Xu, T.; Butterfield, D.; Misner, M. J.; Ryu, D. Y.; Emrick, T.; Russel, T. P.; *Nano Letter* **2005**, *5*, 357. 19. Cui, Y.; Bjork, M.; Liddle, A.; Sonnichsen, C.; Boussert, B.; Alivisatos, P.; *Nano Letter* **2004**, *4*, 1093. 20. Zhou, D. J.; Bruckbauer, A.; Abell, C.; Klenerman, D.; Kang, D.; *J. Adv. Mater.* **2005**, *17*, 1243. 17. Potapova, I.; Mruk, R.; Prehl, S.;. Zentel, R; Baschè, T.; Mews, A.; *J. Am. Chem. Soc.* **2003**, *125*, 320. 18 Eisler, H. J.; Sundar, V. C.; Bawendi, M. G.; Walsh, M.; Smith, H. I.; Klimov, V.; *Appl. Phys. Lett.* **2002**, *80*, 4614. 19 Klimov, V. I.; McBranch, D. W.; Leatherdale, C. A.; Bawendi, M. G.; *Phys. Rev. B* **1999**, *60*, 13740.

P 4.22

Characterization of nanocrystalline semiconductor/metal phthalocyanine hybrid junctions and applications as photoconverter and sensor devices

C. Ingrosso[1], P. Cosma[1,2], P. Fini[2], M. L. Curri[2], G. Giancane[3], L. Valli[3], A. Agostiano[1,2]
[1]*Dip. di Chimica, Univ. di Bari, via Orabona 4 I-70126 Bari, (Italy)*
[2]*CNR IPCF - Sez Bari c/o Dip. di Chimica, Univ. di Bari, via Orabona 4 I-70126 Bari, (Italy).*
[3]*Dip. di Scienza dei Materiali, Univ. di Lecce, via Arnesano 1, 73100 Lecce, (Italy; agostiano@chimica.uniba.it*

In the last decade hybrid junctions formed of thin films of organic molecules and inorganic nanometer-sized semiconductors have been considered appealing frameworks due to the fruitful combination of the peculiar intrinsic properties of both materials that can be exploited in a wide range of applications such as light energy conversion and sensor devices. Phathalocyanines (Pcs) and Metal Phthalocyanines (M(II)Pcs) are promising materials, as the suitable designing of their aromatic macrocycle leads to numerous and different outstanding optical, chemical, electrochemical and semiconducting properties, which can be widely exploited in the transduction processes for sensors[1] and utilized in the sensitization processes of photoconversion devices. Indeed, the incorporation and the modification of the metal ion at the centre of the macroring and/or the peripheral groups[2-4] can result in the modulation of the spectroscopic properties, improving their performance as sensitizers, and in the modification of the sensibility and selectivity of the Pc based active layers towards several analites. Further, these powerful peculiarities and the high chemical and thermal stability, make Pcs appealing materials not only for energy conversion and sensor devices but also for a wide range of applications in which Pcs are involved as catalyst, optical data storage component[5], photoactive material for the photodynamic therapy, photo-sterilizing of blood[6] optical limiting substance[7], non linear optical material[8], active photoreceptor in laser printing system[9] as light emitting

material[10] and CD-R dye[11]. Conversely, inorganic colloidal oxide nanocrystalline (NC) semiconductors are good candidates for energy conversion and sensing applications due to the peculiar properties which exhibit in nanoscopic regime size as the large surface-to-volume ratio that results in a wide superficial area which improve the interactions between the surface atoms and the environment and in very efficient charge transfer processes. Further, colloidal chemistry routes offer the possibility to synthesized on large scale NC materials tuning effectively their morphology, size and size distribution affecting as well the porosity, the structural stability and the topography of the related NC- based films, being the latter fundamental for the charge transfer efficiency, sensitivity and reproducibility of the manifold interaction-based processes. Finally, colloidal methods allow to obtain organic NC solutions easily processable as thin films with handy solution-based deposition techniques. NC materials can thus be relevant for wide areas of applications, ranging from energy conversion to photocatalysis [12,13], and as active layer for sensor devices, as functional materials in electro- and photocromic devices, light emitting diodes and intercalation batteries [14].

Single component-based devices, typically present limited performances and the conjunction of both materials in hybrid junctions will offer the possibility to overcome these drawbacks due to the efficient charge transfer processes occurring at the organic/inorganic interfaces. Thus, the NC peculiar properties such as the size tuneable band gap when properly synthesized in quantum confinement regime[15,16], and the convenient engineering of Pc counterpart, provide the opportunity to optimize the energy level mismatch[17,18], thus improving the efficiencies of the charge exchange processes which can occur in photoconverter and sensor devices.

In this work an extensive chemical physical characterization of the D_{4h} MPcs, zinc phthalocyanine (Zn(II)Pc), magnesium phthalocyanine (Mg(II)Pc) and tetrakis-(isopropoxy-carbonyl)-copper-phthalocyanine (TIPCu(II)Pc) and of the related hybrid junctions formed of ZnO and TiO_2 NCs is presented. UV-vis spectroscopic techniques have been used to widely characterize MPcs in organic solvents as $CHCl_3$, Py, DMSO and DMF. The study reveals as the different chemical structure affects the MPc solubility as well as their aggregation tendency and shows as the different centre metal atom strongly effects the MPc spectroscopic response. Advanced deposition technique as Langmuir-Blodgett has been used to deposit highly ordered films of the $CHCl_3$ soluble TIPCu(II)Pc and its behaviour at the air/water interface has been analyzed on the basis of the Langmuir theory and monitored by Brewsted Angle Microscopy (BAM).

A wide spectroscopic and topographic characterization has been conducted also on thin films of both the bare MPcs and of the related hybrid junctions by means ATR and AFM investigations. The morphologies of the bare phthalocyanine films has been found to be strongly affected by the solvent, temperature and concentration, while that of the corresponding hybrid films is only defined by the topography of the oxide NC semiconductor film. Finally, the efficiency of the hybrid systems has been studied both when they integrated in photoelectrochemical cells and in sensor devices. The study shows that the performances are strongly affected by the temperature treatment of the films, by the solvent, by the shape and nature of the NC oxide and by the concentration of both the NC oxide and MPc.

1. Valli, L.; *Advance in Colloid and Interface Science*, **2005**, *116*, 13. 2. Wróbel, D.; Boguta, A.; *J. Photochem. Photob. A: Chem.* **2002**,*150*, 67. 3. Wróbel, D.; Goc, J.; Ion, R. M.; *J. Mol. Struct.* **1998**, *450,* 239. 4. Wróbel, D.; Boguta, A.; Ion, R. M.; *J. Mol. Struct.* **2001**, *595*, 127. 5. Ferraudi, G.; In Phthalocyanines, Properties and Applications; Leznoff C.C.; Lever A.B.P., Eds.; VCH: New York, **1989**, *1*, p.291. 6. Sharman, W. H.; Allen, S. M.; van Lier, J. E; In *Methods in Enzymology*; Packer L., Sies. 7. Qu, S.; Gao, Y.; Zhao, C.; Wang, Y.; Fu, S.; Song, Y.; Wang, D.; Qiu, J.; Zhu, C.; *Chem. Phys. Lett*. **2003**, *367*, 767. 8. Nordwood, R. A.; Sounik, J. R.; *Appl. Phys. Letter* **1992**, *60*, 295. 9. Mizuguchi, J.; Rihs, G.; Karfunkel, H. R.; *J. Phys. Chem.* **1995**, *99*, 16217. 10. Fujii, A.; Yoshida, M.; Ohmori, Y.; Yoshino, K.; *Jpn. J. Appl. Phys.* **1996**, *35*, L37. 11. Namba, N; In *Phthalocyanine-Chemistry and Functions*; Shirai Y., Kobayashi N., Eds.; IPC: Tokyo, **1997**, p.247. 12. Cozzoli P.D.; Comparelli R.; Fanizza E.; Curri M.L.; Agostiano A.; Laub D.; *J. Am. Chem. Soc.* **2004**, *126*, 3868. 13. Wrobel D.; Goc J.; Ion R.M.; *J. Mol. Struct.* **1998**, *450*, 239. 14. Grätzel M., in: Kamat P.V., Meisel D. (Eds.), *Semiconductor Nanoclusters—Physical, Chemical, and Catalytic Aspects*, Elsevier Science B.V., Amsterdam, **1997**, p. 353. 15 Alivisatos, A.P.; *J. Phys. Chem*. **1996**, *100*, 13226. 16. Alivisatos, A.P.; *Science* **1996**, *271*, 933. 17 Grem, G.; Leitzky, G.; Ullrich, B.; Leising, G.; *Adv. Mater*. **1992**, *4*, 36. 18. Greenham, N. C.; Moratti, S. C.; Bradley, D. D.; Friend, R.; Holmes, A. B.; *Nature* **1993**, *365*, 628

P 4.23

Modification of UHMWPE processed by laser ion implantation

A. Lorusso[1], F. Paladini[2], L. Velardi[1], D. Margarone[3], N. Campo[4], L. Torrisi[3], V. Nassisi[1]

[1]*Laboratorio di Elettronica Applicata e Strumentazione, LEAS, Department of Physics, University of Salento & INFN - Lecce, Via Provinciale Lecce-Monteroni, 73100 Lecce – Italy Tel. +39 0832 297495, Fax. +39 0832 297482, E-Mail: vincenzo.nassisi@le.infn.it*

[2]*Laboratorio di Dinamica Nonlineare, NDL, Department of Physics, University of Salento, Via Provinciale Lecce-Monteroni, 73100, Lecce-Italy*

[3]*Department of Physics, University of Messina; Ctr. Papardo 31, 98166 S. Agata, Messina-Italy*

[4]*Dip.to Di Chimica Ind. E Ing. Dei Materiali, Università di Messina, Ctr. Di Dio, 98166 S. Agata-Messina-Italy*

ABSTRACT

Ultra-high-molecular-weight-polyethylene (UHMWPE) is nowadays utilized in many fields, such as bio-medicine, engineering and microelectronics due its excellent chemical and physical properties.

In medicine, for instance, UHMWPE is employed in many prosthesis devices for its high degree of homogeneity, high mechanical stability and good elastic properties similar to the hard tissue and the bone[1]. Nevertheless, UHMWPE suffers serious alterations especially when it is submitted to high mechanical dynamical stresses, to high temperature and to high corrosive environment. Special attention is voted to the UHMWPE wear as a result of friction against hard surfaces at body temperature typically for polyethylene employed in many mobile prosthesis.

Ion implantation is a good tool to modify the surface characteristics of the polymer in order to reduce the friction wear increasing the whole device lifetime.

In this work, an improvement of the wear resistance of UHMWPE is attempted by using a new ion implantation technique induced by laser-generated plasma at high ion dose.

The "implantation machine" consists of a KrF excimer laser operating at 248 nm wavelength (5 eV photon

energy) and a vacuum chamber made of stainless steel. The laser power density was of $3.5 \cdot 10^8$ W/cm^2 which was able to produced a very high density plasma characterized by ions, electrons and neutral particles. Applying an accelerating voltage, ions with a current density of the order of 10 mA/cm^2 were extracted and accelerated up to 40 kV and implanted onto UHMWPE substrates[2,3].
Polyethylene modifications were obtained in the first superficial layers (up to few hundreds nanometres) by implanting ions of carbon or titanium at a particle fluence of the order of 10^{11} ions/cm^2 per pulse. The implantation was carried out applying some thousands of laser shots at a low repetition rate, ranging from 0.1 to 1 Hz. This low rate value was indispensable to avoid arcs in the plasma.
Our preliminary results showed the surface property modifications of UHMWPE after ion implantation. The surface micro-hardness analysis was performed by applying the "scratch test" method. The SEM photos of Fig. 1 show a typical example of the test performed on the implanted and no-implanted UHMWPE. The resulting scratch width is about 50 µm for the implanted sample (red area of Fig 1a), i.e. 80% lower than that one obtained for no-implanted sample as shown the red area reported in Fig. 1b. Therefore, the smaller scratch indicates a lower tip deep in the sample surface, i.e. that a little increment of the surface hardness occurred in the implanted samples.

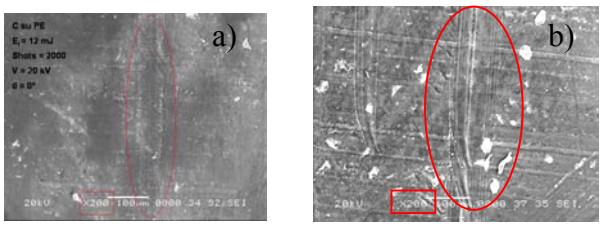

Figure 1: SEM photos for scratch test. a)UHMWPE implanted by C ions; b) no-implanted UHMWPE.

Furthermore, preliminary results have been obtained about the wettability modifications of the polymer after ion implantation. The wettability test was performed by the contact angle measurement. The Fig. 2 shows two examples of contact angle measurements. The Fig 2a) shows the wettability test performed on the surface of the no-implanted UHMWPE, while the Fig. 2b) shows the wettability test made on the surface of UHMWPE sample implanted by Ti ions. The ion implantation modified the contact angle value reporting the values of 96° and of 88.5° for no-implanted sample and for the implanted one, respectively. This result induces to conclude that the processed samples were characterized by an improvement of hydrophilicity respect to no-processed ones.

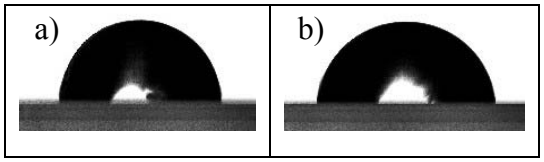

Figure 2: wettability test a) no-implanted UHMWPE; b) UHMWPE sample implanted by Ti ions with 6000 laser shots.

1. L. Torrisi, A. Visco and N. Campo, *Bio-Medical Mater. and Engeneering*, **2004** , *14*, 251.
2. F. Belloni, D. Doria, A. Lorusso, V. Nassisi, L. Torrisi, L. Calcagnile, G. Quarta, D. Bleiner and D. Manno, *Nucl. Instrum. Meth. B* **2005,** *240*, 36.
3. A. Lorusso, J. Krasa, K. Rohlena, V. Nassisi, F. Belloni and D. Doria, *Appl. Phys. Lett.* **2005,** *86*, 081501.

P 4.24

Structure, orientational order and dynamics of HAB by ^{2}H and ^{13}C NMR spectroscopy and DFT calculations

Alberto Marini[1,2], Lucia Calucci[3], Marco Geppi[1], Carlo Alberto Veracini[1]
[1] *Dipartimento di Chimica e Chimica Industriale, Università di Pisa, Via Risorgimento 35, 56126 Pisa, Italy*
[2] *Scuola Normale Superiore di Pisa, Piazza dei Cavalieri 12, 56126 Pisa, Italy*
[3] *Istituto per i Processi Chimico-Fisici del CNR, via G. Moruzzi 1, 56124, Pisa, Italy*

Structural, orientational order properties and dynamics of 4,4'-heptylazoxybenzene (**HAB)** were critically re-investigated in its nematic and smectic A phases combining ^{2}H and ^{13}C NMR techniques, as well as theoretical DFT calculations. To this aim, two isotopomers, **HAB-D$_4$** and **HAB-D$_8$**, partially and fully deuterated on the phenyl rings, respectively, were also studied.

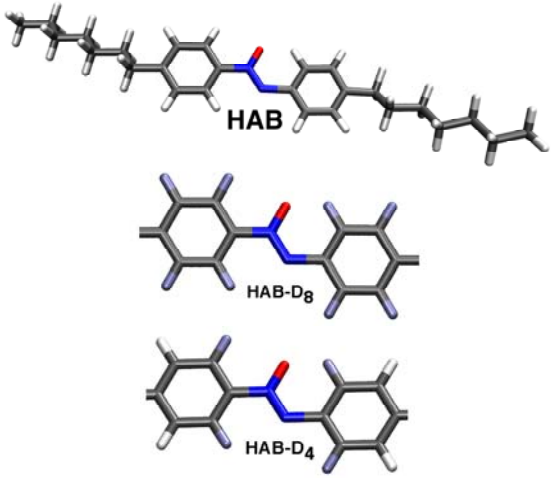

^{13}C-{^{1}H} NMR static spectra were recorded on **HAB** by means of the Linear-Ramped Cross-Polarization technique, under SPINAL-64 decoupling[1] in the whole mesomorphic range. ^{13}C resonances were assigned with the help of solution state spectra and DFT calculations performed using Gaussian'03[2]. Chemical shift anisotropy (CSA) trends with temperature were obtained for all of the chemically distinguishable carbons. Moreover, deuterium quadrupolar and dipolar (deuterium-proton) splittings were determined from ^{2}H NMR quadrupolar echo spectra, recorded on **HAB-D$_4$** at different temperatures within the mesophases. ^{13}C and ^{2}H data were used to determine the complete order matrix and the angle between the *para* axes of the **HAB** phenyl rings through a non-linear least-squares global-fitting procedure, in which geometrical parameters and ^{13}C shielding tensors calculated at the DFT level of theory (B3LYP/6-31G(d) and MPW1PW91/6-311+G(d,p) combination of hybrid functional and basis set; Gauge-Including Atomic Orbitals, GIAO method[3]) were employed. The results were discussed in comparison with those previously obtained from deuterium data only[4].
^{13}C spin-lattice relaxation times (T_1) were determined for all three compounds throughout the liquid-crystalline phases. The combined analysis of these data with the already available deuterium relaxation times[5] allowed detailed information to be obtained on **HAB** reorientational dynamics in the mesophases.

1. Fung, B. M.; *J. Magn. Reson.* 86, 160, **2005**.
2. Gaussian 03, Revision B.05. Frisch, M.J.; et al., Gaussian, Inc., Pittsburgh PA, **2003**.
3. Ditchfield, R.; *Mol. Phys.* 27, 789, **1974**.
4. Catalano, D.; Forte, C.; Veracini, C.A.; Emsley, J. W.; Shilstone, G. N.; *Liq. Cryst.* 2, 345, **1987**.
5. Domenici, V. Czub, J.; Geppi, M.; Gestblom, B.; Urban, S.; Veracini,C. A.; *Liq. Cryst.* 31, 91, **2004**.

P 4.25

Surface structure of nanohydroxyapatite: effects on water and protein adsorption

Luca Bertinetti, Raffaella Ceschino, Gabriele Alberto, Daniele Bollati, Gianmario Martra
Department of Chemistry IFM, NIS Center of Excellence , Università di Torino, via P.Giuria 7, 10125 Torino, Italy, gianmario.martra@unito.it

Introduction. The key role of the surface features of biomaterials has been recognized, leading to the definition, at the beginning of 2000's of the concept of "biological/biomedical" surface science [1,2] The unravelling of the ensemble of surface processes and phenomena actually occurring in vivo is still a challenge, but there is a general consensus in setting the causal sequence: i) biomaterial surface structure, ii) states of adsorbed water molecules and iii) states of adsorbed proteins, that then rule the fate of the interaction of the implant with cells.

On such a basis, we investigated the effect of the modification of the surface features of nanosized, biomimetic hydroxyapatite (HA) materials by i) partial exchange of Ca^{2+} with Mg^{2+}, ii) outgassing at 300 °C, that produces significant changes in the HA surface structure [3] on the interaction with water and a model protein, namely BSA.

Experimental. HA nanoparticles were obtained as the precipitate produced by: i) dropping a H_3PO_4 solution in a $Ca(OH)_2$ aqueous dispersion (material hereafter indicated as HA-A), and ii) by mixing solutions of $Ca(NO_3)_2$ and $(NH_4)_2HPO_4$ (material hereafter indicated as HA-B). Mg^{2+} ions were introduced in aliquots of HA-B by ion-exchange, performed by soaking them in 0.1M and 0.5M $MgCl_2$ solutions (samples HA-B/0.1 and HA-B/0.5, respectively). BSA absorption was carried out by suspending HA-A at 37 °C in protein solutions of due concentration, obtained by dissolving BSA in a phosphate buffer (pH= 7.4).

A multi-technique approached was used. Investigation down to a subnanometric level of the surface structure and morphology of the materials was carried out by UHR-TEM (Jeol EX4000 and 3010). Insights on states of adsorbed water were obtained by Mid- (transmission) and Near IR (diffuse reflectance, DR) spectra of samples kept in atmosphere with controlled levels of water vapour pressure. Quantitative aspects of protein adsorption on HA-A were evaluated by measuring (via UV spectroscopy) the decrease of the BSA concentration in solutions where the samples were suspended. NIR (DR mode) and MIR (ATR mode) spectroscopy were also used for the study of surface water-protein interactions and structural features of adsorbed BSA, respectively.

Results and discussion. HRTEM data indicated that both HA-A and HA-B materials were made of nanoparticles elongated in the direction of the crystallographic c-axis, with length in the 50-150 and 30-60 nm range, respectively. For both materials the particle core appeared crystalline, while surface terminations did not exhibit any flat and sharp profile, suggesting a highly disordered, amorphous-like surface structure (more evident in the case of HA-A). The same features were observed for HA-B/0.1 and HA-B/0.5.

As for the state of adsorbed water, MIR (ν_{OH} and δ_{H2O} regions) and NIR [$(\nu_{out}+\delta)H_2O$ region] spectra indicated that the hydration layer in direct contact with the HA-A and HA-B surfaces was mainly constituted by water molecules involved in both coordination to surface Ca^{2+} through their oxygen atom, and a strong H-bonding with neighbour phosphates. Moreover, H-bonding states of H_2O molecules different from those in bulk water were found to be extended up to three molecular layers adsorbed on the first one. Outgassing at 300 °C of HA-A resulted in an inward relaxation of ca. 60% of surface cations, not longer accessible to water. Interestingly, the IR spectra of adsorbed CO, used as a highly sensitive vibrational molecular probe, monitored the increase Lewis acidity of a relevant part of Ca^{2+} sites left exposed on the surface.

The presence of Mg^{2+} in HA-B/0.1 and HA-B/0.5 resulted in a progressively higher ability of the materials to bind water at the surface. Because of the absence of modification of the surface texture (by UHR-TEM) this feature should be a consequence of the higher Lewis acidity of such surface cations monitored by IR spectra of adsorbed CO.

HA-A material was used for the investigation of the interaction with BSA, also. The adsorption isotherms appeared to follow the Hill model of cooperative adsorption [4]. A maximum amount of adsorbed protein corresponding only to ca. 30% or 40% of the theoretical full monolayer, considering the side-on or end-on adsorption mode, respectively, was obtained. Such a finding indicated that only a fraction of surface sites exhibit structural and energetic features resulting on the ability to absorb the protein. Many studies pointed out that the interaction between protein and surfaces should involve the dehydration of both moieties. We obtained a direct evidence of this process by recording the NIR spectra of HA-A (Fig. 1) in the bare form (solid line) and after BSA absorption (dash-dot line), both outgassed at room temperature. It can be observed that the $(\nu_{out}+\delta)H_2O$ appeared significantly decreased in intensity after BSA adsorption, indicating that protein displaced H_2O molecules originally adsorbed on Ca^{2+} cations.

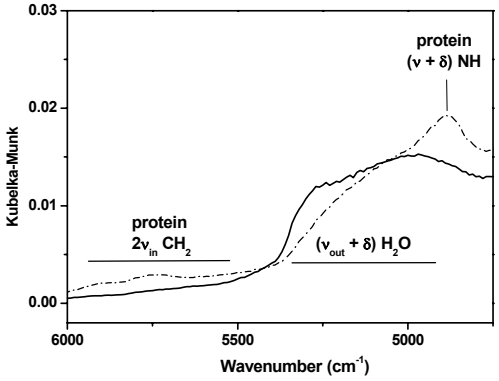

Figure 1: NIR spectra (DR mode) of HA-A before (solid line) and after (dash-dot line) the absorption of BSA. Both spectra were recorded after recovery of the HA powder from the buffered aqueous suspension, washing, drying at r.t. and outgassing at r.t. for 1 h.

MIR spectra (ATR, after exchange with D_2O) indicated that adsorbed BSA retained the native secondary

structure almost unchanged.

BSA adsorption was carried out on HA-A pre-outgassed at 300 °C also. Interestingly, the amount of adsorbed protein appeared slightly increased for all the points of the adsorption isotherm. Such a finding strongly suggests that for hydroxyapatite the amount of adsorbed protein (or, at least, of albumin) is not strictly related to the hydrophilicity of the material (amount of adsorbed water), but to the presence of surface sites with a proper local structure, resulting in cationic centres with a higher polarizing power.

Acknowledgments. Dr. A. Tampieri and Dr. E Landi at CNR-ISTEC (Italy), and Prof. C. Rey and Dr. C. Drouet at INPT-ENSIACET (France), are acknowledged for having kindly provided HA-A and HA-B related materials, respectively.

References

1.. Kasemo, B; *Surf. Sci*., **2002**, *500*, 656-677.
2. Wilson C. J.; Clegg, R. E.; Leavesley, D. I.; Pearcy M. J.; *Tissue Eng*, **2005**, *11*,1-18.
3. Bertinetti L.; Tampieri A.; Landi E.; Ducati C.; Midgley, P.A.; Coluccia S.; Martra G.; *J.Phys Chem. C*, **2007**, *111*, 4027-4035.
4. Luo Q.; Andrade J.D.; J. Colloid Interf. Sci., **1998**, 200, 104-113

P 4.26

Structural and spectroscopic characterisation of $Mo_{1-x}W_xO_{3-\delta}$ oxides.

S. Morandi[a], G. Ghiotti[a], M. C. Paganini[a], E. Giamello[a], M. Bini[b], D. Capsoni[b], V. Massarotti[b].

[a]*Dip. di Chimica I.F.M. and NIS Centre of Excellence, Via Giuria 7, 10125 Torino. e-mail: sara.morandi@unito.it*
[b]*Dip. di Chimica Fisica "M. Rolla" e IENI-CNR, Viale Taramelli 16, 27100 Pavia.*

MoO_3 and WO_3 are well known metal oxides extensively studied for their application in gas sensing devices [1,2]. The interesting optical and electronic properties also make them attractive as electrochromic devices [3]. Moreover, molybdenum and tungsten oxide based materials are highly important compounds in selective oxidation catalysis [4]. They show the capability to lose oxygen in reducing conditions and to restore the lost oxygen in oxidising ones. The introduction of oxygen vacancies in MoO_3 and WO_3 gives rise to electrical conductivity. Thus, sub-stoichiometric molybdenum and tungsten oxides are semiconductors. Upon reduction M^{6+} cations are reduced to M^{5+} or M^{4+}. The additional charge carriers are coupled to the lattice distortion generated in their surroundings, called polaron. Frequently, metal oxide combinations were tailored to achieve desired properties and to modify their electrical behaviour. As an example, recent studies focused on MoO_3-WO_3 mixed oxides report on their promising gas sensing potential [5].

In this work we reported about the preparation and characterisation of Mo-W mixed oxides with different Mo/W molar ratios (4, 1 and 0.25, named MoW4, MoW1 and MoW0.25, respectively) and for comparison purposes also pure MoO_3 and WO_3. All the samples were prepared by precipitation of the hydrated oxides from aqueous solutions of ammonium heptamolybdate and ammonium paratungstate in the right ratio. Morphological and structural characterisations were carried out by SEM and XRD techniques, spectroscopic characterisation by FT-IR, diffuse reflectance UV-Vis-NIR and EPR spectroscopies. FT-IR and DR UV-Vis-NIR spectra were recorded at room temperature (RT) after a pre-treatment in O_2 at 723 K, treatments in vacuum at increasing temperature up to 673 K and subsequent treatments in dry oxygen at the same temperatures. After the same treatments, EPR spectra were recorded in X-band at 77 K.

XRD analysis shows that the Mo-W samples are not single phases, but they are constituted mainly by two crystalline structures. Only MoW4 shows a predominant mixed phase (98.3±0.4 wt.%) with the structure of β-MoO_3 (#89-1554 JCPDS) and W occupancy of 0.22. A second phase (pure monoclinic WO_3 (#83-0950 JCPDS)) is present in very low amount (1.7±0.4 wt.%). Preliminary XRD results for MoW1 and MoW0.25 indicate high percentages of two mixed phases: $Mo_{0.6}W_{0.4}O_3$ (#76-1280 JCPDS) and β-MoO_3 for MoW1 sample; $Mo_{0.29}W_{0.71}O_3$ (#76-1279 JCPDS) and $Mo_{0.14}W_{0.86}O_3$ with the structure of monoclinic WO_3 for MoW0.25 sample. XRD pattern of MoW4 recorded after reducing treatment in vacuum at 723 K shows the appearance of peaks due to a crystalline phase different from those of the completely oxidised sample and related to the presence of $Mo_{0.85}W_{0.15}O_{2.91}$ sub-stoichiometric phase (37.8±1.0 wt.%). This effect is completely reversible for treatment in oxygen at 723 K. Preliminary results for MoW1 and MoW0.25 indicate that the treatment in vacuum at 723 K causes changes in the relative amounts of the phases previously found for the oxidised samples and not the formation of sub-stoichiometric phases. These results enlighten only for MoW4 mixed oxide the capability of losing oxygen not only from the surface but also from the bulk up to a reversible structural rearrangement. On the other hand, pure MoO_3 and WO_3 do not change their XRD patterns after reducing treatments in the same conditions.

FT-IR spectra recorded after reducing treatments in vacuum at increasing temperature show the increase of broad absorptions in the MIR region for pure MoO_3, WO_3 and for MoW4 sample. Absorptions in the MIR region can be related to the presence of electrons trapped at oxygen vacancies. Otherwise, MoW1 and MoW0.25 show only the increase of the tail related to absorptions present at higher energies. As a matter of fact, in the Vis-NIR region all the pure and mixed samples show, beside the absorption edge related to the valence band–conduction band transition, the increase of broad absorptions on increasing the outgassing temperature (see Fig. 1 as an example). These absorptions are related to the presence of polarons. Therefore, the absorptions in the Vis-NIR region can be interpreted as: (i) intervalence charge transfers of the type $[M^{5+}\text{-O-}M^{6+}]$–$[M^{6+}\text{-O-}M^{5+}]$ also called polaronic transitions; (ii) M^{5+} d-d transitions; (iii) M^{5+}-O^{2-} ligand to metal charge transfers.

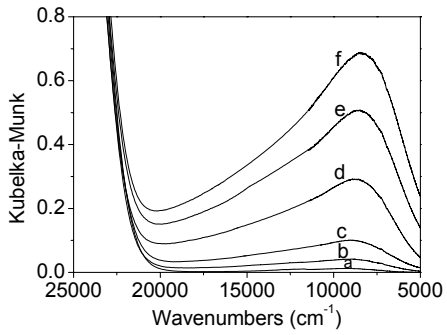

Figure 1. Vis-NIR spectra recorded at RT for MoW1 sample after pre-treatment in oxygen at 723 K (a) and subsequent outgassing at RT (b), 373 K (c), 473 K (d), 573 K (e) and 673 K (f).

EPR spectra confirm the presence of electrons trapped at oxygen vacancies for pure MoO_3, WO_3 and MoW4 with the presence of isotropic signal at g-value characteristic of electron that does not interact with a neighbouring nucleus (g = 2.00). This is the only one signal for WO_3 and for this reason it is possible to postulate that the absorption observable in the Vis-NIR region is related to EPR-silent bipolarons. For MoO_3, MoW4, beside the isotropic signal, and for MoW1 and MoW0.25 several EPR signals related to Mo^{5+} and W^{5+} in different states of coordination and symmetry are observable (see Fig. 2 as an example).

All the electronic absorptions in the MIR and Vis-NIR region and EPR signals are gradually eroded for treatments in oxygen at increasing temperature. This confirms that they are related to defect originated from oxygen loss.

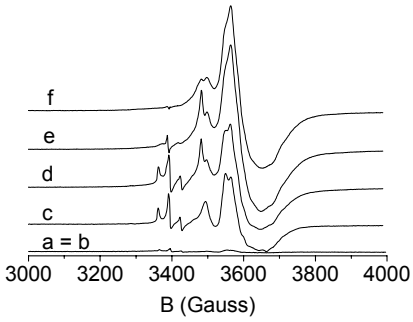

Figure 2. EPR spectra recorded at 77 K for MoW0.25 sample after pre-treatment in oxygen at 723 K (a) and subsequent outgassing at RT (b), 373 K (c), 473 K (d), 573 K (e) and 673 K (f).

1. Prasad, A. K.; Gouma, P. I., Kubinski, D. J.; Visser, J. H.; Soltis, R. E.; Schmitz, P. J.; *Thin Solid Films*, **2003**, *436*, 46-51. 2. Choi, Y. G.; Sakai, G.; Shimanoe, K.; Yamazoe, N.; *Sens and Act. B, Chem.*, **2004**, *101*, 107-111. 3. Djaoued, Y.; Ashrit, P. V.; Badilescu, S.; Brüning, R.; *J. Sol-Gel Sci. Tec.*, **2003**, *28*, 235-244. 4. Dieterle, M.; Mestl, G.; Jäger, J.; Uchida, Y.; Hibst, H.; Schlögl, R.; *J. Mol. Catal,* **2001**, *174*, 169. 5. Galatsis, K.; Li, Y.; Wlodarski, W.; Cantalini, C.; Passacantando, M.; Santucci, S.; *J. Sol-Gel Sci. Tec.*, **2003**, *26*, 1097-1101.

P 4.27

Redox behaviour of Co species in microporous CoAPO-5: a spectroscopic study

M. Vishnuvarthan [a,b*], G. Berlier [b], E. Gianotti [b], D. Davit [b], V. Murugesan [a], S. Coluccia [b]

[a] *Department of Chemistry, Anna University, Chennai-600025, India. e-mail: visvar_cit@yahoo.com*

[b] *Dipartimento di chimica IFM, Università di Torin, V.P. Giuria 7, I-10125 Torino, Italy.*

Transition metal ions incorporated aluminophosphate molecular sieves such as CoAPOs, show attractive catalytic properties due to the variable and reversible oxidation state of cobalt (Co^{2+}/Co^{3+}) in addition to the BrØnsted Co^{2+}(OH)Al functionality. Among these, CoAPO-5 samples, prepared by direct hydrothermal synthetic methods, were characterized by XRD, TEM, Surface area measurements, DR-UV-Vis and FTIR techniques. DR-UV-Vis spectra were used to identify the local geometry and redox behaviour of cobalt centres. In the calcined samples tetracoordinated Co^{2+} ions sites were observed. Upon oxidation at 673 K, the conversion of a small fraction of Co^{2+} ions into Co^{3+}, which are reversibly transformed into Co^{2+} ions by hydrogen treatment at 573K was observed [1]. FTIR spectra were utilized to study the surface binding nature and reactivity of NO and CO molecular probes with cobalt ions. FTIR spectra of NO adsorbed on both oxidized and reduced CoAPO-5 showed the presence of two distinct $Co^{2+}(NO)_2$ complexes (1893 and 1812 cm^{-1}, 1921 and 1844 cm^{-1}) with different stability, confirming the presence of two different kinds of coordination environment for Co^{2+} in the matrix [2]. No evidence for the formation of $NO_2^{\delta+}$ species on the surface of the catalyst on both oxidized and reduced samples could be found. Adsorption of CO resulted in the formation of two different bands at 2184 cm^{-1} and 2047 cm^{-1}. While the former is typical of CO linearly adsorbed on framework tetrahedral or tetragonal Co^{2+} ions, the latter, which appears only on reduced samples, can be explained with the formation of Co^0 or Co^+ carbonyls. This indicates the presence of small extraframework clusters with reversible redox behaviour that could not be detected by XRD or DR-UV-Vis techniques.

1. Barrett, P.A.; Sankar, G.; Catlow, C.R.A; Thomas, J. M.; *Journal of Physical Chemistry*, **1996,** 100, 8977-8985. 2. Gianotti, E.; Marchese, L.; Martra, G.; Coluccia, S.; *Catalysis Today*, **1999**, 54, 547-552.

P 4.28

Effect of the substrate type/composition and deposition techniques on the photocatalytic activity of semiconducting nanocrystalline films for environmental applications

A. Panniello[a], R. Comparelli[b], D. Diso[c], A. Licciulli[c], G. Mascolo[d], A. S. Franza[e], M. Striccoli[b], A. Agostiano[a,b], M.L. Curri[b]

[a] *Università di Bari – Dip. Chimica, Via Orabona 4, Bari, I-70126, Italy*

[b] *CNR-IPCF Sede Bari, c/o Dip. Chimica – Via Orabona 4, Bari, I-70126, Italy; r.comparelli@ba.ipcf.cnr.it*

[c] *Dipartimento Ing. Dell'Innovazione, Universita` di Lecce, via per Arnesano, Lecce, I-73100, Italy*

[d] *CNR-IRSA – Sez. Bari, Viale De Blasi, Bari, I-70100, Italy*

[e] *Salentec SRL, via dell'esercito 8, 73020 Cavallino Le, Italy*

Nanostructured semiconductors immobilized onto appropriate substrates are very promising in catalysis applications thanks to the matched effects of their very high surface area, ascribed to the improved surface to volume ratio of the nanoparticles, and the facile recovery of the catalyst, due to the effects of the deposition.[1] Therefore considerable efforts are devoted to identify the more suitable substrates and the deposition techniques to set up the optimal conditions in order to develop efficient photocatalysts that could be easily recovered from the

reaction system and likely recycled in following experiments.[2-4]
The present work is devoted to the optimization of deposition conditions of nanostructured titania thin films for environmental photocatalysis. For this purpose anatase TiO_2 nanorods and nanodot were prepared both by synthesis in hot coordinating solvent and sol-gel process. The as-prepared materials were characterized by XRD and TEM measurements. The films roughness and catalyst adhesion was investigated by AFM and SEM measurements either before and after the photodegradation experiment.
The films were prepared by exploiting two different deposition techniques (casting and dip-coating) and different supports (glass slides, glass fibers, alumina fibers), in order to get the optimal deposition conditions. The photocatalytic activity of the obtained films was evaluated in the oxidative photodegradation of an organic dye (Methyl Red) in aqueous matrix under UV irradiation.
Photocatalysis experiments were monitored by UV-Vis, HPLC-MS and TOC analysis. Finally, the experimental condition which showed the higher photoactivity and better catalyst adhesion were replicated in a scaled up reactor in order to test the catalyst activity in large scale processes.
Acknowledgment. This work was partially supported by Progetto MIUR D.M. no. 1105 (9 October 2002) funding programme and by Explorative Project "Photocatalytic degradation of organic pollutants in aqueous solutions by nanostructured semiconductors" funded by "Apulia" Region within the Scientific Research Framework Program 2006

1. Comparelli, R.; Fanizza E.; Curri M. L.; Cozzoli P. D.; Mascolo G.; Passino R.; Agostiano A.; *Applied Catalysis B: Environmental*, **2005**, *55*, 81-91.2. Pozzo R. L.; Giambi J. L.; Baltanas M. A.; Cassano A. E.; *Catalysis Today* **2000**, 62, 175-187. 3. Horikoshi S.;Watanabe N.; OnishiH.; Hidaka H.; Sermone N.; *Applied Catalysis B: Environmental*, **2002,** *37*, 117–129. 4. Yu H.; Lee S.C.; Yu J.; Ao C.H.; *Journal of Molecular Catalysis A: Chemical*, **2006,** *246*, 206–211

P 4.29

Silver ions mediated photochemical synthesis of water soluble gold nanoparticles with control over size and morphology

T. Placido[a], R. Comparelli[a], P.D. Cozzoli[b] M. Striccoli[a], G. Capitani[c], F. Giannici[d] M.L. Curri[a],
[a] *CNR-IPCF Sez. Bari, c/o Dip. Chimica – Via Orabona 4, Bari, I-70126, Italy – r.comparelli@ba.ipcf.cnr.it*
[b] *National Nanotechnlogy Laboratory of CNR-INFM, Distretto Tecnologico ISUFI, via per Arnesano Km 5, I-73100 Lecce, Italy*
[c] *Università di Bari – Dip. Geomineralogico, Via Orabona 4, Bari, I-70126, Italy*
[d] *Università di Palermo – Dip. di Chimica Inorganica e Analitica - Parco d'Orleans II, I-90128 Palermo, Italy*

Gold nanoparticles with nanometer-scale dimensions are of great interest due to their unusual physical and chemical properties with respect to their bulk counterpart. The optical properties of metal nanoparticles are tunable throughout the visible and near-infrared region of the spectrum as a function of size, shape, aggregation state and local environment, thus making them very promising for optical, electronic, catalytic, and biomedical applications[1] Current research has been focused on one-dimensional nanoparticles such as nanorods (NRs) since the morphological anisotropy results in very complex physical properties.[2] In fact, the plasmon absorption of gold NRs splits into two bands corresponding to the oscillation of the free electrons along and perpendicular to the long axis of the rods. In particular, the resonance of the longitudinal mode is red shifted and strongly depends on the nanorod aspect ratio.[3] Water soluble gold nanospheres and nanorods have been synthesized by using various methods such as templating,[4] photochemistry,[5] seeding[6] and electrochemistry[7].
In this work, we propose a silver ion mediated photochemical synthesis of gold nanoparticles (NPs) in micellar template under UV irradiation. We performed a systematic study on the role of Ag^+ ions in directing the growth of gold NRs, in order to elucidate the mechanism that produces anisotropic particles rather than spheres.
The effect of reaction time and silver ion concentration has been deeply investigated. The samples have been characterized by UV-Vis-NIR absorption spectroscopy, High Resolution Transmission Electron Microscopy (HR-TEM), Energy Dispersive Spectrometry (EDS), Inductively Coupled Plasma (ICP), and Extended X-ray Absorption Fine Structure Spectroscopy (EXAFS) measurements. Moreover the size and shape distribution has also been investigated by statistical analysis of the experimental data. The overall obtained results allowed us to finely tune the size and the shape distribution of gold NPs and to propose a reasonable mechanism describing the role played by silver ions in directing the growth of gold NRs.
Acknowledgment. This work was financially supported by the EC-funded Project NOVOPOLY (Contract no. STRP 013619).

1. Daniel, M.C.; Astruc, D.; *Chem. Rev.* **2004**,*104,* 293. 2. Kim, F.; Kwan, S.; Akana, J.; Yang, P. *J. Am. Soc.* **2001**, *123*, 4360. 3. Link, S.; El-Sayed, M.A.; *J. Phys. Chem. B* **1999,** *103* ,8410-8426. 4. Bohmer, M. R.; Fokkink, L. G. J.; Scho¨nenberger, C.; van der Zande, B. M. I. *J. Phys. Chem. B* **1997**, *101*, 852. 5. Esumi, K.; Matsuhisa, K.; Torigoe, K. *Langmuir* **1995**, *11*, 3285. 6. Murphy C. J.; Jana N. R. *Adv. Mater*. **2002**, *14*, 80. 7. Yu, Y. Y.; Chang, S. S.; Lee, C. L.; Wang, C. R. C. *J. Phys. Chem. B* **1997**, *101*, 6661-6664.

P 4.30

Protein Adsorption on Chemically and Topographically Nanopatterned Polymer Surfaces

C. Satriano, G.M.L. Messina, and G. Marletta
Laboratory for Molecular Surfaces and Nanotechnologies (LAMSUN), Department of Chemical Sciences, University of Catania and CSGI, Viale Andrea Doria, 6, 95125 Catania, Italy. csatriano@unict.it

The preferential adsorption of two model globular proteins, lactoferrin (Lf) and albumin (HSA) was investigated onto chemically nanostructured polysiloxane surfaces, as function of the pattern geometry and chemical contrast.
The nanopatterned surfaces consisted of 2D nanopore arrays, having hydrophilic internal area (O_2-plasma treated polysiloxane) surrounded by hydrophobic polysiloxane or the reverse.

The pattern geometry was modulated by using two different methods. The first one was based on colloidal self-assembly driven by dewetting, followed by polymer infiltration due to capillarity. The second method, based on spin coating of suitable colloidal and polymer solutions, to vary experimental parameters as ionic strength, pH, solution concentrations.
The nanometric features of adsorbed proteins were investigated by AFM, while the corresponding homogeneous surfaces were studied by QCM-D, for the adsorption kinetics, and XPS, for chemical structure and coverage of the protein adlayers.
A good spatial separation of HSA and Lf was obtained, prompted by opposite preferential adsorption behaviours, involving increased adsorption of Lf and HSA into the hydrophilic or hydrophobic areas of the nanopores, respectively.
The driving chemical factors were identified in terms of surface free energy and chemical termination of the different surfaces.

P 4.31

A quantum-mechanical study on the adsorption of CO on TiO_2: comparison between the Lewis acidity of the rutile (110) and the anatase (101) surfaces.

Jessica Scaranto[a], Santi Giorgianni[a]
[a]*Università Ca' Foscari di Venezia, Dorsoduro 2137, 30123, Venezia, jeyscar@unive.it*

Titanium dioxide represents one of the most interesting metal oxides as it is widely employed in the field of heterogeneous catalysis. The two natural allotropic forms mainly used are the rutile and anatase ones, whose the most stable surfaces are represented by the (110) and the (101), respectively.
Here, we present the main results obtained from a periodic quantum-mechanical study on the adsorption of carbon monoxide on the two surfaces. This study has been done to compare the electrophilicity of the two different surface Lewis acid sites (Ti^{4+}). In fact, as it is well-known, the CO molecule binds to the cation of the metal oxide and the magnitude of the shift of the vibrational frequency of the CO stretching gives information on the strength of the adsorbate-substrate interaction. All the calculations have been performed at DFT/B3LYP level using the CRYSTAL program[1,2]. The two surfaces have been simulated by two slabs whose thickness converges with respect both the structural relaxation and the surface formation energy[3]. The adsorption has been investigated by considering different surface coverages and periodicities; the obtained adsorbate-substrate system has been characterised by means of not only the binding energy but also the interaction and distortion ones. The lateral effects between the CO molecules, consisting in a direct and a surface-mediated repulsion, have been analysed by using a simple model of nearest and next-nearest neighbours; this model allows also the determination of the energies in the limit of an isolated adsorbed molecule. Furthermore, the vibrational frequency of the adsorbed CO molecule has been computed. The study reveals that the adsorbate-substrate interaction is slightly stronger in the case of the CO-rutile system and then, it is possible to conclude that the surface Lewis acid site of the rutile (110) is slightly more electrophilic than that of the anatase (101).

1. Saunders, V.R.; Dovesi, R.; Roetti C., Orlando, R.; Zicovich-Wilson, C.M.; Harrison, N.M.; Doll, K.; Civalleri, B.; Bush, I.J.; D'Arco, P.; Llunell, M.; *CRYSTAL03 User's Manual*, Università di Torino, Torino (**2003**). 2. Dovesi, R.; Saunders, V.R.; Roetti C., Orlando, R.; Zicovich-Wilson, C.M.; Pascale, F.; Civalleri, B.; Doll, K.; Harrison, N.M.; Bush, I.J.; D'Arco, P.; Llunell, M.; *CRYSTAL06 User's Manual*, Università di Torino, Torino (**2006**). 3. Scaranto, J.; Ph. D. thesis, University of Venezia, **2006**: (see web site http://venus.unive.it/molspectragroup/LowResolutionTiO2/TiO.htm.)

P 4.32

Photocatalytic H_2 production from water splitting on one step flame synthesised TiO_2 and Au/TiO_2

Elena Selli, Gian Luca Chiarello, Ilenia Rossetti, Lucio Forni
Dipartimento di Chimica Fisica ed Elettrochimica, Università degli Studi di Milano, Via Golgi 19, 20133 Milano, elena.selli@unimi.it

TiO_2 and 1 wt% Au/TiO_2 were synthesised by a continuous, single-step flame spray pyrolysis method (FP) [1,2] and characterized by BET, XRD, HRTEM and UV-vis reflectance analyses. Both materials consisted of crystalline well dispersed 5-10 nm nanospheres, with high surface area (106 $m^2\ g^{-1}$). XRD analysis showed the presence of *ca.* 75% anatase and 25% rutile, whereas no peaks ascribable to metal gold could be recognized, because of the low noble metal loading. Both materials exhibited a UV-vis adsorption threshold at *ca.* 400 nm; the gold containing oxide also displayed the typical plasmonic band of gold nanoparticles (< 20 nm), centred at 550 nm, *i.e.* red shifted compared to the pure gold plasmon peak (520 nm), indicating interaction between gold and the titania support.
The photocatalytic activity of the materials was tested in a appositely set up, closed recirculation laboratory scale photoreactor (Fig. 1), designed to investigate the activity of suspended particles in water photosplitting, to produce H_2 and O_2. The reactor consisted of a 45 mL, magnetically stirred quartz vessel (A) containing the photoactive suspension, connected to a closed stainless steel circulation system, in which an inert gas (nitrogen) was continuously flowed by means of a bellow pump (C). The analysis of the species evolved from the aqueous suspension under irradiation was performed by gas chromatography with TC detector (D), after calibration by injections of known volumes of H_2 (or O_2) through a six ways valve (E).

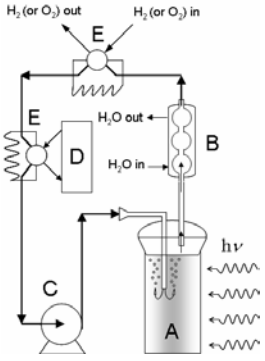

Fig. 1: sketch of the experimental set up

The light source was an iron halogenide mercury arc lamp, emitting in the 315-400 nm wavelength range with an irradiation intensity of 3 x 10^{-7} Einstein s^{-1} cm^{-2} on the reactor. All photocatalysts (14 mg) were suspended in water, in the absence or in the presence of 6 vol.% methanol as sacrificial agent, sonicated for 20 min and thoroughly flushed with inert gas in the photoreactor, before starting irradiation.
H_2 production occurred at constant rate, apart from a sort of initial induction time, possibly dependent on the residual oxygen content of the suspension and on temperature (usually 35°C under irradiation).
The FP-prepared TiO_2 photocatalyst displayed a higher activity with respect to the commercial Degussa P25, usually employed as benchmark of photocatalytic activity (0.27 *vs* 0.17 mmol H_2 h^{-1}). H_2 production on the FP-synthesised Au/TiO_2 photocatalyst was so high (6 NmL produced in 2 h), that outgassing was required every 2 h, to prevent H_2 overpressure. Successive irradiation cycles were thus performed, with an outgassing in the dark in between (Fig. 2). No induction period in hydrogen evolution on Au/TiO_2 was ever observed, with only a slight decrease in the H_2 production rate in successive cycles (7.89, 7.53 and 7.18 mmol H_2 h^{-1}, hence *ca.* 25 times higher with respect to the Au free FP-photocatalyst).

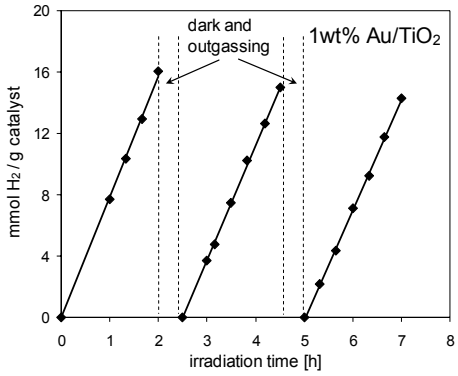

Fig. 2: Hydrogen production from photocatalytic water splitting on FP-synthesised 1% Au/TiO_2.

Thus, FP appears to be a very promising preparation method for the direct synthesis of TiO_2–based photocatalysts active in water splitting.

1. Chiarello, G.L.; Rossetti, I.; Forni, L.; *Journal of Catalysis*, **2005**, *236*, 251-261. 2. Mädler, L.; Stark, W.J.; Pratsinis, S.E.; *Journal of Materials Research*, **2003**, *18*, 115-120.

P 4.33

Si nanocrystals obtained in SiO_2 matrix by low energy ion implantation

L. Velardi[1], A. Lorusso[1], M. Traversa[2], P. Prete[3], V. Nassisi[1], N. Lovergine[2]
[1] *Laboratorio di Elettronica Applicata e Strumentazione, LEAS, Department of Physics, University of Salento & INFN - Lecce, Via Provinciale Lecce-Monteroni, 73100 Lecce – Italy Tel. +39 0832 297495, Fax. +39 0832 297482, E-Mail: vincenzo.nassisi@le.infn.it*
[2]*Laboratorio di Fisica e Tecnologia dei Semiconduttori, Department of Innovation Engineering, University of Salento, CNISM, Unità di Lecce, Via Provinciale Lecce-Monteroni, 7310 Lecce-Italy*
[3]*Institute for Microelectronics and Microsystems (IMM) of CNR, Unità di Lecce, Via Provinciale Lecce-Monteroni, 73100 Lecce – Italy*

We present a new "implantation machine" utilized to process SiO_2 samples by Si ions. The practical consequence consists to obtain composite materials containing silicon nanocrystals (NCs) in SiO_2 matrix obtained by ion implantation and annealing. These NCs have the potentiality to emit photons in the visible light region which is very useful in integrated photonic and optoelectronic devices. The production Si NCs by ion implantation offers an advantage respect to other techniques, i.e a controllable dose of ions at a given depth.
The ion source was developed by laser ablation of Si target. The employed laser is an excimer laser operating at 248 nm wavelength, 23 ns pulse time duration providing a power density of 3.5x10^8 W/cm^2. The laser beam strikes the target producing a very high density plasma which expands adiabatically into the vacuum. The success of the present device was reached inserting a removable expansion chamber (EC) which allowed an initial free expansion of the plasma before the ion extraction reducing, in this way, the probability of arcs during the acceleration which could decrease the implanting ion dose. Figure 1 shows the experimental apparatus developed at LEAS laboratory where it is possible to see the EC equipped by a quartz window (W) in order to close the plasma in the proximity of the target. The EC works as anode, while a ground electrode (GE) as cathode. On GE, we put the sample to be implanted. For metallic samples we utilized a GE having a central hole behind which the samples were placed. The extracted ion dose, utilizing 40 keV accelerating voltage, was estimated by using a fast Faraday cup (FC) in front the ion beam. It was negatively polarized (500 V) in order to collect only plasma positive particles. By our experimental conditions, the applied ion dose was of the order of 10^{12} ions/cm^2 per laser pulse.

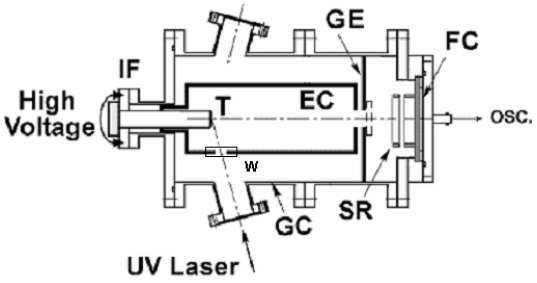

Figure 1. Schematic drawing of the experimental apparatus. GC: Generation Chamber; EC: Expansion Chamber; W: quartz window IF: Insulating Flange; T: Target; GE: Grounded Electrode; FC: Faraday Cup. The accelerating gap is established between the EC, biased at high voltage, and the GE.

Considering the whole charge due to practically to the ions with +1 charge state [1,2] and applying one thousand laser shots, we obtained a total implanted dose of 10^{15} ions/cm^2.
The experiment was performed with a p-type (B doped) Si(100) wafer of 225 μm thickness, target. The wafer was suitably rotated during the implantation process in order to avoid the formation of a unique crater, which may decrease the ion emission yield. Samples consisted of 300

nm thick thermal SiO_2 films on Si(100) and were implanted with some thousand shots at a maximum accelerating voltage of 40 kV. The laser was operated at 0.5 Hz repetition rate. The vacuum chamber was evacuated by two turbo-molecular pumps down to 10^{-6} mbar.
Implanted samples were subsequently annealed at 1000 °C in a tubular resistance furnace flowed with 6.0N pure N_2 gas for a few hours to induce Si precipitation and the formation of Si NCs. In order to evidence changes in the material crystallinity degree upon annealing, as-implanted ad annealed samples were then studied by X-ray diffraction (XRD) in both Bragg and glancing incidence geometry. An example of XRD pattern performed on no-implanted and implanted and annealed samples is reported in Fig. 2. The dimension of the generated nanocrystals was estimated of about 36 nm by using Debye-Scherrer equation.

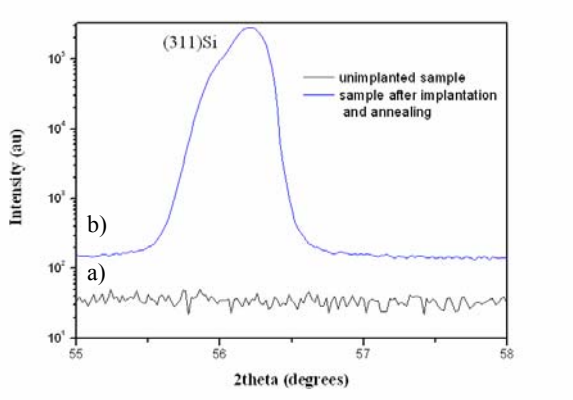

Figure 2. X-ray diffraction is used to value the effectiveness of the implantation. a) no-implanted sample; b) implanted and annealed at 1000°C sample obtained at an incident angle.

1) V. Nassisi and A. Pedone, *Rev. Sci. Instrum.* **2003**, *74*, 68.
2) D. Doria, A. Lorusso, F. Belloni, V. Nassisi, L. Torrisi and S. Gammino, *Laser Part. Beams* **2004**, *22*, 461.

P 4.34

New methodology for Brønsted quantification in microporous materials: FTIR and themogravimetry

G. A. V. Martins [a], G. Berlier [a], G. Gatti [b], S. Coluccia [a], and L. Marchese[b]
[a]*Dipartimento di Chimica IFM, Università di Torino, Turin I-10125 Italy, gesley.martins@unito.it,*
[b]*Dipartimento di Scienze e Tecnologie Avanzate, Università del Piemonte Orientale, Alessandria I-15100, Italy*

H-SAPO-34, a silico-aluminophosphate (SAPO) with chabazite structure and Brønsted functionality, has shown peculiar activity and selectivity in MTO processes, and is now central to the UOP/Norsk Hydro MTO technology. The ability of tuning concentration and strength of Brønsted acid sites in solid catalysts could improve the process performances and catalysts lifetime. As a consequence, a careful characterization of Brønsted sites in terms of acid strength and number represents a fundamental advance in catalysis. In this work we concentrate on H-SAPO-34 material, where the presence of three distinct Brønsted sites (one of them showing an acid strength comparable to zeolite homologues) was recently proved by a careful spectroscopic analysis. In this work, a quantitative method for the determination of total Brønsted content is proposed. This method is based on the combination of FTIR data (spectra of CO and NH_3) and gravimetric analysis of ammonium decomposition. The measured value is combined with the relative fraction of the three Brønsted sites estimated before, in order to calculate the extinction coefficients of distinct sites with different acidity. The calculated values are of general validity for chabasite-like SAPO materials and are of great importance for catalysts optimization.

SEZIONE

CHIMICA TEORICA E COMPUTAZIONALE

P 5.1

DPD Simulations to investigate polymer nanocomposites morphology

E.Bianchino[a,b], S.Piotto[b], C. Sciancalepore[a], M. L. Curri[c], A. Agostiano[a,c], M. Striccoli[c], F.Ciriaco[a], F.Mavelli[a]
[a] *Chemistry Department, University of Bari, Via Orabona 4 – 70125 Bari*
[b] *Pharmaceutical Science Department, University of Salerno via Ponte don Melillo 84084 Fisciano (Salerno)*
[c]*CNR-IPCF Sez. Bari c/o Chemistry Department, University of Bari, Via Orabona 4 – 70125 Bari*

Dense polymer-particle mixtures, or polymer nanocomposites, are of major scientific and technological interest[1]. Fundamental issues include equilibrium miscibility, dispersion and spatial organization of particles, particle-induced modification of polymer conformation and packing, structure of the polymer-particle interface, and the calculation of new thermo-mechanical emerging properties. Diverse theoretical and simulation approaches have begun to be employed to study fundamental aspects of model polymer-particle mixtures: Monte Carlo and Molecular Dynamics methods, both at atomistic and coarse grain levels, and mesoscopic methods such as like Dissipative Particle Dynamics[2] and Mean-Field Dynamics[3].
In this contribution, TiO_2 nanocrystals (NCs) synthesised in surfactant solutions (hot injection method) have been investigated[4]. As a consequence of the preparation method, NCs are coated by amphiphilic molecules, i.e. oleic acid and trioctilphosphin oxide –TOPO-, that, once NCS are embedded in a polymer host matrix, can also play a role in defining the morphology of the blend. This work aims to evaluate the possibility to describe and foresee the characteristic features of the investigated polymer nonocomposites by using both a commercially available software (Materials Studio® by Accelerys Inc.) and a simulation package issued free under licence to academic institutions (DL_MESO developed at Daresburry Laboratory). In particular, Dissipative Particle Dynamics has been used to simulate the morphological features of PMMA/Oleic Acid/Colloidal oxide NCs and PMMA/TOPO/Colloidal oxide NCs mixtures, respectively. Indeed, this mesoscale method applies classical simulation techniques to coarse-grained systems. In this perspective polymer and surfactant molecules can be thought as decomposed in a collection of linked beads, representing homogeneous domains with approximately the same volume. Critical points in this approach stand on the description of NCs as rigid particles of different shapes and sizes and the calculation of the interaction parameters for the different type of beads in order to correctly simulate the dynamic behaviour .
of the studied system.
Some preliminary results will be presented and discussed. In particular, the formation of continuous surfactant domains in PMMA has been investigated as a function of the mixture composition. Finally a comparison of the obtained theoretical results with the experimental data will be shown.

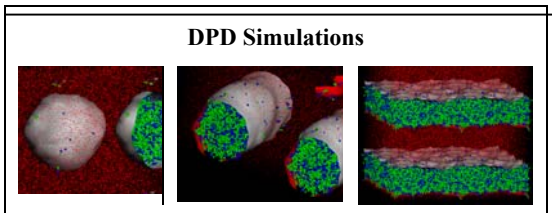

Different morphologies observed in DPD simulations of PMMA/Oleic Acid mixtures with different compositions: surfactant molecules are represented by blue (hydrophilic head) and green (hydrophobic tail) spheres, while polymers are not explicitly reported. The gray surface is the interface between the two domains

Acknowlegment
This work was financially supported by the EC-funded Project NOVOPOLY (Contract no. STRP 013619).

P 5.2

Polarizzabilità ed iperpolarizzabilità statiche di semplici molecole: studio degli effetti vibrazionali.

S. Bruzzone[a], U.T. Lamanna[b], C. Guidotti[a], G.P. Arrighini[a]
[a]*Dipartimento di Chimica e Chimica Industriale,Università di Pisa, Via Risorgimento 35, 56100 Pisa; sama@dcci.unipi.it*
[b]*Dipartimento di Chimica, Università di Bari, Campus Via Orabona 4, 70125 Bari.*

In questo lavoro è presentata una valutazione delle performance di set di base di orbitali atomici di Slater (STO) nel calcolo di contributi vibrazionali a proprietà di risposta elettromagnetica statica, lineare e non lineare, a livello TDHF (Time Dependent Hartree Fock). In particolare, i contributi vibrazionali alla polarizzabilità ed alla prima e seconda iperpolarizzabilità statiche sono stati valutati impiegando le formule perturbative derivate da Bishop e Kirtman[1]. Queste formule, basate su una iniziale approssimazione di tipo armonico, includono correzioni che tengono conto dell'anarmonicità meccanica del potenziale vibrazionale e dell'anarmonicità elettrica dipendente dal potenziale di polarizzazione del campo elettrico sulle coordinate vibrazionali. Il metodo richiede preliminarmente la conoscenza della superficie di energia potenziale in funzione delle coordinate normali della molecola, accompagnata dal contemporaneo calcolo del momento di dipolo elettrico totale, della polarizzabilità e della prima iperpolarizzabilità per ogni geometria molecolare esaminata, alla frequenza studiata. Elementi fondamentali della procedura sono le derivate prime,

[1] Wang, M.-J. Rubber *Chem. Technol.* **1998**, 71, 520; **1999**, 72, 430; Huber, G.; Vilgis, T. A. Macromolecules **2002**, 35, 9204; Vieweg, S.; Unger, R.; Heinrick, G.; Donth, E. *J. Appl. Polym. Sci.* **1999**, 73, 495;
Ajayan, P. M.; Schadler, L. S.; Braun, P. V. In *Nanocomposite Science and Technology*; Wiley-VCH: Weinheim, **2003**, p 77; Ash, J.; Schadler, L. S.; Siegel, R. W. *Mater. Lett.* **2002**, 55, 83; Mackay, M. E.; Dao, T. T.; Tuteja, A.; Ho, D. L.; van Horn, B.; Kim, H.-C.; Hawker, C. *J. Nat. Mater.* **2003**, 2, 762.

[2] Español, P., Warren, *Europhys. Lett.*, **1995**, 30, 191; P. Groot R.D., Warren P.B. *J. Chem. Phys.,* **1997**, 107, 4423.

[3] Fraaije, J.G.E.M., van Vlimmeren, B.A.C., Maurits, N.M., Postma, M., Evers, O.A., Hoffman, C., Altevogt, P., Goldbeck-Wood, G., *J. Chem. Phys.*, **1997**, 106, 4260; Altevogt, P., Evers, O.A., Fraaije, J.G.E.M., Maurits, N.M., van Vlimmeren, B.A.C., *J. Mol. Struct.* (THEOCHEM) **1999**, 463, 139.

[4] Manera, M.G.; Leo, G.; Curri, M.L.; Comparelli, R.; Rella, R.; Agostiano, A.; Vasanelli, L., *Sensors and Actuators B: Chemical,* **2006,** 115, 365.

seconde e terze di tutte queste grandezze rispetto alle coordinate normali.
I risultati, accompagnati da dati di confronto tratti dalla letteratura, sono presentati per piccole molecole isolate: HF, LiH, H_2O, D_2O.

1. a) Kirtman, B.; Bishop, D.M.; *Chem. Phys. Lett*.,**1990,** *175*, 601-607. b) Bishop, D.M.; Kirtman, B.; *J. Chem. Phys*., **1991**, *95*, 2646-2658.

P 5.3

Characterization of a New Candidate as Contrast Agent for Magentic Resonance Molecular Imaging

U. Cosentino[a], D. Pitea[a], G. Moro[b], G.A.A Saracino[b] , L. Cipolla[b], M. Gregori[b], F. Nicotra[b], A. Villa[c]
[a]*Università di Milano-Bicocca, Dipartimento di Scienze dell'Ambiente e del Territorio, Piazza della Scienza 1, 20126 Milano, Italy, ugo.cosentino@unimib.it*
[b]*Università di Milano-Bicocca, Dipartimento di Biotecnologie e Bioscienze, Piazza della Scienza 3, 20126, Milano, Italy*
[c]*J.W. Goethe University, Institute for Physical and Theoretical Chemistry, Max-von-Laue-Strasse 7, D-60439 Frankfurt am Main, Germany*

Contrast agents based on paramagnetic metals such as gadolinium ion are routinely used in magnetic resonance imaging (MRI) diagnostic technique to shorten relaxation times of water protons and enhance image contrast. Chelating moieties are typically octadentate PolyAminoCarboxylate (PAC) ligands that form kinetically and thermodynamically stable complexes with gadolinium. The ninth coordination site of the ion, not saturated by the ligand, allows fast exchanging water molecules to transmit the paramagnetic relaxation effect to bulk solvent.
Contrast agents for clinical use, such as the Gd-DOTA complex (**1**), are confined to extracellular spaces and distribute nonspecifically throughout vascular and interstitial tissues.

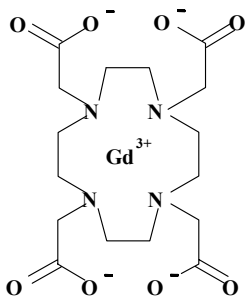

(**1**)

Development of new MRI contrast agents concerns systems presenting increased sensitivity and specificity toward biological targets: this defines a new class of contrast agents suited for the so called *molecular imaging*. In general, the design of these new contrast agents involves the linkage of the gadolinium complex with moieties able to bind to specific receptors, cell surface antigens, proteins, or sensible to enzymatic activity.

Levels of several types of glycosidases, such as *sialidases*, have been shown to be elevated in the interstitial fluid of tumors. In particular, over-expression of *Neu3 sialidase* inhibits apoptosis and promotes cellular proliferation. Thus, this enzyme could be a useful target for diagnostic and therapeutic agents.[1]
With this aim, we propose a new gadolinium complex (**2**) as molecular imaging contrast agent candidate. It consists of a DOTA-like ligand covalently linked to the sialic acid moiety. Based on similar examples reported in literature,[2] design of this structure relies on the following hypothesis: the sialic moiety prevents the contrast agent activity, hindering coordination of a water molecule to the ninth coordination site of the gadolinium ion; in presence of *sialidases*, the sialic acid is cleaved from the chelate allowing coordination of a water molecule and restoring the contrast agent activity.
Here we present preliminary results concerning characterization of the conformational behaviour in aqueous solution of complex (**2**) performed by means of MD simulations based on a previously developed force fields.[3] The chemical synthesis of complex (**2**) is underway.

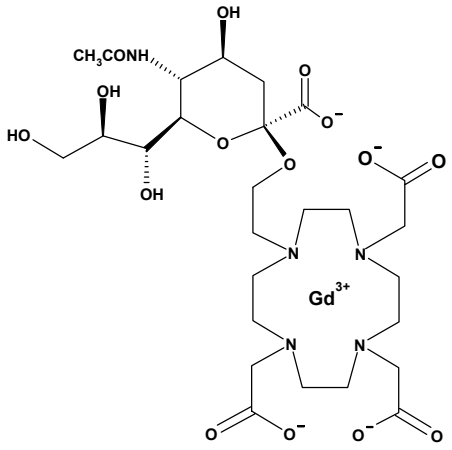

(**2**)

1. Kakugawa, Y.; Wada, T.; Yamaguchi, K.; Yamanami, H.; Ouchi, K.; Sato, I.; Miyagi, T.; *Proc. Natl. Acad. Sci. USA,* **2002**, 99, 10718–10723.
2. Louie, A.Y.; Huber, M.M.; Ahrens, E.T.; Rothbacher, U.; Moats, R.; Jacobs, R.E.; Fraser, S.E.; Meade, T.J.; *Nature Biotechnology*, **2000**, *18*, 321-325.
3. Cosentino, U.; Moro, G.; Pitea, D.; Villa, A.; Fantucci, P.C.; Maiocchi, A.; Uggeri, F.; *J. Phys. Chem. A*, **1998**, *102*, 4606-4614. (b) Villa, A.; Cosentino, U.; Pitea, D.; Moro, G.; Maiocchi, A.; *J. Phy. Chem A*, **2000**, *104*, 3421-3429.

P 5.4

Theoretical and experimental studies of layered alkylamine-aluminophosphates.

M. D'Amore[a], C.Bisio[a], G. Talarico[b], M. Cossi[a], L. Marchese[a].
[a]*Dipartimento di Scienze e Tecnologie Avanzate, Università del Piemonte Orientale "A. Avogadro", Via Bellini 25/G, 15100 Alessandria, leonardo.marchese@mfn.unipmn.it*
[b]*Dipartimento di Chimica, Università di Napoli "Federico II", Complesso di Monte S. Angelo, Via Cintia, 80126 Napoli*

Lamellar aluminophosphates modified by intercalation of alkylamines are key intermediates in the synthesis of aluminophosphates (ALPOs) and silicoaluminophosphates (SAPOs) molecular sieves and can be also used as host framework in the fields of nanocomposites. However, until the CAL-n family of microporous silicoaluminophosphate molecular sieves was presented[1], there were no good candidates as layered reactants, that is lamellar aluminophosphates and silicoaluminophosphates with structures similar to the hydrated layered silicates. It is from the work of Cheng et al.[2], who reported the synthesis of the layered aluminophosphate ALPO-ntu (whose empirical formula is $AlPO_2(OH)_2[NH_2(CH_2)_xCH_3]$, x=3, 5, 7), employing amines as structure directing agents, that the perspective to obtain ALPOs and SAPOs molecular sieves using layered materials as precursors became possible[1]. In addition, layered aluminophosphates, especially those organically modified by intercalation of different n-alkylamines, have the assets of a larger interlayer distance and organophilic galleries between the sheets to host either organic molecules or polymer chains. Moreover, the interaction between organic molecules and inorganic aluminophosphate may influence the acidity of sites present on the surfaces and drive the interfacial phenomena in polymer composites.

The experimental data available on this class of layered aluminophosphates were not sufficient to fully resolve both their local and long range structural features. For this reason computational approaches are proposed to model structure and surface properties of these materials thus obtaining useful insights on their chemical behaviour. Reliable models may also help a better understanding of experimental data. The acidity of sites on ALPO layers and the interactions between organic molecule and the inorganic substrate have been specifically addressed.

Since all experimental (X-ray powder diffraction patterns, IR, ^{27}Al and ^{31}P MAS NMR) data relative to the alkylamine-aluminophosphates are in agreement with a kanemite-like structure, ab-initio computational models of butylamine-ALPO-kanemite were built starting from a reasonable structure of silica kanemite[3].

The computational tools to simulate these solids were based on density functional theory (DFT) employing localized basis sets: both cluster and periodic models were taken into account, and IR spectra were simulated for optimised structures. Results were compared with the IR experimental spectrum of butylamine-ALPO-kanemite. The harmonic vibrational spectra were computed (PBE0/6-31 G(d), LANL2DZ level) for all the cluster minima, to identify the chemical species present in the material and support the interpretation of the experimental data.

Computations on cluster of ALPO surface show that the P-OH moiety is markedly more acidic than Al-OH and the structure of relative anion is stabilized by $PO^-\cdots$H-O-Al hydrogen bond. The results are interpreted in terms of an acid-base reaction between protons P-OH groups in the inorganic layer and the butylamine molecules.

The actual position of the positive butylamonium heads was determined by a bidimensional PBC calculation on the ALPO layer in presence of an equivalent layer of NH_3 molecules close to the surface. During the optimisation all the surface P-OH groups reacted with NH_3 molecules and were quickly deprotonated forming NH_4^+ ions: as a consequence, the Al-OH groups rotated and the intramolecular H-bond observed in the isolated anion were lost in favour of the stronger interaction with NH_4^+. In the $AlPO\text{-}NH_4^+$ periodic layer the ammonium ion was substituted by $CH_3(CH_2)_3NH_3^+$ ion: the optimised structure shows tridentate butylammonium ions i.e. the ion interacting via three hydrogen bonds, one with oxygen atom on Al and the other two with oxygen atoms on phosphorous in the layer, these H bonds are not equivalent (Fig. 1).

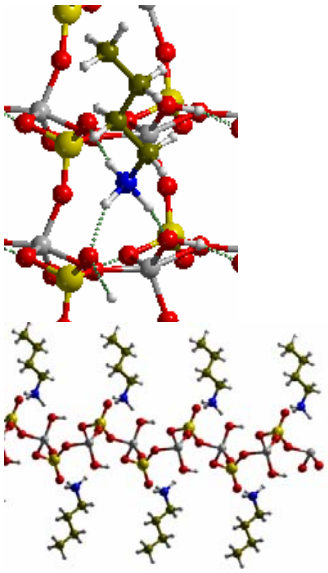

Fig. 1. Detail of optimized structure (PBC/PBE/6-21G level) of a layer of butyl-ALPO-kan

This position of butylamonium ion on surface leads to a downward shift of the $-NH_3^+$ stretching frequencies, which were found in the region 3200-3000 cm^{-1} (Fig. 2), significantly lower than the isolated NH vibration. Al-OH groups in Butyl-ALPO-Kan point on lattice oxygens in a well ordered network of H-bonds, and give a sharp peak at 3584 cm^{-1} in the IR spectrum.

The IR spectrum presents also bands around 2550 cm^{-1} and 2090 cm^{-1}, which derive from both strong H-bonds in $R\text{-}NH_3^+\cdots^-OP$ complexes and combination of rotations of RNH_3^+ with the bendings at 1635 cm^{-1} and 1555 cm^{-1}. The positions of the bands strongly depends upon the strength of hydrogen bonds between protons in $R\text{-}NH_3^+$ groups and both PO^- and basic surface oxygens. The shape of the combination bands derives from the interactions with vibrational states of the ν (NH) band of hydrogen bonded groups. A Fermi resonance between fundamental stretching modes and the overtones and/or combinations, which pronounce an Evans window around 2180 cm^{-1}, is in fact clearly observable.

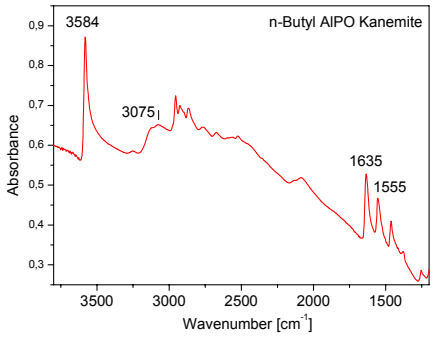

Fig.3: IR spectrum of butylammonium intercalated in ALPO-kan.

1. (a): Pastore, H.O.; Coluccia, S. and Marchese, L.; *Annu. Rev. Mater. Res.*,**2005**, 35, 351; (b): Pastore, H.O.; Martins, G.A.V.; Strauss,M.; Pedroni, L.G.; Superti, G.B.; de Oliveira, E.C.; Gatti , G. and Marchese, L.; *Micropor. Mesopor. Mater.*, (in press).

2.Cheng, S.; Tzeng, J.; HSU,B.; *Chem. Mater.* **1997**, 9, 1788-1796.
3.Garvie, L.A.J. ; Devouard, B.; Groy, T.L.; Camara, F. ; Buseck; P.R.; *American Mineralogist,* **1999**, 84, 1170-1175.

P 5.5

Sviluppo e applicazione di metodi basati su Orbitali Molecolari Estremamente Localizzati

Michela Ghitti[a], Alessandro Genoni[a,b], Stefano Pieraccini[a], Maurizio Sironi[a]
[a]*Dipartimento di Chimica Fisica ed Elettrochimica,Università degli Studi di Milano, via Golgi 19, 20133 Milano, michela.ghitti@unimi.it*
[b]*Quantum Theory Project, University of Florida, P.O. Box 118435, 32611 Gainsville, Florida, U.S.A.*

Gli Orbitali Molecolari Estremamente Localizzati (ELMOs), ovvero orbitali strettamente localizzati su frammenti molecolari, risultano essere un efficace strumento per la costruzione della distribuzione elettronica di sistemi di grandi dimensioni.
L'affidabile trasferibilità degli ELMOs, già ampiamente dimostrata, è stata sfruttata nel nostro laboratorio, per sviluppare un programma per la determinazione della densità elettronica *ab-initio* di polipeptidi, attraverso l'utilizzo di un database di ELMOs[1] determinati su molecole modello opportunamente costruite.
Poiché gli ELMOs risultano essere orbitali non ortogonali, il calcolo della corrispondente matrice densità risulta essere dispendioso. Per realizzare un algoritmo di calcolo efficiente si è quindi impiegato un approccio "Divide and Conquer", particolarmente adatto a sfruttare la natura localizzata degli ELMOs.
Al fine di migliorare l'accuratezza nella descrizione di proprietà molecolari "locali", quali ad esempio le barriere rotazionali, è stata messa a punto una nuova strategia che permette di rilassare selettivamente solo gli ELMOs che rivestono un ruolo cruciale nella determinazione delle proprietà in esame.

1. Genoni, A.; Ghitti, M.; Pieraccini, S.; Sironi, M.; *Chem. Phys. Lett.*, **2005,** 415, 256 – 260. 2. Genoni, A.; Sironi, M.; *Theor. Chem. Acc.*, **2004**, *112*, 254 – 262. 3. Sironi, M., Genoni, A.; Civera, M.; Pieraccini, S.; Ghitti, M.; *Theor. Chem. Acc.*, in press.

P 5.6

Potenziali chimici in eccesso in liquidi ionici tramite 1D-RISM

M. Malvaldi[a], S.Bruzzone[b], C. Chiappe[a].
[a] *Dipartimento di Chimica Bioorganica e Biofarmacia, Università di Pisa, Via Bonanno 33, 56126 Pisa.*
e-mail corresponding author: marco@dcci.unipi.it
[b]*Dipartimento di Chimica e Chimica Industriale, Università di Pisa, Via Risorgimento 35, 56126 Pisa.*

I liquidi ionici sono una nuova classe di sistemi organici sempre più frequentemente studiata e utilizzata nella sintesi organica in virtù delle peculiari proprietà riscontrate. Poiché i liquidi ionici sono principalmente usati come solventi nella sintesi organica e in molte altre applicazioni, come l'elettrodeposizione, è particolarmente importante stimare quantitativamente la solubilità di molecole organiche ed inorganiche in questi composti. La grandezza termodinamica rilevante per stabilire l'eventuale solubilità di un possibile soluto in un dato solvente è il potenziale chimico in eccesso. Il potenziale chimico in eccesso per numerosi soluti in liquidi ionici recentemente è stato stimato teoricamente attraverso simulazioni molecolari [1, 2] e in alcuni casi comparato a risultati sperimentali [2]. Nel presente lavoro gli effetti della solvatazione, tra cui appunto il potenziale chimico in eccesso, per molecole organiche ed inorganiche (H_2O, Acetone, Metanolo e CO_2) sono stati valutati seguendo un trattamento alternativo alle simulazioni e non ancora applicato nel campo dei liquidi ionici, basato sulla teoria Reference Interaction Site Model monodmensionale (1D-RISM)[3]. Questo metodo, che fornisce le funzioni di distribuzione radiale atomo-atomo (g(r)) risolvendo le equazioni integrali RISM, presenta due vantaggi: richiede uno sforzo computazionale estremamente contenuto e le soluzioni ottenute sono libere dal rumore statistico e dagli artefatti numerici, tipici delle simulazioni. Inoltre, il potenziale chimico può essere espresso analiticamente a partire dalle funzioni di distribuzione, evitando le difficoltà insite nelle tecniche di simulazione molecolare sviluppate per stimare grandezze termodinamiche in eccesso. I risultati ottenuti per una serie di liquidi ionici modello ([mmim][Cl],[mmim][BF_4] e [mmim][PF_6]) sono in accordo qualitativo con precedenti dati ottenuti da simulazioni MD e MC; la deviazione è data dalla differenza tra le g(r) simulate e quelle ottenute per via RISM. Un accordo quantitativamente più soddisfacente è possibile tramite vari approcci [4]. Un primo miglioramento è ottenibile introducendo delle correzioni in grado di migliorare l'accordo delle g(r) calcolate con quelle simulate, tramite procedure già applicate in letteratura appositamente per il calcolo di potenziali chimici in eccesso tramite 1D-RISM.

1. Lynden-Bell, R. M.; Atams, N. A.; Vasilyuk, A.; Hanke, C. G.; *Mol. Phys.*, **2002**, *100*, 3225 – 3229. 2. Shah, J. K.; Maginn, E. J.; *J. Phys. Chem. B*, **2005**, *109*, 10395 – 10405. 3. Chandler, D.; Andersen, H. C.; *J. Chem. Phys.*, **1972**, *57*, 1930. 4. Kast, S. M.; *ChemPhysChem*, **2004**, *5*, 449 – 455.

P 5.7

Synthetic, electrochemical and theoretical investigation of encumbered triangular cluster units

Gabriele Manca[a], Alberto Albinati[b], Samantha Bruzzone[a], Fabrizia Fabrizi de Biani[c], Carla Guidotti[a], Piero Leoni[a], Lorella Marchetti[a], Swagat K.Mohapatra[a], Eliseo Ruiz[d], Piero Zanello[c]

.
[a] *Dipartimento di Chimica e Chimica Industriale, Università di Pisa, via Risorgimento 35, Pisa.56126 Email:g.manca@dcci.unipi.it, sama@dcci.unipi.it*
[b] *Dipartimento di Chimica Strutturale e Stereochimica Inorganica, via Venezian 21, Milano*
[c] *Dipartimento di Chimica,Università di Siena, via A. Moro, Siena.*
[d]*Department de Quimica Inorganica,Universidad de Barcelona (Spain)*

In the last years we have synthesized a new family of 44 e^- triangular platinum clusters of general formula $Pt_3(\mu\text{-}PBu^t_2)_3(CO)_2X$ (X =, halide, CCR), with a limited number of reactive sites, which proved to be useful precursors of ordered molecular structures containing several cluster units connected by conjugated spacers. A new member of this of this family of cluster $[Pt_3(PBu^t_2)_3I_3$, (**1**) Fig. 1], showing peculiar properties and a different valence electrons count (42 e^-), has been prepared and characterized in the last months. As shown by electrochemical studies, cluster **1** undergoes two reversible mono-electronic reductions, reaching 44 e^-; the salt $[Pt_3(PBu^t_2)_3I_3]PPN$ [(**2**), PPN = bis-triphenylphosphinimini-um], containing the 43 e^- radical anion, has also been prepared and isolated by chemical reduction of **1**, while the 44 e^- dianion is unstable and undergoes rapid decomposition.

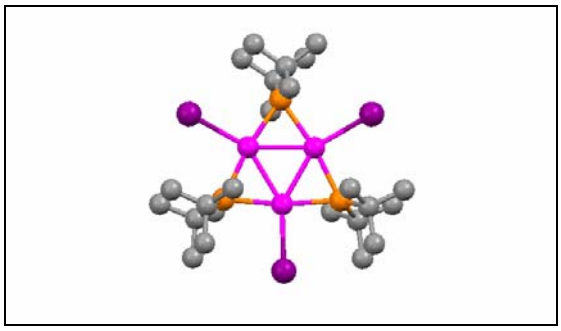

Figure 1

During the first reduction the colour changes from purple to green. All the three (neutral, mono reduced and direduced forms) have been studied using density functional methods. Herein we report the comparison between computational and experimental results for all the three different oxidation states.

1) M,. Stener, K. Albert, N. Rosch, *Inorganica Chimica Acta,* **1999,** 286, 30-36

P 5.8

Combined X-ray absorption spectroscopy and Molecular Dynamics study of the Hg2+ aqua ion.

Giordano Mancini[a,b] Nico Sanna[b], Vincenzo Barone[c], Paola D'Angelo[a], Giovanni Chillemi[b]
[a] *Department of Chemistry, Università di Rome "La Sapienza", P.le Aldo Moro 5, 00185 Roma. gmancini@caspur.it*
[b] *CASPUR, Consorzio Applicazioni di Supercalcolo per Università e Ricerca,Via dei Tizii 6b, 00185 Roma.*
[c] *Dipartimento di Chimica, Università di Napoli Federico II, Via Cintia, 80126 Napoli*

Molecular Dynamics simulations of the Hg^{2+} ion in aqueous solution have been carried out using an effective two body potential. This potential is obtained from quantum mechanical ab initio calculations in which the many-body ion-water terms are accounted for by the polarizable continuum method (PCM). This approach is computationally very efficient and has allowed us to carry out extremely long molecular dynamics simulations, indispensable to reproduce the dynamic properties of ionic system with a flexible first hydration shell derived from quantum mechanical calculations. A stable hepta-coordinated structure of the Hg^{2+} first hydration shell has been observed. This result is confirmed by the analisys of extended X-ray absorption fine structure (EXAFS) and X-ray absorption near-edge structure experimental data, which unambiguously show the preference for a sevenfold instead of a sixfold coordination..

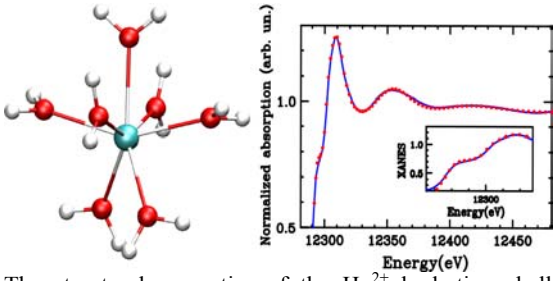

The structural properties of the Hg^{2+} hydration shells have been investigated using radial and angular distribution functions, while the dynamical behavior has been discussed in terms of reorientational correlation functions, mean residence times of water molecules in the first and second hydration shells, and self-diffusion coefficients. The effect of water-water interactions on the Hg^{2+} hydration properties has been evaluated using the SPC/E and TIP5P water models

1. Chillemi G., D'Angelo P., Pavel N. V., Sanna N., Barone V.; *J. Am. Chem. Soc.* **2002**, *124*, 1968.
2. Chillemi G., Barone V., D'Angelo P., Mancini G., Persson I., Sanna N.; *J. Phys. Chem. B.* **2005**, *109* , 9186.
3. G. Chillemi, G. Mancini, N. Sanna, V. Barone, S. Della Longa, M.
Benfatto, N. V. Pavel, P. D'Angelo; *J. Am. Chem. Soc*. **2007**, *129*, 5430

P 5.9

Ab Initio calculation and experimental determination of ^{13}C And ^{19}F Chemical Shielding Tensors of some fluorinated toluenes dissolved in a nematic LC mixture

Alberto Marini[a,b], Donata Catalano[a], Benedetta Mennucci[a], Carlo Alberto Veracini[a]
[a] *Dipartimento di Chimica e Chimica Industriale, Università di Pisa, Via Risorgimento 35, 56126 Pisa, Italy. a.marini@sns.it*
[b] *Scuola Normale Superiore di Pisa, Piazza dei Cavalieri 12, 56126 Pisa, Italy.*

In recent years, the comparison between theoretical predictions and experimental determinations of chemical shielding tensors has become a good test bench in analyzing electronic structures of molecules[1]. In anisotropic media the chemical shift interaction is described by the chemical shielding tensor (σ) in an arbitrary coordinate system. *Ab initio* methods give the complete nine-elements shielding matrix for each chemically distinguishable resonant nucleus, thus the orientation of the principal axis system of each tensor can be easily determined. The principal values of σ tensors (or, at least, some components of such tensors in an outstanding molecular frame) can also be determined by using NMR spectroscopy of small molecules dissolved in liquid crystals, if the molecular order parameters are known from independent experimental data[2].

In this work we present a detailed study of the magnetic shielding properties of some fluorotoluenes, in order (i) to build up a shielding tensors database for fluorinated aromatic molecules, which constitute models of the rigid core of modern fluorinated liquid crystals[3], and (ii) to rationalize the effects of the presence of fluorine atoms on the principal values and orientations of the ^{13}C chemical shielding tensors investigated.
The chemical shielding tensors have been obtained by means of quantum-mechanical calculations, using Gaussian'03[4]. Geometries and carbon nuclear shielding tensors of the different probes have been determined at the DFT level of theory using the B3LYP/6-31G(d) and MPW1PW91/6-311+G(d,p) combination of hybrid functional and basis set, respectively. NMR chemical shielding tensors have been calculated by the method of Gauge-Including Atomic Orbitals, GIAO[5]. On these model systems we have also performed an analysis in terms of paramagnetic and diamagnetic contributions as given by the Natural Chemical Shielding (NCS) approach[6].
^{13}C and ^{19}F NMR spectra of *para* and *meta* fluorotoluene dissolved in the nematic mixture ZLI1167, recorded at various temperatures, have been analyzed, finally obtaining (i) the orientational order parameters from ^{13}C-^{19}F dipolar couplings and (ii) some σ components from the temperature trends of chemical shift anisotropies.
The agreement between computed and experimental results is excellent.

1. "*Calculation of NMR and EPR Parameters*", eds.: Kaupp, M.; Buhl, M.; Malkin, V. G.; WILEY-VHC Verlag GmbH & Co. KGaA, Weinheim, **2004**.
2. Fung, B. M.; *Journal of Magnetic Resonance*, **2005**, *86*, 160.
3. Kirsch, P.; Bremer, M.; *Angewandte Chemie Int. Ed.,* **2000**, *39*, 4216.
4. Gaussian 03, Revision B.05. M.J. Frisch et al., Gaussian, Inc., Pittsburgh PA, **2003**.
5. Ditchfield, R.; *Molecular Physics* **1974**, *27*, 789.
6. Bohmann, J. A.; Farrar, T. C.; and Weinhold, F.; *Journal of Chemical Physics,* **1997**, *107*, 1173.

P 5.10

A non conventional molecular dynamics approach for determining interactions in MAPKs protein complexes.

M. C. Menziani[a], F.Filomia[a], F. De Rienzo[a]
[a]*University of Modena and Reggio Emilia, via Campi, 183, 41100 Modena, filomia.federico@unimore.it, http://multiscale-school.unimore.it*

Mitogen Activated Protein Kinase (MAPK) family has been one of the most popular target in bio-farmacological research in the last decade for its prominent role in a number of diseases, including cancer, diabetes and inflammation. In particular, the p38α subfamily is tightly involved in proinflammatory signal transduction. A large variety of inhibitors [1] have been designed to interfere with signal transduction. This can be achieved by competing with ATP or inducing conformational changes detrimental for activation.
In this study the conformational plasticity of the p38α activation loop has been simulated by means of Molecular Dynamics techniques and the distribution of dynamics states of p38α in the absence and presence of inhibitor binding has been compared with recently published mechanistic hypothesis derived from experiments.

1. P. Cohen, Nature Reviews in drug Discovery, **1**, 309-315, 2006.

P 5.11

Interpretation of CW-ESR spectroscopy of tempo-palmitate in the 5CB liquid crystal

Antonino Polimeno[a], Mirco Zerbetto[b], Paola Cimino[b]
[a]*Dipartimento di Scienze Chimiche, Università di Padova, Via Marzolo 1, 35131, Padova / antonino.polimeno@unipd.it*
[b]*Dipartimento di Chimica, Università di Napoli "Federico II", Complesso Universitario di Monte Sant'Angelo Via Cintia, I-80126 Napoli*

We present the interpretation of continuous wave electron spin resonance (CW-ESR) spectra of tempo-palmitate dissolved in the 5CB liquid crystal via our *ab initio* integrated computational approach (ICA) *[1]*. The methodology, already applied for the study of molecules in isotropic media *[2]*, is based on the stochastic Liouville equation (SLE) approach *[3,4]* in which the time evolution of the density matrix depends on the spin Hamiltonian and on relaxing processes included as stochastic Fokker Planck/diffusive operators. The spin Hamiltonian is averaged over the fast vibrational motions and the magnetic tensors (Zeeman and hyperfine) are characterized by quantum-mechanical density functional calculations *[5,6]* in both isotropic and nematic phases.
The molecule is described as a non-rigid rotator with one internal degree of freedom which was chosen to be the torsional angle describing the orientation of the tempo nitroxide with respect to the alchilic chain. So, dynamic is described by two stochastic coordinates: *1)* the set of Euler angles ($\boldsymbol{\Omega}$) giving the overall tumbling of the molecule with respect to an inertial laboratory frame and *2)* the internal angle (θ). The overall tumbling is subjected to an external orienting potential in the nematic phase while the internal angle θ is affected by the internal torsional potential obtained from QM calculations. Dynamical parameters (rotational, internal and mixed parts of the diffusion tensor) are obtained with calculations based on a hydrodynamic model *[7]*. CW-ESR spectra of the tempo-palmitate spin probe were simulated in the range of temperatures from 299 K (nematic phase) to 317 K (isotropic phase).

1. Barone, V.; Polimeno, A.; *Phys. Chem. Chem. Phys.*, **2006**, *8*, 4609 – 4629.
2. Polimeno, A.; Zerbetto, M.; Franco, L.; Maggini, M.; Corvaja, C.; *J. Am. Chem. Soc.*, **2006**, *28*, 4734 – 4741; Barone, V.; Brustolon, M.; Cimino, P.; Polimeno, A.; Zerbetto, M.; Zoleo, A.; *J. Am. Chem. Soc.*, **2006**, *128*, 15865 – 15873; Zerbetto, M.; Carlotto, S., Polimeno, A.; Corvaja, C.; Franco, L.; Toniolo, C.; Formaggio, F.; Barone, V.; Cimino, P.; *J. Phys. Chem. B.*, **2007**, *110*, 2668 – 2674.
3. Schneider, D. J.; Freed, J. H.; *Adv. Chem. Phys.*, 1989, *73*, 387 – 527.
4. Polimeno, A.; Freed, J. H.; *J. Phys. Chem.*, **1995**, *99*, 10995 – 11006.
5. Neese, F.; *J. Chem. Phys.*, **2001**, *115*, 11080 – 11096.
6. Ciofini, I.; Adamo, C.; Barone, V.; *J. Chem. Phys.*, **2004**, *121*, 6710 – 6718.
7. Moro, G.; *Chem. Phys.*, **1987**, *118*, 181 – 197.

P 5.12

Multivariate analysis of glass structures obtainted by molecular dynamics simulations

M. Pota, A. Pedone, G. Malavasi, M. Cocchi, U. Segre, M. C. Menziani
Dipartimento di Chimica, Università di Modena e Reggio Emilia, Via Campi 183, 41100, Modena. mpota@unimo.it.
Scuola di Dottorato: http://multiscale-school.unimore.it.

The correct understanding of their structure-property relationships is required to meet predefined physical properties of glass forming systems and ever-changing industrial needs, but the elucidation of glass structures is still a difficult task.
In this paper, Molecular Dynamics (MD) simulation procedures used to produce glasses are investigated in order to find the optimal combination of the simulation parameters. To do this, a design of experiments (DOE) methodology [1] has been used; the parameters of the simulation procedure (e.g. starting relaxation temperature and length, cooling rate and final relaxation length) and those concerning the MD algorithm (e.g. the cut-off and the ensemble used) have been considered as *factors*. The DOE approach allows us to examine simultaneously the influence of different simulation parameters and their interactions and to find an approximate model that can explain the dependencies between the response values and the parameters considered. As the optimization objective is to produce simulated glasses with structural properties in good agreement with experimental results, firstly we restrict our study to silica and 30% Na2O silica glasses for which experimental radial distribution function are available. Moreover, multivariate analysis is applied to understand how structural properties described by functions (e.g. distances and angles distribution functions) are related with mean properties described by single points and with the simulation parameters.

1. Chagarov, E.; Adams, J. B.; Kieffer, J.; *Modelling Simul. Mater. Sci Eng*. **2004**, *12*, 337-356.

P 5.13

Molecular dynamics simulation of carboxy and deoxy murine Neuroglobin

Massimiliano Anselmi[a], Beatrice Vallone[b], Maurizio Brunori[b] and Alfredo Di Nola[a]
[a]*Dipartimento di Chimica Università di Roma La Sapienza, P.le Aldo Moro 5, 00100 Roma, m.anselmi@caspur.it*
[b]*Dipartimento di Scienze Biochimiche Università di Roma La Sapienza, P.le Aldo Moro 5, 00100 Roma*

Globins are respiratory proteins that reversibly bind dioxygen and other small ligands at the iron of a heme prosthetic group. Hemoglobin (Hb) and myoglobin (Mb) are the most prominent members of this protein family. Unexpectedly a few years ago a new member was discovered and called neuroglobin (Ngb) being predominantly expressed in the brain[1]. Ngb is a single polypeptide of 151 amino acids and despite the small sequence similarity with other globins, it displays the typical globin fold. Oxygen, nitric oxide or carbon monoxide can displace the distal histidine which in ferrous Ngb (as well as ferric) is bound to the iron, yielding a reversible adduct. Recent crystallographic data on carboxy Ngb show that binding of an exogenous ligand is associated to structural changes involving heme sliding and a topological reorganization of the internal cavities; in particular the huge internal tunnel that connects the bulk with the active site (peculiar to Ngb) is heavily reorganized[2,3]. We report the results of extended (90 ns) molecular dynamics simulations in water of ferrous deoxy and carboxy murine neuroglobin, which are both coordinated on the distal site, in the latter case by CO and in the former one by the distal His64(E7). The long time scale of the simulations allowed us to characterize the equilibrated protein dynamics and to compare protein structure and dynamical behaviour coupled to the binding of an exogenous ligand. We have characterized the heme sliding motion, the topological reorganization of the internal cavities, the dynamics of the distal histidine and particularly the conformational change of the CD loop (see figure), whose flexibility depends ligand binding[4].

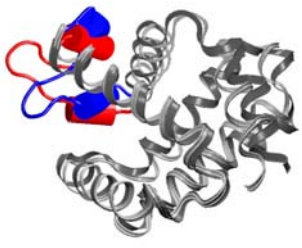

1. Burmester, T.; Weich, B.; Reinhardt, S.; Hankeln, T.; *Nature,* **2000**, 407, 520 - 523. 2. Vallone, B.; Nienhaus, K.; Brunori, M.; Nienhaus, G. U.; *Proteins,* **2004**, 56, 85 - 92. 3. Vallone, B.; Nienhaus, K.; Matthes, A.; Brunori, M.; Nienhaus, G. U.; *Proc. Natl. Acad. Sci. U.S.A.,* **2004**, 101, 17351 - 17356. 4. Anselmi, M.; Vallone, B.; Brunori, M.; Di Nola, A.; *Biophys. J.,* **2007,** in press

P 5.14

Studio DFT della riduzione catalitica di acetofenone ad 1feniletanolo mediante $[Ru(HPN)(pcym)Cl]^+$.

V.Verdolinoa, R.Cammi, P.Pelagatti, M.Balordi, C.Pelizzi
Università degli Studi di Parma, Dip. di Chimica GIAF, Viale G.P. Usberti 17/A, 43100 Parma

Lo studio teorico presentato si propone di dare una descrizione meccanicistica del trasferimento d'idrogeno da alcol isopropilico ad acetofenone catalizzato da $[Ru(HPN)(pcym)Cl]^+$ (HPN = 2(difenilfosfino)anilina, pcym= pcimene) riservando particolare interesse alla possibile enantio selettività della reazione. Il meccanismo è articolato in due fasi: I) formazione della specie cataliticamente attiva (C) mediante coordinazione di isopropossido al centro metallico (sfera interna di coordinazione) con conseguente formazione di una specie RuH, II) avvicinamento dell'acetofenone alla specie idrurica mediante legame idrogeno tra l'ossigeno del chetone e la funzione amminica del legante (sfera esterna di coordinazione). In questa fase hanno origine gli stati di transizione (ST1,ST2) relativi alle conformazioni proR e S.
Gli intermedi che caratterizzano la fase I sono il precursore catalitico [Ru(HP)(pcym)Cl2] (P), il

complesso clorodissociato $[Ru(HP)(pcym)Cl]^+$ (PC1), quello chelato $[Ru(HPN)(pcym)Cl]^+$ (PC2), il complesso Rualcossido coordinato (C) e la specie idrurica nelle due possibili forme, $[Ru(HP)(pcym)HCl]^+$ (C1) e $[Ru(HPN)(pcym)H]^+$ (C2).
Da evidenze sperimentali la specie idrurica risulta essere C2 da cui la caratterizzazione dell'intermedio Rualcolato coordinato è stata effettuata a partire dal complesso PC2 seguendo tre possibili direzioni d'avvicinamento dello ione ipropossido. Solo una di queste vie conduce ad un intermedio idoneo a formare il precursore C2.
La fase II comprende lo studio degli stati di transizione che conducono ai due alcoli enantiomeri (R) ed (S) dell' 1feniletanolo. Partendo da geometrie ottimizzate sotto condizione di vincolo strutturale (distanza RuC carbonilico di 4 Å) sia dei reagenti (C2+acetofenone), che dei prodotti (residuo mettallorganico + feniletanolo), si è effettuata una ottimizzazione dei due stati di transizione ST1 (proS) e ST2 (proR).
E' stato inoltre verificato che entrambi gli ST ottimizzati possiedono un solo modo vibrazionale immaginario e che tale modo normale corrisponda alla c.r. relativa al trasferimento sincrono di H dal metallo e di H+ dall'azoto (fig.1).

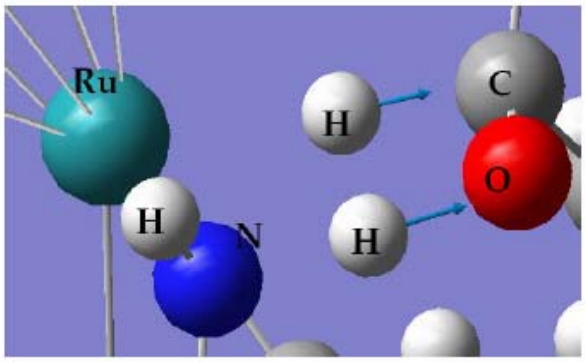

Fig.1 Coordinata di reazione per gli stati di transizione ST1 ed ST2

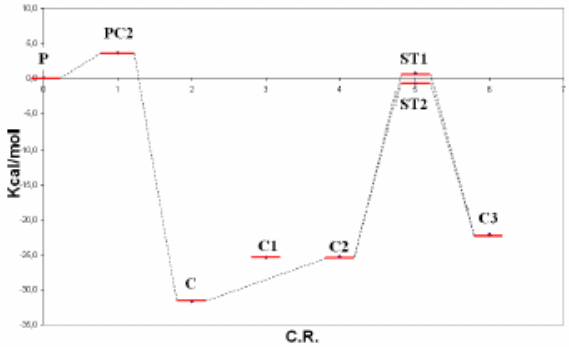

Fig.2 Schematizzazione del processo riduttivo

Si è quindi ottenuto il profilo completo del percorso reattivo (fig.2) ottenendo come prodotti [Ru(PN)(pcym)Cl] e 1feniletanolo. E' possibile quindi effettuare alcune considerazioni di carattere strutturale ed elettroniche in relazione agli stati di transizione ST1 e ST2: 1) i calcoli di energia effettuati introducendo l'effetto del solvente mostrano che ST1 ed ST2 differiscono di soli 1.5 Kcal/mol giustificando il dato sperimentale secondo cui non vi è riscontro d'eccesso enantiomerico, II) la configurazione proR è energeticamente favorita nonostante sia la più ingombrata stericamente, III) la distanza H(pcym)-C(fenile) (2.89 Ang) è paragonabile alla somma dei loro raggi di Van der Waals (2.90 Å), presupponendo un'interazione specifica (fig3). Anche l'analisi popolazionale ha messo in evidenza tale interazione; i valori della carica di Mulliken su H(44) (0.294) e su C(3) (-0.380) ben si adattano a descrivere l'avvicinamento elettrofilo(H)-nucleofilo(C). Ciò potrebbe essere alla base di una strategia sintetica per favorire selettivamente la riduzione dell'enantiofaccia proR.

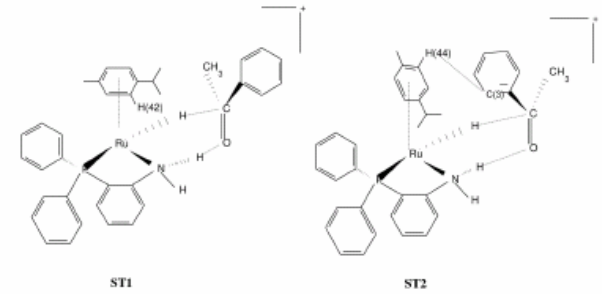

Fig.3 Rappresentazione schematica dei due possibili stati di transizione a) ST1 e b) ST2

Tutti i calcoli sono stati effettuati mediante il programma *Gaussian03*[1] al livello di calcolo DFT/B3LYP/Lanl2dz[2-4].
Tutti gli intermedi stabili sono stati ottimizzati in vuoto e le energie valutate in single point in vuoto e simulando la presenza del solvente (isopropanolo come ambiente di reazione) mediante il modello PCM[5]. Gli stati di transizione sono stati individuati al medesimo livello di calcolo mediante ottimizzazione con metodi sincroni (STQN) in vuoto, e determinandone il single point introducendo il solvente.

RIFERIMENTI

[1] M. J. Frisch et al. Gaussian 03 (Gaussian, inc., Pitzburgh, PA, '03)
[2] P. J. Hay and W. R. Wadt, *J. Chem. Phys.* 82, 270 (1985).
[3] W. R. Wadt and P. J. Hay, *J. Chem. Phys.* 82, 284 (1985).
[4] P. J. Hay and W. R. Wadt, *J. Chem. Phys.* 82, 299 (1985).
[5] C.Amovilli, V.Barone, R.Cammi, E.Cances, M.Cossi, B.Mennucci, C.S.Pomelli, and J.Tomasi. In Quantum System in Chemistry and Physics part II vol.32 of Advances in Quantum Chemistry 227261.

INDICE COMPLESSIVO
AUTORI E COMUNICAZIONI

ELENCO DELEGATI

Aggravi	Marianna	Università di Siena	aggravi4@unisi.it
Agostiano	Angela	Università di Bari	agostiano@chimica.uniba.it
Amelia	Matteo	Università degli Studi di Perugia	ameliamat@libero.it
Anedda	Roberto	Università di Cagliari	aneddar@unica.it
Angelini	Emma	Politecnico di Torino	emma.angelini@polito.it
Anselmi	Massimiliano	Università di Roma "La Sapienza"	m.anselmi@caspur.it
Baglioni	Piero	Università di Firenze e CGSI	baglioni@csgi.unifi.it; piero.baglioni@unifi.it
Balucani	Nadia	Università degli Studi di Perugia	nadia@dyn.unipg.it
Barone	Guido	Università di Napoli Federico II	guido.barone@unina.it
Barone	Vincenzo	Università di Napoli "Federico II"	baronev@unina.it
Basosi	Riccardo	Università di Siena	basosi@unisi.it
Becucci	Maurizio	Università di Firenze	maurizio.becucci@unifi.it
Bee	Antonio	Costruzioni Solari srl	c.s@costruzionisolari.it
Bennici	Simona	Università degli Studi di Milano	simona.bennici@catalyse.cnrs.fr
Bertolino	Chiara Alessandra	Università degli Studi di Torino	chiara.bertolino@unito.it
Bianchino	Erminia	Università di Bari	mavelli@chimica.uniba.it
Binetti	Simona	Università di Milano Bicocca	simona.binetti@mater.unimib.it
Bisio	Chiara	Università del Piemonte Orientale "A. Avogadro"	bisio@mfn.unipmn.it
Bocchinfuso	Gianfranco	Università di Roma "Tor Vergata"	gianfranco.bocchinfuso@uniroma2.it
Bonicelli	Maria Grazia	Università di Roma "La Sapienza"	mariagrazia.bonicelli@uniroma1.it
Bozio	Renato	Università di Padova	renato.bozio@unipd.it
Brustolon	Marina	Università degli Studi di Padova	marinarosa.brustolon@unipd.it
Brutti	Sergio	Università di Roma "La Sapienza"	sergio.brutti@uniroma1.it
Bruzzone	Samantha	Università di Pisa	sama@ns.dcci.unipi.it
Bystrenova	Eva	Institute for Nanostructured Materials Studies	e.bystrenova@bo.ismn.cnr.it
Caminati	Gabriella	Università di Firenze	caminati@unifi.it
Caminiti	Ruggero	Università di Roma "La Sapienza"	r.caminiti@caspur.it
Cannistraro	Salvatore	Università della Tuscia	cannistr@unitus.it
Capobianco	Amedeo	Università di Salerno	acapobianco@unisa.it
Caponetti	Eugenio	Università di Palermo	caponett@unipa.it
Caracciolo	Giulio	Università di Roma "La Sapienza"	g.caracciolo@caspur.it
Carlotti	Benedetta	Università degli Studi di Perugia	carlotti@unipg.it
Carnasciali	M. Maddalena	Università degli Studi di Genova	marilena@chimica.unige.it
Casarin	Maurizio	Università degli Studi di Padova	maurizio.casarin@unipd.it; casarin@ux1.unipd.it
Casu	Mariano	Università di Cagliari	mcasu@unica.it
Catti	Michele	Università di Milano Bicocca	michele.catti@mater.unimib.it
Catucci	Lucia	Università di Bari	catucci@chimica.uniba.it
Ceccarelli	Raffaella	Politecnico di Torino	raffaella.ceccarelli@polito.it
Chidichimo	Giuseppe	Università della Calabria	chidichi@unical.it
Chiorino	Anna	Università degli Studi di Torino	anna.chiorino@unito.it
Cimino	Paola	Università degli Studi di Salerno	cimino@unisa.it
Coluccia	Salvatore	Università di Torino	salvatore.coluccia@unito.it
Comparelli	Davide	Università di Bari	r.comparelli@ipcf.ba.cnr.it
Convertino	Annalisa	Istituto per lo Studio dei Materiali Nanostrutturati	annalisa.convertino@ismn.cnr.it
Corno	Marta	Università di Torino	marta.corno@unito.it
Corricelli	Michela	IPCF-CNR Bari	m.corricelli@ba.ipcf.cnr.it
Cosentino	Ugo	Università degli Studi di Milano Bicocca	ugo.cosentino@unimib.it
Cosma	Pynalisa	Università di Bari, CNR-IPCF	p.cosma@chimica.uniba.it
Costa	Giorgio Andrea	Università di Genova	costa@chimica.unige.it
Croce	Fausto	Università degli Studi "G. D'Annunzio"	fausto.croce@unich.it

Curri	M. Lucia	CNR-IPCF Bari	lucia.curri@ipcf.ba.cnr.it
D'Amore	Maddalena	Università Piemonte Orientale	mdamore@unina.it
De Benedetto	Giuseppe	Università del Salento	giuseppe.debenedetto@unile.it
De Filpo	Giovanni	Università della Calabria	defilpo@unical.it
De Nicolò	Nicola	IPCF-CNR Bari	n.denicolo@ba.ipcf.cnr.it
De Palo	Nicoletta	Università di Bari	n.depalo@ba.ipcf.cnr.it
De Santis	Pasquale	Università di Roma "La Sapienza"	pasquale.desantis@uniroma1.it
Del Sole	Roberta	Università del Salento	roberta.delsole@unile.it
Di Pietro	Elisa	Università degli Studi di Firenze	dipietro@chim.unifi.it
Dimo	Luigi	Università del Salento	luigi.dimo@unile.it
Donati	Alessandro	Università di Siena	alessandro.donati@unisi.it
Duce	Celia	Università di Pisa	celia@dcci.unipi.it
Elisei	Fausto	Università degli Studi di Perugia	elisei@unipg.it
Fabrizi de Biani	Fabrizia	Università di Siena	fabrizi@unisi.it
Faga	Maria Giulia	Università di Torino	m.faga@to.istec.cnr.it
Faralli	Cristian	Università di Firenze	nayandei98@hotmail.com
Ferrante	Camilla	Università di Padova	camilla.ferrante@unipd.it
Ferretti	Maurizio	Università degli Studi di Genova	ferretti@chimica.unige.it
Fini	Paola	IPCF-CNR Bari	p.fini@ba.ipcf.cnr.it
Fittipaldi	Maria	INSTM	maria.fittipaldi@unifi.it
Flor	Giorgio	Università degli Studi di Pavia	giorgio.flor@unipv.it
Fortunati	Ilaria	Università degli Studi di Padova	ilaria.fortunati@unipd.it
Frola	Francesca	Università di Torino	francesca.frola@unito.it
Galantini	Luciano	Università di Roma "La Sapienza"	l.galantini@caspur.it
Garbin	Eleonora	INSTM	eleoga@gmail.com
Gatti		Università del Piemonte Orientale	
Genga	Alessandra	Università del Salento	alessandra.genga@unile.it
Ghiotti	Giovanna	Università di Torino	giovanna.ghiotti@unito.it
Ghitti	Michela	Università degli Studi di Milano	michela.ghitti@unimi.it
Giancane	Gabriele	Università del Salento	gabriele.giancane@unile.it
Giancola	Tina	Università di Napoli Federico II	giancola@unina.it
Giotta	Livia	Università del Salento	livia.giotta@unile.it
Girlando	Alberto	Università di Parma	girlando@unipr.it
Guldi	Dirk M.	Friedrich-Alexander-Universität Erlangen-Nürnberg	dirk.guldi@chemie.uni-erlangen.de
Ielpo	Piera	Università di Bari	pieraielpo@chimica.uniba.it
Ingrosso	Chiara	Università di Bari	c.ingrosso@ba.ipcf.cnr.it
Iozzi	Maria Francesca	Univ. Piemonte Orientale “Amedeo Avogadro”	francesca.iozzi@mfn.unipmn.it
Italiano	Francesca	IPCF-CNR Bari	
Lamanna	Ugo	Università di Bari	lamanna@chimica.uniba.it
Latterini	Loredana	Università degi Studi di Perugia	loredana@unipg.it
Lazar	Adina	Istituto Studio dei Materiali Nanostrutturati	a.lazar@bo.ismn.cnr.it
Lazzara	Giuseppe	Università degli Studi di Palermo	g.lazzara@unipa.it
Leggio	Claudia	Università di Roma "La Sapienza"	c.leggio@caspur.it
Lo Russo	Antonella	Università del Salento	antonella.lorusso@le.infn.it
Malvaldi	Marco	Università di Pisa	marco@dcci.unipi.it
Manca	Gabriele	Università di Pisa	g.manca@ns.dcci.unipi.it
Mancini	Giordano	Università di Roma "La Sapienza" - CASPUR	gmancini@caspur.it
Mangiapia	Gaetano	Università degli Studi di Napoli "Federico II"	gaetano@chemistry.unina.it
Manno	Daniela	Università del Salento	daniela.manno@unile.it
Manyar	Haresh	Università degli Studi di Torino	hareshmanyar@rediffmail.com
Manzoli	Maela	Università degli Studi di Torino	maela.manzoli@unito.it
Marchese	Leonardo	Università degli Studi del Piemonte Orientale	leonardo.marchese@mfn.unipmn.it
Marchettini	Nadia	Università di Siena	marchettini@unisi.it

Marini	Alberto	Scuola Normale Superiore	a.marini@sns.it; am@ns.dcci.unipi.it
Marletta	Giovanni	Università degli Studi di Catania	gmarletta@dipchi.unict.it
Martino	Luigi	Università di Napoli Federico II	luigi.martino@unina.it
Martra	Gianmario	Università di Torino	gianmario.martra@unito.it
Masia	Marco	Università degli Studi di Sassari	marco.masia@uniss.it
Massarotti	Vincenzo	Università di Pavia	vincenzo.massarotti@unipv.it
Mavelli	Fabio	Università di Bari	mavelli@chimica.uniba.it
Mazzucato	Ugo	Università di Perugina	mazzucat@unipg.it
Melandri	Sonia	Università di Bologna	sonia.melandri@unibo.it
Menziani	Maria Cristina	Università di Modena e Reggio Emilia	menziani.mariacristina@unimore.it
Milano	Francesco	IPCF-CNR Bari	f.milano@ba.ipcf.cnr.it
Milioto	Stefania	Università di Palermo	milioto@unipa.it
Monaco	Guglielmo	Università degli Studi di Salerno	gmonaco@unisa.it
Moncelli	Maria Rosa	Università degli Studi di Firenze	moncelli@unifi.it
Morandi	Sara	Università di Torino	sara.morandi@unito.it
Moro	Giorgio	Università di Padova	giorgio.moro@unipd.it
Morresi	Assuntina	Università di Perugina	morresi@unipg.it
Muratore	Nicola	Università di Palermo	nicola.muratore@unipa.it
Musinu	Anna	Università di Cagliari	musinu@unica.it
Muthusamy	Vishnuvarthan	Università degli Studi di Torino	visvar_cit@yahoo.com
Narducci	Dario	Università di Milano Bicocca	dario.narducci@unimib.it
Ortona	Ornella	Università di Napoli "Federico II"	ortona@chemistry.unina.it
Paduano	Luigi	Università di Napoli "Federico II"	padu@chemistry.unina.it; luigi.paduano@unina.it
Pagano	Bruno	Università degli Studi di Salerno	bpagano@unisa.it
Palumbo	Luisa	Università di Torino	luisa.palumbo@unito.it
Panniello	Anna Maria	Università degli Studi di Bari	a.panniello@ba.ipcf.cnr.it
Pavel	Nicolae Viorel	Università di Roma "La Sapienza"	pavel@caspur.it
Pavone	Michele	Università degli Studi di Napoli "Federico II"	mipavone@unina.it
Peddis	Davide	Ass. Univ. del Sulcis Iglesiente (A.U.S.I.)	dpeddis@hotmail.com
Pedone	Alfonso	Università di Modena e Reggio Emilia	apedone@unimo.it
Piccaluga	Giorgio	Università di Cagliari	piccal@unica.it
Pierri	Paolo	Centro Studi e Ricerche di Sanità Militare	pierrichim@libero.it
Pignataro	Bruno	Università di Palermo	bruno.pignataro@unipa.it
Pignataro	Salvatore	Università di Catania	spignataro@dipchi.unict.it
Pindinelli	Emanuela	Università del Salento	Emanuela.pindinelli@unile.it
Pitea	Demetrio	Università degli Studi di Milano-Bicocca	demetrio.pitea@unimib.it
Placido	Tiziana	IPCF-CNR	t.placido@ba.ipcf.cnr.it
Pogni	Rebecca	Università di Siena	pogni@unisi.it
Polimeno	Antonino	Università di Padova	antonino.polimeno@unipd.it
Ponterini	Glauco	Università di Modena e Reggio Emilia	ponterini.glauco@unimore.it
Pota	Marco	Università di Modena e Reggio Emilia	pota.marco@unimore.it
Pozzi	Daniela	Università di Roma "La Sapienza"	d.pozzi@caspur.it
Puzzarini	Cristina	Università di Bologna	cristina.puzzarini@unibo.it
Rega	Nadia	Università di Napoli Federico II	nadia.rega@unina.it
Ricchiardi	Gabriele	Università di Torino	gabriele.ricchiardi@unito.it
Rich	Peter	University College, London	prr@ucl.ac.uk
Ruocco	Giancarlo	Università di Roma "La Sapienza"	giancarlo.ruocco@roma1.infn.it
Russo	Nino	Università della Calabria	nrusso@nical.it
Rustici	Mauro	Università di Sassari	rustici@ssmain.uniss.it
Sansone	Alberto		alberto_sansone@hotmail.it
Santoro	Fabrizio	Molecular Modelling Lab	f.santoro@ipcf.cnr.it
Satriano	Cristina	Università degli Studi di Catania	csatriano@unict.it
Savino	Maria	Università di Roma "La Sapienza"	maria.savino@uniroma1.it

Scaranto	Jessica	Università Ca' Foscari di Venezia	jeyscar@unive.it
Schettino	Vincenzo	Università di Firenze	vincenzo.schettino@unifi.it
Schiraldi	Alberto	Università degli Studi di Milano	alberto.schiraldi@unimi.it
Scipioni	Anita	Università di Roma "La Sapienza"	anita.scipioni@uniroma1.it
Segre	Ulderico	Università di Modena e Reggio Emilia	segre.ulderico@unimore.it
Selli	Elena	Università degli Studi di Milano	elena.selli@unimi.it
Simoncini	Eugenio	Università degli Studi di Siena	simoncini7@unisi.it
Spalletti	Anna	Università degli Studi di Perugia	faby@unipg.it
Striccoli	Marinella	CNR-IPCF Division of Bari	m.striccoli@ba.ipcf.cnr.it
Suffritti	Giuseppe Baldovino	Università di Sassari	pino@uniss.it
Tabacchi	Gloria	Università dell'Insubria	gloria.tabacchi@uninsubria.it
Tiezzi	Enzo	Università di Siena	tiezzienzo@unisi.it
Tiné	Maria Rosaria	Università di PIsa	mrt@dcci.unipi.it
Tomasi	Iacopo	Università di Pisa	tomasi@dcci.unipi.it
Tonachini	Glauco	Università degli Studi di Torino	glauco.tonachini@unito.it
Torsi	Luisa	Università di Bari	lstr01ch@uniba.it
Trotta	Massimo	CNR-IPCF BARI	m.trotta@ba.ipcf.cnr.it
Turco Liveri	Vincenzo	Università degli Studi di Palermo	turco@unipa.it
Vaccaro	Mauro	Università di Napoli Federico II	mauro.vaccaro@fkem1.lu.se
Valli	Ludovico	Università del Salento	ludovico.valli@unile.it
Vecchio	Stefano	Università di Roma "La Sapienza"	stefano.vecchio@uniroma1.it
Velardi	Luciano	Università del Salento	Nassisi@le.infn.it
Velino	Biagio	Università di Bologna	biagio.velino@unibo.it
Veloso Martins	Gesley Alex	Università degli Studi di Torino	gesley.martins@unito.it
Venanzi	Mariano	Università di Tor Vergata	venanzi@uniroma2.it
Verdolino	Vincenzo	Università degli Studi di Parma	vincenzo.verdolino@nemo.unipr.it
Vergara	Alessandro	Università di Napoli Federico II	alessandro.vergara@unina.it
Verrone	Raffaella	Università degli Studi di Bari	vera.remy@libero.it
Vindigni	Floriana	Università di Torino	floriana.vindigni@unito.it
Vittucci	Vito	Centro Studi e Ricerche di Sanità Militare	vitovittucci@tiscali.it
Zavorotynska	Olena	Università di Torino	olena.zavorotynska@unito.it
Zerbetto	Mirco	Università di Padova	mirco.zerbetto@unipd.it